



**Effet du salage et du séchage sur la dynamique d'évolution de la protéolyse, de la structure et de la texture lors de la fabrication d'un jambon sec. Développement d'un modèle de " jambon numérique " couplant transferts d'eau, de sel et protéolyse**

Rami Harkouss

► **To cite this version:**

Rami Harkouss. Effet du salage et du séchage sur la dynamique d'évolution de la protéolyse, de la structure et de la texture lors de la fabrication d'un jambon sec. Développement d'un modèle de " jambon numérique " couplant transferts d'eau, de sel et protéolyse. Autre. Université Blaise Pascal - Clermont-Ferrand II, 2014. Français. <NNT : 2014CLF22446>. <tel-01162623>

**HAL Id: tel-01162623**

**<https://tel.archives-ouvertes.fr/tel-01162623>**

Submitted on 11 Jun 2015

**HAL** is a multi-disciplinary open access archive for the deposit and dissemination of scientific research documents, whether they are published or not. The documents may come from teaching and research institutions in France or abroad, or from public or private research centers.

L'archive ouverte pluridisciplinaire **HAL**, est destinée au dépôt et à la diffusion de documents scientifiques de niveau recherche, publiés ou non, émanant des établissements d'enseignement et de recherche français ou étrangers, des laboratoires publics ou privés.



N° d'ordre : D. U : 2446  
E D S P I C : 648

**UNIVERSITE BLAISE PASCAL - CLERMONT II**

**ECOLE DOCTORALE  
SCIENCES POUR L'INGENIEUR DE CLERMONT-FERRAND**

**T h è s e**

Présentée par

**Rami HARKOUSS**

pour obtenir le grade de

**DOCTEUR D'UNIVERSITÉ**

**SPECIALITE : GENIE DES PROCEDES**

**Effet du salage et du séchage sur la dynamique d'évolution de la  
protéolyse, de la structure et de la texture lors de la fabrication  
d'un jambon sec. Développement d'un modèle de « jambon  
numérique » couplant transferts d'eau, de sel et protéolyse**

Soutenue publiquement le 17 Mars 2014 devant le jury :

M. DUSSAP Claude-Gilles  
Mme BERRI Cécile  
M. BOHUON Philippe  
M. DELLA VALLE Guy  
M. ASTRUC Thierry  
M. MIRADE Pierre-Sylvain  
Mme PARAFITA Emilie

Président  
Rapporteur et examinateur  
Rapporteur et examinateur  
Examineur  
Examineur  
Directeur de thèse  
Invitée



**AVANT-PROPOS**

---



---

**Publications internationales à comité de lecture**

---

- 1 – Harkouss, R., Mirade, P.S., & Gatellier, P. (2012). Development of a rapid, specific and efficient procedure for the determination of proteolytic activity in dry-cured ham: Definition of a new proteolysis index. *Meat Science*, 92, 84–88 (**article n°2**).
- 2 – Harkouss, R., Safa, H., Gatellier, P., Lebert, A., & Mirade, P.S. (2014). Building phenomenological models that relate proteolysis in pork muscles to temperature, water and salt content. *Food Chemistry*, 151, 7-14 (**article n°3**).
- 3 – Harkouss, R., Astruc, T., Lebert, A., Loison, O., Portanguen, S., Gatellier, P., Parafita, E., & Mirade, P.S. Is there any relationship between proteolysis, structure and texture during the manufacture of dry-cured ham? *Food Chemistry*, submitted, November 2013 (**article n°4**).
- 4 – Harkouss, R., Chevarin, C., Daudin, J.D., & Mirade, P.S. Building a 3D “numerical ham” that simulates and couples water and salt transfers to proteolysis during the dry-cured ham process. Application to the modelling of the salting and post-salting stages of process. *Food and Bioprocess Technology*, paper under preparation (**article n°5**).
- 5 – Harkouss, R., Gatellier, P., & Mirade P.S. Effect of drying and salting on the time course of proteolysis and sensory properties in dry-cured ham. Can sodium be reduced during dry-cured ham manufacture? *Food and Bioprocess Technology*, review under preparation (**article n°1**).

---

**Communications à des congrès et colloques**

---

- 1 – Harkouss, R., Safa, H., Mirade, P.S., & Gatellier, P. (2012). A new method and index for quantifying proteolysis intensity in dry-cured ham. In *58<sup>th</sup> International Congress of Meat Science and Technology*, Montreal, Canada, 12-17 August 2012 (**4 pages + oral**).
- 2 – Harkouss, R., Safa, H., Gatellier, P., Lebert, A., & Mirade, P.S. (2012). Evolution of proteolysis in pork muscles as a function of temperature and water and sodium chloride contents. In *14<sup>èmes</sup> Journées des Sciences du Muscle et Technologies des Viandes*, Caen, France, 13-14 Novembre 2012 (**2 pages + oral**).
- 3 – Harkouss, R., Safa, H., Latour, A., Mirade, P.S., & Gatellier, P. (2012). Effect of temperature, salt and water content on the proteolysis activity in small laboratory pork meat samples. In *2012 European Federation of Food Science and Technology (EFFoST) Annual Meeting*, Montpellier, France, 20-23 November 2012 (**2 pages + oral**).
- 4 – Harkouss, R., Chevarin, C., Gatellier, P., Lebert, A., Daudin, J.D., & Mirade, P.S. (2013). Towards building of a “numerical ham” for simulating proteolysis and salt and water transfers during the dry-cured ham elaboration process. In *59<sup>th</sup> International Congress of Meat Science and Technology*, Izmir, Turkey, 18-24 August 2013 (**4 pages + oral**).
- 5 – Harkouss, R., Safa, H., Gatellier, P., Lebert, A., & Mirade, P.S. (2013). Phenomenological models relating proteolytic evolution of small pork meat samples to temperature and water and salt contents. In *59<sup>th</sup> International Congress of Meat Science and Technology*, Izmir, Turkey, 18-24 August 2013 (**4 pages + poster**).
- 6 – Harkouss, R., Chevarin, C., Gatellier, P., Lebert, A., Daudin, J.D., & Mirade, P.S. (2013). Time-course evolution of protein degradation velocity in pork meat samples: integration in a model simulating dry-cured ham manufacture. In *14<sup>ème</sup> Congrès de la Société Française de Génie des Procédés*, Lyon, France, 8-10 Octobre 2013 (**8 pages + oral**).





**Titre**

**Effet du salage et du séchage sur la dynamique d'évolution de la protéolyse, de la structure et de la texture lors de la fabrication d'un jambon sec. Développement d'un modèle de « jambon numérique » couplant transferts d'eau, de sel et protéolyse.**

**Résumé**

Du fait de problèmes de santé publique, l'industrie agroalimentaire doit réduire la quantité de sel (chlorure de sodium) dans les aliments, et donc dans les charcuteries. Lors de la fabrication des jambons secs, une diminution du taux de sel pourrait se traduire par des problèmes de texture dus à une protéolyse excessive pouvant nuire à l'étape de tranchage industriel, et aussi par des problèmes de stabilité microbiologique. Dans ce contexte, les objectifs de cette thèse sont : (1) d'étudier le lien entre l'évolution de la protéolyse, de la texture et de la structure, tout au long des différentes étapes de fabrication de jambons secs et (2) de développer un modèle de « jambon numérique » afin de prédire spatialement les dynamiques d'évolution des teneurs en eau, en sel et celle de l'activité de l'eau ( $a_w$ ), et de coupler ces évolutions à celle de la protéolyse.

Ce travail combine études expérimentales et modélisation/simulation numérique. Tout d'abord, une méthode de quantification de la protéolyse utilisant la « Fluorescamine » a été développée et validée sur des échantillons de viande de porc et des échantillons extraits de jambons industriels ; un nouvel indice de protéolyse (IP) a été défini. Sur la base d'un plan d'expériences, l'évolution de la protéolyse au sein d'échantillons différemment salés et séchés et préparés à partir de 5 muscles différents d'un jambon de porc, a été quantifiée. Suite à l'application d'une régression linéaire multiple, des lois phénoménologiques ont été construites permettant de calculer la vitesse de protéolyse, pour un muscle donné, en fonction de la température et des teneurs en eau et en sel. Ensuite, au moyen du logiciel Comsol® Multiphysics, ces lois ont été combinées avec des modèles de transferts de matière (eau, sel), de chaleur (température), et de calcul de l' $a_w$ , constituant ainsi un modèle de « jambon numérique ». Enfin, la dynamique d'évolution de l'IP, de 5 paramètres texturaux (dureté, fragilité, cohésion, élasticité et adhésion) et de 4 paramètres structuraux (nombre des fibres, espaces extracellulaires, taille des fibres et surface de tissu conjonctif) a été mesurée sur des échantillons prélevés dans deux muscles extraits de jambons industriels pris à cinq stades de fabrication différents. L'application d'une régression polynômiale multiple à ces données expérimentales a conduit à l'établissement de corrélations permettant de calculer certains paramètres texturaux et structuraux à partir de l'IP et des teneurs en eau et en sel. A court terme, ces lois seront incorporées dans le modèle numérique afin de constituer un vrai simulateur de procédé. A moyen terme, le modèle de « jambon numérique » devra être amélioré afin de tenir compte (1) de la diminution du volume du jambon, du fait du séchage et (2) de la diminution de la vitesse de protéolyse en fonction du temps, du fait de la réduction de la quantité de protéines hydrolysables dans le jambon. Une fois complété et amélioré, le simulateur de procédé pourra aider les professionnels à tester des scénarios visant à réduire la quantité de sodium dans les jambons secs, sans altérer leur qualité finale.

**Mots clés :** jambon sec ; séchage ; salage ; protéolyse ; structure ; texture ; fluorescamine ; plan d'expériences ; loi phénoménologique ; modélisation ; jambon numérique ; simulateur de procédé.



**Title**

**Effect of salting and drying on the time course of proteolysis, structure and texture during the dry-cured ham elaboration process. Building of a “numerical ham” model that couples water and salt transfers to proteolysis.**

**Abstract**

Because of public health problems, the food industry must lower sodium content in all food products, therefore in cured meat products. During the dry-cured ham elaboration process, decreasing salt content may induce microbial safety problems and texture defects due to an excessive proteolysis that could affect later the industrial stage of slicing. On account of that, this work of thesis aims at (1) studying the relationship between proteolysis, structure and texture during the various stages of dry-cured ham manufacture, and (2) building a “numerical ham” model to predict spatially the time course of water and salt content, and thus water activity ( $a_w$ ), and to couple these variations with proteolysis.

This work combines experimental studies and numerical modelling and simulation. Firstly, a new and powerful technique for quantifying proteolysis that uses “Fluorescamine” was developed and validated on pork meat samples and samples extracted from industrial dry-cured hams; a new proteolysis index (PI) was defined. Based on an experimental design, the time course of proteolysis was quantified in laboratory-salted and dried pork meat samples prepared from five different types of pork muscle. Applying multiple linear regression enabled us to build phenomenological models relating, for each pork muscle, PI velocity to temperature, and to water and salt content. Using Comsol<sup>®</sup> Multiphysics software, these phenomenological models were then combined with heat and mass transfer models and associated with calculation of  $a_w$ , thus constituting the “numerical ham” model. In addition, the time course of PI, five textural parameters (hardness, fragility, cohesiveness, springiness and adhesiveness), and four structural parameters (fiber number, extracellular spaces, cross section area, and connective tissue area) was quantified on samples extracted from two different muscles of industrial dry-cured hams removed from the process at five different processing times. Multiple polynomial regression was applied to build phenomenological models relating PI, salt and water content to some textural and structural parameters investigated. These last models could be rapidly incorporated in the “numerical ham” model to constitute a real process simulator. In the future, the “numerical ham” model should be improved in order to take into account (1) the strong decrease in ham volume due to drying and also (2) the decrease in proteolysis velocity with time as a result of the reduction in the amount of protein that can be hydrolysed in the ham. Once completed and improved, the process simulator will be available to professionals to test scenarios allowing sodium content to be reduced in dry-cured hams without altering their final quality.

**Keywords:** dry-cured ham; drying; salting; proteolysis; structure; texture; fluorescamine; experimental design; phenomenological model; modelling; numerical ham; process simulator.



« *Remercier les gens est aussi une autre façon de remercier Dieu* ». Pourtant, il est difficile de savoir par qui ou par où commencer, vu le nombre de personnes qui m'ont aidé à aboutir à cet instant. Je m'excuse, à l'avance, auprès de toutes les personnes que je n'aurai pas nominativement mentionnées, mais qui auraient contribué au développement de ma personne, et aussi de façon significative, à l'avancement de cette thèse durant ces trois dernières années.

Je tiens, tout d'abord, à exprimer mes plus vives reconnaissances à l'encontre de Monsieur **Pierre-Sylvain MIRADE**, qui m'a soutenu tout au long de ce travail, et à la direction avisée, fidèle et exigeante qu'il a eue et à laquelle cette thèse doit beaucoup. Mes sincères remerciements vont aussi à mes encadrants, Messieurs **Philippe GATELLIER** et **Thierry ASTRUC**, pour leurs conseils judicieux, tout au long de la préparation de cette thèse. Je remercie également, Monsieur **Alain KONDJAYAN**, le directeur de l'unité **QuaPA**, et Monsieur **André LEBERT**, Professeur à l'Université Blaise Pascal, le responsable du projet ANR « Na<sup>+</sup> », pour leur aide et leur soutien durant ces trois années de recherche enrichissantes.

Je remercie Madame **Cécile BERRI**, Directrice de Recherches à l'INRA de Nouzilly, ainsi que Monsieur **Philippe BOHUON**, Professeur à Montpellier SupAgro, d'avoir accepté la lourde charge de rapporter mon travail de thèse. Je leur exprime toute ma reconnaissance pour l'intérêt qu'ils ont porté à ce travail. À Monsieur **Guy DELLA VALLE**, Ingénieur de Recherches au sein de l'Unité BIA de l'INRA de Nantes, et Monsieur **Thierry ASTRUC**, Ingénieur de Recherches au sein de l'unité QuaPA, l'un de mes encadrants, j'exprime ma profonde gratitude pour avoir accepté de juger ma thèse en tant qu'examineur. Que Monsieur **Claude-Gilles DUSSAP**, Professeur et responsable de l'axe Génie des Procédés, Energétique et Biosystèmes au sein de l'UMR Institut Pascal de Clermont-Ferrand, soit remercié pour avoir représenté l'Université Blaise Pascal et l'Ecole Doctorale Sciences Pour l'Ingénieur dans mon jury de thèse.

Je remercie aussi les membres de mon comité de thèse : Madame **Véronique Santé-Lhoutellier**, Madame **Marie-Noëlle Maillard**, Monsieur **Pascal Garry**, Monsieur **Laurent Picgirard**, Monsieur **Guy Della Valle**, et Monsieur **André Lebert** pour les conseils précieux qu'ils ont pu et su me donner lors des réunions constructives que nous avons eues.

Que l'Agence Nationale de la Recherche soit également remerciée pour le financement de ma bourse de thèse. Un merci du fond du cœur aussi à L'Association Islamique pour la Spécialisation et les Conseils Scientifiques, pour leur soutien spirituel et financier, tout au long de mes années d'études supérieures en France.

J'adresse aussi mes remerciements à Monsieur **Jean-Dominique DAUDIN** pour tous ses conseils et ses remarques pertinentes en matière de modélisation. Je remercie toute l'équipe Imagerie et Transferts de l'Unité QuaPA, sans exception ; un merci spécial à **Stéphane Portanguen** pour sa

## Remerciements

---

créativité dans les montages expérimentaux, également à **Raphaël Favier** pour son aide durant certaines de mes manipulations, ainsi qu'à **Olivier Loison** et **Annie Vénien** pour m'avoir initié à la microscopie. Un merci « numérique » à **Cyril CHEVARIN** pour tout ce qu'il a fait pour la partie simulation, merci également à **Aurélien LATOUR** pour son aide technique. Un grand Merci à l'équipe **Biochimie et Protéines du Muscle** de QuaPA et à sa responsable Madame **Véronique Santé-Lhoutellier**, pour m'avoir accueilli, et aussi, à **Laurent Aubry** et **Claude Ferreira** pour leur aide technique et leur gentillesse. Je remercie également l'ADIV et spécialement Madame **Emilie Parafita** pour m'avoir permis d'utiliser certains de leurs équipements.

Au cours de ces trois années, j'ai eu l'occasion de rencontrer beaucoup de doctorants et de stagiaires, ce qui a permis de maintenir une très bonne ambiance, à chaque instant. J'adresse de profonds remerciements aux stagiaires qui ont participé à mon projet de thèse, d'abord **Hassan**, pour sa patience et toutes les heures biochimiques qu'il a réalisées, et **Riziki**, pour avoir analysé certaines images de structure et pour sa gentillesse. Un salut à **Laure, Aurélie, Juliana, Daa, Caroline(s), Anne, Marwa, Lina, Julien** et **Malek**. Je remercie également le service informatique, notamment **Jean-Michel Auberger** pour sa disponibilité, ainsi qu'**Eliane Bachelard, Françoise Lassalas, Valérie Guesneau** et **Sophie Poitevin** pour leurs soutiens administratifs et comptables. Finalement, merci à tout le personnel de l'unité **QuaPA** pour l'ambiance générale et leur accueil chaleureux.

Merci à tous les professeurs que j'ai eus depuis mes débuts à l'école jusqu'à ce jour ; sans eux, ce travail n'aurait jamais pu être accompli.

Je remercie du fond du cœur toute ma famille pour leur amour, leur aide, leur patience et leur soutien, tout le long de ma vie. Mes efforts leur sont dédiés.

*A mon père, mon arc en ciel.  
A ma mère, mon espoir immortel.  
A mon frère, mon ange Gabriel.  
A ma sœur, mon sourire exceptionnel.  
Ma vie est une fleur, tu en es le miel,  
Toi Rola, mon amour éternel !*

*A toi, le guide attendu, toute ma reconnaissance...*

## **LISTE des FIGURES et TABLEAUX**

---





## Liste des figures

### Chapitre 1 : Revue bibliographique

- Figure 1.1:** Schematic description of some dry-cured ham elaboration processes in Spain, France and Italy. (article n°1) ..... p 27
- Figure 1.2:** Two dimensional gel electrophoresis maps of a myofibrillar protein fraction from a dry-cured ham at 6 months of process and from Parma and San Daniele dry-cured hams at 12 months of process. Each Parma or San Daniele dry-cured ham is represented by two different maps: (a) MLC - Myosin light chain, and (b): MHC - Myosin heavy chain (from Luccia et al. 2005). (article n°1) ..... p 31
- Figure 1.3:** Example of results obtained after a Texture Profile Analysis test on a dry-cured ham sample. (article n°1) ..... p 38
- Figure 1.4:** Example of salt and water contents and  $a_w$  distribution diagrams of a representative standard-salted (SS) and salted-reduced (SR) ham obtained at different scanning times during the elaboration process (from Santos-Garcés et al. 2012). (article n°1) ..... p 43

### Chapitre 2 : Matériels et méthodes

- Figure 2.1 :** Protocole expérimental de conditionnement des petits échantillons de muscles de porc préparés au laboratoire. .... p 47
- Figure 2.2 :** (a) Positionnement de la coupe transversale d'épaisseur 3 cm prélevée dans chacun des jambons de Bayonne sélectionnés ; (b) Positionnement des prélèvements des échantillons pour les différentes mesures texturales, structurales et biochimiques. .... p 49
- Figure 2.3 :** Protocole expérimental de dosage de l'indice de protéolyse par la nouvelle procédure basée sur la fluorescence mise au point au laboratoire. .... p 52
- Figure 2.4 :** (a) Exemple d'image originale acquise, suite à la coloration HES ; (b) Image binaire des espaces extracellulaires ; (c) Image avec couleur aléatoire permettant d'identifier les fibres musculaires. .... p 55
- Figure 2.5 :** Photographie de l'appareil de chromatographie ionique du laboratoire utilisé pour le dosage des ions chlorure ou sodium. .... p 58

**Figure 2.6 :** Illustration de la création des masques 2D (en vert) à partir des images tomographiques (en gris) d'un jambon acquises au moyen d'un tomographe à rayons X.

..... p 62

**Figure 2.7 :** (a) Vue extérieure de la géométrie 3D de jambon construite et (b) Vue en transparence du maillage volumique et des différents groupes de muscles créés dans la géométrie de jambon. .... p 63

**Figure 2.8 :** Visualisation de la trame grasse existant dans un jambon entre les muscles SM et BF. .... p 67

**Figure 2.9 :** Vue extérieure de la géométrie de jambon et détail des conditions limites appliquées. .... p 68

**Figure 2.10:** Calibration curve of glycine with fluorescamine. Glycine concentrations were those of the initial stock solutions before the TCA treatment. Values were the means  $\pm$  SEM of four independent determinations. (article n°2) ..... p 73

**Figure 2.11:** Proteolysis kinetics in *M. biceps femoris* at 25°C under different processing conditions. Values were the means  $\pm$  SEM of four independent determinations. At the end of ageing, values not bearing common superscripts differed significantly ( $p < 0.001$ ). (article n°2) ..... p 75

**Figure 2.12:** Proteolysis kinetics in three muscles of different Bayonne dry-cured hams. The zero time values corresponded to PI in the unsalted raw meats. Values were the means  $\pm$  SEM of 24 determinations. Values not bearing common superscripts differed significantly ( $p < 0.05$ ). (article n°2) ..... p 76

**Figure 2.13:** Relation between the classic proteolysis index (nitrogen index) and the new proteolysis index (fluorescamine index). (article n°2) ..... p 78

### **Chapitre 3 : Résultats et discussion**

**Figure 3.1:** Experimental protocol for laboratory preparation of the pork meat samples used in this study to determine proteolysis rates. (article n°3) ..... p 87

**Figure 3.2a:** Time course of proteolysis index at 3 °C for muscle BF as a function of various salt and water contents, and corresponding to some of the experiments listed in Table 3.1. (article n°3) ..... p 90

<b>Figure 3.2b:</b> Time course of proteolysis index at 13 °C for muscle SM as a function of various salt and water contents, and corresponding to some of the experiments listed in Table 3.1. <b>(article n°3)</b> .....	<b>p 92</b>
<b>Figure 3.2c:</b> Time course of proteolysis index at 24 °C for muscle ST, as a function of various salt and water contents, and corresponding to some of the experiments listed in Table 3.1. <b>(article n°3)</b> .....	<b>p 93</b>
<b>Figure 3.3:</b> Response surface plot of the combined effect of temperature and water content on the proteolysis rate in an ST pork muscle, at 4% sodium chloride content (% dry matter). <b>(article n°3)</b> .....	<b>p 95</b>
<b>Figure 3.4:</b> View of the location where the samples were extracted from the dry-cured hams: (a) general view and (b) view of the cross sectional area cut performed on each dry-cured ham. <b>(article n°4)</b> .....	<b>p 102</b>
<b>Figure 3.5 :</b> Example of typical result obtained after a texture profile analysis (TPA) test performed on a dry-cured ham sample. <b>(article n°4)</b> .....	<b>p 105</b>
<b>Figure 3.6:</b> Time course of proteolysis index (PI) measured on two muscles (biceps femoris and semimembranosus) of different Bayonne dry-cured hams. Values were the means +/- SEM of six independent determinations. Significance: *** $p < 0.001$ , ** $p < 0.01$ , * $p < 0.05$ , NS $p \geq 0.05$ . <b>(article n°4)</b> .....	<b>p 107</b>
<b>Figure 3.7:</b> Time course of lipid oxidation measured on two muscles (biceps femoris and semimembranosus) of different Bayonne dry-cured hams: (a) TBARS values; values were the means +/- SEM of three independent determinations; Significance: *** $p < 0.001$ , ** $p < 0.01$ , * $p < 0.05$ , NS $p \geq 0.05$ , and (b) relation between the proteolysis index and TBARS values for the first 21 weeks of dry-cured ham manufacture. <b>(article n°4)</b> .....	<b>p 109</b>
<b>Figure 3.8:</b> Time course of three structural parameters investigated in this study on two muscles (biceps femoris and semimembranosus) of different Bayonne dry-cured hams: (a) cross sectional fiber area, (b) extracellular space surface area, and (c) fiber numbers. Values not bearing common superscripts for each muscle differed significantly ( $p < 0.05$ ). <b>(article n°4)</b> .....	<b>p 111</b>
<b>Figure 3.9:</b> Views of (a) the 3D ham geometry and its dimensions built using Mimics® software and (b) the volumetric tetrahedral mesh with the different groups of muscle inside the ham imported into Comsol® Multiphysics software. <b>(article n°5)</b> .....	<b>p 121</b>

**Figure 3.10:** External view of the ham geometry and details of the boundary conditions applied in the “numerical ham” model. **(article n°5)** ..... p 125

**Figure 3.11:** Distribution of PI, salt and water contents predicted by the “numerical ham” model during the salting stage, at mid-salting (after one week of process) and at the end of salting (after two weeks). **(article n°5)** ..... p 127

**Figure 3.12:** Distribution of PI, salt and water contents predicted by the “numerical ham” model during the post-salting stage, at mid-period (after six weeks of process) and at the end of post-salting (after eleven weeks). **(article n°5)** ..... p 128

**Figure 3.13:** Time course of profiles of salt content predicted by the “numerical ham” model during the salting and post-salting stages and extracted on the location indicated in the upper part of this figure, on the right-hand side. **(article n°5)** ..... p 130

**Figure 3.14:** Time course of profiles of water content predicted by the “numerical ham” model during the salting and post-salting stages and extracted on the location indicated in the lower part of this figure, on the right-hand side. **(article n°5)** ..... p 131

**Figure 3.15:** Time course of mean values of salt content predicted by the “numerical ham” model during the salting and post-salting stages and calculated in the SM muscle, in the ‘BF + ST’ muscles and in the entire ham. **(article n°5)** ..... p 133

**Figure 3.16:** Time course of mean values of water content predicted by the “numerical ham” model during the salting and post-salting stages and calculated in the SM muscle, in the ‘BF + ST’ muscles and in the entire ham. **(article n°5)** ..... p 133

**Figure 3.17:** Time course of mean values of PI predicted by the “numerical ham” model during the salting and post-salting stages and calculated in the SM muscle, in the ‘BF + ST’ muscles and in the entire ham. **(article n°5)** ..... p 135

**Figure 3.18:** Time course of mean values of water activity predicted by the “numerical ham” model during the salting and post-salting stages and calculated in the SM muscle, in the ‘BF + ST’ muscles and in the entire ham. **(article n°5)** ..... p 135

**Figure 3.19:** Weight loss kinetic of the ham predicted by the “numerical ham” model during the salting and post-salting stages. **(article n°5)** ..... p 136

**Figure 3.20 :** Comparaison de mesures d’indice de protéolyse (IP) réalisées par 2 méthodes de dosage différentes (méthode classique de dosage de l’azote et méthode développée au laboratoire utilisant la fluorescamine) sur des échantillons prélevés sur 3 muscles (SM, BF et ST) de jambons de Bayonne sélectionnés à 3 stades de fabrication : fin de repos (11 semaines), fin de séchage (21 semaines) et fin d’affinage (12 mois). ..... p 140

- Figure 3.21 :** Dynamique d'évolution du pourcentage de teneur en sel mesurée par chromatographie ionique dans 2 muscles (*Semimembranosus* et *Rectus femoris*) de jambons de Bayonne et exprimé en : (a) kg sel.kg matière totale<sup>-1</sup>, (b) kg sel.kg matière sèche dessalée<sup>-1</sup> et (c) kg sel.kg eau<sup>-1</sup>. Chaque point de la figure correspond à la moyenne et à l'écart-type calculés à partir d'une mesure sur 3 échantillons. .... **p 143**
- Figure 3.22 :** Différentes vues d'une géométrie 3D de jambon avant salage (jambon « frais ») et en fin d'affinage (après 12 mois) indiquant les variations de volume ( $V_{viande}$ ), de surface (S) et d'épaisseur (Ep.). Cette géométrie a été construite avec le logiciel Mimics® à partir d'images de tomographie X. .... **p 145**
- Figure 3.23 :** Graphique type représentant la concentration en produit apparu [P] au cours du temps, lors d'une réaction chimique catalysée par une enzyme dite « michaélienne ». .... **p 147**

## Liste des tableaux

### Chapitre 1 : Revue bibliographique

**Table 1.1:** Information on dry-cured ham production process for each main ham production line in four countries. (article n°1) ..... p 27

**Table 1.2:** Potential activities of cathepsin **B** and **L** after each stage of Jinhua dry-cured ham process (from Zhao et al. 2005). (article n°1) ..... p 29

**Table 1.3:** Texture profile analysis (TPA) and stress relaxation (SR) data of several textural parameters measured on dry-cured hams at two different ages and salt contents (from Benedini et al. 2012). (article n°1) ..... p 38

**Table 1.4:** General information on methods of salting, on salt reduction and salt substitution, plus other details in the dry-cured ham elaboration process. (article n°1) ..... p 42

### Chapitre 2 : Matériels et méthodes

**Tableau 2.1 :** Détails du plan de Doehlert avec les 13 cinétiques de mesure de protéolyse à réaliser pour chaque muscle ; le centre (cinétique n°1) a été répété 2 fois. .... p 51

**Table 2.2:** Characteristics of the Bayonne dry-cured hams at the end of each main processing stage. Water and NaCl contents were calculated on the basis of dry matter. Values were the means +/- SEM of three determinations (one determination per muscle). Values not bearing common superscripts differed significantly ( $p < 0.05$ ). (article n°2) ..... p 72

### Chapitre 3 : Résultats et discussion

**Table 3.1:** Details of the Doehlert design built and results of proteolysis rate obtained as a function of pork muscle type (SM: semimembranosus, BF: biceps femoris, ST: semitendinosus, RF: rectus femoris and GM: gluteus medius). (article n°3) ..... p 89

**Table 3.2 :** Details of multiple linear regression coefficients calculated from experimentally-quantified proteolysis rates for five different pork muscles, plus another one combining muscles SM, BF, ST and RF.  $T$  represents the temperature (°C),  $S$  the salt content (% dry matter) and  $W$  the water content (% total matter). (article n°3) ..... p 94

**Table 3.3:** Calculation of proteolysis indices (PIs) and their variation as a function of temperature, water and salt contents during each main stage of the dry-cured ham production process using the phenomenological models built in this study, for three different pork muscles (SM: semimembranosus, BF: biceps femoris, and RF: rectus femoris). **(article n°3)**  
 ..... p 97

**Table 3.4:** Time course of the five textural parameters investigated (hardness, fragility, cohesiveness, springiness and adhesiveness) on two muscles (biceps femoris and semimembranosus) of different Bayonne dry-cured hams. Values were the means +/- SEM of two independent determinations. **(article n°4)** ..... p 112

**Table 3.5:** Details of multiple polynomial regression coefficients calculated from experimentally quantified textural and structural parameters, for BF and SM pork muscles. PI represents the proteolysis index (%), T the temperature (°C), S the salt content (% dry matter) and W the water content (% total matter). **(article n°4)** ..... p 114





## **SOMMAIRE GENERAL**

---



**AVANT-PROPOS**

Liste des communications .....	p 1
Résumé .....	p 3
Abstract .....	p 5
Remerciements .....	p 7
Liste des figures .....	p 9
Liste des tableaux .....	p 14

**SOMMAIRE GENERAL** ..... p 17**INTRODUCTION GENERALE** ..... p 19**Chapitre 1 : REVUE BIBLIOGRAPHIQUE**

1.1. Introduction .....	p 23
1.2. Article n°1 (projet à soumettre à Food and Bioprocess Technology) .....	p 24
1.3. Conclusions bibliographiques .....	p 45

**Chapitre 2 : MATERIELS et METHODES**

2.1. Préparation des échantillons et plan d'expériences (articles n°2, 3 et 4) .....	p 47
2.1.1. Protocole expérimental de préparation des petits échantillons au laboratoire (article n°3) .....	p 47
2.1.2. Préparation des échantillons issus de jambons de Bayonne (articles n°2 et 4) .....	p 48
2.1.3. Plan d'expériences de type surface de réponse / Doehlert (article n°3) .....	p 50
2.2. Mesures biochimiques .....	p 51
2.2.1. Dosage de l'indice de protéolyse par fluorescence (article n°2) .....	p 51
2.2.2. Dosage de l'oxydation des lipides (article n°4) .....	p 53
2.3. Analyses structurales (article n°4) .....	p 54
2.3.1. Protocole expérimental (article n°4) .....	p 54
2.3.2. Quantification de la morphologie par analyse d'images (article n°4) .....	p 54
2.3.3. Seuillage sur les niveaux de gris et calcul des propriétés structurales .....	p 55
2.4. Analyses texturales (article n°4) .....	p 56
2.5. Mesures physico-chimiques (articles n°2, 3 et 4) .....	p 57
2.5.1. Teneur en sel (articles n°2, 3 et 4) .....	p 57

2.5.1.1. Le chloruromètre (articles n°2 et 3) .....	p 57
2.5.1.2. La chromatographie ionique (article n°4) .....	p 58
2.5.2. Teneur en eau (articles n°2, 3 et 4) .....	p 59
2.5.3. pH (articles n°2, 3 et 4) .....	p 59
<b>2.6. Analyses statistiques .....</b>	<b>p 59</b>
2.6.1. Régression linéaire (ou polynomiale) multiple (articles n°3 et 4) .....	p 60
2.6.2. Analyse de variance (articles n°2, 3 et 4) .....	p 60
<b>2.7. Modélisation multi-physique (article n°5) .....</b>	<b>p 61</b>
2.7.1. Construction géométrique et maillage volumique (article n°5) .....	p 62
2.7.2. Implémentation des différents modèles (article n°5) .....	p 63
2.7.2.1. Modèle de protéolyse (article n°5) .....	p 63
2.7.2.2. Modèle de transfert de chaleur (article n°5) .....	p 64
2.7.2.3. Modèle de transfert de matière (article n°5) .....	p 65
<b>2.8. Article n°2 (publié dans Meat Science 92, 2012, 84-88) .....</b>	<b>p 69</b>
<b>2.9. Conclusions .....</b>	<b>p 80</b>

### **Chapitre 3 : RESULTATS et DISCUSSION**

<b>3.1. Introduction .....</b>	<b>p 81</b>
<b>3.2. Article n°3 (publié dans Food Chemistry 151, 2014, 7-14) .....</b>	<b>p 82</b>
<b>3.3. Article n°4 (soumis à Food Chemistry en Novembre 2013) .....</b>	<b>p 99</b>
<b>3.4. Article n°5 (projet à soumettre à Food and Bioprocess Technology) .....</b>	<b>p 117</b>
<b>3.5. Discussion .....</b>	<b>p 138</b>
3.5.1. Nouvelle méthode de mesure de l'indice de protéolyse .....	p 138
3.5.2. Comparaison de la dynamique d'évolution de la protéolyse mesurée dans des échantillons préparés au laboratoire et extraits de jambons industriels .....	p 140
3.5.3. Modèle de « jambon numérique » .....	p 141
3.5.3.1. Variation de volume .....	p 141
3.5.3.2. Dynamique d'évolution de la protéolyse prédite par le modèle ..	p 145
<b>3.6. Conclusions partielles .....</b>	<b>p 149</b>

### **CONCLUSION GENERALE et PERSPECTIVES** ..... **p 151** |

### **REFERENCES BIBLIOGRAPHIQUES** ..... **p 157** |

Annexe I : Harkouss, Mirade & Gatellier (2012). *Meat Science*, 92, 84–88.

Annexe II : Harkouss, Safa, Gatellier, Lebert & Mirade (2014). *Food Chemistry*, 151, 7-14.

## **INTRODUCTION GENERALE**

---



La fabrication du jambon sec repose sur un procédé de conservation combinant salage et séchage, et requiert une durée totale généralement comprise entre 5 et 12 mois, parfois plus dans le cas de certaines productions. Les qualités organoleptiques finales du produit obtenu dépendent de la qualité de la matière première (teneur et composition de la matière grasse, poids, pH), mais aussi du bon déroulement de l'ensemble des étapes technologiques suivies, *i.e.* par ordre chronologique : salage, repos, étuvage, séchage-maturation et affinage. Dans les pays méditerranéens, le processus de salage est réalisé à sec, soit par enfouissement total des jambons dans le sel (chlorure de sodium), soit par apport en surface d'une quantité de sel limitée, proportionnelle au poids du jambon. Suite à la phase de salage réalisée à basse température (2 à 4°C) qui dure généralement 2 semaines, une phase de repos, aussi réalisée à basse température (température inférieure à 5°C), est mise en place pendant 8 à 10 semaines environ dans le but de conduire à une distribution du sel la plus homogène possible à l'intérieur du jambon, ainsi qu'à une légère déshydratation en surface et donc d'éviter la prolifération de micro-organismes d'altération indésirables par l'effet barrière créé, du fait de l'abaissement de l'activité de l'eau ( $a_w$ ) (Leistner, 1985). A ces 2 phases conduites à basse température, succède, parfois, une phase d'étuvage à température élevée (environ 23°C), d'une durée d'une semaine, dont le but est d'intensifier la déshydratation de la surface du produit, tout en amplifiant les phénomènes biochimiques de protéolyse (dégradation des protéines suite à leur hydrolyse par action enzymatique) et de lipolyse (dégradation de la matière grasse suite à une hydrolyse par action enzymatique), à l'origine de la saveur du produit. L'ensemble de ces phénomènes (déshydratation, protéolyse, lipolyse, génération d'arômes) se poursuit lors des phases de séchage-maturation et d'affinage qui durent de nombreux mois et qui sont conduites à des températures intermédiaires, généralement comprises entre 13 et 18°C environ.

Dans l'alimentation humaine, le chlorure de sodium est un élément indispensable au bon fonctionnement du corps humain : il aide à la régulation de la pression sanguine, contribue à la transmission de l'influx nerveux et joue un rôle dans l'activité musculaire, notamment cardiaque. Toutefois, d'un point de vue nutritionnel, la consommation de jambon sec et de charcuteries, en général, doit être modérée du fait d'une teneur en sel et en sodium très élevée. Par exemple, la teneur en sel d'un jambon espagnol de type Serrano, exprimée par rapport à la matière sèche, est comprise entre 8 et 15%, à la fin de la phase de séchage/maturation (Costa-Corredor *et al.*, 2009). Or, certaines études scientifiques ont montré qu'une consommation excessive de sodium dans l'alimentation humaine favorisait l'hypertension artérielle et accroissait le risque de maladies cardiovasculaires, d'ostéoporose

(AFSSA, 2002 ; He and Macgregor, 2009 ; Heaney, 2006), de cancers gastriques (Nazario *et al.*, 1993) et de maladies rénales (Mc Mahon et al., 2012). Dans ce contexte, l'Académie Nationale des Sciences, aux Etats-Unis, et l'AFSSA (Agence Française de Sécurité Sanitaire des Aliments), en France, ont recommandé que la consommation journalière de chlorure de sodium n'excède pas 6 g, ce qui implique de réduire la consommation courante d'environ 30 à 50%, dans des pays comme les Etats-Unis, l'Irlande et la France (Desmond, 2006 ; AFSSA, 2008). Dans la plupart des pays Européens et Nord-Américains, les organisations en charge de la santé humaine ont toutes incité, ces dernières années, les industriels de l'agro-alimentaire à réduire la teneur en sel des produits manufacturés. Par exemple, en France, dès 2002, l'AFSSA a préconisé de réduire la teneur en sel des produits alimentaires de 20%, en 5 ans. Or, malgré les efforts engagés par les différentes filières de l'industrie agro-alimentaire, celles-ci n'ont que partiellement atteint la réduction visée de 20%. Par exemple, entre 1993 et 2007, la baisse de la teneur médiane en sel n'a été que d'environ 5,6% pour le jambon sec, en France (données IFIP). La raison principale, dans le cas spécifique du jambon sec, outre des problèmes de stabilité et de sécurité microbiologiques éventuels, est qu'une réduction trop importante du taux de sel lors de la fabrication entraîne des problèmes de texture (produit trop mou), rendant difficile, voire impossible, l'étape finale de tranchage industriel à haute cadence.

Dans ce contexte, le projet « Na<sup>-1</sup> », initié et coordonné par André Lebert (Université Blaise Pascal (UBP) de Clermont-Ferrand) et porté par l'unité QuaPA, a été bâti et financé par l'Agence Nationale de la Recherche (ANR) sur la période 2010-2013. Ce projet associe 6 partenaires : l'unité QuaPA, l'Institut de la Filière Porcine (IFIP), l'Association pour le Développement de l'Institut de la Viande (ADIV), le Laboratoire de Génie Chimique et Biochimique (LGCB) de l'UBP, l'AFSSA et la Fédération française des Industriels Charcutiers, Traiteurs et transformateurs de viandes (FICT), qui est le représentant des professionnels du secteur des charcuteries. L'objectif du projet « Na<sup>-</sup> » est de développer des connaissances sur les phénomènes physiques (transferts de matière, de chaleur...) et biologiques (évolutions biochimique, structurale, texturale, microbiologique...) qui ont lieu dans la viande de porc lors des procédés de fabrication de pièces crues et séchées (cas du jambon sec), mais aussi cuites (cas du jambon cuit), de coupler l'ensemble de ces connaissances afin de développer des outils de simulation (des « simulateurs ») pour aider les professionnels dans leur quête de réduction du taux de sel et de sodium. Ces simulateurs ont

---

<sup>1</sup> Site internet : <http://www.na-project.eu/>



pour vocation de conduire à une conception raisonnée de produits de charcuterie allégés en sodium, tout en contribuant au maintien de leurs qualités sanitaires et organoleptiques.

Ce travail de thèse, financé par le projet « Na<sup>-</sup> », a trait à la partie « jambon sec ». Il a pour cadre général la conception de nouveaux produits par de nouveaux procédés. Cette conception rend indispensable le développement d'outils basés sur des approches de modélisation et de simulation numérique visant à décrire, puis à coupler, en fonction du temps et de l'espace, l'ensemble des phénomènes physiques et biologiques se produisant tout au long de la fabrication d'un jambon sec : transferts de chaleur et de matière (eau, sel), évolutions biochimiques (protéolyse, lipolyse), évolution des propriétés structurales, texturales et microbiologiques du produit.

Ce travail de recherche, qui est présenté sous la forme de 5 publications scientifiques, combine des approches expérimentales et numériques qui sont décrites au cours de trois grands chapitres.

En premier lieu, une revue bibliographique, écrite sous la forme d'un article scientifique, présente et détaille plusieurs aspects inhérents à l'élaboration des jambons secs : le procédé de fabrication, le rôle du sel et du séchage, les phénomènes biochimiques, en particulier la protéolyse, ainsi que les propriétés sensorielles, notamment la texture, qui évoluent pendant toute la durée du procédé, et enfin des pistes potentielles permettant de réduire la teneur en sodium des jambons secs, sans altérer leurs qualités organoleptiques et sanitaires finales.

Le deuxième chapitre décrit les matériels et méthodes utilisés, mais aussi développés dans ce travail, pour quantifier les évolutions biochimiques (protéolyse, oxydation lipidique), les modifications de structure et de texture, et décrire les propriétés physicochimiques au cours de la fabrication d'un jambon sec. Le modèle de « jambon numérique » qui a été bâti avec le logiciel Comsol® Multiphysics, et qui couple phénomènes physiques de transferts (séchage, diffusion de sel, migration d'eau) et protéolyse est aussi présenté dans cette partie. Au cours de ce chapitre, un deuxième article est présenté ; il décrit et détaille la nouvelle procédure utilisant la technique de fluorescence, mise au point au laboratoire, pour quantifier rapidement, et avec peu de matière, l'intensité de la protéolyse dans des échantillons de jambon sec. Un nouvel indice de protéolyse (IP) a ainsi été défini.

Enfin, au cours du troisième et dernier chapitre, sont présentés et discutés les principaux résultats obtenus dans ce travail, principalement par l'intermédiaire de 3 nouveaux articles. En s'appuyant sur une approche « plan d'expériences de type surface de réponse associé à la régression linéaire multiple », le premier article (article n°3) a pour objectif de quantifier les

effets de la température, du séchage et du salage sur la dynamique d'évolution de la protéolyse dans des échantillons de viande de porc issus de 5 muscles différents et conditionnés en température, teneurs en eau et en sel. L'analyse statistique de l'ensemble des résultats expérimentaux obtenus a conduit à la construction de modèles phénoménologiques permettant de quantifier l'intensité de l'activité protéolytique en fonction de ces différents facteurs, durant les différentes étapes de la fabrication d'un jambon sec. Sur la base de travaux expérimentaux faits sur des échantillons prélevés sur 2 muscles différents extraits de vrais jambons secs, l'article suivant (article n°4) vise à répondre à la question suivante : existe-t-il des corrélations significatives entre les dynamiques d'évolution de la protéolyse, de la structure et de la texture au sein d'un jambon sec ? Enfin, la plupart des modèles phénoménologiques obtenus et présentés dans les 2 articles précédents, sont combinés dans le dernier article de ce chapitre (article n°5), avec les modèles physiques de transferts de chaleur et de masse, pour, au final, obtenir le modèle de « jambon numérique ». Ce modèle, résultat majeur de ce travail de thèse, constitue un simulateur permettant de prédire quantitativement, en 3 dimensions (3D), la dynamique d'évolution de l'état d'avancement de la protéolyse, de l'activité de l'eau ( $a_w$ ) et des concentrations en eau et en sel, à l'intérieur d'une géométrie réelle de jambon. Un focus particulier sur la période de fabrication qui se déroule à basse température (phase de salage suivi d'un repos) est réalisé dans cet article. La dernière partie de ce chapitre consiste en une discussion critique et objective des résultats majeurs de ce travail.

## **Chapitre 1 : REVUE BIBLIOGRAPHIQUE**

---



## 1.1. Introduction

Le jambon sec est considéré comme un produit typique, traditionnel et authentique par la plupart des consommateurs. La fabrication du jambon sec dépend de plusieurs facteurs : entre autres, du type génétique, des conditions d'élevage et d'abattage de l'animal, de la masse initiale du jambon frais, et aussi des différentes étapes subies par le jambon frais lors de sa transformation en jambon sec, qui confère au produit sa qualité finale. Cette qualité finale dépend de plusieurs phénomènes biochimiques (comme la protéolyse, la lipolyse) qui affectent la texture et la structure, tout au long de la transformation du produit.

Sur la base des informations précédentes, une étude approfondie de la protéolyse est indispensable et une meilleure maîtrise de sa dynamique d'évolution pourra être utile pour mieux contrôler la qualité finale du jambon sec. Ceci implique que la revue bibliographique traite de la protéolyse, en présentant, notamment, les enzymes protéolytiques responsables de la dégradation des protéines en acides aminés libres et peptides dans le muscle, à tous les stades de fabrication du jambon sec. L'action du salage et du séchage sur l'activité de ces enzymes, et donc sur la protéolyse, mérite également d'être précisée.

Afin de compléter la discussion, un point bibliographique relatif à la texture du jambon sec est fait, en essayant de comprendre le lien entre la protéolyse et la texture du produit. Dans cette partie, plusieurs techniques de mesure, classiquement utilisées pour caractériser la texture du jambon sec, sont présentées, et quelques corrélations obtenues dans la littérature sont décrites, permettant de relier certaines propriétés physiques ou biochimiques (teneur en eau, protéolyse) à certains paramètres texturaux, comme la cohésion.

Ensuite, comme le jambon sec est un produit salé, l'étude bibliographique se devait de faire le point sur le rôle particulier du sel lors de la fabrication des jambons secs, ainsi que sur les leviers technologiques (réduction directe ou substitution partielle du chlorure de sodium) à la disposition des professionnels, permettant de réduire la quantité finale de sodium dans le produit. Cette partie a été étendue à la présentation de quelques travaux établissant des modèles pour décrire la diffusion du sel dans la viande. La dernière partie de cette revue fait le point sur les outils de mesures et de calculs existants, permettant d'estimer la teneur en sel, tout au long de la fabrication des jambons secs.

Il convient, enfin, de préciser que la partie biochimie de la revue bibliographique consacrée à la protéolyse, a été précédée d'une partie générale ayant pour but d'éclaircir plusieurs points traités dans la suite de la revue, tel le procédé de la fabrication des jambons

secs. Pour cela, les étapes essentielles de ce procédé ont été détaillées, *i.e.* le salage, le repos, l'étuvage, le séchage et l'affinage.

En résumé, la revue bibliographique qui a été faite, et qui est présentée sous la forme d'un article scientifique, s'attache à faire un point précis sur le procédé d'élaboration du jambon sec, en faisant un focus sur la protéolyse, l'évolution des propriétés sensorielles, notamment la texture, et sur les leviers technologiques possibles pour réduire la teneur en sodium d'un jambon sec.

## 1.2. Article n°1 (projet à soumettre à Food and Bioprocess Technology)

### **Effect of drying and salting on the time course of proteolysis and sensory properties in dry-cured ham. Can sodium be reduced during dry-cured ham manufacture?**

Rami Harkouss<sup>a</sup>, Philippe Gatellier<sup>a</sup> and Pierre-Sylvain Mirade<sup>a</sup>

<sup>a</sup> INRA, UR370 Qualité des Produits Animaux, F-63122 Saint-Genès-Champanelle, France.

#### **Abstract**

Consumers consider dry-cured ham a typically authentic product. Dry-cured ham is a highly-salted food, as the production process relies on salt for the microbiological stabilization of the product and the development of its sensory properties. However, sodium intake is already excessive in developed countries. In this context, this review is focused on the dry-cured ham elaboration process, especially proteolysis, sensory properties, and options for reducing sodium content in dry-cured ham. Further research is needed to gain better knowledge of the texture-structure-proteolysis relationship in a sodium-reduced ham, and dedicated numerical models would appear to be the way forward.

#### **Introduction**

Dry-cured ham is an important traditional staple in many diets worldwide and is considered a typically authentic product by consumers throughout Europe. Spanish dry-cured ham is one of the most traditional cured meat products in the Mediterranean area, at over 40 million pieces produced per year and average consumption estimated at 4.5 kg per person per year (Cruz 2005). French dry-cured ham production has quietly progressed from 13,500 T in the 1970s to 47,700 T in 2011. Italy produced more than 160 kT of dry-cured hams per year, while Norway produces more than 1,870 T (Nielsen 2009), with Germany, Portugal and other

countries also posting significant output. From an economic standpoint, these statistics show how Southern European dry-cured ham production is important enough to rank as a driver of commerce in this area. In general, the majority of countries producing dry-cured ham follow roughly the same core process, with slight modifications in operational conditions depending on several factors: type of dry-cured ham, fresh ham weight, final quality aimed for by producers... The aim of the process is to stabilize the ham by decreasing water activity ( $a_w$ ) and to facilitate the development of its sensory characteristics (flavor, texture, color...), essentially via salt penetration into muscles in conjunction with progressive dehydration.

Dietary salt is important for regulation of blood pressure, water transport into/out of cells, tissue osmolality and transmission of nerve cell impulses. In developed countries, most estimates put average salt consumption at 6-8 g per person per day, whereas 2 g per day for a 60 kg person is physiologically sufficient. This excessive sodium intake is thought to cause hypertension linked to risk of stroke and cardiovascular disease, as well as increasing calcium excretion which can lead to osteoporosis (Karppanen and Mervaala 2006; Lawes et al. 2006). Consequently, there are a number of research projects investigating ways to reduce salt content in the food industry to obtain healthier products. In the dry-cured ham industry, salt is a multifunctional ingredient that affects both quality and safety. Note that dry-cured ham salt content generally ranges from 5 to 7% of total mass, but can reach 15% (expressed on dry basis) at the end of ripening in Spanish Serrano dry-cured ham (Costa-Corredor et al. 2009).

This paper set out to review the dry-cured ham production process, giving special focus to how sodium content can be reduced in this food product. With this objective in mind, we start with a general overview of the dry-cured ham process before zooming in on enzymes and their activities at the origin of proteolysis, one of the key biochemical phenomena occurring during the process and shaping the texture of the product. We then move on to discuss the most important sensory properties of dry-cured hams, i.e. appearance, color and texture. The crucial salting step is then described, followed by analysis of the technological solutions for cutting sodium content in dry-cured hams, before rounding off with a discussion.

### **Overview of the dry-cured ham process**

There are various well-known dry-cured hams worldwide (USA, France, Spain, Italy, China...). American Country dry-cured ham is salty due to long curing, and sometimes contains pepper. Some smoked with a variety of hardwoods are usually aged 5–9 months. French Bayonne dry-cured ham is an air-dried, salted ham normally aged 10–12 months. It has been awarded EU Protected Geographical Indication (PGI) status and represents about

20% of national ham production. It is characterized by a homogeneous pink color, tender texture and slightly salted taste. Spain boasts two famous dry-cured hams: Iberian and Serrano. Iberian dry-cured ham is made essentially from black-footed Iberian pigs. The hams are aged for at least 18 months and develop a characteristic special flavor due to their high intramuscular fat (IMF) levels. Serrano dry-cured ham, protected under the EU Traditional Specialities Guaranteed scheme, is made from white pigs, typically a Landrace or Large white cross-breed fed a mixture of quality grains. It is aged 7–15 months, and the flavor is sweet with just a hint of saltiness. Parma, a popular Italian dry-cured ham obtained from heavy pigs, is gently salted and long-aged, at least 12 months. Salt is the only additive permitted, although pepper is sometimes added to the head of the femur or the fat used to cover the ham (Parolari 1996). Finally, Chinese Jinhua dry-cured ham is known for its characteristic flavor character, pink meat color, golden yellow skin and pure white fat (Zhou and Zhao 2007).

There are several steps in the dry-curing ham process: ham selection, salting, post-salting, any pre-ripening applied, and drying/ripening. pH value is a critical factor for ham selection (5.5–6.2). Then, based on weight, the hams are split into two categories: small hams weighing an average 8 kg and big hams weighing an average 12 kg. During the salting step, hams are exposed to curing agents (salts) to ensure safe development in the following stages. Generally, there are two salting procedures: (a) hams are completely covered by salt during a salting time ranging from 1–1.5 day per kg of raw meat, or (b) “limited salt input” on the muscle part without salting the rind; this method can be done in one step (60–75 g salt per kg of ham) or two successive steps (22–58 g salt per kg of ham at each step). It takes 11–21 days depending on the amount of salt rubbed into the muscle given the initial ham weight. In both methods, hams are placed in a cold room (1–3°C at 80–90% RH), during which salt starts to diffuse from outside and penetrates into the first few centimeters depth. After that comes the post-salting stage that aims to distribute salt into the inner zones of the ham so as to obtain the minimum salt concentration needed to stabilize the product in the next stages. Salted hams are kept at 2–5°C to avoid microbiological hazard at 70–80% RH for 60–80 days depending on salting method. Hernandez-Cazares et al. (2011) showed that from as early as the initial salting and post-salting stages, nucleotide degradation starts to generate several compounds, which affects meat flavor and contributes to umami taste. Finally, the ripening stage usually takes a minimum of 6 (excluding American dry-cured ham) to a maximum of 16 months, during which the temperature is increased (13–16°C) and RH is decreased (60–70%) compared to the salting/post-salting stages. Hams lose water during this stage, with the result that  $a_w$  also decreases to some extent, so the hams become stable at room temperature. This



allows biochemical mechanisms to take place, such as proteolysis and lipolysis which are responsible for sensory characteristics and the production of flavor compounds. There is also an optional pre-ripening stage directly after post-salting where temperature is increased to 22–24°C for 7–10 days to accelerate biochemical evolution during ripening. At the end of the process, estimates put weight loss of dry-cured ham at 25–35% and salt concentration at 5–7% of total mass (Andres et al. 2005; Antequera et al. 2007). Figure 1.1 and Table 1.1 summarize how dry-cured hams are produced in the different countries.

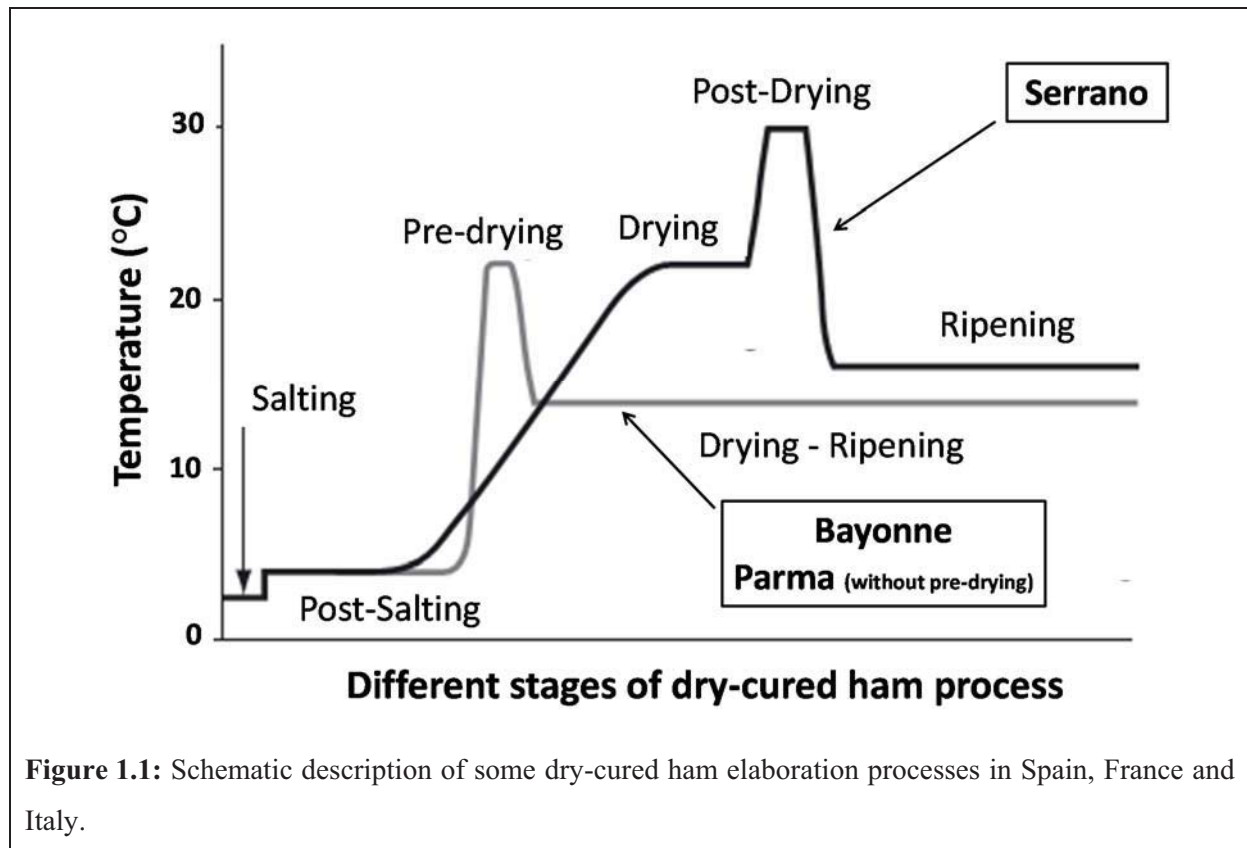


**Figure 1.1:** Schematic description of some dry-cured ham elaboration processes in Spain, France and Italy.

This brief general overview already highlights how obtaining a final product with high quality hinges on controlling and finding the right trade-off between all the above-stated factors. Knowing that several factors can simultaneously affect different aspects that shape final product quality (e.g. water content affecting proteolysis, flavor, texture), the paper now turns to give detailed discussion of each of these aspects, such as biochemical evolution (enzymes and proteolysis) and sensory properties (texture, flavor) during dry-curing ham processing.

**Table 1.1:** Information on dry-cured ham production process for each main ham production line in four countries.

Stages of dry-cured ham process	In Spain (main production: 'Serrano')	In France (main production: 'Bayonne')	In Italy (main production: 'Parma')	In the USA
Raw material	with hip bone and V-shaped rind trimming	without hip bone (coxal bone) and with rind		
Salting	1 day per kg raw meat T = 1 – 3°C RH > 75%	1 – 1.5 day / kg T = 2 – 4°C RH = 85 – 95%	3 – 4 weeks T = 1.5 – 4.5°C RH = 70 – 90%	≈ 3 weeks (3 rubbings)
Post-salting		T < 5°C RH = 70 – 80% 1.5 – 2.5 months		Resting Washing Smoking (≈ 24 h)
Washing	At the end of salting	At the end of post-salting ≈ 1 week	No	
Pre-drying	No	RH = 60 – 75% 8h 24h 48h 14°C 24°C 20° C	No	No
Drying	T = 10 – 34°C 3 – 4 months RH = 60 – 80%	T = 13 – 16°C 2 – 3 months RH = 65 – 75%	T = 12 – 16°C 7 – 14 months RH = 60 – 80%	T ≈ 18°C 3 – 6 months RH = 55 – 65%
Ripening	T = 12 – 20°C RH = 50 – 80% 7 – 9 months	T = 16 – 18°C RH ≈ 70% 3 – 4 months		

T: Air Temperature; RH: Air Relative Humidity

### Biochemical evolution of dry-cured ham throughout the process: focus on proteolysis

Dry-cured ham is a great source of proteins and free amino acids. It contains all the essential amino acids needed by humans. In developed countries, basic amino acid needs are generally properly provided by diet. Nevertheless, some populations, like elderly or seriously ill people, can present significant deficiencies in amino acids due to altered assimilation of proteins. These populations have higher essential amino acid requirements to curb the process of degenerative loss of skeletal muscle mass and strength (Jiménez-Colmenero et al. 2010). Many of these free amino acids come from proteolysis, which is a central biochemical reaction in dry-cured ham processing. This section first discusses the role of enzymes responsible for this biochemical phenomenon as well as some of the process factors influencing their activity that leads to protein degradation and thus affects final dry-cured ham quality. Proteolysis during dry-cured ham processing facilitates the complete degradation of proteins and the bioaccessibility of amino acids once ingested and digested by humans.

Proteolysis generally refers to endogenous enzyme activity (Cordero and Zumalacarregui 2000). The main endopeptidases responsible for muscle protein degradation are cathepsins,

followed by calpains and to some extent exopeptidases (aminopeptidases) and cytosolic enzymes (Luccia et al. 2005). According to Hortos et al. (1994), the most active enzymes are cathepsin B, L, H and D. Cathepsin B is responsible for the degradation of low-molecular-weight proteins to free amino acids as well as myofibrillar proteins like actin and myosin (Parreño et al. 1994; Toldra et al. 1997), which could be a good argument for studies showing that fresh hams with higher cathepsin B activity were more proteolysed. Zhao et al. (2005) studied the effect of several factors on cathepsin B and L in Jinhua ham and showed that temperature had a strong influence on these enzymes, especially at low pH values. They did not find any obvious effect of pH on cathepsin B activity at <10 °C, and increasing pH value weakened the temperature effect on cathepsin L activity. There is strong evidence that salt also greatly affects proteolytic enzyme activity. Gandolfi et al. (2011) studied the influence of several porcine gene polymorphisms to relate them with enzyme activity in muscle and meat quality, and concluded that the CAST gene affected post-mortem activation time of calpain. Sarraga et al. (1993) observed that calpains lost their activity after salting. These results were in line with Zhao et al. (2005) who highlighted that salting led to constant decrease in potential activities of cathepsin B and L mid-process down to 83.35% and 86.16%, by the end of salting stage of original potential activity of cathepsin B and L, respectively, and to only 9.31% and 13.66%, by the end of the process where salt content became higher (Table 1.2), thus confirming the inhibitory role of salt.

**Table 1.2:** Potential activities of cathepsin **B** and **L** after each stage of Jinhua dry-cured ham process (from Zhao et al. 2005).

<b>Time</b>		<b>Cathepsin B activity</b>		<b>Cathepsin L activity</b>	
<i>Stage</i>	<i>day</i>	<i>M ± S.E. (U/g)</i>	<i>Remains (%)</i>	<i>M ± S.E. (U/g)</i>	<i>Remains (%)</i>
<i>Prior-salting</i>	1	11332 ± 717	<b>100</b>	9955 ± 468	<b>100</b>
<i>End of salting</i>	31	9444 ± 1167	<b>83.35</b>	8577 ± 916	<b>86.16</b>
<i>End of loft-ageing</i>	203	1988 ± 459	<b>17.55</b>	2281 ± 365	<b>22.92</b>
<i>End of post-ageing</i>	264	1055 ± 138	<b>9.31</b>	1359 ± 212	<b>13.66</b>

However, the duration of mid-process enzyme activity differs between studies: cathepsins B, L and H kept persistent activities when dry-curing ham – with cathepsin B remaining active

up to 15 months – while calpains and cathepsin D were restricted to the first few months of the process. Therefore, controlling the action of these factors – temperature, salt, duration – on proteolytic enzyme activity enables safe and normal proteolysis during dry-cured ham processing.

Deeper investigation into protein degradation profiles gives a better understanding of proteolysis rates to optimize texture. The key proteins involved can be collapsed into 3 groups: (a) myofibrillar proteins (55–60% of total protein) such as myosin and actin that are soluble at high ionic strengths, (b) sarcoplasmic proteins (30%) such as myoglobin that are soluble at low ionic strengths and in water, and (c) connective tissue proteins (5–10%) such as collagen that are insoluble. Studies indicate that soluble proteins are more degraded than insoluble proteins (Larrea et al. 2006; Rodriguez-Nunez et al. 1995). Some studies report that the myofibrillar fraction is more proteolysed (Del Olmo et al. 2013) whereas others show that the sarcoplasmic fraction is more vulnerable (Mora et al. 2009). Most myofibrillar proteins are completely hydrolyzed after 12 months of dry-curing (Luccia et al. 2005), although myosin heavy chain fragments can still be found in some Parma and San Daniele dry-cured ham samples (Figure 1.2).

According to Monin et al. (1997), during the ripening stage the main modifications were detected in myosin heavy chain (MHC), myosin light chain and troponin C and I, by the formation of 50–100 and 14.4–45 kDa fragments. On the other hand, several studies showed that most free amino acids and small peptides were accumulated continuously during the process. Virgili et al. (2007) demonstrated that free amino acids content continued to rise even after 23 months of process in Italian *Biceps femoris* (BF) muscle, while Zhao et al. (2008) demonstrated that more than 90% of the NPN compounds coming from protein degradation were free amino acids and peptides of less than 1 kDa molecular weight. These results and others showed that the combination of these small fragments produces the characteristic taste and aroma of dry-cured hams (Buscailhon et al. 1994; Larrea et al. 2006; Sentandreu et al. 2003; Sforza et al. 2001). Hence, it is vital to track protein hydrolysis to free amino acids and peptides during the process, since this biochemical phenomenon plays a huge role in both nutritional and sensory quality.

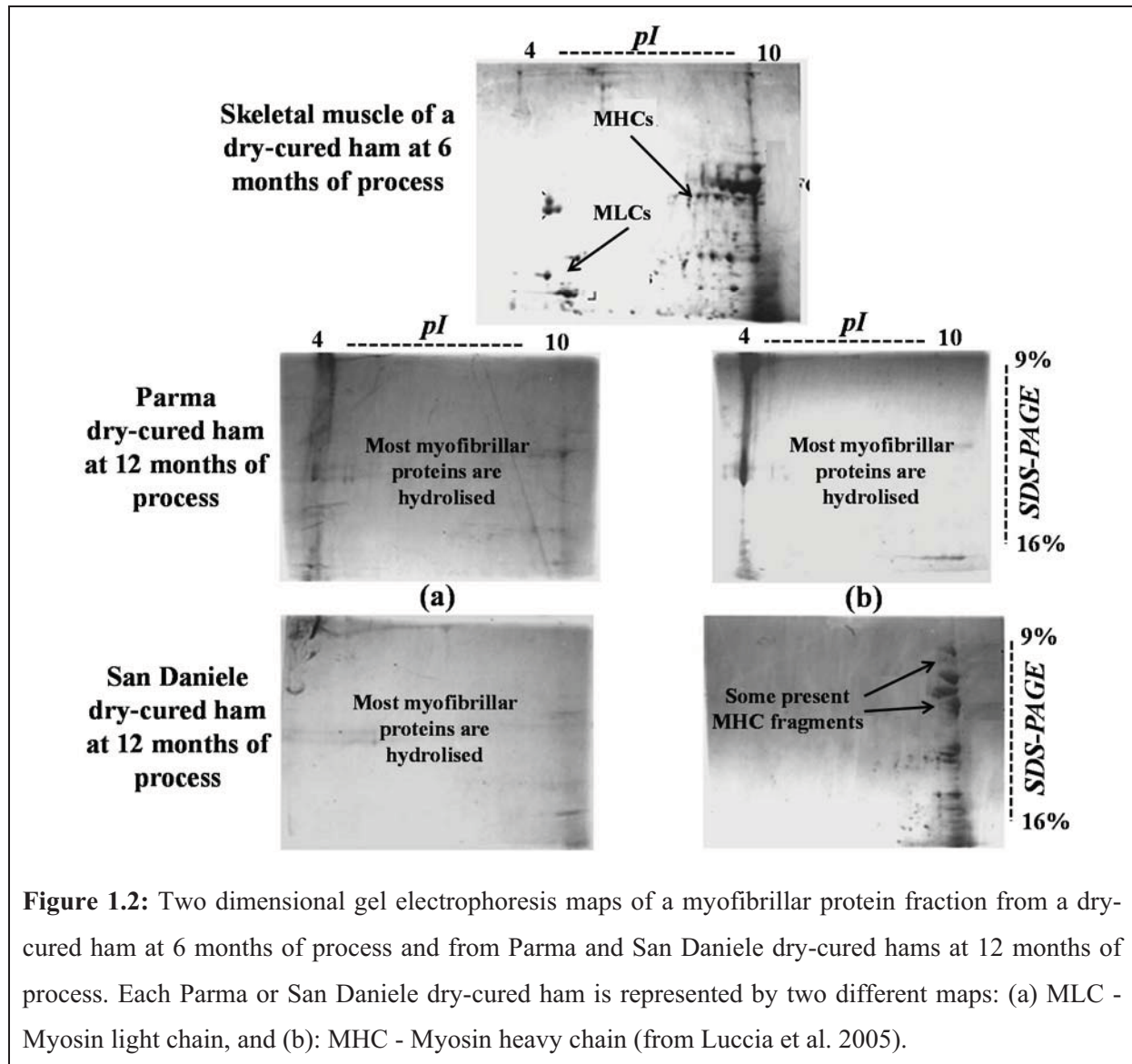


**Figure 1.2:** Two dimensional gel electrophoresis maps of a myofibrillar protein fraction from a dry-cured ham at 6 months of process and from Parma and San Daniele dry-cured hams at 12 months of process. Each Parma or San Daniele dry-cured ham is represented by two different maps: (a) MLC - Myosin light chain, and (b): MHC - Myosin heavy chain (from Luccia et al. 2005).

In dry-cured ham, proteolysis affects the final texture (hardness, cohesiveness...) of the product and is considered essential to obtain acceptable-quality taste and flavor characteristics (Arnau et al. 1998; García-Garrido et al. 2000; Toldra 1998; Zhao et al. 2008). Many authors have found that besides the proteolytic enzymes discussed above, proteolysis rate is also impacted by the convergence of pH and processing parameters such as salt concentration, water content, ageing temperature and time (Arnau et al. 2003; Pearson et al. 1983; Ruiz-Ramirez et al. 2006; Toldra et al. 1997). Andres et al. (2005) showed that temperature promotes lipase activities and lipid oxidation leading to the generation of volatile and non-volatile compounds responsible for flavor in dry-cured ham. Moreover, Sforza et al. (2001) showed that high temperature in the final ageing period played an important role in lowering ham dryness. Furthermore, geometrical location of muscles inside the ham – external as

*Semimembranosus* (SM) and internal as BF – also plays a key role in the time-course evolution of proteolysis due to various salt and water transfer behaviors in each muscle during curing and drying. In fact, during the initial stage of the drying process, BF has a lower salt content than SM (Barat et al. 2005) but a higher water content (Arnau et al. 1995), which ultimately leads to a higher proteolysis rate in BF than in SM (Garcia-Garrido et al. 2000). Research to date has focused solely on the influence of factors affecting proteolysis and sometimes their interactions, but without ever correlating proteolysis to these factors.

Experimental methods have been developed to estimate the level of proteolysis evolution. In dry-cured ham, proteolysis is classically quantified through a proteolysis index (PI) commonly defined as the percentage ratio of NPN content to total nitrogen content (TN) determined by the Kjeldahl method. This procedure is standardized (the reference method is ISO 937:1978) and widely used in industry. As a rule, PIs vary according to ham type and processing conditions. For example, after post-ripening, PI values in good-quality Italian and French dry-cured hams, at 22–30 and 12–32, respectively, were higher than PI values in Jinhua hams, at 14–20 (Zhao et al. 2008). The authors attributed these differences to different total processing times, i.e. 9–14 months for European dry-cured hams vs. 8–10 months for Jinhua hams, and to the loss of soluble nitrogen fraction during the Jinhua ham salting stage that caused lower PIs. In general, proteolysis activity should not exceed a specific level; otherwise, a huge amount of lipophilic amino acids and oligopeptides such as leucine and phenylalanine would be generated, leading to perception of unpleasant bitter taste in the final product. The literature reports a negative effect on the final product texture when PI exceeds 30, with samples recorded as having an excessively soft texture at a PI >35.

### **Sensory properties of dry-cured ham: appearance, flavor and texture**

Sensory properties of ham have been widely studied for several years and found to be forged through a complicated chain of chemical and biochemical reactions during processing. These characteristics are closely related to raw meat properties and processing conditions (Toldra et al. 1997; Virgili and Parolari 1991) and highly influence consumers (Skinner and Rao 1986). In general, sensory quality is evaluated by appearance, flavor and texture. The influence of ham genotype on final texture has been studied, and several authors have found that distinctions in ham structure and anatomy, IMF content and other characteristics according to genetic origin of the ham were related to textural differences observed in dry-cured hams (Gou et al. 1995; Guerrero et al. 1999). Recently, Santé-Lhoutellier et al. (2012) studied the effect of two polymorphisms (PRKAG3 and CAST) on the quality characteristics of French



Bayonne ham and showed a significant relationship between these polymorphisms and textural properties. Arnau et al. (1998) highlighted that textural problems such as pastiness, flavor as bitterness or appearance problems like pale color often turn into economic damage for producers. Thus, sensory aspects continue to be the focus of intensive research aiming to obtain a high final product trait, which is equally important for both producers and consumers. Color is considered the main parameter influencing appearance which is so important to consumer satisfaction. After slicing, color should exhibit the typical red of the cured product; a lack of color probably results from low content of nitrifying agent due to chemical reactions or low pH which increases the transformation of nitrite to nitric oxide. Consumers react negatively to pale color as an appearance defect, whereas the formation of white film or white spots is given less importance by butchers since it appears several days after slicing.

Appearance alone is not enough to evaluate the final quality of the product, and is always followed by another important aspect of sensory properties, i.e. flavor. In the last twenty years, advanced research has focused on flavor formation in dry-cured ham. Results show that flavor development is a very complex process and that almost all flavor compounds originate from enzymatic actions and/or chemical reactions such as lipid oxidation, Maillard reactions and Strecker degradations in muscle protein and fat (Antequera et al. 1992; Coutron-Gambotti and Gandemer 1999; Motilva et al. 1993; Sforza et al. 2001; Virgili et al. 1998). For these reasons, raw meat characteristics and processing factors are equally important drivers of flavor quality. Morales et al. (2008a) demonstrated that the key characteristics for consumers were salty taste and matured flavor. Sforza et al. (2001) also proved that bitterness in most proteolysed hams occurs as a result of a higher quantity of lipophilic amino acids and oligopeptides. Although color and taste are highly important to attain a very good final product quality, texture remains the major sensory characteristic to be tested.

Some producers of dry-cured hams including “Prosciutto di Parma” and “Jamon Serrano” have obtained certifications based on their texture properties, yet for consumers texture is an equally significant index (MAPA 2005). Texture can be qualified by various characteristics, the most important being pastiness and softness. Pastiness implies a lack of elasticity when pressing gently on the zone concerned, together with oily handling. It occurs mainly in BF muscle, where it is accompanied with a kind of bitterness and piquant flavor. Garcia-Garrido et al. (2000) reported that pasty ham texture can also occur with a metallic taste and less salty flavor. Parolari et al. (1994) gave evidence that pastiness was also affected by raw muscle material and the amount of salt diffused during the salting stage. Garcia-Rey et al. (2004b) related pasty texture to physicochemical properties, high NPN and moisture and observed that

color parameters were to somehow high, prompting them to conclude that pastiness could be a result of anomalous proteolysis. Softness happens when ham has not attained the predicted typical firmness and consistency and can be tested if slicing is deformed on slight pressing with a finger. Softness, like pastiness, is also related to raw material and process characteristics (Virgili and Schivazappa 2002). It is reportedly affected by high cathepsin activity (Virgili et al. 1995), processing temperature (Arnau et al. 1997) and high water content (Ruiz-Ramirez et al. 2006). Finally, Garcia-Rey et al. (2004b) concluded that softness might be a result of improper dehydration rather than abnormal proteolysis.

The pH value also seems to be a good predictor of meat quality and could affect the sensory properties of the final product. Most authors do not recommend using green hams with a pH above 6.2 or below 5.6 to prevent both microbial growth (Newton and Gill 1981) and texture-related problems (Gou et al. 2008). Guerrero et al. (1999) found that high pH values were related to softness of dry-cured ham due to the higher solubility of meat proteins. In contrast, Garcia-Rey et al. (2004a) and Ruiz-Ramirez et al. (2006) found that low pH values were related to softness as a result of higher non-protein nitrogen (NPN) and proteolytic activity, which Schivazappa et al. (2002) also found to be affected by pH and other factors such as NaCl content and temperature in meat products. Moreover, water-holding capacity increases when pH increases, thus affecting texture properties in dry-cured ham. On the other hand, Buscaillon et al. (1994) showed that in hams coming from different countries, a low pH did not have the same influence on texture. They found that French dry-cured ham had higher proteolysis and texture characteristics – high firmness and low mellowness – whereas Spanish dry-cured ham results showed the opposite pattern. Results reported by Buscaillon et al. (1994) suggest that pH alone is not a crucial factor for texture, and that it would be better to take other factors into account, since their interaction is highly important. Tabilo et al. (1999) stated that duration of the ripening stage should be adapted to the initial pH to obtain more uniform sensory quality. Similar results were obtained by Cilla et al. (2005), Ruiz et al. (1998) and Soresi-Bordini et al. (2004), who showed that extending the ripening stage leads to better taste and aroma properties and enhances muscle firmness.

Generally speaking, water content is related to sensory properties. Buscaillon et al. (1995) showed that reducing water content by dehydration allowed a durable aroma. Serra et al. (2005) found a negative non-linear relationship between moisture content and hardness. On the other hand, Ruiz-Carrascal et al. (2000) failed to find a significant relationship between water content and sensory textural characteristics (hardness, dryness and juiciness) in Iberian dry cured-ham. Tabilo et al. (1999) stated that hams from sows have lower hardness values



than hams from boars due to their higher moisture contents (57.4% vs. 53.2%), which is consistent with Ruiz-Ramirez et al. (2005) who reported that high moisture content leads to softer dry-cured hams. The fact that increasing water content decreases hardness in dry-cured ham appears logical.

Excessive pastiness and softness lead to a defective texture (Garcia-Rey et al. 2004b). In general, softness and pastiness have been associated with high temperature during the last month of ageing. Many studies tended to focus on the influence of low-moderate temperature treatment for many months on the quality of dry-cured ham (Cilla et al. 2006). Morales et al. (2008a) studied the effect of thermal treatment at 30°C for one week at the end of the drying stage and showed it decreased pastiness in BF without increasing hardness in SM muscle or affecting their physicochemical parameters (moisture,  $a_w$ , PI). Gou et al. (2008) also demonstrated that soft texture problems could be reduced by a 10-day ageing at 30°C without influencing the flavor of the product. Moreover, both studies proved that this thermal treatment had no effect on crusting formation, which is an excessive hardness affecting mainly superficial muscles. This texture defect occurs when water migration from inside the ham does not counterbalance the rapid dehydration at the surface (Serra et al. 2005). Texture defects usually make slicing more difficult and produce a mouth-coating sensation, and statistical studies done in Spain proved that texture problems (softness, pastiness and crusting) reduced consumers acceptability and were highly important factors for butchers. Morales et al. (2008b) declared that butchers were interested in processing time, smell/aroma and texture properties, whereas consumers were attracted by sensory indicators such as salty taste and aged/matured flavor. In fact, most texture problems in dry-cured hams could be related to a short processing time and low salt content. Given these statistics, studies should be more centered on processing factors – time, salt amount, temperature – combined with textural properties – hardness – and biochemical evolutions – proteolysis – to obtain a high-final-quality dry-cured ham. Thus, in order to better understand textural characteristics, hams have been classified into different groups. Garcia-Rey et al. (2004b) used four texture types: very pasty, pasty, soft and normal, each characterized by various properties. Normal hams contained less water than other types but also had a higher NaCl content than pasty and soft hams. NPN values were highest in pasty hams and lowest in soft hams. In addition, the authors found that pH could be a key property for very pasty hams, since pH was highest in this type-group.

Moving forward, studies show that texture can differ from muscle to muscle. Parolari et al. (1994) and Virgili et al. (1995) found that PI values are higher in BF than SM, with an effect

on texture, while Ruiz-Ramirez et al. (2005) showed that the lower water content in SM influenced product firmness. According to reports by Ruiz-Ramirez et al. (2006) and Serra et al. (2005), SM is the hardest muscle in dry-cured ham enabling crust development, while BF is more liable to show a high degree of soft and pasty texture.

Texture is generally found positively related to muscle dehydration; in fact, as a muscle dries, its consistency increases. However, Benedini et al. (2012) showed that even at the same moisture content, PI sometimes differed significantly, attributing this to the mechanism related to protein breakdown which leads to an alteration in texture properties. Tabilo et al. (1999) stated that the disappearance of 150 kDa and 85 kDa fragments would help get optimum texture in dry-cured ham, but Del Olmo et al. (2013) recently showed that the 150 kDa peak increased significantly as a result of MHC and sarcoplasmic degradation and aggregation. Either way, it is clear that protein degradation can affect texture, depending on the final fragments obtained. On the other hand, an ageing time higher than 20 months decreased moisture significantly while proteolysis remained the same, probably as a result of meat muscle shrinkage. These changes explain the loss of consistency found mid-processing and its subsequent complete recovery by the end of the process. The role of salt on texture has been also studied. Gou et al. (2008) showed that when NaCl content decreased, texture problems increased. NaCl inhibits proteolytic activity and influences the compression of myofibrillar proteins, thus explaining the higher hardness and lower adhesiveness and pastiness of hams at longer salting times. This important understanding of texture properties makes it possible to relate texture to other factors such as proteolysis or fatty acids and lipids. Proteolysis is thought to be the main biochemical mechanism responsible for progressive meat tenderization, where high proteolytic activity is considered the central cause of excessive softness and high pastiness in dry-cured ham texture (Careri et al. 1993; Cilla et al. 2005; Garcia-Garrido et al. 2000). Several studies demonstrated that when PI decreases, cohesiveness and springiness decrease too; in fact, high enzyme activity results in uncontrolled hydrolysis and a potential loss of protein structure that leads to product texture and color defects. Virgili et al. (1995) found a negative correlation between PI and hardness in Parma hams, in line with Ruiz-Ramirez et al. (2005) who demonstrated that hardness decreased when PI increased. Ruiz-Ramirez et al. (2005) found that dry-cured hams with lower PI were more able to form harder texture at the surface, and suggested that a high PI with low water content could be useful for reducing crust formation. Furthermore, Garcia-Garrido et al. (2000) showed how the residual enzyme activity of cathepsin B+L could be a good indicator to identify textural defects in ham due to strong proteolysis during curing,

which means efforts should be made to minimize the effect of cathepsin B+L on proteolysis during the ham curing process. According to Parolari et al. (1994), using raw hams with a controlled enzyme activity, especially cathepsin B, would improve final product quality. Hence, proteolysis should be firmly controlled to get a desirable tenderness of meat and ensure consumer acceptability.

Moreover, texture is greatly related to fat and lipids content. Fat that acts as a flavor modifier or “salt destroyer” has attracted a fair amount of research in food and meat products (Phan et al. 2008; Ruusunen and Puolanne 2005). Many studies have tackled the influence of fat content and fatty acid on texture in dry-cured ham: Ruiz-Carrascal et al. (2000) observed that variations in fatty acid composition in different parts of Iberian hams were highly influenced by IMF, which positively influences some texture characteristics, such as oiliness and juiciness, but negatively influences others, such as dryness and hardness. However, Buscaillon et al. (1994) failed to find a relationship between texture and lipid fraction. In addition, fat oiliness and softness increased when PUFA and MUFA levels increased (St John et al. 1987; Warnants et al. 1996). Based on these insights, it is evidently necessary to be aware of all associations relating texture, proteolysis and fat together to assure final dry-cured hams of high quality.

The texture of dry-cured ham is determined using both sensorial and instrumental methods. Sensory testing is time- and resource-intensive and requires a lot of samples, so the preferred approach is to use instrumental methods. In general, texture profile analysis (TPA) and stress relaxation (SR) are the most popular tests for characterizing dry-cured ham texture. Morales et al. (2007a) showed that SR was better at differentiating soft and normal texture in BF and SM muscles. The SR test informs on the physical properties of food materials correlated with sensory characteristics such as hardness, softness and brittleness. The formula  $Y(t) = [F(t) - F_0]/F_0$  – where  $Y(t)$ : force decay at instant  $t$ ,  $F_0$ : initial force,  $F(t)$ : force at  $t$  [in general,  $Y$ (at 2s) and  $Y$ (at 90s) are calculated] – can be used to quantify textural characteristics. TPA is also good for evaluating the essential textural characteristics described in Figure 1.3, i.e. hardness (kg), cohesiveness (dimensionless), springiness (dimensionless), adhesiveness (g.s), and chewiness which is obtained by multiplying hardness, cohesiveness and springiness. In Figure 1.3, height  $H$  characterizes hardness,  $b/a$  ratio characterizes springiness,  $area2/area1$  ratio characterizes cohesiveness, and  $area3$  characterizes adhesiveness.

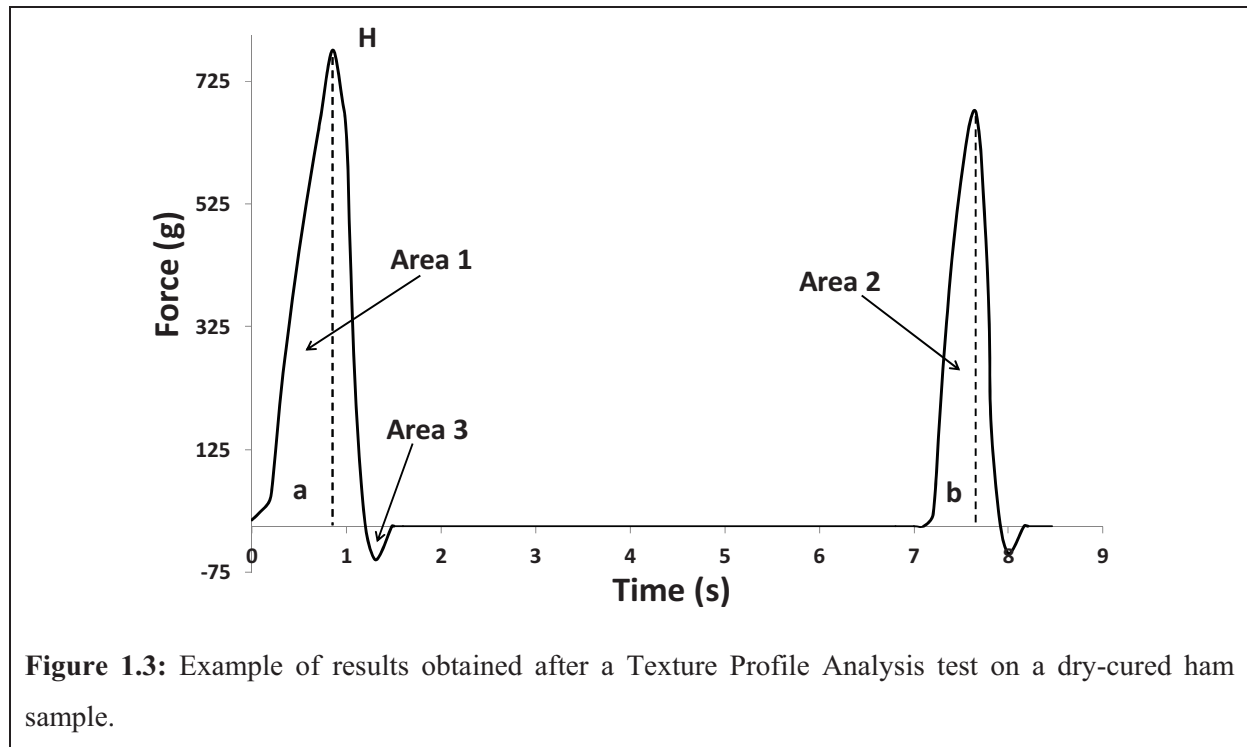


**Figure 1.3:** Example of results obtained after a Texture Profile Analysis test on a dry-cured ham sample.

Benedini et al. (2012) evaluated sensory characteristics using both methods. Using the TPA test, they observed that salting increased rigidity and stiffness, thus confirming previous results by Gou et al. (2008) and Ruiz-Ramirez et al. (2006). TPA and SR appeared to give globally similar evaluations and could both be used to describe texture (Table 1.3).

**Table 1.3:** Texture profile analysis (TPA) and stress relaxation (SR) data of several textural parameters measured on dry-cured hams at two different ages and salt contents (from Benedini et al. 2012).

<u>Texture Profile Analysis</u>	<u>Age of hams (months)</u>		<u>Salt content (%TM)</u>	
	<b>14 - 15</b>	<b>20 - 22</b>	<b>5.3 – 5.7</b>	<b>6.3 – 6.7</b>
Work	57.8	82.2	63.8	68.8
Springiness	0.72	0.68	0.72	0.66
Adhesiveness	1.36	1.22	1.41	0.95
<u>Stress Relaxation</u>				
Y <sub>2</sub>	0.37	0.36	0.39	0.36
Y <sub>90</sub>	0.68	0.67	0.69	0.65

However, Morales et al. (2007a) found that sample temperature during the test affects TPA measurements and so identified the best conditions for performing each of the two tests as a function of muscle type in dry-cured hams: the SR test – performed at 4°C and at 1 mm/s –

should be applied on BF muscle, while the TPA test – performed at 4°C and 20°C and at 10 mm/s – is preferable for SM muscle.

The TPA test was also used to relate texture to water content. Serra et al. (2005) established a negative non-linear relationship between hardness,  $a_w$  and water content, showing a dramatic increase in hardness below a water content threshold of  $X=0.55$  kg H<sub>2</sub>O/kg dry matter and  $a_w=0.7$ ; on the other hand, cohesiveness and springiness showed a positive relationship. Although these tests proved of huge utility, they are still destructive and time-consuming. Other viable techniques for estimating texture include Near Infra-Red Spectroscopy (NIRS). NIRS is a fast and effective, easy-to-use, non-destructive tool for meat quality assessment that also makes it possible to simultaneously determine several parameters such as fat content, moisture and protein content (Brøndum et al. 2000). Garcia-Rey et al. (2005) presented NIRS as a good tool for classifying dry-cured hams based on texture and color characteristics, with similar precision to expert sensory evaluation. Note that Ruiz-Ramirez et al. (2006) established different statistical models allowing hardness, cohesiveness and springiness to be assessed from water content and PI values. These kinds of models are very rare but could be introduced in future numerical models predicting water and salt transfers and proteolysis in order to also predict the final texture of dry-cured hams.

### **Salting, a crucial step in dry-cured ham production: focus on sodium reduction**

In dry-cured ham production, salt is a multifunctional ingredient that affects both quality and safety. First, salt acts as a barrier against pathogens and spoilage microorganisms (Rastelli et al. 2005; Taormina 2010). Curing salts and sodium chloride at specific pH and temperature obtain a redox potential and low  $a_w$  during drying that lead to an inhibitory effect on the microorganisms responsible for food spoilage. Second, salt contributes to water holding capacity, texture, color and flavor development (Arnau et al. 1998; Benedini et al. 2012). It has been shown that salt could influence the formation of tyrosine crystals in hams, i.e. a white film appearing on the surface in contact with air that modifies textural properties. Note too that NaCl is not the only factor responsible for saltiness: Careri et al. (1993) reported that glutamic acid and other compounds generated by proteolysis increased the salty taste of dry-cured hams. Several authors have studied the effect of salt on proteolytic enzymes – as detailed in the ‘biochemical section’ – proteolysis and lipolysis (Zanardi et al. 2004; Andres et al. 2005). These last years, efforts have been made to reduce the amount of salt in foods, with the target being products with 25% less salt (EC 2006; FDA 2008). In dry-cured hams, NaCl

reduction is mainly limited to two approaches: (a) direct reduction of NaCl content, mainly by reducing salting time or (b) partial substitution of NaCl by other salts (KCl, CaCl<sub>2</sub>, MgCl<sub>2</sub>...).

#### Direct reduction of NaCl content

Regarding the first approach, results show that longer post-salting times are needed for lower-sodium hams to reach the same  $a_w$  values as hams normally salted with 100% NaCl. Thus, manufacturers aiming to reduce sodium while conserving approximately the same final ham quality should extend the ham maturation stage. As an alternative solution, Grau et al. (2008) proved that freezing then thawing Iberian hams before the salting process yields hams with a lower salt content at the final stages; in fact, this procedure entails modifications in muscle structure that affect salt and water diffusion so that faster salt uptake reduces salting time. In addition, reducing ham thickness, using boned ham and trimming away subcutaneous and IMF would also help reduce salt concentration (Arnau et al. 2007; Marriott et al. 1987).

Although this first approach seems to be a good solution to reduce sodium content, limiting NaCl opens up risks in terms of microbiological stability and issues in terms of (1) reduction of salty flavor and aroma (Ventanas et al. 2010), (2) defective color and texture – Desmond (2006) showed that limiting salt tends to decrease fiber swelling, leading to poor texture – and (3) poor cohesiveness and sliceability as a result of abnormal softness occurring at high proteolysis rates (Ruiz-Ramirez et al. 2005). Given these issues, and based on the fact that increased potassium, magnesium and calcium intake may slightly decrease blood pressure (Geleijnse et al. 1994; Jee et al. 2002), there has been a surge in research on NaCl substitution by potassium chloride, calcium chloride, magnesium chloride and K-lactate in dry-cured ham, thus constituting the second approach that can be used.

#### Partial substitution of NaCl

From a processing point of view, salt mixtures with low-sodium content may imply several modifications in some stages, especially post-salting time at low temperature or during the ripening/drying period. Aliño et al. (2010) showed that hams salted with a combination of 50% NaCl and 50% KCl needed up to 16 days more post-salting time to reach similar  $a_w$  values to hams salted with 100% NaCl, while hams salted with a combination of 55% NaCl, 25% KCl, 15% CaCl<sub>2</sub> and 5% MgCl<sub>2</sub> needed up to 26 days more post-salting time. However, no differences in microbial counts were observed between these different formulations (Blesa et al. 2008). Looking at ripening stage, knowledge of the sorption isotherm is important to avoid crust formation; as substituting NaCl with KCl could affect sorption isotherms at the



product surface, it may also influence the drying kinetics of meat products. Comaposada et al. (2007) worked on lean surface of *Gluteus medius*-muscle dry-cured hams and highlighted that 35% of NaCl (in moles) could be substituted by KCl without change in sorption isotherm. Although KCl is one of additives most frequently proposed for NaCl substitution, its use is limited to a certain threshold (40%-50%) beyond which a bitter or astringent taste starts to emerge.

K-lactate also looks a good candidate to partially replace NaCl in dry-cured hams. It has been well studied, extensively evaluated, and described as effective at inhibiting most spoilage and pathogenic bacteria. Fulladosa et al. (2009) studied the effect of adding K-lactate to reduced-NaCl dry-cured ham and the use of boned ham as a strategy to speed up the salt distribution and drying process. They found that K-lactate could facilitate microbiological stabilization during the early process stages with no negative effect on physicochemical properties. Furthermore, they showed that restructuring hams with 50% NaCl + 36% substitution of NaCl by K-lactate (in moles) did not significantly influence texture, flavor or color. Costa-Corredor et al. (2009) showed that adding K-lactate did not modify chloride uptake and tended to reduce sodium uptake. They also observed that K-lactate significantly reduced the lightness ( $L^*$ ) of the product, which could be perceived as darker by consumers. Furthermore, as  $a_w$  should be kept over 0.7 to prevent crust formation, K-lactate looks to be a good protector against excessive hardening at the surface of dry-cured hams (Muñoz et al. 2009). So, besides KCl, K-lactate looks an effective NaCl alternative commonly used in meat and poultry products to extend shelf-life and increase food safety.

There are several strategies for partially replacing NaCl by other salts mentioned above, but all require perfect knowledge of their diffusion properties. In general, the diffusion coefficient of salt ( $D$ ) in meat depends on muscle type (Djelveh and Gros 1988), which differs by fat content (Fox 1980), connective tissue content (Hansen et al. 2008) and fiber orientation (Thorvadsson and Skjoldebrand 1996). Lautenschläger (1995) showed that pH could also affect  $D$  values, unlike Vestergaard et al. (2005) who failed to find any pH effect.  $D$  is also modified by salt ion concentration (Graiver et al. 2006) as well as processing temperature and the presence of other ions in salting brine.  $D$  values were significantly lower for lactate than other ions due to its higher molecular size. Potassium can pass through narrow pores more easily than sodium ion, especially in smaller channels (1.5 Å) (Marañón Di Leo and Marañón 2005), and its  $D$  value is higher than that of NaCl (Barat et al. 2011). It penetrated meat muscle more easily than other cations (calcium, magnesium), consequently decreasing salting time compared to NaCl (Blesa et al. 2008). Bearing this in mind, using salts that rapidly

diffuse inside hams would help greatly accelerate salt distribution, leading to a lower salting time and, ultimately, low-sodium dry-cured ham. Table 1.4 summarizes this section, giving more detailed information on ingredients of a normal salting mixture, on factors affecting the salt penetration and on some industrial salt substitutes used in the dry-cured ham process.

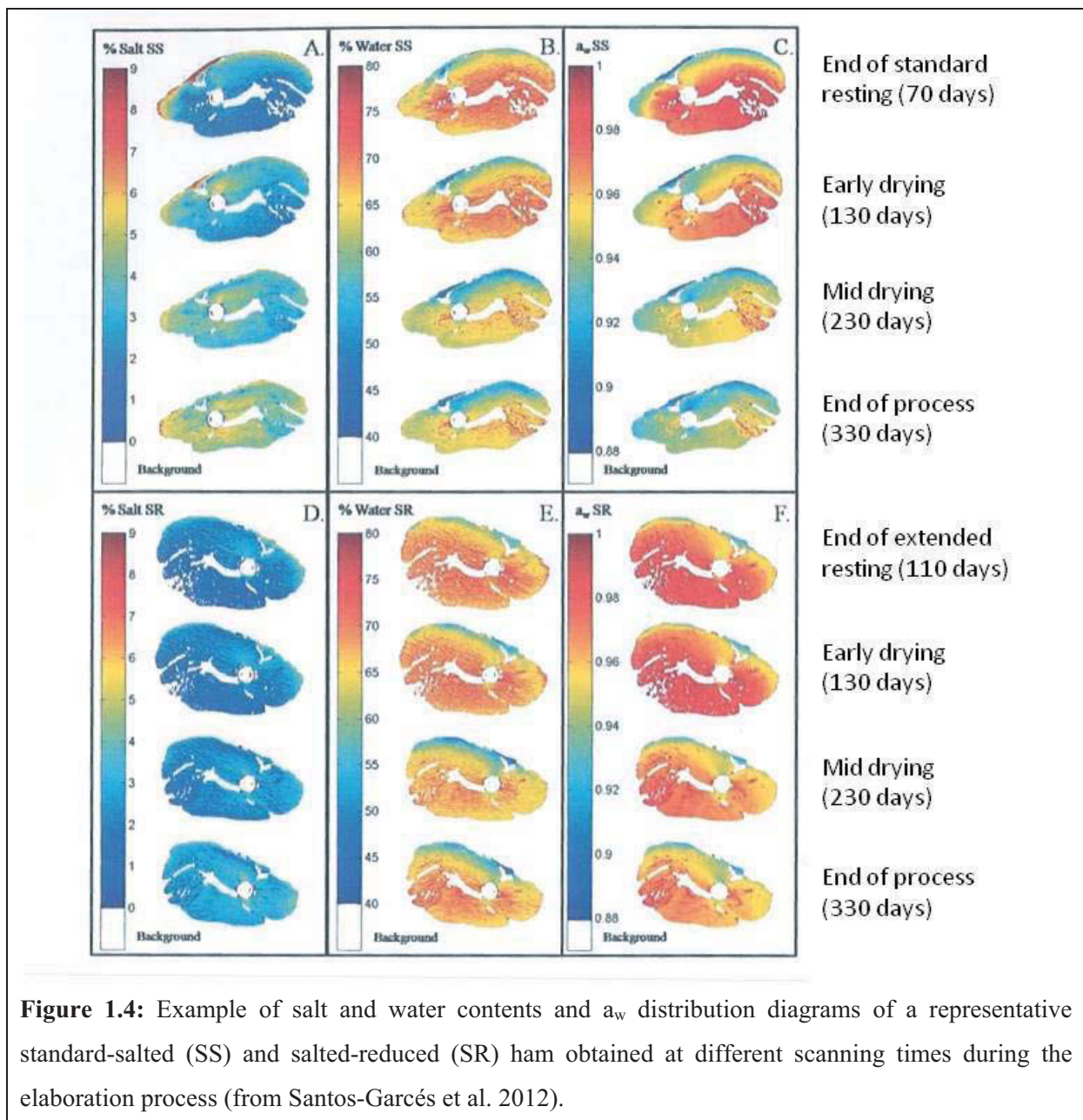
**Table 1.4:** General information on methods of salting, on salt reduction and salt substitution, plus other details in the dry-cured ham elaboration process.

<b><u>Dry-cured ham regulations</u></b>				
<b><u>Characteristics of ham</u></b>	Weight: 7.5 kg minimum		Trimming: Round or V shaped rind	
<b><u>Ingredients of salting mixture</u></b>	Salt, sugar (saccharose/dextrose), spices, wine, alcohol, aroma, potassium nitrate...			
<b><u>Methods of salting</u></b>				
<b><u>Complete cover with salt</u></b>	<u>In excess</u>	9-13 days	11-16 weeks (end of post-salting)	
	100-120 g of salt mixture	1j/kg of ham	11-12 weeks (end of post-salting)	
<b><u>Limited salt input</u></b>	<u>1 step</u>	40-75 g salt/kg ham	13-18 days	
(without nitrate)	<u>2 steps</u>	27-58 g salt/kg ham	11-21 days	7-10 weeks (end of post-salting)
<b><u>Some factors affecting salt penetration</u></b>				
Salt particle size	Salting method	Trimming	Freezing of fresh ham	Duration of salting
<b><u>Salt reduction</u></b>				
<b><u>Direct reduction of salt by:</u></b>	Reduction of salting time	Reduction of ham thickness	Freezing and thawing fresh ham	Using boned ham
<b><u>Drawbacks</u></b>	Reduction of salty flavor and aroma	Poor texture	Defective color	Poor sliceability
<b><u>Partial substitution of sodium by:</u></b>	Potassium	Potassium lactate	Magnesium	Calcium
<b><u>Drawbacks</u></b>	Increasing post-salting time	Could affect the drying kinetics	May involve the crust formation	
<b><u>Some industrial salt substitutes</u></b>				
<b><u>Ksalt®</u></b>	Organic salts of potassium		Salty taste without bitterness	
<b><u>Lite Salt® (USA)</u></b>	KCl	NaCl	Potassium iodide	Flavor approving
<b><u>Losalt® (Scotland)</u></b>	KCl (66%)	NaCl (30%)		Anti-agglomerating
<b><u>Pansalt® (Finland)</u></b>	NaCl (57%)	KCl (28%)	MgSO <sub>4</sub> (12%)	Silica Flavor approving (no bitterness)



## Discussion

Salting and drying are mass transfer processes that create water/salt distribution profiles that will change during the dry-cured ham production process. It is of great importance to know the time-course evolution and precisely quantify these two parameters to better understand their effects on the biochemical evolution and textural properties of the product. Traditional measurement techniques are time- and product-consuming. Non-destructive methodologies are now gaining currency in the meat industry. Nuclear Magnetic Resonance (NMR), Magnetic Resonance Imaging (MRI) and Computed Tomography (CT) are potential non-invasive techniques for estimating local salt and water values inside dry-cured ham. CT is a X-ray imaging technique that measures density in detailed cross-sectional images of a sample.



Using CT, tissues with various density can be separated and quantitative information can be obtained once CT images have been analyzed. Fulladosa et al. (2010) and Santos-Garcés et al. (2012) used CT to build salt and water content models in different stages of dry-curing hams (Figure 1.4) and concluded that CT is a suitable technology for characterizing and optimizing dry-cured ham salting processes. Haseth et al. (2012) also evaluated the ability of CT to predicting salt content in 26 Norwegian dry-cured hams at different processing times and studying salt distribution during the elaboration process. MRI also provides quantitative information on salt diffusion and moisture content, as shown by Fantazzini et al. (2009) in their study based on the analysis of NMR images of internal sections of Parma dry-cured ham at different processing stages. Although these analysis tools are not destructive, they have to be used many times throughout the dry-cured ham production process that lasts several months in order to periodically track water migration and salt diffusion patterns in the ham. Moreover, calibration models have to be established to evaluate salt and water contents from the X-ray images. For this objective, numerical modeling and simulation could be a good candidate to replace the experimental tools mentioned above, since it is non-invasive, non-destructive, and less expensive, and requires relatively little time to obtain the desired information. Indeed, using a multi-physical modeling approach, it is now possible to simulate dynamically how physical phenomena such as heat transfer, salt diffusion, and water migration occur inside a 3D geometry.

There is precious little published information on salt/water transfer models during salting, post-salting and ripening stages in dry-curing hams. Gou et al. (2004) determined effective moisture diffusivity coefficients in SM and BF muscles, but they built a simple diffusive model. Barat et al. (2011) described salt transfer using mathematical models and determined the NaCl and KCl diffusion coefficients on pork meat samples. We found only one study dealing with bacon pork meat in which Said et al. (2007) numerically simulated salt diffusion. On the other hand, there has not been a single study to model proteolysis evolution and its link with structure/texture during the ham production process. A specific model is sorely needed to allow proteolysis to be quantified as a function of muscle type, temperature, water and salt content. In dry-cured ham, proteolysis is currently quantified using a standardized procedure via a PI commonly defined as percent ratio of NPN to TN. However, this procedure has many drawbacks: it is time- and product-consuming, and lacks specificity. This recently prompted Harkouss et al. (2012) to develop a fluorometric-based procedure that specifically determines the level of N-terminal  $\alpha$ -amino groups of peptides and amino acids and so reflects the real intensity of proteolytic activity occurring mid-process. A new PI was thus defined as

the percent ratio of N-terminal  $\alpha$ -amino group content to total protein content of the ham sample. Quantifying proteolysis using this procedure is faster, more sensitive and more specific than the classic nitrogen method, and the new PI can easily be related to the classic PI by a linear regression reported in Harkouss et al. (2012). Once built, the proteolysis model could be combined with salt penetration, water migration and heat transfer models to dynamically simulate the processes at work during dry-curing. This complete 3D multi-physical numerical model would let professionals test different production process scenarii in order to reduce the final salt content of dry-cured ham without significantly altering final product quality, i.e. texture, aroma, appearance and flavor.

### **Acknowledgements**

This work was funded by the Na- integrated program (ANR-09-ALIA-013-01) financed by the French National Research Agency (ANR). This review was written within the framework of a thesis by Rami Harkouss who works for this research program.

### **1.3 Conclusions bibliographiques**

Cette revue bibliographique a montré que plusieurs facteurs, outre le pH, influençaient la protéolyse lors de la fabrication de jambons secs, notamment la température, les teneurs en sel et en eau. Par contre, aucune corrélation, ni aucun modèle prédictif, permettant de quantifier la protéolyse en fonction des facteurs cités précédemment n'ont été trouvés dans la littérature. Le développement de ce type de modèle est donc indispensable. Cela implique (1) de mettre au point un protocole expérimental permettant de conditionner rapidement en température, mais surtout en teneurs en eau et sels, plusieurs centaines d'échantillons de viande de porc, et ce, en tenant compte du type de muscle, et (2) de mettre au point une technique de mesure permettant de quantifier rapidement, en utilisant très peu de matière première, la protéolyse au sein des échantillons précédents.

D'après la littérature, beaucoup de travaux ont eu pour objectif d'analyser la texture des jambons secs, notamment en fin de procédé de fabrication ; toutefois, des recherches plus approfondies mériteraient d'être conduites afin d'étudier clairement la relation existant entre protéolyse, texture et structure dans un jambon en cours de séchage. Enfin, sur le plan de la modélisation et de la simulation numérique, aucun modèle couplant les transferts de matière (sel et eau) et/ou thermiques avec les évolutions biochimiques, structurales,

texturales, voire microbiologiques se déroulant dans un jambon, n'a été développé. Construire un tel modèle de « jambon numérique » serait, de toute évidence, un outil précieux permettant d'aider les professionnels dans leur quête de développement de jambons secs à teneur réduite en sodium, mais aux qualités organoleptiques et microbiologiques préservées.

## **Chapitre 2 : MATERIELS et METHODES**

---

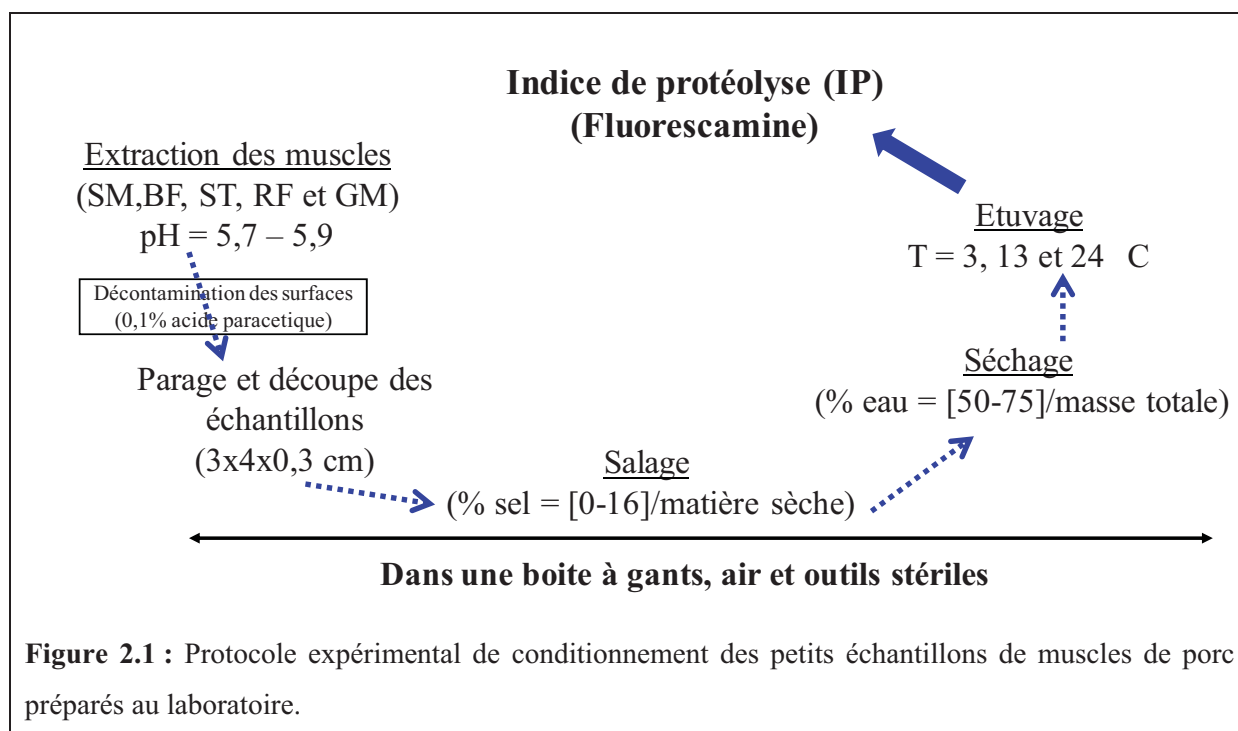


## 2.1. Préparation des échantillons et plan d'expériences (articles n°2, 3 et 4)

### 2.1.1. Protocole expérimental de préparation des petits échantillons au laboratoire (article n°3)

Ce travail de thèse requérait la préparation d'un grand nombre d'échantillons de viande de porc parfaitement conditionnés en température, en teneurs en sel et en eau, en fonction de valeurs prédéfinies dans le plan d'expériences mis en place (cf. partie 2.1.3). Très rapidement, il a été décidé de travailler directement à partir de muscles de porc extraits de jambons frais plutôt qu'à partir d'échantillons directement prélevés dans de vrais jambons secs, pour lesquels il était impossible d'obtenir des échantillons ayant les teneurs en eau et en sel désirées.

Dans cette optique, un protocole expérimental a été construit afin de préparer au mieux au laboratoire ces petits échantillons, en tenant compte de la pratique industrielle et des paramètres physico-chimiques affectant la protéolyse. Ce protocole, qui est décrit sur la Figure 2.1, a nécessité plusieurs semaines de travaux pour sa mise au point et pour bien établir les conditions des différentes étapes : décontamination initiale, découpe, salage, séchage et étuvage, de façon à permettre une homogénéisation rapide (inférieure à 24 h) des teneurs en eau et en sel dans ces échantillons.



La microbiologie et la croissance bactérienne à la surface d'un muscle sont des facteurs affectant la protéolyse, du fait des enzymes protéolytiques qui peuvent être secrétées par ces microorganismes. Pour cela, une étape de décontamination du muscle entier a été introduite dans le protocole et réalisée sous une hotte aspirante, munie de gants. Pour cela, dans un sac en plastique, le muscle a été immergé dans de l'acide peracétique pendant 3 min, puis rincé 2 fois, pendant 1 min, avec de l'eau stérile. Le muscle a ensuite été disposé dans une boîte à gants, ventilée par de l'air stérile, et contenant des outils de découpe stériles ; tout ceci, afin d'éviter toute contamination microbienne extérieure pouvant affecter les mesures biochimiques de protéolyse. Après décontamination de la surface du muscle, la partie de plusieurs millimètres d'épaisseur abimée par l'acide a été ôtée et le morceau paré a été découpé, en tranches de même épaisseur, afin de préparer des échantillons ayant une masse finale, après salage et séchage, supérieure à 5 g. Ensuite, les morceaux ont été déposés sur un portoir et un volume de saumure ( $C=30\text{g}/100\text{ml}$ ) nécessaire a été ajouté (Multipette plus, Eppendorf AG, Hamburg, Germany) pour avoir la teneur en sel désirée lors de chaque expérimentation. Compte tenu de la faible épaisseur des tranches de viande (3 à 4 mm), la diffusion du sel se faisait en un temps très court (quelques heures). Après le salage, les morceaux ont été séchés toujours dans la boîte à gants, avec de l'air stérile, à  $15^{\circ}\text{C}$ , afin d'atteindre le plus rapidement possible la teneur en eau désirée (24 h au maximum). Les échantillons séchés et salés ont ensuite été mis sous vide et laissés dans différentes étuves (Model 14 D-78532, Binder GmbH, Tuttlingen, Germany), dont la température de consigne correspondait à la température de la cinétique correspondante du plan d'expériences de Doehlert (cf. Tableau 2.1). Le prélèvement des échantillons dans les étuves a été fait selon un plan de prélèvement spécifique pour chaque cinétique. Les sacs contenant les échantillons de viande de porc conditionnés en température et en teneurs en sel et en eau, ont été ensuite stockés dans un congélateur à  $-80^{\circ}\text{C}$  (Bio Memory, Froilabo, France) jusqu'à ce que les différents dosages soient effectués : teneur en sel, teneur en eau, pH et mesure de l'indice de protéolyse par la méthode de la « Fluorescamine ».

### 2.1.2. Préparation des échantillons issus de jambons de Bayonne (articles n°2 et 4)

En plus des très nombreuses mesures réalisées sur les échantillons préparés au laboratoire, des mesures complémentaires ont été aussi faites sur des échantillons de muscles extraits de vrais jambons secs.



Pour l'expérimentation portant sur l'étude de l'applicabilité de la nouvelle procédure mise au point au laboratoire à mesurer l'indice de protéolyse (IP) dans de vrais jambons secs (article n°2), un total de 9 jambons de Bayonne ont été achetés. Trois muscles, BF, ST et SM, ont été extraits de chacun des 3 jambons pris à 3 stades de fabrication différents : à la fin du repos à basse température (*i.e.* 11 semaines), à la fin du séchage (*i.e.* 21 semaines) et à la fin de l'affinage (12 mois). De chacun de ces muscles, 8 échantillons ont été prélevés pour mesurer l'IP selon la nouvelle procédure, autorisant ainsi 24 mesures par muscle et par temps de prélèvement. De plus, un échantillon d'environ 50 g a été prélevé sur chaque muscle de chaque jambon et adressé à une technicienne d'ADIV Performances, à Clermont-Ferrand, pour une mesure de l'IP selon la méthode « classique ». Les 2 types de mesure de l'IP ont ensuite été comparés, de façon à voir si une corrélation pouvait être établie.

Pour l'expérimentation portant sur l'étude de la relation entre protéolyse, texture et structure au sein d'un jambon durant sa fabrication (article n°4), un total de 15 jambons de Bayonne, provenant d'un même éleveur, ont été achetés et acheminés au sein du laboratoire. Ces jambons ont été sélectionnés sur la base d'un pH à 24 h dans le muscle SM ( $\text{pH}_{\text{SM}24}$ ) compris entre 5,6 et 5,9, et d'une même classe de poids frais (9,5-10,5 kg). Deux muscles, BF et SM, ont été extraits de chacun des trois jambons pris à cinq stades différents de fabrication : état « frais » (4 jours post-mortem), à la fin du repos à basse température (*i.e.* 11 semaines), à la fin du séchage (*i.e.* 21 semaines), à mi-période pendant l'affinage (*i.e.* 35 semaines) et en fin d'affinage (12 mois). À une distance de 10 cm de l'os coaxial, une coupe transversale de 3 cm d'épaisseur a été faite sur chacun des 15 jambons (Figure 2.2a). Sur chacune des coupes, un parallélogramme horizontal (2x3x5 cm) a été extrait dans le muscle BF, à 2 cm du bas du jambon (côté couenne) et un autre parallélogramme de mêmes dimensions a été prélevé dans le muscle SM, à 2.5 cm du haut du jambon (côté muscle).

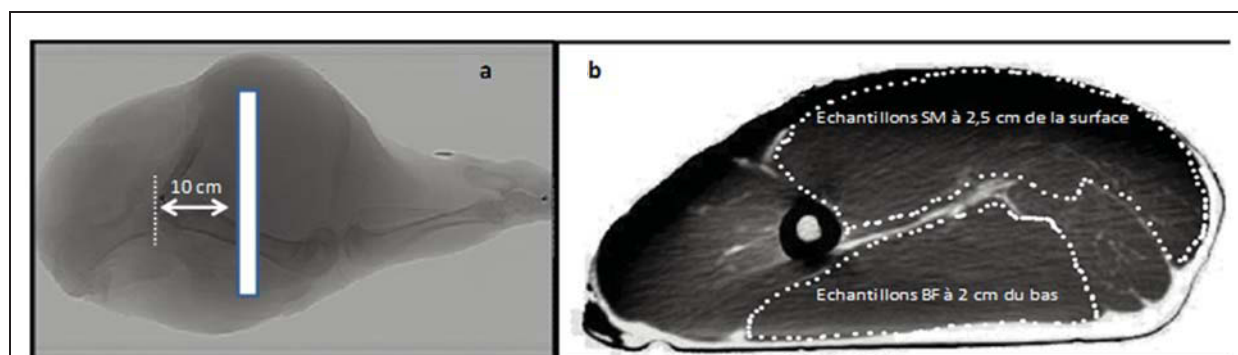


**Figure 2.2 :** (a) Positionnement de la coupe transversale d'épaisseur 3 cm prélevée dans chacun des jambons de Bayonne sélectionnés, (b) Positionnement des prélèvements des échantillons pour les différentes mesures texturales, structurales et biochimiques.

Ce protocole d'extraction avait pour objectif de conserver au mieux la position géométrique des prélèvements pour le lot de jambons, et ce, afin d'obtenir des teneurs en sel et en eau semblables dans tous les échantillons prélevés dans chaque jambon pour les différents dosages (Figure 2.2b). Enfin, les échantillons extraits ont été stockés dans un congélateur à -80°C, en attendant de procéder aux différents dosages et mesures.

### 2.1.3. Plan d'expériences de type surface de réponse / Doehlert (article n°3)

Pour les quantifications de la protéolyse (mesures de l'IP) réalisées dans les échantillons préparés au laboratoire, un plan d'expériences de type surface de réponse a été bâti. Du fait de différences anatomiques, morphologiques et fonctionnelles et compte tenu du fait qu'un jambon frais est un mélange de muscles, 5 types de muscle ont été étudiés : *Semimembranosus* (SM), *Biceps femoris* (BF), *Semitendinosus* (ST), *Rectus femoris* (RF) et *Gluteus medius* (GM). Sur la base de données industrielles, la plage de variation de la teneur en eau retenue pour l'étude a été 50-75%, exprimée en matière totale, et celle du sel a été 0-16%, exprimée en matière sèche. Concernant la température, une plage de variation 2-26°C a été choisie. Dans un souci de simplification, le facteur pH a été exclu des paramètres étudiés et du plan d'expériences, mais il a été toujours vérifié qu'il était compris entre 5,6 et 5,9 dans les muscles frais de porc, ce qui correspond à l'intervalle généralement admis par les industriels. Au final, un plan d'expériences de type Doehlert surface de réponse a été retenu (Tableau 2.1).

Ce plan peut être résumé ainsi : pour chacun des muscles (BF, SM, ST, RF et GM), 3 facteurs (température, teneur en sel et teneur en eau) ont été étudiés, avec 3 niveaux pour la température (centre à 13°C), 5 niveaux pour la teneur en eau (centre à 62,5% par rapport à la matière totale) et 7 niveaux pour la teneur en NaCl (centre à 8% par rapport à la matière sèche). Ce plan a permis de diminuer le nombre des manipulations de 105 à 13. Toutefois, deux manipulations supplémentaires ont été ajoutées, correspondant à une double répétition du point central du plan d'expériences afin de tenir compte de la variabilité animale ; au total, 15 manipulations x 5 muscles x 9-10 échantillons par cinétique : plus de 650 échantillons ont été analysés.

**Tableau 2.1** : Détails du plan de Doehlert avec les 13 cinétiques de mesure de protéolyse à réaliser pour chaque muscle ; le centre (cinétique n°1) a été répété 2 fois.

	Teneur en eau (%MT)	Teneur en sel (% MS)	Température (°C)
centre 1 (x3)	62,5	8	13
2	75	8	13
3	68,5	14,9	13
4	68,5	10,3	23,6
5	50	8	13
6	56,25	1,07	13
7	56,25	5,68	2,4
8	68,5	1,07	13
9	68,5	5,68	2,4
10	56,25	14,9	13
11	62,5	12,6	2,4
12	56,25	10,3	23,6
13	62,5	3,38	23,6

## 2.2. Mesures biochimiques

### 2.2.1. Dosage de l'indice de protéolyse par fluorescence (article n°2)

Dans la fabrication de jambons secs, la protéolyse est un facteur clé vis-à-vis de la qualité finale de ces produits transformés. L'intensité de la protéolyse est quantifiée au travers d'un indice de protéolyse (IP). En général, la méthode de Kjeldahl, appelée aussi méthode « classique », est la procédure couramment appliquée pour cette mesure, depuis plusieurs décennies, notamment en milieu industriel. Selon cette méthode, l'IP, qui s'exprime en pourcentage (%), est donc défini comme étant le rapport de la concentration de l'azote non protéique sur la concentration en azote total de l'échantillon. Bien que cette méthode soit standardisée, elle présente plusieurs inconvénients. En effet, elle nécessite un minimum de 10 à 20 g de matière et environ 2 jours pour le dosage d'un échantillon ; de plus, elle manque de spécificité vis-à-vis de l'ensemble des dérivés azotés présents dans la viande, dont certains ne sont pas issus de la protéolyse et pour lesquels elle ne fait aucune différenciation.

La première partie expérimentale de ce travail de thèse a nécessité de quantifier l'indice de protéolyse dans plus de 650 échantillons de viande de porc. Ce nombre important d'échantillons à analyser a requis la mise au point d'une méthode de dosage rapide et sensible

de l'activité protéolytique. Pour ce faire, une procédure basée sur la fluorescence a été développée au sein du laboratoire ; elle permet d'évaluer la quantité des groupes 'N-terminal  $\alpha$ -amino' des peptides et acides aminés libres. Cette procédure qui permet au final de déterminer l'intensité de l'activité protéolytique est décrite sur la Figure 2.3.

La nouvelle procédure de dosage comprend les différentes étapes suivantes. Tout d'abord, un extrait musculaire (0,5 g) est réalisé par broyage des échantillons de viande dans de l'eau (dilution de 1:10) au moyen d'un Polytron PT-MR 2100 (Kinematica AG, Switzerland). Dans cette technique, les peptides et les acides aminés issus de la protéolyse sont séparés des protéines par précipitation à l'acide trichloracétique (TCA) à 12,5%, suivie d'une centrifugation à 4000 rpm. Après neutralisation au borate de sodium (2M, pH 10), la fraction soluble contenant les produits de protéolyse est incubée 1 h avec la sonde fluorescente (0,6 mg de fluorescamine/ml d'acétone). Le dosage des produits d'addition de la fluorescamine sur les fonctions amines libres est réalisé par fluorescence dans le visible (excitation à 375 nm et émission à 475 nm), à l'aide d'un spectrofluorimètre (Perkin-Elmer LS 50B) équipé d'un lecteur de microplaque. Une gamme étalon de glycine, traitée dans les mêmes conditions, permet de calculer le taux de protéolyse, exprimé en équivalent glycine. En parallèle, la quantité totale de protéines de l'extrait brut initial est évaluée par la méthode du biuret (Gornall *et al.*, 1949) et est exprimée en mg/ml.

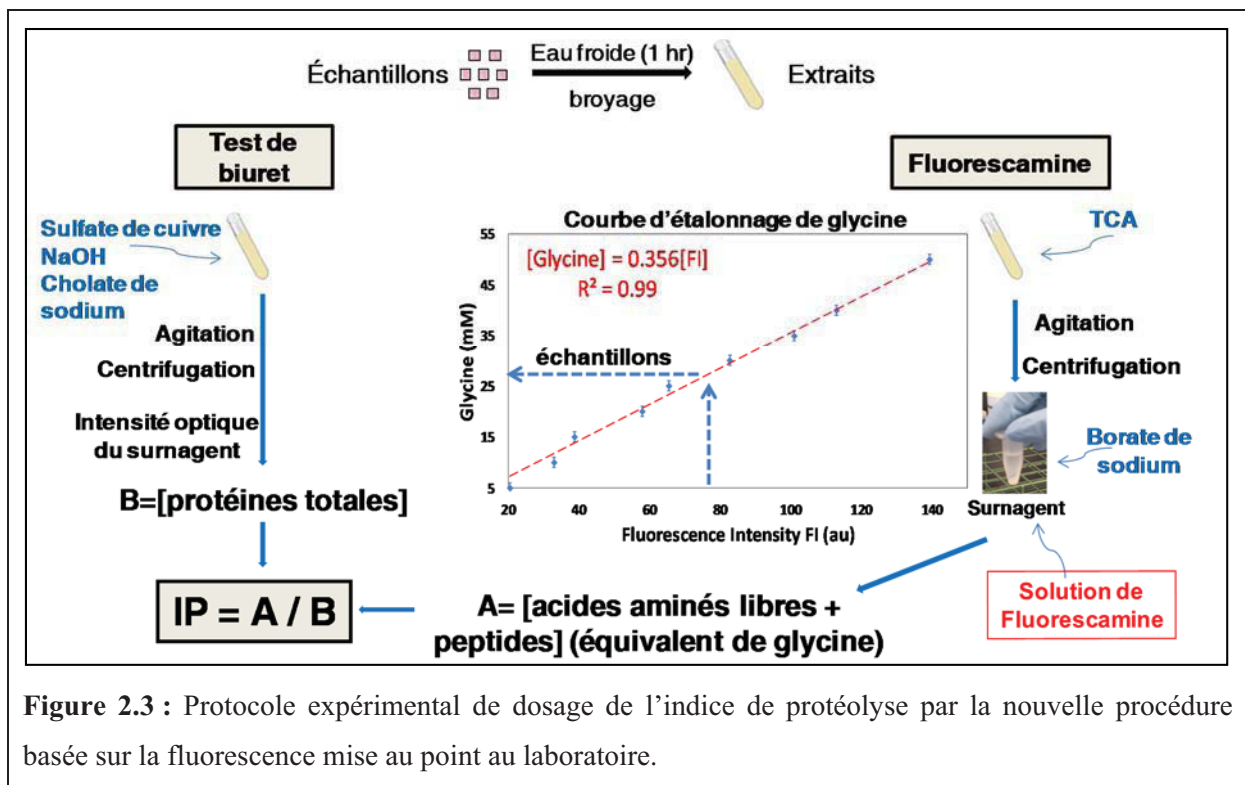


Figure 2.3 : Protocole expérimental de dosage de l'indice de protéolyse par la nouvelle procédure basée sur la fluorescence mise au point au laboratoire.

Le nouvel indice de protéolyse, par la méthode de la « fluorescamine », est au final défini comme étant le pourcentage du rapport de la concentration des groupes 'N-terminal  $\alpha$ -amino' des peptides et acides aminés libres sur la concentration en protéines totale de l'échantillon. Cette technique présente l'avantage d'être rapide, peu coûteuse en termes de quantité de matière (0,5 g) et d'être très sensible, du fait de la détection par fluorescence. Une comparaison entre les deux méthodes (classique et « fluorescamine ») a été établie sur des échantillons industriels de jambons de Bayonne et une corrélation liant ces deux mesures a été obtenue afin de convertir le nouvel indice à partir du premier.

### 2.2.2. Dosage de l'oxydation des lipides (article n°4)

Le niveau d'oxydation lipidique peut renseigner sur le développement aromatique qui s'opère durant la fabrication des jambons secs. Pour l'expérimentation portant sur l'étude de la relation entre protéolyse, texture et structure au sein d'un jambon durant sa fabrication (article n°4), la quantification de l'oxydation lipidique a été effectuée en parallèle des mesures de l'IP. Ce second type de mesure biochimique a été réalisé selon la méthode développée par Mercier *et al.* (1998), elle-même étant adaptée de la technique mise au point par Lynch et Frei (1993). Le principe de cette méthode est basé sur le dosage des composés carbonylés provenant de la décomposition des hydro-péroxydes lipidiques. En effet, la peroxydation des lipides de la viande produit des aldéhydes, dont environ 95% le sont sous forme de malondialdéhyde (MDA) ou aldéhyde malonique. En milieu acide et à chaud, le MDA réagit avec l'acide thiobarbiturique (TBA), pour former un complexe de couleur rose présentant un maximum d'absorbance à 535 nm. Cette technique donne, au final, une approximation du taux d'oxydation des lipides dans la viande. Pour réaliser ce dosage, 0,5 ml d'extrait de viande a été prélevé, suite au broyage d'1 g d'échantillon de jambon de Bayonne dans 10 ml d'eau ultra-pure. A cet extrait, 0,25 ml d'acide trichloroacétique (TCA) à 2.8% (préparé dans de l'eau) a été ajouté, afin de maintenir le milieu à un pH acide, ainsi que 0,25 ml de TBA à 1%, préparé dans une solution de soude à 50 mM. L'ensemble des réactifs a été incubé à 100°C, pendant 10 min, afin de faciliter la réaction, puis refroidi, au minimum, 30 min, à température ambiante. Ensuite, les produits d'oxydation des lipides ont été extraits, à 4°C, suite à l'ajout de 2 ml de n-butanol, par centrifugation à 4000 rpm, pendant 15 min. La phase organique a été prélevée et sa densité optique a été mesurée au spectrophotomètre à 535 nm par comparaison à un blanc de n-butanol. Afin de tenir compte des erreurs de mesure liées à la turbidité de l'échantillon, deux densités optiques ont été mesurées : l'une à 535 nm, qui est le

maximum d'absorption du complexe TBA-MDA-TBA, et l'autre à 760 nm, représentative de la turbidité de l'échantillon ; la densité optique a ensuite été corrigée à partir de la simple différence entre les 2 densités optiques. Au final, les taux d'oxydation des lipides ont été exprimés en unités TBA (UTBA), *i.e.* en mg de MDA par kg d'échantillon.

### 2.3. Analyses structurales (article n°4)

#### 2.3.1. Protocole expérimental (article n°4)

Pour l'expérimentation portant sur l'étude de la relation entre protéolyse, texture et structure au sein d'un jambon durant sa fabrication (article n°4), les échantillons de muscles SM et BF ont été prélevés, pour les 15 jambons de Bayonne, toujours dans la même zone anatomique, puis cryofixés à l'isopentane maintenu à -160 °C, et enfin stockés quelques jours à -80°C, jusqu'à la réalisation des analyses histologiques. Des coupes histologiques de 10 µm d'épaisseur, perpendiculaires au sens des fibres musculaires, ont été confectionnées, à une température de -25°C, à l'aide d'un cryostat (Modèle Microm HM 560, Thermo-Fisher Scientific Inc., Etats-Unis). Ces coupes ont ensuite été montées sur des lames de verre, puis colorées à l'hématoxyline-éosine-safran (HES) pour visualiser les fibres musculaires et les espaces extracellulaires, et au rouge sirius (RS) pour mettre en évidence le tissu conjonctif, avant d'être protégées par une résine synthétique (Eukitt, Kindler GmbH & Co, Allemagne).

#### 2.3.2. Quantification de la morphologie par analyse d'images (article n°4)

Pour chacune des coupes préparées, 6 images numériques ont été faites aléatoirement, avec un grossissement x10, au moyen d'un microscope en transmission couplé à un système d'acquisition d'images (Microscope Olympus BX61, Caméra Olympus DP71, Olympus France SAS, France). L'analyse des images a été faite à l'aide du logiciel gratuit ImageJ. Le but était de fournir une description quantitative de l'image : nombre de cellules musculaires, surface moyenne de ces cellules, taille de l'espace extracellulaire et surface du tissu conjonctif. Dans un premier temps, une calibration de l'image était nécessaire, afin de convertir les pixels en micromètre. Pour cela, l'image d'une lame graduée tous les 10 µm a été acquise dans les mêmes conditions que les images à analyser. Ensuite, le logiciel ImageJ a permis de mesurer les graduations de l'image et d'établir la correspondance entre la longueur



en  $\mu\text{m}$  et le nombre de pixels mesurés, de façon à pouvoir extraire les paramètres structuraux désirés : nombre de cellules, surface des cellules...

### 2.3.3. Seuillage sur les niveaux de gris et calcul des propriétés structurales

Sur chaque image acquise (dont un exemple est donné sur la Figure 2.4a), le bruit de fond a été compensé en soustrayant le blanc de l'image à analyser. L'image couleur a été décomposée en ses trois composantes monochromatiques : rouge, bleu et vert. Au final, les analyses ont été réalisées sur le canal vert qui offrait le meilleur contraste. Ensuite, une segmentation par seuillage sur les niveaux de gris a été appliquée, puis une transformation en image binaire (noir et blanc) a permis d'identifier les objets à mesurer (Figure 2.4b). Le seuillage constitue une étape clé de l'analyse d'images, car c'est grâce à cette opération que le logiciel identifie les objets à mesurer. La surface relative de chaque objet ainsi extrait a été évaluée par quantification du nombre de pixels la composant. De manière identique, la surface relative des fibres musculaires a été quantifiée, en prenant la précaution d'éliminer les fibres coupées au bord de l'image. Le nombre de fibres a été déterminé après individualisation de ces dernières et mise en évidence par application de couleurs aléatoires, ce qui facilite grandement leur visualisation, et donc leur comptage (Figure 2.4c).

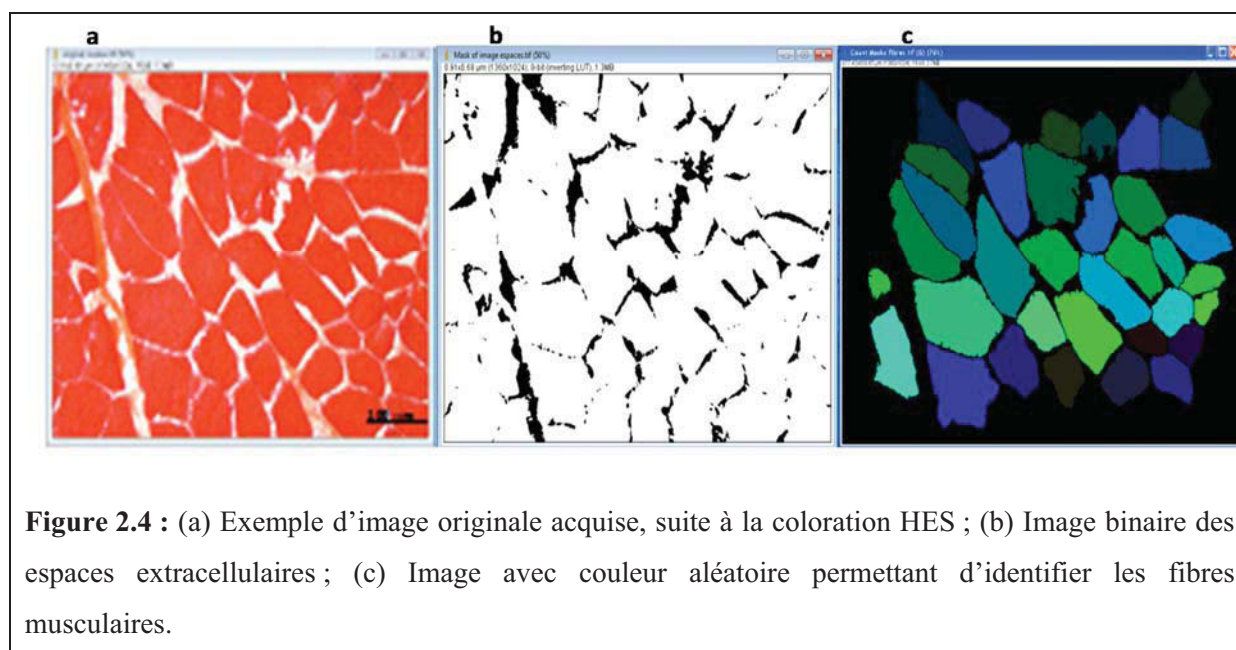


**Figure 2.4 :** (a) Exemple d'image originale acquise, suite à la coloration HES ; (b) Image binaire des espaces extracellulaires ; (c) Image avec couleur aléatoire permettant d'identifier les fibres musculaires.

Au final, les grandeurs identifiées suite à l'analyse des images ont été consignées dans un premier tableau affichant le résumé des résultats : nombre de fibres, surface totale des fibres, surface du tissu conjonctif, taille moyenne et densité de fibres sur la surface étudiée, et

dans un second tableau détaillant chacun des résultats pour chaque objet mesuré. Enfin, les données ont été importées dans le logiciel Excel afin de les mettre en forme, faire les premières analyses statistiques et construire les figures et histogrammes permettant l'interprétation des résultats.

#### **2.4. Analyses texturales (article n°4)**

Pour l'expérimentation portant sur l'étude de la relation entre protéolyse, texture et structure au sein d'un jambon durant sa fabrication (article n°4), les échantillons congelés de muscles SM et BF prélevés sur les 15 jambons de Bayonne, ont été décongelés, à 4°C, pendant 24 h environ. La mesure de la texture des échantillons a été faite selon la méthode de « Texture Profile Analysis (TPA) » (Bourne, 2002), à température ambiante, en utilisant un texturomètre universel (Modèle TA.XT plus, Stable MicroSystems Ltd., Surrey, England) présent à l'ADIV. Deux cubes de 10 mm d'arrête ont été analysés pour chacun des deux muscles, SM et BF, de chaque jambon. Les échantillons ont été disposés de telle façon que les fibres musculaires soient placées parallèlement à la surface de contact du disque de compression, de diamètre 50 mm. Les échantillons ont été compressés axialement deux fois successivement, à 50 % de leur hauteur originale, avec un laps de temps de 2 s entre les deux compressions. Concrètement, la mesure consiste à enregistrer des courbes force-temps, suite à l'application d'une charge de 15 kg appliquée à une vitesse de 1 mm/s sur l'échantillon. Finalement, les paramètres mesurés à l'aide du logiciel XT.RA Dimension associé au texturomètre sont : la dureté, la fragilité, l'élasticité, l'adhésion et la cohésion. La dureté est définie par la force maximale pendant le premier cycle de compression (F1) et est exprimée en N. La fragilité correspond au rapport F2/F1 (Figures 1.3 et 3.5). La cohésion est calculée par le ratio entre la surface située sous le second pic (Area2) et la surface située sous le premier pic (Area 1). L'élasticité est définie comme le ratio entre le temps enregistré entre le début du second pic et le second renversement de sonde (b) et le temps enregistré entre le début du premier pic et le premier renversement de sonde (a). Enfin, l'adhésion est définie comme étant la surface « négative », située sous la courbe obtenue entre les 2 cycles (Area 3) ; elle est exprimée en N.s (Figure 1.3 et 3.5).



## 2.5. Mesures physico-chimiques (articles n°2, 3 et 4)

### 2.5.1. Teneur en sel (articles n°2, 3 et 4)

Le chlorure de sodium (NaCl) a été dosé dans les échantillons de viande de porc par deux techniques différentes : le chloruromètre (articles n°2 et n°3) et la chromatographie ionique, technique récemment acquise par le laboratoire (article n°4). A noter que la préparation des échantillons est presque la même pour ces 2 techniques de mesure, seules quelques différences mineures existent entre les deux. Toutefois, le principe de mesure est radicalement différent entre les 2 techniques.

#### 2.5.1.1. Le chloruromètre (articles n°2 et 3)

Le principe de base de dosage au moyen de cette technique consiste à précipiter les ions chlorure contenus dans une solution sous forme de chlorure d'argent (AgCl). Un flux constant d'ions argent est généré par application d'un courant constant entre les électrodes d'argent plongées en milieu acide. L'intensité du courant électrique, qui dépend de la quantité d'ions présents dans ce milieu, est enregistrée en continu grâce à deux autres électrodes. Au fur et à mesure de la disparition des ions chlorure, par précipitation sous forme d'AgCl, cette intensité diminue. Une fois que tous les ions chlorure ont précipité, la production d'ions argent a pour effet d'augmenter la quantité d'ions présents dans la solution et l'intensité du courant électrique augmente. Le chloruromètre détecte alors le minimum de l'intensité du courant électrique. Le temps nécessaire pour atteindre ce minimum correspond à la quantité d'ions chlorure. La valeur indiquée par l'appareil est déduite de ce temps, par comparaison au temps enregistré lors d'un essai effectué avec une solution de calibration contenant 200 mg/L de NaCl. Du fait de l'instabilité éventuelle du courant appliqué entre les électrodes d'argent, de l'usure et de l'encrassement de ces électrodes, il est nécessaire de calibrer fréquemment l'appareil, à savoir tous les 5 à 8 dosages.

Concernant la préparation de la solution à analyser, 0,5g d'échantillon a été broyé, dans 20 ml d'eau déminéralisée, pendant 2 x 45 s, en utilisant l'Ultra-Turrax T25 (Ika, Allemagne). Le broyat a été stocké pendant quelques heures, à 4°C. Ensuite, 1 ml de surnageant a été centrifugé, pendant 10 min, à 13000 tr/min. Enfin, 500 µl du surnageant a été dosé au chloruromètre (MKII Chloride Analyser 926, Sherwood, Cambridge, UK). Au final, la teneur en sel est exprimée en pourcentage par rapport à la matière sèche (% MS).

### 2.5.1.2. La chromatographie ionique (article n°4)

La chromatographie ionique (Modèle 850 professional IC, Metrohm France SAS, France) permet d'optimiser les séparations chromatographiques en gradient basse ou haute pression (Figure 2.5). Ce système peut recevoir différents modes de détection et comprend différents modules pour automatiser les préparations d'échantillons. Il est piloté par le logiciel Mag IC Net, qui présente une grande convivialité de par son interface graphique. Il propose également des fonctionnalités de calcul intéressantes permettant de réaliser des dilutions « intelligentes » avec les automates d'injection. Deux types de dosage peuvent ainsi être évalués : les anions et les cations ; ce qui permet de doser soit les ions sodium, calcium ou magnésium existants dans la viande, soit les ions chlorure, moyennant un changement de la colonne de séparation.



**Figure 2.5 :** Photographie de l'appareil de chromatographie ionique du laboratoire utilisé pour le dosage des ions chlorure ou sodium.

La préparation de la solution à analyser consiste à homogénéiser 1 g d'échantillon de viande dans 10 ml d'eau déminéralisée, en utilisant l'Ultra-Turrax T25 (Ika, Allemagne). Après quelques heures de repos, une centrifugation a été faite pour 10 min à 13000 tr/min. Le surnageant a été dilué avec de l'eau déminéralisée et les ions chlorure ont été mesurés au moyen de l'appareil de chromatographie ionique présenté sur la Figure 2.5. Comme avec le chloruromètre, au final, la teneur en sel a été exprimée en pourcentage par rapport à la matière sèche de l'échantillon (% MS).

### 2.5.2. Teneur en eau (articles n°2, 3 et 4)

Pour la mesure de la teneur en eau des échantillons de viande de porc (soit préparés au laboratoire, soit extraits de jambons de Bayonne), 1,5 à 2,5 g de viande ont été découpés en petits cubes et déposés dans une coupelle, dont la masse à vide avait été préalablement mesurée et notée ( $m_c$ ). La masse de la coupelle contenant l'échantillon ( $m_i$ ) a été aussi mesurée et notée, puis le tout a été placé dans une étuve (Modèle FT127U, Firlabo, France), à 104°C +/- 2°C, pendant 24 h. Après étuvage, la masse finale de la coupelle contenant l'échantillon ( $m_f$ ) a été de nouveau mesurée. Au final, la teneur en eau de l'échantillon, exprimée par rapport à la masse totale (MT), a été calculée par la formule suivante :

$$X_{eau} = \frac{m_i - m_f}{m_i - m_c} \quad \text{Eq. (2.1)}$$

### 2.5.3. pH (articles n°2, 3 et 4)

Comme indiqué précédemment, bien que le pH ne soit pas un facteur physico-chimique dont l'effet sur l'évolution de la protéolyse a été pris en compte dans ce travail, le pH a été systématiquement mesuré dans les muscles frais et a été un critère de sélection, de par sa valeur qui devait être comprise entre 5,6 et 5,9.

Pour la mesure du pH, 0,6 g d'échantillon de viande a été broyé dans 0,3 ml d'eau déminéralisée, pendant 2 x 30 s, en utilisant l'Ultra-Turrax T25 (Ika, Allemagne). Ensuite, le broyat a été mis dans un tube Eppendorf et la mesure du pH a été faite avec la sonde de pénétration d'un pH-mètre (Modèle InLab427, Mettler Toledo, France), préalablement calibré avec des solutions standards de pH 4 et pH 7.

## 2.6. Analyses statistiques

Les analyses et traitements statistiques des résultats expérimentaux obtenus dans ce travail ont été effectués avec la version 3.0.1 du logiciel R (R Development Core Team, 2013), à laquelle ont été adjoints les ensembles statistiques 'car' (Fox & Weisberg, 2011), 'HH' (Heiberger, 2013), 'leaps' (Lumkey, 2009) et l'ensemble graphique 'rgl' (Adler & Murdoch, 2013). Toutes ces analyses ont été faites en étroite collaboration avec André Lebert (Institut Pascal, Université Blaise Pascal, Clermont-Fd).

### 2.6.1. Régression linéaire (ou polynomiale) multiple (articles n°3 et 4)

Un des grands objectifs de ce travail de thèse était de développer un modèle d'évolution protéolytique permettant de calculer la valeur de l'IP d'un échantillon de muscle de porc salée et séchée, connaissant la température et les teneurs en eau et en chlorure de sodium. Pour cela, une approche plan d'expériences de type surface de réponse (plan de Doehlert – cf. partie 2.1.3) couplée à une régression polynomiale multiple a été mise en place. Pour chacun des 5 muscles étudiés, une régression polynomiale quadratique a été appliquée aux données de vitesse de protéolyse déterminées suite au plan d'expériences. Cette régression avait pour forme :

$$Y = \alpha_0 + \sum \alpha_i \cdot X_i + \sum \alpha_{ii} \cdot X_{ii}^2 + \sum \sum \alpha_{ij} \cdot X_i \cdot X_j + \lambda_i \quad \text{Eq. (2.2)}$$

où Y est la vitesse de la protéolyse (réponse du modèle),  $\alpha_0$  est la constante du modèle,  $\alpha_i$  est le coefficient linéaire,  $\alpha_{ii}$  est le coefficient quadratique,  $\alpha_{ij}$  est le coefficient d'interaction des facteurs deux à deux, et  $\lambda_i$  est l'erreur du modèle. Cette équation décrit les effets linéaires, quadratiques, ainsi que les effets des interactions des trois facteurs T (température), E (teneur en eau) et S (teneur en sel) sur la valeur de la réponse, *i.e.* la vitesse de protéolyse (%/jour).

Un deuxième objectif de ce travail de thèse était de comprendre la relation entre protéolyse, structure et texture au cours de la fabrication des jambons secs. De manière identique à ce qui a été réalisé lors du développement des modèles protéolytiques, des régressions polynomiales multiples ont été effectuées, pour chaque muscle (SM et BF), puis les meilleurs modèles, permettant à chacun des paramètres structuraux et texturaux étudiés d'être calculé en fonction de l'IP (IP, IP<sup>2</sup> ou IP<sup>1/2</sup>), des teneurs en eau et en sel et de l'interaction eau-sel, ont été identifiés. Le choix du meilleur modèle pour chaque paramètre investigué a été fait en fonction d'une valeur de R<sup>2</sup><sub>ajusté</sub> la plus grande possible, associée à une valeur de l'erreur standard sur le résidu la plus petite possible. Pour un paramètre, aucun modèle n'a été retenu dans le cas où le R<sup>2</sup><sub>ajusté</sub> restait inférieur à 0,25.

### 2.6.2. Analyse de variance (articles n°2, 3 et 4)

De multiples analyses de variance (ANOVA) ont été réalisées au cours de ce travail de thèse. Dès l'application de la nouvelle procédure de mesure de l'IP développée au laboratoire à des échantillons de muscle extraits de jambons de Bayonne (article n°2), une première

ANOVA a été faite sur les mesures de protéolyse afin d'étudier l'effet de la période (fin de repos, fin du séchage, fin d'affinage) et du type de muscle (BF, SM et ST).

Concernant l'étude de la protéolyse sur les petits échantillons préparés au laboratoire (article n°3), une ANOVA à 3 facteurs a été effectuée sur l'ensemble des pentes issues des différentes cinétiques obtenues pour les 5 muscles étudiés : ST, SM, BF, RF et GM. Le but était d'étudier l'effet de chacun des facteurs étudiés (température, teneurs en eau et en chlorure de sodium), ainsi que leur significativité, sur la valeur des pentes des cinétiques de protéolyse. L'effet muscle a été aussi apprécié. Un ensemble de tests statistiques a été aussi utilisé, comme les tests de Fisher et Post-hoc, pour classer les niveaux de chaque facteur en groupe ayant un effet homogène sur les pentes des cinétiques de protéolyse.

L'expérimentation portant sur l'étude de la relation entre protéolyse, texture et structure dans un jambon durant sa fabrication (article n°4) a nécessité la réalisation de plusieurs ANOVA, à différentes étapes de l'étude. Une première ANOVA a été faite pour étudier les effets des 5 périodes investiguées (« frais », fin de repos, fin de séchage, mi-affinage et fin d'affinage) et des 2 muscles (SM et BF) sur les valeurs mesurées de l'IP et de l'oxydation lipidique (TBA). Quand un effet significatif a été mis en évidence par l'ANOVA, le test de Student a été appliqué pour déterminer les niveaux de significativité entre les différents groupes. De plus, chaque donnée morphométrique issue de l'analyse des images faites sur les coupes histologiques a été exprimée en valeur moyenne +/- erreur standard à la moyenne (SEM). Les modifications en fonction du temps de la taille des fibres, de la surface des espaces extracellulaires et du nombre de fibres ont été ensuite analysées au moyen d'une ANOVA à 1 facteur. Comme précédemment, l'ANOVA a été complétée par un test de Student, dès qu'un effet significatif a été observé. Enfin, l'ensemble des données structurales et texturales acquises pour les 2 muscles étudiés (SM et BF) a fait l'objet d'une ANOVA à 3 facteurs afin d'étudier l'effet des facteurs IP, teneur en sel et teneur en eau. Dans ce dernier cas, tout effet significatif décelé a été suivi de tests Post-Hoc et de Fisher.

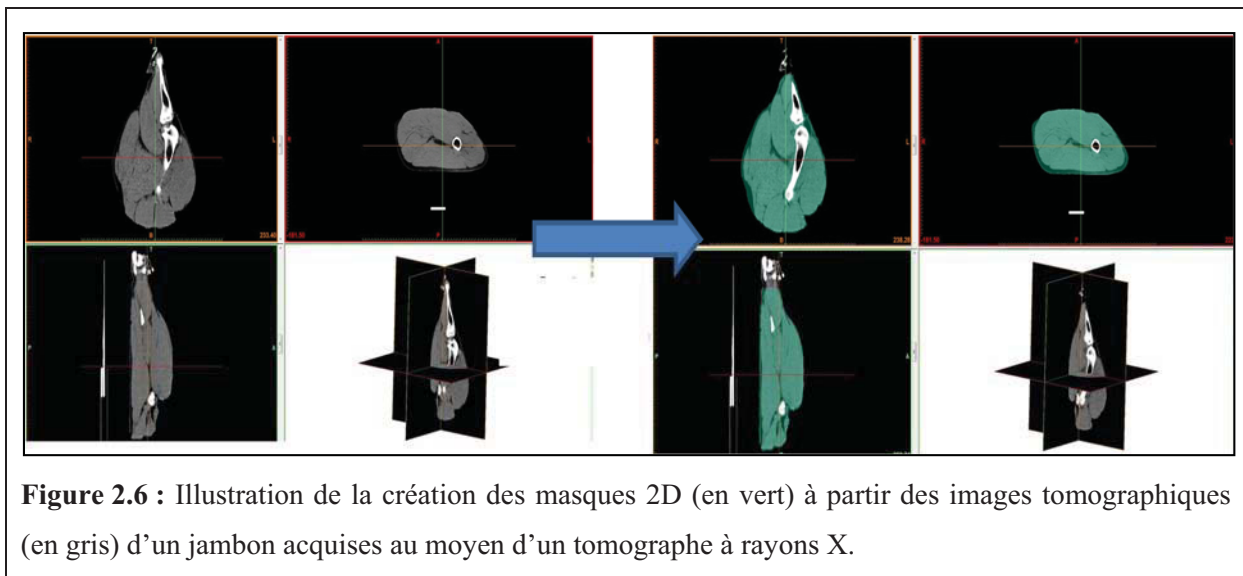
## **2.7. Modélisation multi-physique (article n°5)**

Une géométrie complète 3D d'un vrai jambon incluant plusieurs groupes de muscles a été construite et maillée au moyen d'un logiciel utilisé dans le milieu médical, *i.e.* le logiciel Mimics®. Sur la base de cette géométrie maillée, les modèles phénoménologiques permettant de calculer des vitesses de protéolyse ont ensuite été intégrés et combinés avec des modèles physiques de transferts de chaleur et de matière (eau, sel) afin de constituer le modèle de

« jambon numérique ». L'intégration de ces différents modèles a été faite sous le logiciel Comsol® Multiphysics 4.3a.

### 2.7.1. Construction géométrique et maillage volumique (article n°5)

Une géométrie 3D réaliste d'un jambon a été construite à partir d'une série de 181 images 2D d'un jambon frais, acquises à l'aide d'un appareil de tomographie à rayons X et gracieusement fournies par l'IFIP. Les images traitées ont été préalablement choisies sur la base de la qualité des contrastes afin de faciliter les étapes ultérieures d'analyse, de segmentation, d'extraction de contours et de construction 3D. Sous le logiciel Mimics®, plusieurs techniques de lissage, de remplissage et de contraste ont été utilisées afin de séparer les enveloppes des principaux muscles du jambon. Une étape de seuillage en niveaux de gris a été automatisée de façon à aussi identifier et isoler les principaux constituants du jambon : la couenne, les muscles, l'os et le gras. Enfin, un traitement particulier et des opérations de lissage ont été réalisés pour rendre les surfaces continues et les frontières lisses, et obtenir des masques en 2D de très bonne qualité afin de faciliter l'étape ultérieure de construction 3D (Figure 2.6).



Enfin, l'empilement et la connexion de tous les masques de toutes les coupes 2D ont conduit à la construction de la géométrie de jambon en 3D (Figure 2.7). Ensuite, sur cette géométrie 3D, un maillage surfacique comportant un nombre limité de mailles ayant une forme la plus régulière possible a été créé. La dernière étape a consisté à générer, à partir du maillage surfacique, le maillage volumique avec des cellules de forme tétraédrique. Cette



étape a requis plusieurs opérations de lissage. Afin de limiter le nombre total de mailles, l'intérieur de l'os du jambon n'a pas été maillé. Au final, la géométrie de jambon 3D bâtie fait 42 cm de long, 32 cm de large au maximum et a une épaisseur maximale de 15,8 cm. Au total, cette géométrie comporte 202 000 mailles tétraédriques et cinq groupes de muscles différents qui ont pu être clairement définis à l'intérieur de cette géométrie (Figure 2.7b). C'est cette géométrie qui a été importée dans le logiciel Comsol<sup>®</sup> Multiphysiques (Figure 2.7) et qui a servi de base au modèle de « jambon numérique ».

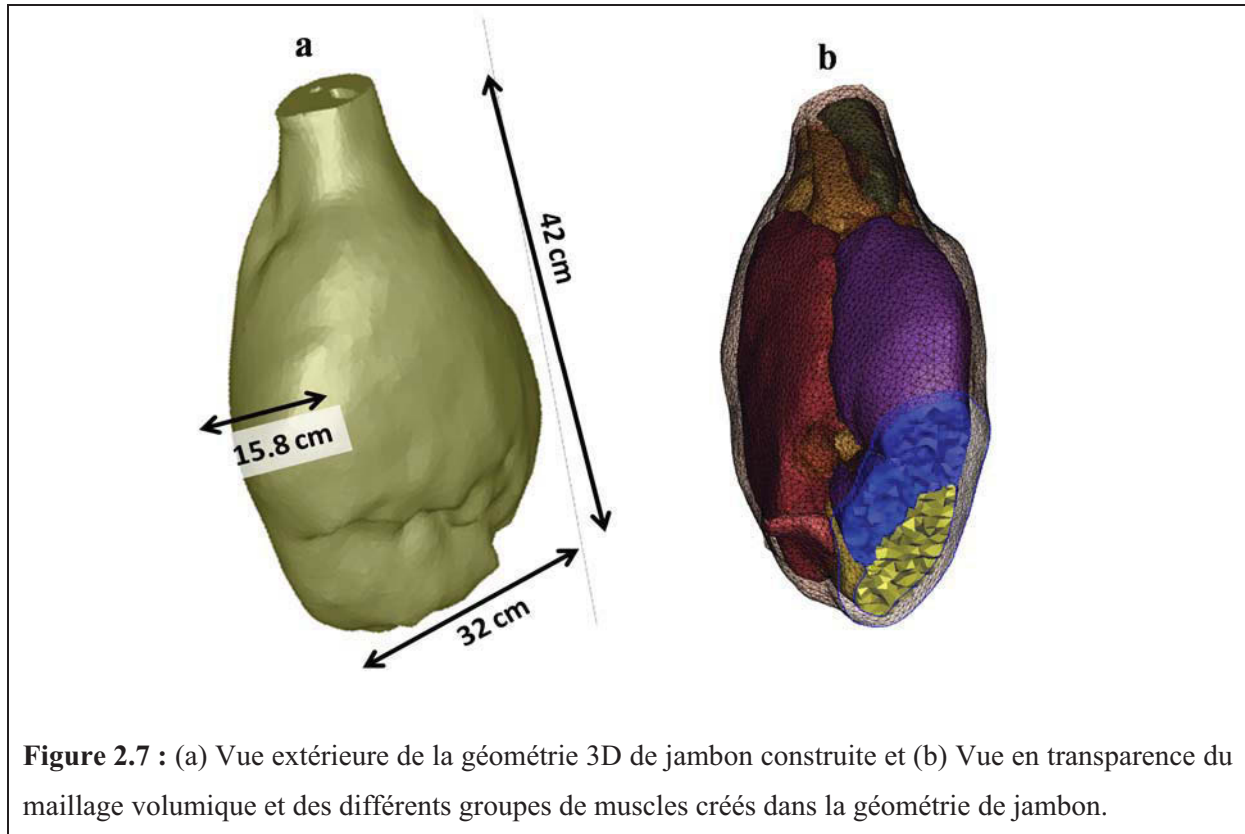


**Figure 2.7 :** (a) Vue extérieure de la géométrie 3D de jambon construite et (b) Vue en transparence du maillage volumique et des différents groupes de muscles créés dans la géométrie de jambon.

## 2.7.2. Implémentation des différents modèles (article n°5)

### 2.7.2.1. Modèle de protéolyse (article n°5)

Le calcul de la protéolyse dans le modèle de « jambon numérique » est fait en résolvant l'équation suivante, où IP représente l'indice de protéolyse (%) :

$$\frac{d IP}{d t} = R_i \quad \text{Eq. (2.3)}$$

$R_i$  correspond à un terme réactionnel ; il est donné par l'équation du modèle phénoménologique choisi pour calculer la vitesse de protéolyse (cf. article n°3) en fonction des valeurs locales de température, de teneurs en eau et en sel. Dans la version actuelle du

modèle de « jambon numérique », c'est le modèle moyen établi pour les 4 muscles SM, ST, BF et RF qui a été implémenté dans tous les groupes de muscles, *i.e.* celui correspondant à l'équation (3.7) p 122. L'équation (2.3) a été appliquée à l'ensemble des domaines de calcul du modèle, sauf à l'intérieur de l'os puisque ce dernier n'a pas été maillé et qu'aucun phénomène de protéolyse n'intervient à cet endroit. Enfin, une valeur initiale a été imposée pour la protéolyse, à savoir un  $IP_0$  égal à 2,5%, correspondant à la valeur moyenne de l'IP mesurée avec la méthode de mesure mise au point au laboratoire sur un grand nombre d'échantillons de viande de jambon de porc frais préparés à partir de différents muscles.

#### 2.7.2.2. Modèle de transfert de chaleur (article n°5)

Le transfert de chaleur est simulé dans le jambon au moyen de la loi de Fourier (Eq. (2.4)). La résolution de cette équation permet de prédire le changement de la température à l'intérieur du jambon suite aux modifications de la température de l'air lors des étapes d'étuvage et de séchage/maturation. La loi de Fourier qui est résolue s'écrit, sous une forme simplifiée, de la manière suivante :

$$\rho \cdot c_p \cdot \frac{\partial T}{\partial t} = \nabla(k \cdot \nabla T) \quad \text{Eq. (2.4)}$$

où  $t$  représente le temps (s),  $\rho$  est la masse volumique du jambon égale à  $1072 \text{ kg.m}^{-3}$ ,  $c_p$  est la chaleur spécifique du jambon égale à  $3200 \text{ J.kg}^{-1}.\text{K}^{-1}$  et  $k$  est la conductivité thermique du jambon égale à  $0,45 \text{ W.m}^{-1}.\text{K}^{-1}$ .

L'équation de transfert de chaleur a été appliquée à tous les domaines du jambon, sauf dans l'os qui n'a pas été maillé et dont la surface a été considérée comme isolée thermiquement. Au temps  $t=0$ , *i.e.* au début de l'étape de salage, il a été supposé que le jambon, dont la température initiale était homogène et égale à  $3^\circ\text{C}$ , a été placé dans une chambre froide où la température de l'air était de  $4^\circ\text{C}$ .

A l'interface air-jambon, une condition limite thermique particulière a été imposée de façon à calculer la densité du flux de chaleur à la surface du jambon, en prenant en compte les phénomènes de convection thermique et d'évaporation de l'eau. Cette condition limite s'écrit de la manière suivante :

$$q = h (T_{air} - T_{surface}) + \varphi_{eau} \cdot L_v \quad \text{Eq. (2.5)}$$

Dans cette relation,  $h$  représente le coefficient de transfert de chaleur convectif. Une valeur de  $h$  égale à  $7 \text{ W.m}^{-2}.\text{K}^{-1}$  a été choisie pour cette étude en raison de l'existence de très faibles vitesses d'air autour du jambon (Kondjoyan & Daudin, 1997). La grandeur  $T_{surface}$



représente soit la température de la surface correspondant au côté muscle recevant le sel, soit la température de la surface correspondant au côté couenne du jambon où aucun salage n'a été appliqué. En effet, seule une condition de salage de type « apport limité » a été simulée au moyen du modèle de « jambon numérique » créé, consistant à apporter et à apposer une masse de sel donné uniquement sur le côté viande du jambon, à la différence d'un salage par enfouissement où la totalité de la surface du jambon est mise en contact avec le sel. Enfin, dans l'équation (2.5), le terme  $L_v$  représente la chaleur latente de vaporisation de l'eau ( $2450 \text{ kJ.kg}^{-1}$ ) et  $\varphi_{\text{eau}}$  correspond à la densité de flux d'eau qui s'évapore de la surface du jambon. Le calcul de cette grandeur se fait selon une équation présentée dans la partie suivante traitant du 'transfert de matière' (cf. Eq. (2.8)).

### 2.7.2.3. Modèle de transfert de matière (article n°5)

Les phénomènes de transferts de matière qui se déroulent lors de la fabrication d'un jambon sec, *i.e.* la diffusion du sel et la migration de l'eau, ont été considérés, par hypothèse, comme purement Fickiens. Ils ont donc été modélisés au moyen de la loi de Fick suivante :

$$\frac{\partial c_i}{\partial t} + \nabla \cdot (-D_i \nabla c_i) = 0 \quad \text{Eq. (2.6)}$$

dans laquelle  $c_i$  représente la concentration en sel ou en eau ( $\text{kg.m}^{-3}$ ).

Dans la loi de Fick, le terme  $D_i$  correspond au coefficient de diffusion de l'eau et du sel dans le jambon. Le coefficient de diffusion du sel dans la viande maigre du jambon a été considéré comme constant et égal à  $5.10^{-10} \text{ m}^2.\text{s}^{-1}$ , tandis que celui de l'eau a été considéré comme variant en fonction de la teneur locale en eau selon la relation suivante (Ruiz-Cabrera *et al.*, 2004) :

$$D_{\text{water}} = 4 \cdot 10^{(0.625 \cdot X_{\text{water}} - 12)} \quad \text{Eq. (2.7)}$$

Comme pour les équations précédentes, les deux équations de Fick (une pour l'eau et une pour le sel) ont été résolues dans tous les domaines du jambon, sauf dans l'os. Une teneur initiale en sel de 0% MT et une teneur en eau initiale de 75% MT ont été introduites dans le modèle numérique, soit des valeurs correspondant à celles de la viande fraîche.

Dans un premier temps, le modèle de « jambon numérique » a été utilisé pour simuler les transferts d'eau et de sel et coupler ces transferts avec un calcul de protéolyse au cours des 11 premières semaines de fabrication d'un jambon sec, durant lesquelles le jambon est placé dans une ambiance à basse température. Ce laps de temps inclue une première étape de salage,

d'une durée de 15 jours, réalisée selon la méthode consistant à apporter une quantité limitée de sel uniquement sur la surface correspondant au côté viande du jambon (cf. Figure 2.9). Sur le plan numérique, le salage du côté viande a été modélisé au travers de l'application d'une saumure constituée d'une masse de sel variable (655 g initialement) ajoutée à un volume d'eau constant (100 ml). A chaque pas de temps de l'étape de salage, la masse de sel qui a pénétré à l'intérieur du jambon a été calculée par intégration volumique, ainsi que la masse de sel restant à la surface du jambon et donc la nouvelle concentration en sel de la saumure présente sur la surface de salage. L'étape de salage a été suivie d'une étape de repos, d'une durée de 62 jours, pendant laquelle le sel diffuse à l'intérieur du jambon. Il est à noter que la diffusion du sel s'opère depuis la surface du jambon vers l'intérieur, alors que la migration de l'eau se fait en sens inverse, depuis l'intérieur vers la surface où se déroule le phénomène d'évaporation. De ce fait, des conditions limites particulières ont été imposées à l'interface air-jambon.

La densité de flux d'eau à la surface du jambon est donnée par la relation suivante :

$$\varphi_{eau} = k \cdot \left( a_{w,surface} \cdot P_{sat,T_{surface}} - \frac{HR_{air}}{100} \cdot P_{sat,T_{air}} \right) \quad \text{Eq. (2.8)}$$

avec une humidité relative de l'air  $HR_{air}$  égale à 70%.

Dans la gamme de température 0-40°C, la pression de vapeur saturante, à une température T donnée, peut être calculée selon l'équation suivante :

$$P_{sat,T} = \exp \left( -\frac{6764}{T} - 4.915 \cdot \log T + 58.75 \right) \quad \text{Eq. (2.9)}$$

Dans l'équation (2.8), k, le coefficient de transfert d'eau ( $\text{kg} \cdot \text{m}^{-2} \cdot \text{Pa}^{-1} \cdot \text{s}^{-1}$ ), est calculé à partir du coefficient de transfert de chaleur convectif h grâce à cette relation (Kondjoyan & Daudin, 1997) :

$$k = \frac{h \cdot M_{eau}}{Cp_{air} \cdot M_{air} \cdot P_{atm} \cdot Le^{2/3}} \quad \text{Eq. (2.10)}$$

où  $M_{eau}$  est la masse molaire de l'eau ( $18 \text{ g} \cdot \text{mol}^{-1}$ ),  $Cp_{air}$  est la chaleur spécifique de l'air ( $1004 \text{ J} \cdot \text{kg}^{-1} \cdot \text{K}^{-1}$ ),  $M_{air}$  représente la masse molaire de l'air ( $29 \text{ g} \cdot \text{mol}^{-1}$ ) et  $P_{atm}$  est la pression atmosphérique exprimée en atm. Dans la relation précédente,  $Le$  est le nombre de Lewis qui vaut 0,777 pour l'air.

Du côté couenne du jambon, il a été admis arbitrairement que le coefficient de transfert d'eau k était divisé par un facteur égal à 20 par rapport à celui calculé du côté viande par la relation (2.10), de façon à indirectement tenir compte de l'effet barrière vis-à-vis du transfert d'eau joué par la couche de graisse située juste sous la couenne.

Dans l'équation (2.8), le terme de 'surface' est à associer, soit à la surface correspondant au côté viande du jambon (surface de salage), soit à la surface correspondant au côté couenne du jambon, en fonction de la condition limite considérée. Du côté couenne, il a été admis que l' $a_w$  sur cette surface était et restait égale à 1,0, du fait de la présence d'une couche de gras faisant quelques millimètres d'épaisseur. Par contre, du côté viande, *i.e.* sur la surface de salage, compte tenu de la présence du sel, l' $a_w$  sur cette surface obéit aux équilibres décrits dans les équations suivantes (Rougier, 2006 ; Rougier *et al.*, 2007) :

$$a_{w_{viande\ salée}} = a_{w_{viande\ non\ salée}} \cdot a_{w_{eau\ salée\ de\ la\ viande}} \quad \text{Eq. (2.11)}$$

dans laquelle:

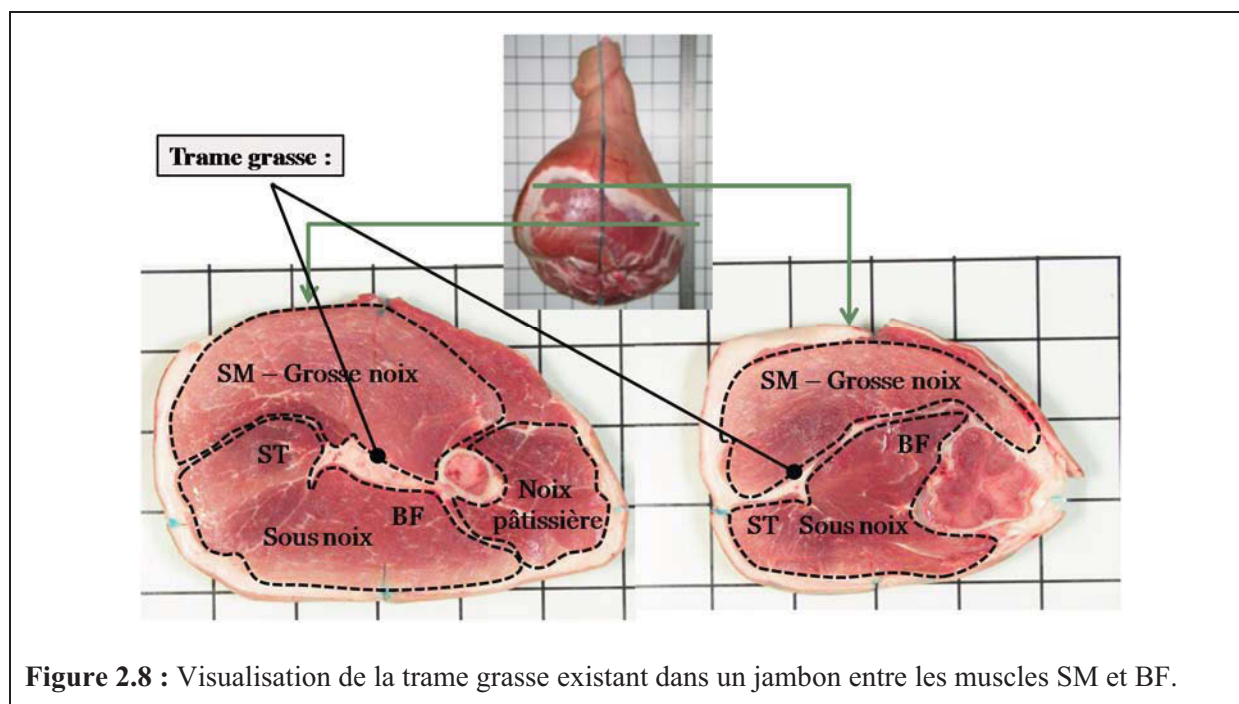
$$a_{w_{viande\ non\ salée}} = a_{w_{gelatine\ sans\ sel}} = 0.993 \cdot \exp(-0.0204 \cdot X_{eau}^{-1,96}) \quad \text{Eq. (2.12)}$$

et

$$a_{w_{eau\ salée\ de\ la\ viande}} = -0.4553 \cdot X_{sel}^{eau^2} - 0.5242 \cdot X_{sel}^{eau} + 0.999 \quad \text{Eq. (2.13)}$$

où  $X_{sel}^{eau}$  représente la concentration en sel exprimée par rapport à la concentration en eau (kg sel.kg eau<sup>-1</sup>).

Dans un jambon frais, il existe une trame de gras appelée veine grasse, qui fait entre 2 et 5 mm d'épaisseur environ, localisée entre les muscles SM, d'un côté, et BF et ST, de l'autre. Cette trame sépare la partie supérieure du jambon de sa partie inférieure (Figure 2.8). Dans la pratique, cette veine grasse est connue pour affecter les transferts de sel et d'eau dans cette zone du jambon.



En conséquence, la présence de cette trame grasse a été incluse dans le modèle de « jambon numérique », en imposant à l'interface entre les groupes de muscles 'grosse-noix' et 'sous-noix' (Figure 2.8), une condition limite de type 'paroi de diffusion mince' avec les caractéristiques suivantes : une épaisseur moyenne de 3 mm et des coefficients de diffusion de l'eau et du sel réduits par rapport à ceux dans la viande maigre, et égaux à, dans cette zone grasse, respectivement,  $10^{-12} \text{ m}^2.\text{s}^{-1}$  et  $10^{-10} \text{ m}^2.\text{s}^{-1}$  (Lebert & Daudin, 2013).

Comme indiqué précédemment, le salage de la surface située côté viande du jambon a été modélisé au travers de l'application d'une saumure sur cette surface (Figure 2.9).

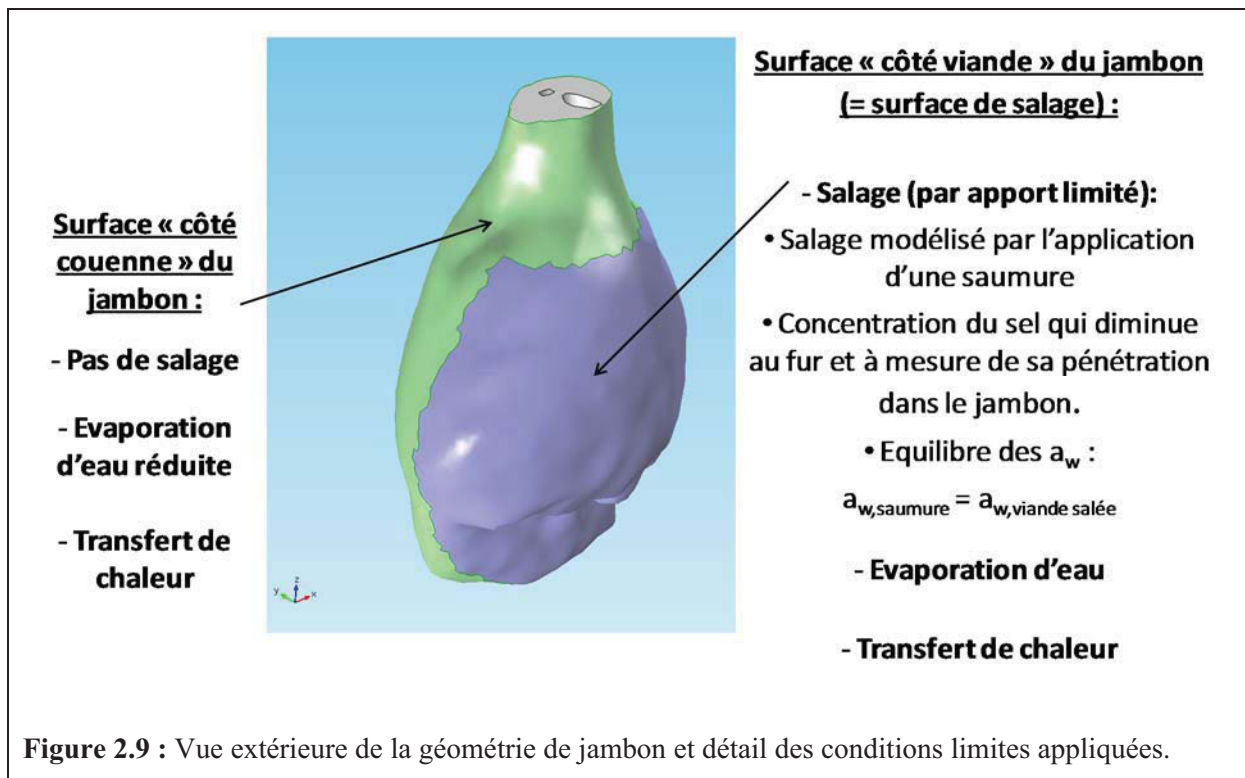


Figure 2.9 : Vue extérieure de la géométrie de jambon et détail des conditions limites appliquées.

Concernant le salage, la condition limite appliquée sur la surface de salage a consisté à écrire l'égalité des  $a_w$  entre la saumure, d'un côté, et la première couche de viande salée en contact avec cette saumure, de l'autre. Cette hypothèse conduit à la relation suivante :

$$a_{w_{saumure}} = a_{w_{viande\ salée}} \quad \text{Eq. (2.14)}$$

Le premier terme de cette équation est calculé à partir de la relation (2.13) et à partir du bilan de sel réalisé à chaque pas de temps lors de l'étape de salage, qui permet de calculer la masse de sel restante et donc la concentration en sel de la saumure (*i.e.* le terme  $X_{sel}^{eau}$ ). Notons, au passage, que dans les conditions de salage simulées dans le modèle numérique présenté dans ce travail (masse initiale de chlorure de sodium de 655 g et volume d'eau de

100 ml), la saumure reste saturée tout au long du salage, ce qui donne une valeur d' $a_w$  de la saumure constante et égale à 0.759.

Le terme de droite de l'équation (2.14) correspond à la relation (2.11). La résolution de l'équation (2.14) permet donc, dans le cas de la viande salée, d'évaluer la concentration en sel exprimée par rapport à l'eau ( $X_{sel}^{eau}$ ), et donc ensuite la concentration en sel de la première couche de viande en équilibre avec la saumure.

Le modèle de « jambon numérique » a été utilisé, dans un premier temps, pour modéliser les transferts de sel et d'eau, ainsi que l'évolution de la protéolyse pendant les étapes de salage réalisé selon la méthode par apport limité et de repos à basse température. La résolution de l'ensemble des équations a été conduite sur un PC doté de 8 processeurs, de 48 Go de RAM et cadencé à 3 GHz, et a nécessité un temps de calcul de 3,5 h pour la période de procédé modélisée.

## **2.8. Article n°2 (publié dans Meat Science 92, 2012, 84-88)**

### **Development of a rapid, specific and efficient procedure for the determination of proteolytic activity in dry-cured ham: Definition of a new proteolysis index**

Rami Harkouss, Pierre-Sylvain Mirade, Philippe Gatellier

INRA, UR370 Qualité des Produits Animaux, F-63122 Saint-Genès-Champanelle, France

#### **Abstract**

A new method was developed to determine proteolysis activity in dry-cured ham using fluorescamine-specific labelling of N-terminal  $\alpha$ -amino groups of peptides and amino acids. Proteins were separated from peptides and amino acids by 10% trichloroacetic acid treatment of ham extracts. Fluorescamine derivation was optimized to prevent reaction with the  $\epsilon$ -amino groups of lysine. Fluorescence of the complex was measured using a microplate procedure and optimum excitation and emission wavelengths of 375 nm and 475 nm, respectively. A new proteolysis index (PI) was defined as the percentage ratio of the N-terminal  $\alpha$  amino group content to the total protein content of the ham extract. The robustness of the method was evaluated by measuring PI in laboratory pork meat samples subjected to standardized processing conditions and in samples extracted from industrial hams taken at different stages of processing. For the industrial samples, a comparison with the classic nitrogen procedure of PI determination was performed and a formula relating the two PIs was established. The

rapidity, sensitivity and specificity of the procedure make it a good candidate for a screening test to evaluate ham quality in industry.

Keywords: Dry-cured ham; Proteolysis index; Fluorescamine; Fluorescence

## Introduction

In dry-cured ham, the main factor affecting final product quality is proteolytic activity. It impacts the flavour and the texture, i.e. the hardness, cohesiveness, and springiness of the product (Arnau, Guerrero, & Sárraga, 1998; García-Garrido, Quiles-Zafra, Tapiador, & Luque de Castro, 2000; Toldrá, & Flores, 2000; Virgili, Parolari, Schivazappa, Bordini, & Borri, 1995; Zhao et al., 2008). Proteolytic activity depends on many factors, such as pH, water content, NaCl content and drying conditions (Arnau, Gou, & Comaposada, 2003; Arnau, Gou, & Guerrero, 1994; Arnau, Guerrero, & Gou, 1997; Arnau, Guerrero, Maneja, & Gou, 1992; Martín, Córdoba, Antequera, Tímon, & Ventanas, 1998; Toldrá, Flores, & Sanz, 1997). In dry-cured ham, a proteolysis index (PI), defined as the percentage ratio of non-protein nitrogen content to total nitrogen content, is widely used to characterize the intensity of proteolytic activity; nitrogen content is determined by the Kjeldahl method, which consists in measuring ammonia after mineralization of the organic matter (Careri et al., 1993; Ruiz-Ramírez, Arnau, Serra, & Gou, 2006; Schivazappa et al., 2002). Although this procedure is commonly used and is standardized (ISO 937-1978 E reference method), it has many drawbacks. It is time- and product-consuming, and it lacks specificity, as there are many nitrogen compounds in meat (ammonium salts, urea, uric acid, creatinine, etc.) that can interfere in the determination of the proteolysis index. A more rapid and efficient assay of peptides and amino acids would thus greatly facilitate the evaluation of proteolysis in dry-cured ham. To this end, we developed a simple, specific fluorometric procedure to determine the level of N-terminal  $\alpha$ -amino groups of peptides and amino acids, which reflects the intensity of proteolytic activity during the curing process. Our procedure is based on the fluorescamine-specific labelling of the N-terminal  $\alpha$ -amino groups present in the fractions of the ham extracts soluble in 10% trichloroacetic acid (TCA). A new proteolysis index was then defined as the percentage ratio of the N-terminal  $\alpha$ -amino group content to the total protein content of the ham extract. Because of the high sensitivity of fluorometric detection, fluorescamine has been extensively used for the quantification of amino acids, peptides and proteins (Bantan-Polak, Kassai, & Grant, 2001; Castell, Cervera, & Marco, 1979; Friguet, Stadtman, & Szewda, 1994; Lorenzen & Kennedy, 1993; Miedel, Hulmes, & Pan, 1989). In



meat, we used this fluorophore to evaluate the proteolysis of skeletal muscle myofibrillar proteins (Morzel et al., 2006).

The new procedure is described here. Its applicability to the analysis of proteolysis was evaluated in small laboratory samples of pork meat processed under well-defined salting and drying conditions, and in industrial dry-cured hams at different stages of processing. For industrial dry-cured hams, a comparison of this new procedure with the commonly used nitrogen content procedure was performed, and a formula was established to convert the new proteolysis index to the classic one.

## **Materials and methods**

### **Preparation of the laboratory salted and dried pork meat samples**

This preparation mimicked the different steps used in industry processing, but was adapted to small samples. Three different muscles, *biceps femoris* (BF), *semi tendinosus* (ST), and *semi membranous* (SM), were used in the preparation of the laboratory samples. First, muscle surfaces were decontaminated by a treatment using 0.1% peracetic acid for 3 min followed by a 1 min rinse with sterile water. This operation was repeated twice. The muscle superficial layers damaged by the acid treatment were discarded, and samples were cut into small parallelepipeds ( $5 \times 4 \times 0.3$  cm). These operations were performed under sterile air using sterile tools. The small pork meat samples were then salted by covering the surface of the piece with a  $300 \text{ g.L}^{-1}$  NaCl solution using a multichannel pipette (Multipette plus, Eppendorf AG, Hamburg, Germany) adjusted to 4  $\mu\text{l}$  per spot. In these conditions, salt diffused so as to achieve a homogenous distribution in a few hours. The quantity of salt added was calculated on the basis of the salt concentration (4% to 13% of the dry matter) and water content (50% to 75%) required in the final pork meat samples. Drying was then performed at 15°C for different times (up to 16 h for the driest samples) until each sample reached the weight corresponding to the selected water content. After checking the water content by determining the dry matter and salt content by chlorometry (MKII Chloride Analyser 926, Sherwood, Cambridge, UK), samples were placed under vacuum in plastic bags and kept in temperature-controlled chambers (Model 14 D-78532, Binder GmbH, Tuttlingen, Germany) at different temperatures (4°C, 14.5°C and 25°C) to obtain various proteolysis kinetics. At the end of the processing, samples were stored at  $-80^\circ\text{C}$  until analysed. Four samples were prepared for each processing condition to make replicates.

### Preparation of the samples extracted from industrial dry-cured hams

PI determinations were performed on Bayonne dry-cured hams. Bayonne ham obtained a Protected Designation of Origin (PDO) certification in 1998 and its characteristics have been described by Robert and Lanore (2003). Three muscles (*biceps femoris*, *semi tendinosus*, and *semi membranosus*) were extracted from three different hams at the end of each main processing stage, i.e. the resting period (11 weeks), drying period (21 weeks), and ageing period (12 months). Samples were taken from each muscle to calculate the new proteolysis index, allowing 24 determinations per muscle type per time (3 hams × 8 samples). For the calculation of the classic proteolysis index, only one sample weighing about 50 g was taken from each muscle of the three hams. Some physical and chemical characteristics of these Bayonne hams (pH, water content and salt content) were determined and are given in Table 2.2.

**Table 2.2:** Characteristics of the Bayonne dry-cured hams at the end of each main processing stage. Water and NaCl contents were calculated on the basis of dry matter. Values were the means  $\pm$  SEM of three determinations (one determination per muscle). Values not bearing common superscripts differed significantly ( $p < 0.05$ ).

		pH	Water content (%)	NaCl content (%)
11 weeks	SM	5.85 $\pm$ 0.05 a	69.8 $\pm$ 0.6 ab	2.67 $\pm$ 0.42 ab
	ST	5.95 $\pm$ 0.09 a	68.0 $\pm$ 0.1 a	4.63 $\pm$ 0.13 a
	BF	5.90 $\pm$ 0.04 a	71.6 $\pm$ 0.2 b	2.39 $\pm$ 0.28 b
21 weeks	SM	5.88 $\pm$ 0.11 a	61.1 $\pm$ 1.2 a	3.38 $\pm$ 0.47 a
	ST	5.87 $\pm$ 0.11 a	65.3 $\pm$ 1.0 ab	3.40 $\pm$ 0.54 a
	BF	5.95 $\pm$ 0.13 a	68.2 $\pm$ 0.5 b	3.72 $\pm$ 0.59 a
12 months	SM	5.68 $\pm$ 0.05 a	56.4 $\pm$ 1.0 a	4.94 $\pm$ 0.22 a
	ST	5.78 $\pm$ 0.03 a	57.2 $\pm$ 1.4 a	5.41 $\pm$ 0.26 a
	BF	5.83 $\pm$ 0.03 a	60.5 $\pm$ 0.7 a	5.72 $\pm$ 0.33 a

### Determination of the new proteolysis index

Pork meat samples were placed for 1 h in cold water (0.7 g in 7 ml) to facilitate subsequent grinding. Extracts from the pork meat samples were prepared by homogenization with a Polytron PT-MR 2100 (Kinematica AG, Switzerland) for 30 s at maximum speed (30,000 rpm); 150  $\mu$ l aliquots of the extract were then removed and diluted with 600  $\mu$ l of 12.5% trichloroacetic acid to precipitate proteins (TCA final concentration 10%). Samples



were shaken for 15 min at 4°C. After centrifuging at 2000g for 10 min, the concentration of peptides and amino acids in the supernatant was measured by the method of Friguet et al. (1994) with slight modifications. First, 300 µl of the supernatant was neutralized with 300 µl of 2 M potassium borate, pH 10. In these conditions, the final pH of the solution was 9.2 +/- 0.1, a value suitable for the reaction with fluorescamine. Second, 180 µl of fluorescamine (Sigma) at a concentration of 0.6 mg.ml<sup>-1</sup> in acetone was added. Free fluorescamine does not fluoresce, but its reaction with primary amines yields a fluorescent pyrrolinone moiety. Fluorescence was measured 1 h after adding fluorescamine by means of a Perkin-Elmer LS 50B spectrofluorometer. A front surface accessory (Perkin Elmer Plate Reader) was installed for measurement in 96-well polystyrene microplates designed for fluorescence. A volume of 200 µl was placed in each well. Analyses were performed at the optimum excitation and emission wavelengths ( $\lambda_{\text{excitation}} = 375 \text{ nm}$  and  $\lambda_{\text{emission}} = 475 \text{ nm}$ ) with excitation and emission slit settings of 10 nm. The non-specific fluorescence of corresponding fluorescamine-untreated samples was subtracted. The level of amino groups in the pork meat extracts was determined by reference to a calibration curve of glycine from 5 mM to 50 mM (concentration of the stock solution before TCA treatment) treated in exactly the same conditions and at the same time as the pork meat extracts. Figure 2.10 shows that fluorescence increased linearly with glycine throughout the range of concentrations used here ( $R^2 = 0.993$ ).

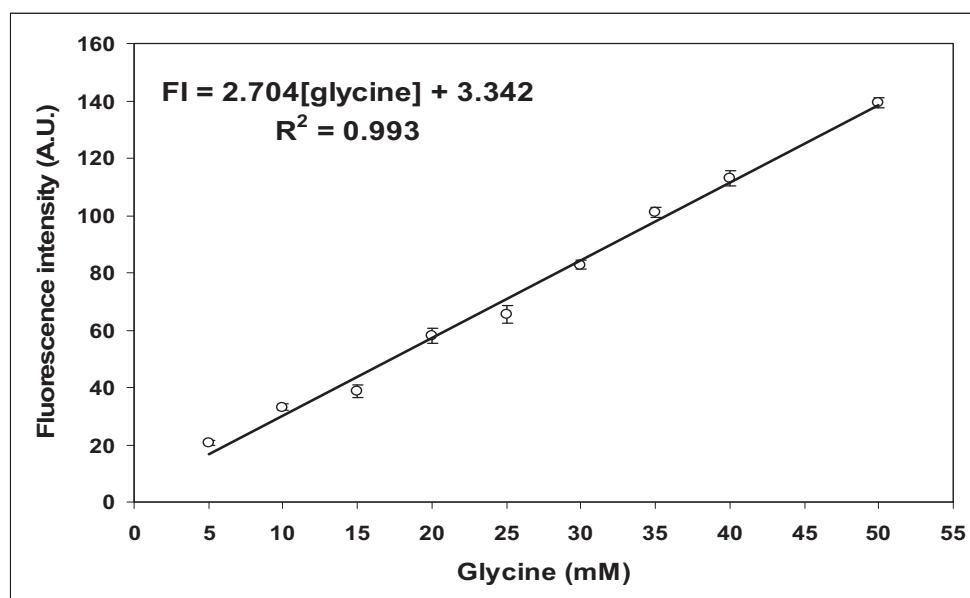


**Figure 2.10:** Calibration curve of glycine with fluorescamine. Glycine concentrations were those of the initial stock solutions before the TCA treatment. Values were the means +/- SEM of four independent determinations.

The level of N-terminal  $\alpha$  amino groups was then expressed in grams of “glycine equivalent” per gram of ham (*A*). In parallel, the total protein content was estimated in the pork meat extract, before treatment, by the biuret method (Gornall, Bardawill, & David, 1949). Results were expressed in grams of protein per gram of ham (*B*). The new proteolysis index was then expressed as the percentage ratio of N-terminal  $\alpha$  amino group content to total protein content according to:

$$\text{PI \%} = (A / B) \times 100 \quad (2.15)$$

### **Determination of the classic nitrogen proteolysis index**

Total nitrogen (TN) was determined by the Kjeldahl method according to the ISO 937-1978(E) reference method, and non-protein nitrogen (NPN) content by precipitation of proteins with TCA followed by determination of nitrogen in the extract by the Kjeldahl method. The proteolysis index was determined as the percentage ratio of NPN to TN (Careri et al., 1993; Ruiz-Ramírez et al., 2006, Schivazappa, et al., 2002).

### **Statistics**

ANOVA was performed at the end of the resting, drying and ageing periods to test the effects of the processing periods and muscle types on the PI values. When a significant effect was observed by ANOVA, the unpaired Student *t*-test was used to determine the levels of statistical significance between groups.

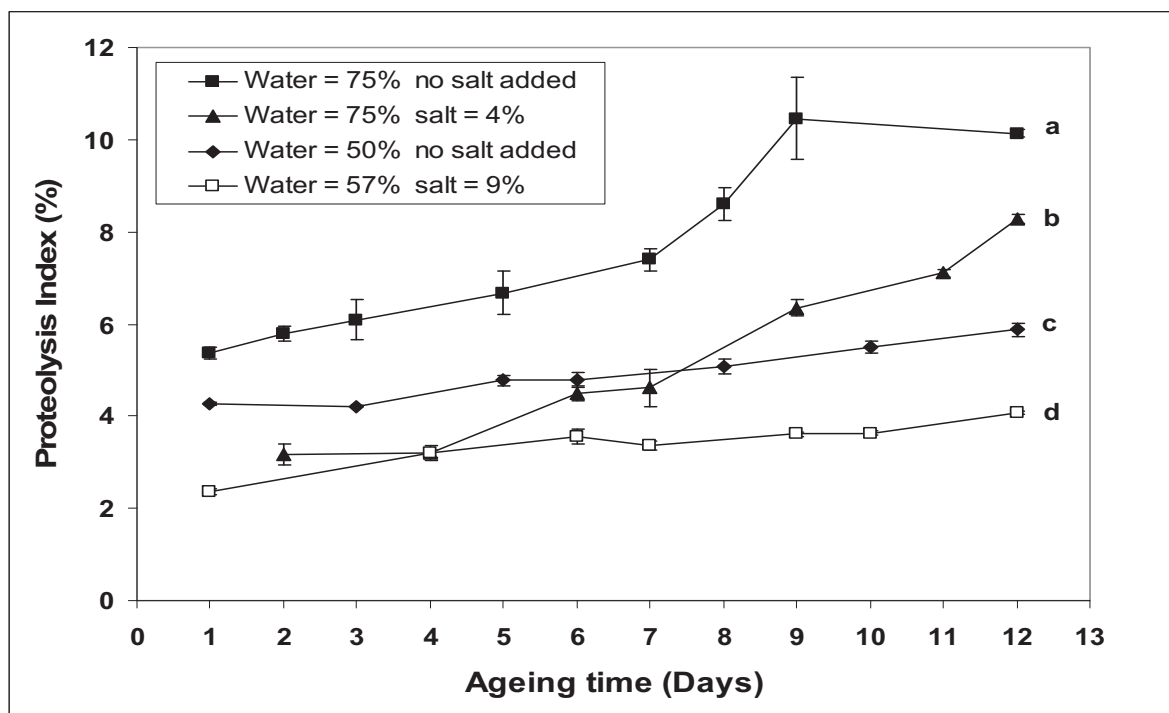
## **Results**

### **Determination of the new proteolysis index in laboratory-dried and salted pork meat samples**

The applicability of the new procedure to characterize proteolysis kinetics was tested first in different laboratory samples processed under well-defined salting and drying conditions. The use of small pork meat samples enabled us to test a large number of conditions in muscles of a single animal, thus circumventing lack of reproducibility due to animal effect. In this case, PI variation cannot be produced by differences in raw material (protease activity, inhibitors, pH, etc.). Another advantage of reducing the product size is that rapid salt diffusion and drying, considerably shortens preparation time (16 h at the very most). A large number of conditions (salting, drying, temperature, time, and muscle type) were tested, but the complete results will

be presented and discussed in a forthcoming paper. The purpose of the present work was only to illustrate the potential of the new procedure for PI determination in a restricted number of conditions and in one muscle only.

The initial value of PI, measured in the *biceps femoris* muscle before processing, was very low (1.04%  $\pm$  0.33%). In Figure 2.11, we see the time course of the PI in pork meat samples prepared from muscle *biceps femoris* and stored under vacuum for 12 days at 25°C. The mean coefficient of variation (ratio of standard deviation to mean value) of this parameter calculated from the whole conditions was 5.3%, demonstrating the good reproducibility of the procedure.



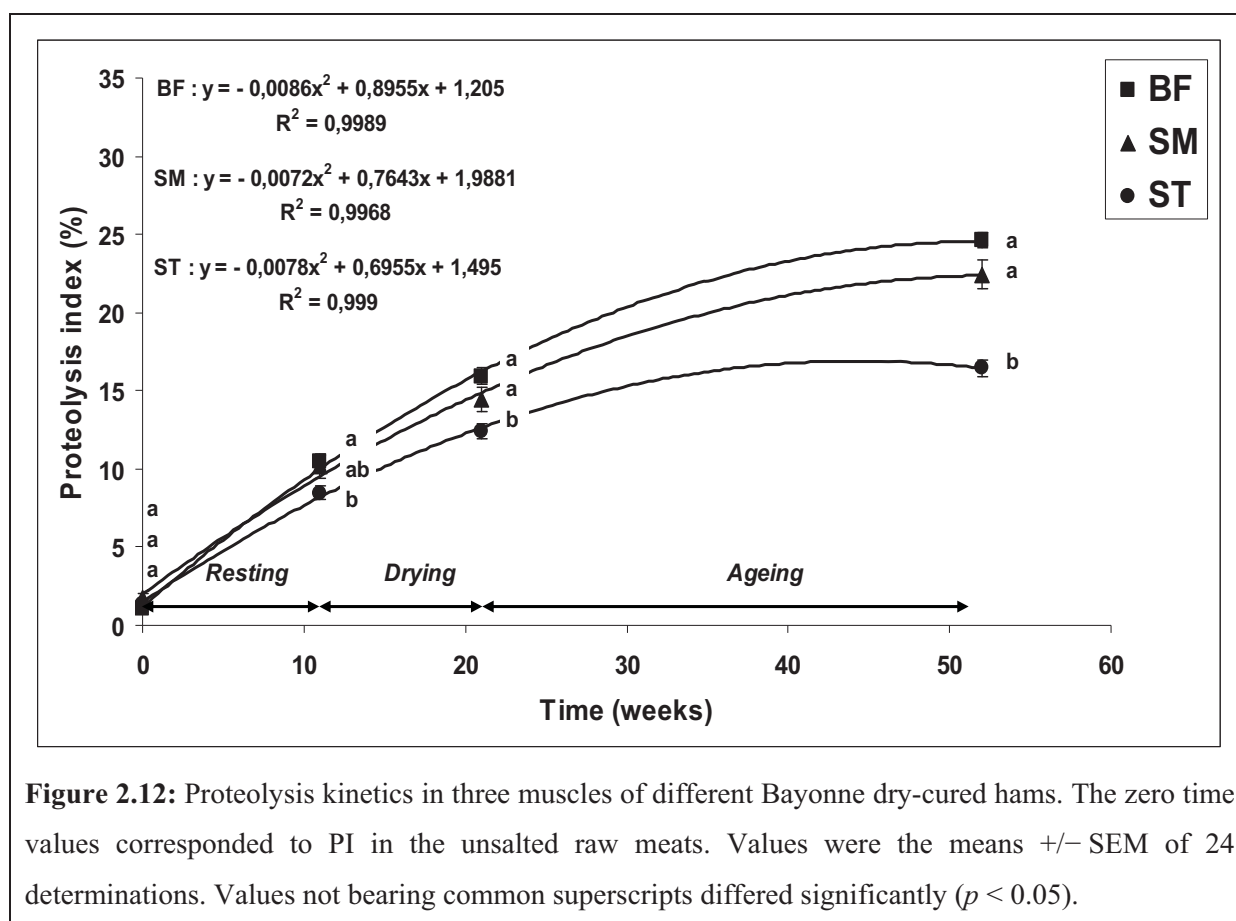
**Figure 2.11:** Proteolysis kinetics in *M. biceps femoris* at 25°C under different processing conditions. Values were the means  $\pm$  SEM of four independent determinations. At the end of ageing, values not bearing common superscripts differed significantly ( $p < 0.001$ ).

Figure 2.11 shows that the untreated samples (75% water and no salt added) exhibited the highest proteolysis index. In this case PI reached a maximum of 10.5% after 9 days of ageing and remained stable for the following 3 days of ageing. Salting alone (to 4% of the dry matter) and drying alone (to 50% of water content) reduced the proteolysis intensity. This effect was much more pronounced when both salting and drying processes were applied (9% salt and 57% water). In this case a 60% decrease in PI value was observed after 12 days of

ageing, compared with the untreated samples. After 12 days of ageing, the four conditions tested exhibited significant differences in PI values among themselves ( $p < 0.001$ ). At lower temperatures (14.5°C and 4°C), the PI increase was considerably reduced (data not shown). These results were in line with those generally reported in the literature demonstrating a decrease in proteolysis activity with increasing salt content (Martin et al., 1998; Robert & Lanore, 2003; Ruiz-Ramírez et al., 2006) and with decreasing temperature (Martin et al., 1998; Robert & Lanore, 2003) or water content (Toldra, Cerveró, & Part, 1993; Toldra et al., 1997).

### Determination of the new proteolysis index in industrial dry-cured ham samples

The applicability of the new procedure to the characterization of proteolysis kinetics was then tested in more realistic conditions by measuring PI in industrial Bayonne hams over a 12-month period (Figure 2.12).



**Figure 2.12:** Proteolysis kinetics in three muscles of different Bayonne dry-cured hams. The zero time values corresponded to PI in the unsalted raw meats. Values were the means  $\pm$  SEM of 24 determinations. Values not bearing common superscripts differed significantly ( $p < 0.05$ ).

Probably owing to the animal effect, the mean coefficient of variation of PI, calculated from the whole conditions, was higher than that previously calculated in laboratory-dried and salted pork meat samples derived from the same animal (19.6% vs. 5.3%). To characterize the

kinetics of proteolysis, the increase in PI with time was fitted by a second-order polynomial regression. Despite the biological variability, good correlation coefficients were obtained from the different curves ( $R^2 > 0.99$ ). As we see in Figure 2.12, the three muscles tested here can be ranked in order of increasing proteolysis speed: BF > SM > ST. BF and SM did not display any significant differences in terms of proteolysis intensity, while proteolysis in ST was always lower than in BF and SM. In the case of BF muscle, a proteolysis increase of 2200% was observed during the overall observation period and of 55% during the ageing period only. These results were in line with those of Zhao et al. (2008), who reported a PI increase in BF muscle of 60% during the last 7 months of ageing. Ruiz-Ramírez et al. (2006) and Toldrá et al. (1997) also reported higher proteolysis in BF muscle than in SM muscle. Like these authors, we can attribute the higher proteolysis in the BF muscle to its higher residual moisture content (Table 2.2), which allows a higher activity of endogenous proteases. Differences between SM and ST muscles could be explained by the fact that for similar water content, ST muscle exhibited higher salt content (Table 2.2).

#### **Relationship between the classic and the new proteolysis indices**

Most of the literature data on dry-cured ham proteolysis have been gained with the classic nitrogen proteolysis index, and so industrial operators have used this index routinely. Hence although we have demonstrated the applicability of this new procedure in different conditions and its many advantages compared with the classic procedure (see Section ‘discussion’), to be accepted by scientists and professionals in the dry-cured ham industry, the new proteolysis index must be easily convertible into the classic index. For this purpose, a conversion equation was established by comparison of the two indices in these same Bayonne hams at the end of the resting, drying and ageing periods. Figure 2.13 shows the relation between the two PIs. The relationship was well fitted with a linear regression model:

$$PI_{\text{classic}} = 0.779 PI_{\text{new}} + 11.081 \quad (r = 0.824, p < 0.001) \quad \text{Eq. (2.16)}$$

Clearly, this conversion formula is valid only so long as the determinations are performed in the conditions described above (see ‘Materials and methods’). Other protocols will require new formulas.

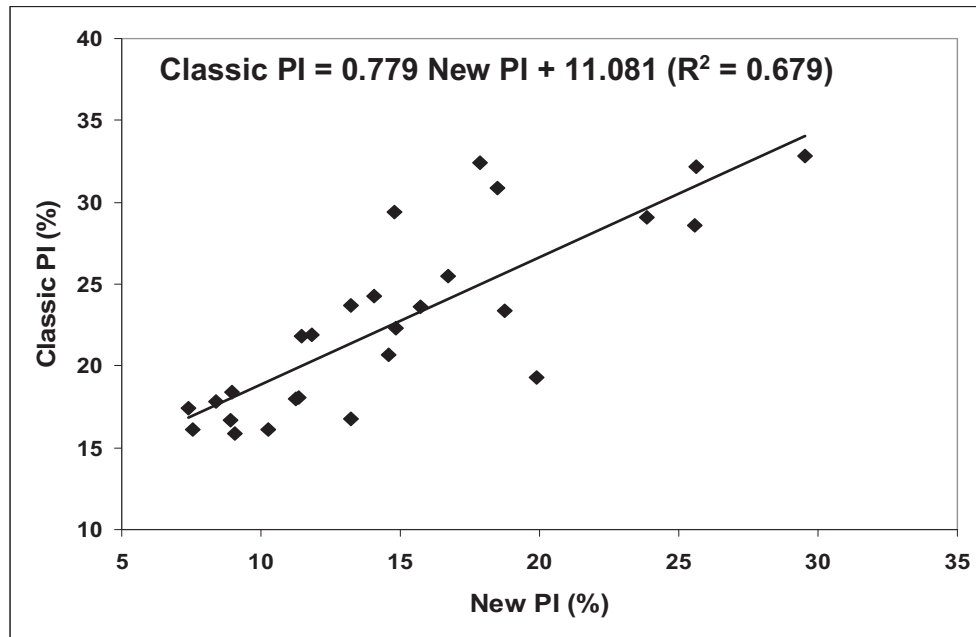


**Figure 2.13:** Relation between the classic proteolysis index (nitrogen index) and the new proteolysis index (fluorescamine index).

## Discussion

This new procedure of PI determination offers many advantages over the classic nitrogen procedure. The fluorometric detection lends it a high sensitivity, which allows work on very small product quantities. Samples of 0.7 g were used in the present study, but we have successfully tested this procedure with smaller quantities of meat (less than 0.1 g, data not shown). Using this procedure, dry-cured hams could be tested during industrial fabrication by punching a small hole in the muscle, without depreciation of the products. In addition, the procedure is rapid; the use of a microplate reader allows fluorescence measurement of 96 samples in less than one minute. The limiting factor in the procedure is the muscle extract preparation, but with trained personnel more than 50 determinations can be performed daily. This procedure also offers a high specificity; fluorescamine does not react with the major non-protein nitrogenous substances commonly present in muscle, i.e. urea, uric acid, creatinine and ammonia (Klein & Standaert, 1976). Fluorescamine can react with the  $\epsilon$ -amino groups of lysine (Dhaunta, Fatima, & Guptasarma, 2011), which are not specific products of the proteolysis. To avoid this, we used conditions such that the reaction of fluorescamine with amino groups was specific for adduction of fluorescamine only to the N-terminal  $\alpha$ -amino groups. The reaction with fluorescamine requires the amino group to be in its unprotonated form (Bohlen, Stein, & Udenfriend, 1974; Castell et al., 1979; Mendez & Gavilanes, 1976;

Bantan-Polak et al., 2001). Since the  $pK_a$  of the N-terminal  $\alpha$ -amino groups of peptides (8.0) is lower than the  $pK_a$  of lysine  $\epsilon$ -amino groups (10.8) (Berg, Tymoczko, & Stryer, 2007), we minimized the conjugation of the label to the lysine compared with the N-terminal  $\alpha$ -amino groups by performing the labelling reaction at pH 9.2; using the Henderson equation, we determined that at pH 9.2, 94% of the N-terminal  $\alpha$ -amino groups were in the reactive unprotonated form ( $NH_2$ ), while the  $\epsilon$ -amino groups of lysine were almost entirely (98%) in the non-reactive protonated form ( $NH_3^+$ ). It was for that very reason that in peptides containing lysine residues, Dhaunta et al. (2011) failed to detect any evidence of labelling of this residue with fluorescamine in a reaction pH range of 8.0 to 10.0. Also, fluorescamine does not react with secondary amines such as the amino groups of histidine and arginine side chains (Dhaunta et al. 2011; Weigele, De Bernardo, Teng, & Leimgruber, 1972). Finally, it may be safely asserted that the new procedure is more powerful than the classic procedure in that it describes the progress of the proteolytic activity more finely. For example, in the case of the complete degradation of a decapeptide, the classic procedure cannot discriminate between the decapeptide containing 10 nitrogen atoms and the sum of the 10 corresponding amino acids each containing one nitrogen atom. In such a case, the PI remains unchanged. By contrast, our new procedure distinguishes between the decapeptide (one N-terminal  $\alpha$ -amino group) and the corresponding amino acids (10 N-terminal  $\alpha$ -amino groups). In this case the PI is multiplied by ten.

## **Conclusion**

Based on these results, the fluorescamine-specific labelling of the N-terminal  $\alpha$ -amino groups of peptides and amino acids offers a powerful technique to determine proteolysis intensity in dry-cured ham. In addition, we have developed a procedure for the easy detection of labelled amino groups in a fluorescence microplate reader. This study demonstrates some advantages of this procedure over the classic nitrogen procedure. It offers the possibility of rapidly determining peptides produced during the process on small amounts of sample. The easy conversion of PI values obtained with this new procedure into the classic PI values allows the fluorescamine method to be used directly in industry as a reference method for PI determination in dry-cured hams.

## Acknowledgments

This work was funded by the Na-integrated programme (ANR-09-ALIA-013-01) financed by the French National Research Agency. We thank H. Safa for participating in some of the laboratory work, S Portanguen, L. Aubry and J.D. Daudin for discussing the protocol of preparation of the laboratory pork meat samples, ADIV for measuring the classic PI in industrial Bayonne ham samples, and ATT for language editing.

## 2.9. Conclusions

Au cours de ce travail de thèse, sur le plan des méthodes, une nouvelle procédure de détermination de l'indice de protéolyse a été mise et au point et validée sur des échantillons extraits de jambons de Bayonne. Cette procédure est rapide et nécessite moins de 0,5 g de matière. Parallèlement au développement de cette méthode de mesure de l'IP, de façon à s'affranchir des contraintes liées à l'utilisation et au coût de jambons industriels, un protocole expérimental particulier a été établi, permettant de conditionner rapidement au laboratoire, en minimisant au maximum le risque d'action microbienne, des échantillons de muscles de porc « frais », selon des conditions de salage et de séchage bien maîtrisées et correspondant au plan d'expériences de type surface de réponse mis en place. Au final, l'ensemble de cette démarche expérimentale autorise une quantification de l'évolution de la protéolyse au sein d'un grand nombre d'échantillons de muscle de porc préalablement salés et/ou séchés. Cela était la condition *sine qua non* de l'établissement de lois robustes de calcul de la protéolyse dans différents muscles de porc, en fonction de la température de traitement et des teneurs en eau et en chlorure de sodium, suite à l'application d'une approche statistique de type régression polynomiale multiple ; ces lois devant ensuite être intégrées et couplées aux lois physiques de transferts (chaleur, matière) dans un modèle 3D de « jambon numérique ».

De plus, le même type d'approche statistique a été rigoureusement employé afin de bâtir des lois d'évolution permettant de relier plusieurs paramètres caractérisant la structure (nombre et taille des fibres musculaires, espaces extracellulaires...) et la texture (dureté, fragilité, cohésion, souplesse, adhésion) d'un jambon sec en cours de fabrication, à l'évolution de l'IP et des teneurs en eau et en sel.



## **Chapitre 3 : RESULTATS et DISCUSSION**

---



### 3.1. Introduction

Outre la méthode de dosage de l'intensité de protéolyse mise au point au cours de ce travail de thèse et qui a été détaillée dans le chapitre précédent, les autres résultats majeurs sont présentés et discutés dans ce troisième chapitre, principalement par l'intermédiaire de 3 articles scientifiques.

Le premier article (article n°3) décrit le cheminement scientifique : préparation des échantillons, plan d'expériences de type surface de réponse, analyse statistique par régression linéaire multiple, qui a conduit à l'établissement de modèles phénoménologiques permettant de calculer l'indice de protéolyse dans des échantillons de viande de porc, salés et séchés, préparés à partir de différents muscles d'un jambon, connaissant la température de traitement et leurs teneurs en eau et en sel. Le conditionnement de ces échantillons a été imaginé et mis en place, de façon à reproduire au mieux ce qui se passe, en termes de transferts (chaleur, eau, sel), dans un jambon de porc lors des différentes étapes de fabrication : salage, repos, étuvage, séchage et affinage/maturation.

Sur la base de travaux expérimentaux (mesures de l'IP, de paramètres structuraux et de paramètres texturaux) conduits sur des échantillons de viande de porc prélevés sur 2 muscles différents extraits de jambons de Bayonne et suite à une analyse statistique consistant à faire une régression polynomiale multiple sur les données expérimentales, l'article n°4 a pour objectif principal de rechercher des corrélations significatives entre les dynamiques d'évolution de la protéolyse, de la structure et de la texture au sein d'un jambon sec, tout au long de sa fabrication.

Le dernier article de ce chapitre (article n°5) présente le couplage réalisé numériquement entre les modèles phénoménologiques de quantification de la protéolyse décrits dans l'article n°3 et des modèles physiques de transferts de chaleur et de masse. Cet ensemble de modèles constitue, au final, le modèle de « jambon numérique ». Cet outil numérique permet de prédire quantitativement, en 3D, la dynamique d'évolution de l'intensité de la protéolyse, des concentrations en eau et en sel, ainsi que de l' $a_w$ , à l'intérieur d'une géométrie réelle de jambon. Les résultats numériques analysés dans l'article n°5 correspondent aux phases de fabrication se déroulant à basse température, *i.e.* la phase de salage suivi d'un repos.

La dernière partie de ce chapitre consiste en une discussion critique et objective des principaux résultats de ce travail. Elle repose sur 3 axes majeurs de réflexion relatifs à :

- La mise au point de la méthode rapide et sensible de mesure de l'indice de protéolyse et sa comparaison par rapport à la méthode de dosage classique ;
- La dynamique d'évolution de la protéolyse mesurée dans des échantillons de viande de porc préparés au laboratoire, mais aussi dans des échantillons directement extraits de jambons secs industriels ;
- Le développement du modèle de « jambon numérique », avec, d'une part, l'intégration des modèles phénoménologiques de calcul de l'indice de protéolyse en fonction de la température et des teneurs en sel et en eau, et d'autre part, le fait que ce simulateur, dans sa version actuelle, ne tienne pas compte de la diminution du volume du jambon au cours du séchage qui équivaut à environ 40% de son volume initial.

### 3.2. Article n°3 (publié dans *Food Chemistry* 151, 2014, 7-14)

#### **Building phenomenological models that relate proteolysis in pork muscles to temperature, water and salt content**

Rami Harkouss<sup>a</sup>, Hassan Safa<sup>a</sup>, Philippe Gatellier<sup>a</sup>, André Lebert<sup>b</sup>, Pierre-Sylvain Mirade<sup>a</sup>

<sup>a</sup> INRA, UR370 Qualité des Produits Animaux, F-63122 Saint-Genès-Champanelle, France.

<sup>b</sup> Institut Pascal, UMR6602 UBP/CNRS/IFMA, 24 avenue des Landais, BP80026, 63171

Aubière Cedex, France.

#### **Abstract**

Throughout dry-cured ham production, salt and water content, pH and temperature are key factors affecting proteolysis, one of the main biochemical processes influencing sensory properties and final quality of the product. The aim of this study was to quantify the effect of these variables (except pH) on the time course of proteolysis in laboratory-prepared pork meat samples. Based on a Doehlert design, samples of five different types of pork muscle were prepared, salted, dried and placed at different temperatures, and sampled at different times for quantification of proteolysis. Statistical analysis of the experimental results showed that the proteolysis index (PI) was correlated positively with temperature and water content, but negatively with salt content. Applying response surface methodology and multiple linear

regressions enabled us to build phenomenological models relating PI to water and salt content, and to temperature. These models could then be integrated into a 3D numerical ham model, coupling salt and water transfers to proteolysis.

Keywords: proteolysis; pork muscle; water and salt content; temperature; Doehlert design; response surface methodology; multiple linear regression.

### **Introduction**

During dry-cured ham production, the main biochemical mechanism affecting the tenderization of meat and the quality of the final product (texture, flavour and appearance) is proteolysis, resulting from the action of proteolytic endogenous enzymes, such as cathepsins and calpains, which remain active for a long time (Arnau, Guerrero, & Sárraga, 1998; Garcia-Garrido, Quiles-Zafra, Tapiador, & Luque de Castro, 2000; Tabilo, Flores, Fiszman, & Toldra, 1999; Toldra & Eheringnton, 1988; Toldrá & Flores, 2000; Virgili, Parolari, Schivazappa, Bordini, & Borri, 1995; Zhao, Tian, Liu, Zhou, Xu, & Li, 2008). A literature review showed that many factors influence proteolytic activity, such as temperature, salt content, water content and pH. The effect of temperature has been described in previous studies (Arnau, Guerrero, & Gou, 1997; Parolari, Virgili, & Schivazappa, 1994, among others). Morales, Serra, Guerrero, and Gou (2007b) showed that letting Biceps femoris (BF) muscle age at 30 °C increased PI significantly compared with hams aged at 5 °C. It is well known that temperature rise promotes cathepsin B and L activity and it has been observed that high temperatures during the drying-ageing stage favour the formation of non-protein nitrogen compounds, which increases PI. However, at the same time, a high enzyme activity results in uncontrolled hydrolysis, leading to an anomalous texture or even an undesirable colour in the product. The effect of NaCl content has also been widely demonstrated (Garrido, Domínguez, Lorenzo, Franco, & Carballo, 2012; Rico, Toldrá, & Flores, 1990; Sárraga, Gil, Arnau, Monfort, & Cussó, 1989). Studies report that PI increases in hams as salting time is shortened. A high concentration of NaCl may inhibit the enzymes responsible for proteolytic activity. For example, cathepsin D, the most active cathepsin throughout the dry-curing of ham, loses more than 70% of its activity at a salt concentration of 5%. However, the reduction of salt may pose a major problem in terms of colour formation and stability, as reported by Benedini, Parolari, Toscani, and Virgili (2012). High salt concentration significantly affected the yellow colour of fat as a result of a high rate of autoxidation, and the red colour of meat as a result of greater penetration of nitrate and nitrite, generating nitrosomyoglobin, responsible for the characteristic pink colour of cured meats. Martin, Cordoba, Antequera, Timon, and Ventanas

(1998) related pasty texture to the amount of salt adsorbed during the salting stage. Garrido et al. (2012) also related increased hardness of meat to an increase in salt content. Studies have often found a relation between salt concentration and water content, another factor affecting proteolysis and texture. High water content increased water activity ( $a_w$ ) and in turn, the proteolytic activity. Serra, Ruiz-Ramirez, Arnau and Gou (2005) highlighted a negative non-linear relationship between hardness and water content, but a positive relationship with cohesiveness and springiness. Time is also important for proteolysis. Some studies have shown that one month storage at 30 °C augments proteolysis, thereby increasing the pastiness of BF muscle (Arnau et al., 1997), whereas at the same temperature after one week, pastiness, adhesiveness and softness decrease in BF, without obviously affecting  $a_w$  or proteolysis (Morales et al., 2007b). Finally, the activity of proteases, like that of all enzymes, depends on an optimal pH. In dry-cured ham, since the pH rarely exceeds 6.2, only proteases acting in slightly acid pH will be active, such as cathepsins B, D, H and L (García-Garrido et al., 2000). By contrast, several studies found greater hardness in hams with  $pH_{24} < 5.8$  than in hams with  $pH_{24} > 6.2$ , whereas others highlighted harder dry-cured hams with  $pH_{24}$  between 5.6 and 6 than with  $pH_{24} < 5.6$  (Arnau et al., 1998). In addition to these physicochemical factors (pH, temperature, water and salt content), the type of muscle may also affect the time course of proteolysis during the ham dry-curing process, since the percentage of myofibrillar and sarcoplasmic proteins differs from one muscle to another. Studies have reported that the above factors act on proteolysis in meat. However, the interaction between these factors has not yet been elucidated. Also, no study describes the time course of proteolysis as a function of temperature, salt content, water content and muscle type.

Response surface methodology (RSM) is commonly defined as a collection of mathematical and statistical techniques that explore the relationships between several independent variables, termed input or explanatory variables, and one or more response (or output) variables. RSM is generally based on fitting a polynomial equation to the experimental data obtained through a designed sequence of experiments. Many applications of RSM can be found in the literature, e.g. in analytical chemistry (Bezerra, Santelli, Oliveira, Villar, & Escaleira, 2008), and in meat science. For example, Zhao, Zhou, Wang, Xu, Huan, and Wu (2005) evaluated the effects of temperature, salt content, pH and nitrite content on the activities of cathepsin B and L, using RSM based on a Box-Behnken design, and calculated the actual activities of these cathepsins during Jinhua ham processing. Jakobsen and Bertelsen (2000) developed a response surface model to predict the effects of temperature, storage time and oxygen partial pressure on the colour stability and lipid oxidation of fresh beef muscle. They concluded that

RSM was a very promising tool for modelling chemical quality changes in meat stored under various conditions, providing that the broad biological variability among animals could be controlled. From the combined use of a RSM approach and a full factorial design with six factors, Møller, Jakobsen, Weber, Martinussen, Skibsted, and Bertelsen (2003) found that the interactions between packaging and storage conditions were crucial to limiting light-induced oxidative discoloration of cured ham packaged in a modified atmosphere during the 14 days of chill storage. More recently, Jin, He, Zhang, Yu, Wang, and Huang (2012) used RSM coupled with central composite design to investigate the effects of temperature (from 15 to 35 °C) and sodium chloride content (from 0.5 to 4.0%) on lipid oxidation in minced pork muscle, demonstrating that both temperature and NaCl content had significant pro-oxidant effects, and also extremely significant interaction for lipid oxidation.

In the present study, RSM was investigated in a way similar to that detailed in Zhao et al. (2005) and Jin et al. (2012) to spotlight the interactive effect of the different factors affecting proteolysis time course in dry-cured ham, and so build phenomenological models that map proteolysis throughout the process. The objective of this study was to quantify the effects of salt content, temperature, water content and muscle type, together with their interactions, on proteolytic activity in laboratory-prepared, dried, salted small pork meat samples, and thereby to determine models to quantify PI as a function of these factors. In future work, these models could be incorporated into a global finite-element model coupling salt and water transfers with proteolysis in a 3D “numerical” ham that is cured and dried for several months.

## Materials and methods

### Preparation of the laboratory pork meat samples

This study required a very large number of pork meat samples to be prepared rapidly under pre-defined, accurate temperature, salt content and moisture values. To do this, we decided to work from fresh pork muscles rather than from samples taken directly from dry-cured hams, from which it is very difficult to obtain samples with the desired salt and water content.

Fig. 3.1 details the experimental protocol followed to prepare and condition the small salted and/or dried pork meat samples, before quantifying proteolysis. Every stage in this figure, i.e. decontamination, cutting, salting, drying, and proteolysis quantification, required much preliminary experimental work to determine the best way to proceed. Eight fresh hams of average weight  $10.6 \pm 0.75$  kg were selected at a local slaughterhouse. Five different muscles,

Biceps femoris (BF), Semitendinosus (ST), Semimembranosus (SM), Rectus femoris (RF) and Gluteus medius (GM) were extracted from each ham four days *post mortem*. Their moisture content and pH were respectively  $74.7 \pm 1.7\%$  and  $5.74 \pm 0.13$ . Entire muscles were vacuum-packed in plastic bags, frozen in an ultra-low temperature freezer (Bio Memory, Froilabo) at  $-80\text{ }^{\circ}\text{C}$  and stored for later use. Muscle surfaces were decontaminated twice under an extractor fan by treatment with 0.1% peracetic acid for 3 min followed by 1 min rinsing-out with sterile water. Samples were then cut into small slabs ( $5 \times 4 \times 0.3\text{ cm}$ ) after discarding the superficial muscle layers damaged by the acid treatment. These operations were performed under sterile air conditions using sterile tools. Samples were prepared so as to obtain a final mass greater than 5 g per sample in order to perform all the biochemical tests; samples were then vacuum-packed in bags and frozen at  $-80\text{ }^{\circ}\text{C}$  until needed. The small pork meat samples were then thawed and salted by covering the surface of the piece with a  $300\text{ g.L}^{-1}$  NaCl solution using a pipette (Eppendorf AG, multipette plus, Hamburg, Germany) adjusted to  $4\text{ }\mu\text{l}$  per spot. The thinness of the samples allowed the salt to diffuse rapidly, in a few hours, and homogeneously. The quantity of salt added was calculated on the basis of the salt concentration (1 to 15% of the dry matter - DM) and the water content (50 to 75% of the total matter - TM) required in the final pork meat sample. The uncertainty of salting of these small pork meat samples was evaluated from preliminary experiments; it was found to range from 0.1% DM for the least salted (1.1% DM) samples to 0.8% DM for the most salted (14.9% DM) samples. The next step was drying; this was carried out under sterile air conditions at  $15\text{--}16\text{ }^{\circ}\text{C}$  for different periods of time (up to 22 hours for the most thoroughly dried samples) until each sample reached the weight corresponding to the selected water content. Applying this simple procedure allowed the uncertainty of drying to be maintained below 1% TM, whatever the final desired water content (from 56.3 to 68.5% TM). Samples were then vacuum-packed in plastic bags and kept in controlled-temperature chambers (Model 14 D-78532, Binder GmbH, Tuttlingen, Germany) at various temperatures (3, 13 and  $24\text{ }^{\circ}\text{C}$ ) in order to study the proteolysis kinetics.

Preliminary tests gave an estimation of 35, 25 and 13 days, respectively, for the shelf-life of these small samples at these three temperatures, without observing any microbiological growth, so that only proteolysis resulting from endogenous enzyme activity occurred, i.e. that taking place inside hams during the drying and curing processes, and not the degrading action of some microorganisms, which leads to an exponential increase in PI and an increasingly unbearable odour. Once prepared, the samples were finally stored at  $-80\text{ }^{\circ}\text{C}$  before final



analysis (PI, salt and water contents). Four samples were prepared for each processing condition.

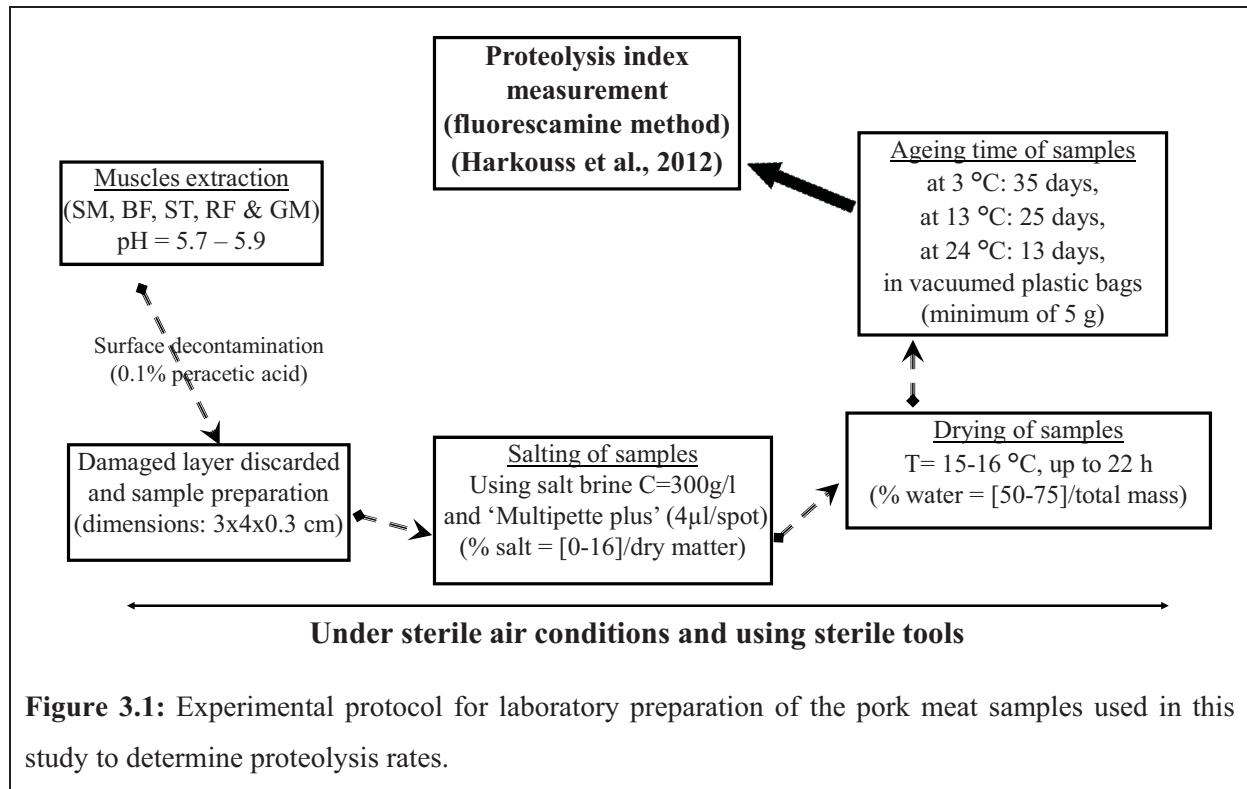


**Figure 3.1:** Experimental protocol for laboratory preparation of the pork meat samples used in this study to determine proteolysis rates.

### Quantification of the proteolysis

In parallel to the preparation of the laboratory pork meat samples, to cope with the large number of samples to be analysed, a rapid, accurate, fluorometry-based procedure was developed to determine sample PI. In this procedure, the new PI is defined as the percentage of the ratio of the N-terminal  $\alpha$ -amino group content (A) to the total protein content (B). The content (A), which reflects the real intensity of proteolytic activity occurring during the process, was measured by the fluorescamine method (Harkouss, Mirade, & Gatellier, 2012), and content (B) by the biuret method (Gornall, Bardawill, & David, 1949). This procedure is more rapid, more specific and more economical in raw materials than classical methods, e.g. the classic nitrogen method, and could also be easily used in industry. Full information on this powerful technique can be found in Harkouss et al. (2012).

Preliminary tests of quantification of proteolysis performed on some small laboratory-prepared pork meat samples revealed that over the periods of time investigated (i.e. 13, 25 and 35 days, depending on temperature) proteolysis kinetics could be approximated by straight lines, and thus characterized by a slope representing a rate of protein degradation.

### Response surface methodology and Doehlert design

In the present study, a response surface methodology based on a Doehlert design was used to investigate the interaction between temperature, water and salt content on the proteolysis time course in small laboratory pork meat samples, with the final objective of building phenomenological models allowing proteolysis to be quantified in pork muscles as a function of these factors.

A Doehlert design (Doehlert, 1970) was implemented on the basis of three factors for each muscle: temperature, water content and salt content. This particular design offers a uniform distribution of points over the whole experimental region, arranged in a rhomboidal figure. In the case of three-variable designs, a cuboctahedron is produced geometrically. It is important to note that in a Doehlert design, the number of levels is not the same for all variables: in a three-factor problem, the first factor is studied at three levels, the second at five levels and the third at seven levels. Although pH is also a key factor for the proteolysis time course, pH was not included in the present Doehlert design. The pH of green muscles had been previously measured and found to range between 5.6 and 5.9. The selection of the independent variables and their levels was made in accordance with values commonly found in industrial production of dry-cured ham. The different levels of each factor were chosen as: five levels for water content, centred at 62.5% (50 to 75% TM), seven levels for salt content, centred at 8% (0 to 16% DM) and three levels for temperature, centred at 13 °C (approximately 2 to 26 °C). This design allowed the number of manipulations to be decreased from 105 to 13 experiments per muscle (Table 3.1). Also, the centre of this experimental design was repeated twice to take into account animal variability; at this particular design point, kinetics of proteolysis were recorded on ten small samples prepared from muscles belonging to a different animal each time. Finally, 15 proteolysis kinetics were determined for each muscle, with 10 points (samples) per plot and four measurements per sample, i.e. a total of 3,000 experimental proteolysis quantification items for all five muscles.

For each muscle investigated, the quadratic polynomial regression equation was taken as given by RSM:

$$Y = \alpha_0 + \sum \alpha_i \cdot X_i + \sum \alpha_{ii} \cdot X_{ii}^2 + \sum \sum \alpha_{ij} \cdot X_i \cdot X_j + \lambda_i \quad \text{Eq. (3.1)}$$

where  $Y$  is the response variable (proteolysis),  $\alpha_0$  is the constant coefficient (intercept),  $\alpha_i$  is the linear coefficient,  $\alpha_{ii}$  is the quadratic coefficient,  $\alpha_{ij}$  is the two-factor interaction coefficient, and  $\lambda_i$  is the random error. Eq. (3.1) describes the linear, quadratic and interaction

effects of the three variables  $T$  (temperature),  $W$  (water content) and  $S$  (salt content) on the response value (proteolysis rate).

**Table 3.1:** Details of the Doehlert design built and results of proteolysis rate obtained as a function of pork muscle type (SM: semimembranosus, BF: biceps femoris, ST: semitendinosus, RF: rectus femoris and GM: gluteus medius).

List of experiments of Doehlert design	Temperature (°C)	Salt content (% dry matter)	Water content (% total mass)	Muscle SM (% PI/day)	Muscle BF (% PI/day)	Muscle ST (% PI/day)	Muscle RF (% PI/day)	Muscle GM (% PI/day)
Exp. 1a (centre)	13	8.0	62.5	0.09	0.06	0.10	0.09	0.06
Exp. 1b (centre)	13	8.0	62.5	0.10	0.07	0.09	0.09	0.05
Exp. 1c (centre)	13	8.0	62.5	0.09	0.08	0.08	0.10	0.07
Exp. 1 (mean)	13	8.0	62.5	0.09	0.07	0.09	0.09	0.06
Exp. 2	13	8.0	75.0	0.08	0.10	0.13	0.22	0.08
Exp. 3	13	14.9	68.5	0.11	0.11	0.10	0.10	0.08
Exp. 4	24	10.3	68.5	0.31	0.17	0.26	0.37	0.35
Exp. 5	13	8.0	50.0	0.05	0.06	0.05	0.06	0.05
Exp. 6	13	1.1	56.3	0.06	0.08	0.08	0.13	0.08
Exp. 7	3	5.7	56.3	0.04	0.04	0.05	0.06	0.04
Exp. 8	13	1.1	68.5	0.13	0.12	0.16	0.19	0.13
Exp. 9	3	5.7	68.5	0.03	0.06	0.08	0.12	0.06
Exp.10	13	14.9	56.3	0.02	0.05	0.04	0.02	0.03
Exp. 11	3	12.6	62.5	0.04	0.05	0.09	0.04	0.04
Exp. 12	24	10.3	56.3	0.12	0.18	0.13	0.24	0.17
Exp. 13	24	3.4	62.5	0.25	0.21	0.33	0.27	0.35

### Statistical analysis

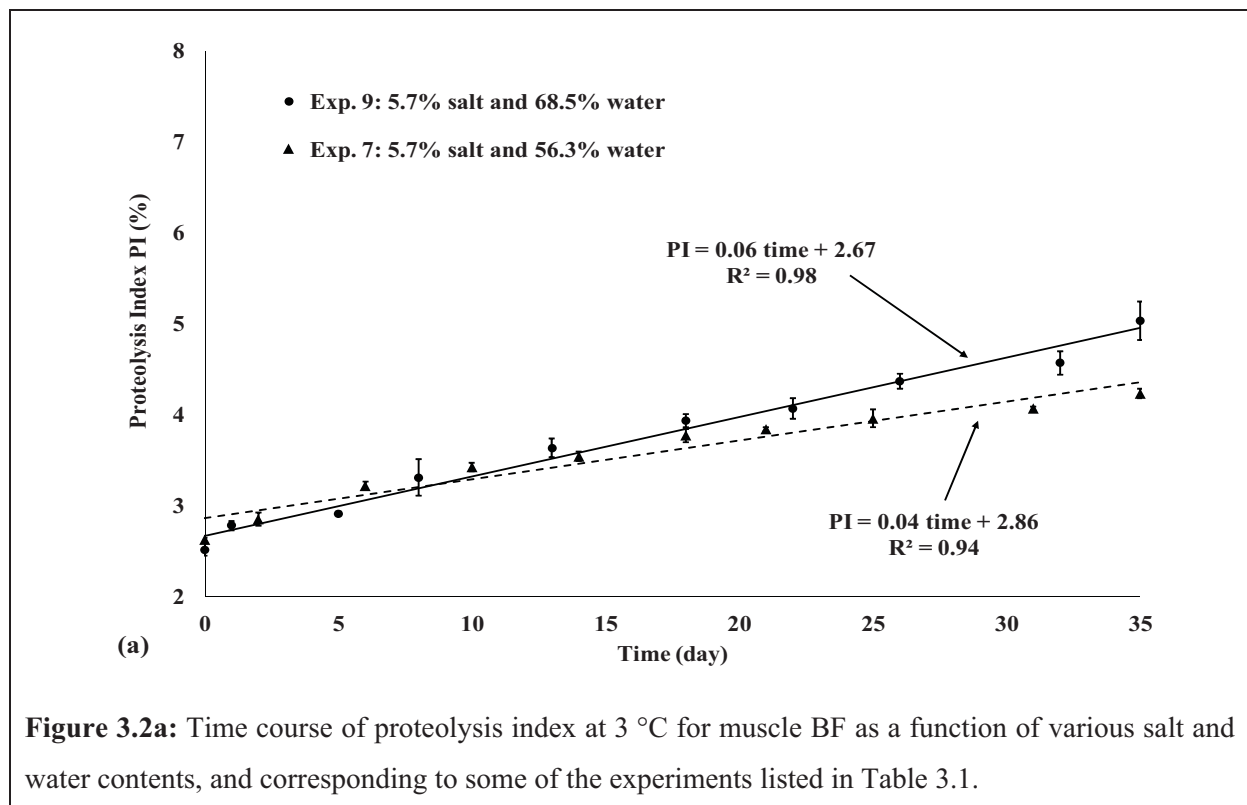
All statistical analyses were performed using R 3.0.1 software (R Development Core Team, 2013), the statistical packages ‘car’ (Fox & Weisberg, 2011), ‘HH’ (Heiberger, 2013), ‘leaps’ (Lumkey, 2009) and the graphical package ‘rgl’ (Adler & Murdoch, 2013). A three-way analysis of variance (ANOVA) was performed on all the proteolysis kinetics obtained for the five muscles ST, SM, BF, RF and GM. The objective was to assess the effect of each factor (temperature, water and salt content) on PI. The effect of muscle type was also studied. *Post hoc* procedures were used when the  $F$ -test was significant ( $p < 0.05$ ). Multiple comparisons among means were examined by the Fisher’s least significant difference (LSD) test, for temperature, water and salt content. Multiple linear regressions were performed in order to find the best model of proteolysis time course as a function of the factors studied for each muscle, and their interactions. As advocated by Fox and Weisberg (2011), regression diagnostics such as ‘Component+Residual’ plots were performed to investigate non-linearity problems, hat values, Studentized residuals and Cook’s distances to identify outlier points, and finally model factors selection by exhaustive search, forward or backward stepwise, or

sequential replacement (Mallows's  $C_p$  and Schwartz's information criterion: BIC). Using the previous models, the response surface of proteolysis rate was plotted in 3D as a function of temperature, salt and water content.

## Results and discussion

### Time course of proteolysis at low temperature (3 °C)

Results confirmed that the proteolysis time course could be described linearly with time ( $R^2 \geq 0.93$ ) in the laboratory-prepared pork meat samples, at 3 °C. In general, at this temperature protein degradation of the different muscles was very slow ( $0.06 \pm 0.02\%$  PI/day). Similar results were obtained by Costa-Corredor, Serra, Arnau and Gou (2009), who indicated that increasing post-resting temperature to above 5 °C reduced processing time. Hence at low temperature, proteolysis needs more time to progress. In the present study, at 3 °C, the proteolysis indices were generally low; more than 35 days being required to increase PI from  $2.97 \pm 0.59$  to  $4.95 \pm 0.99\%$ . The same results have been reported in several previous studies, thus confirming that PI at low temperature ( $\leq 5$  °C) is lower than at higher temperatures (Martin et al., 1998). Fig. 3.2a shows that there was also a slight effect of drying on proteolytic activity of the enzymes, clearly visible from day 20 (Fig. 3.2a).

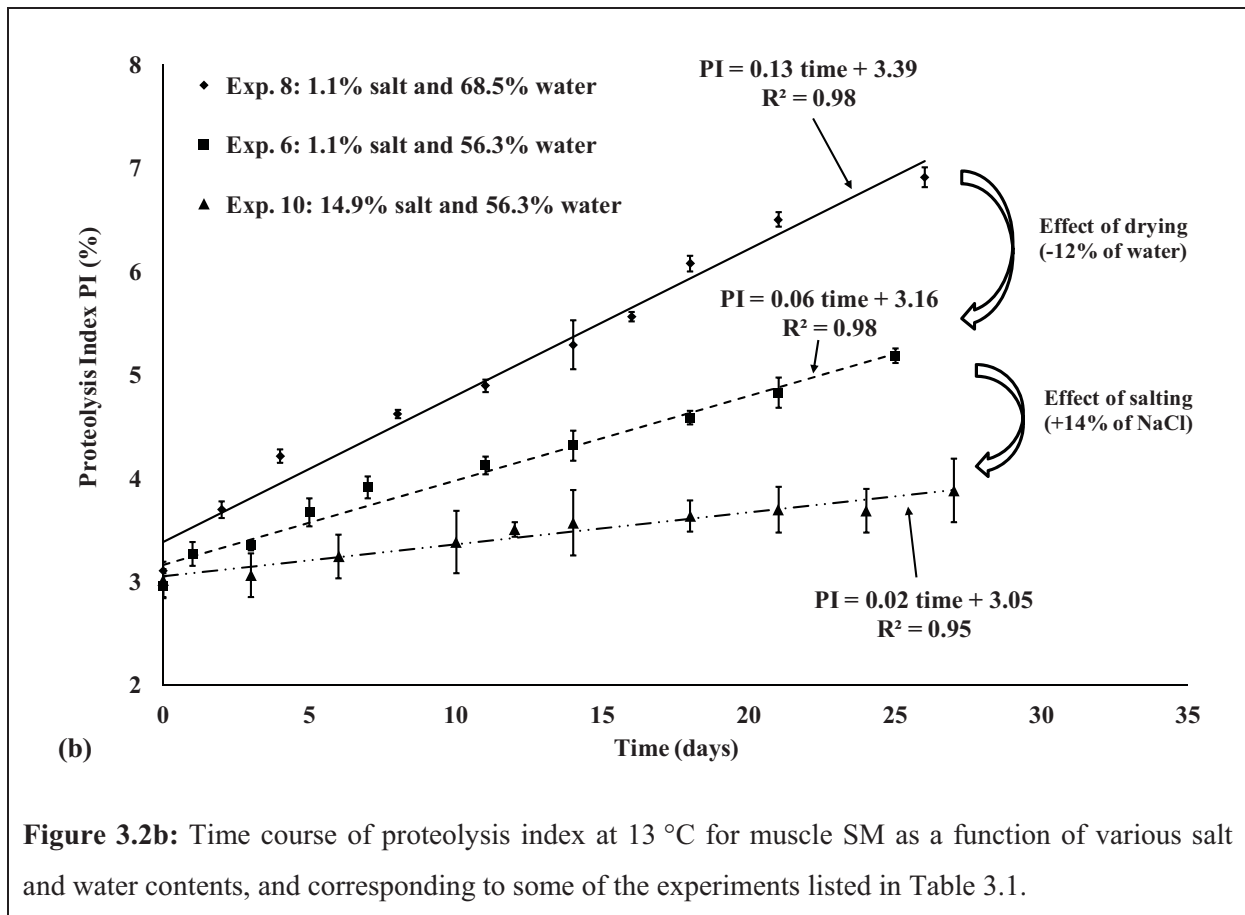


Similar results were reported by Toldra (2006) in his review, denoting that drying decreased water activity values, which affected the muscle proteolytic enzymes activity. The averages of proteolysis kinetics slopes for all muscle types at 5.7% DM salt content, and 68.5% TM and 56.3% TM water content were  $0.07 \pm 0.03\%$  PI/day and  $0.05 \pm 0.01\%$  PI/day, respectively (Experiments 7 and 9, Table 3.1). This could be because at low temperature there is not enough energy to sufficiently activate the enzymes (cathepsins, calpains, etc.) responsible for protein degradation. Unfortunately, the effect of salt at 3 °C could not be investigated directly from graph analysis because the Doehlert design did not provide for experiments at this temperature (Table 3.1). The interpretation of salt effect will therefore be discussed later when analysing the 3D response surface plots. The overall conclusion is that all muscles behaved in approximately the same way at 3 °C in terms of the proteolysis time course.

#### **Time course of proteolysis at moderate temperature (13 °C)**

As at low temperature, proteolysis index increased markedly and linearly with time ( $R^2 \geq 0.95$ ), at 13 °C (Fig. 3.2b). Generally, the progress of proteolysis at moderate temperature was faster and stronger than at low temperature; the average of slopes of all the muscle proteolysis kinetics at 13°C were globally higher than at 3 °C ( $0.11 \pm 0.04\%$  PI/day), except for kinetics with high salt content combined with low water content, where low values of slope were obtained, e.g. for the 14.9% DM salt-56.3% TM water curve in Fig. 3.2b (Experiment 10, Table 3.1). When pork meat samples were weakly dried and salted (i.e. the 1.1% DM salt-68.5% TM water curve of Fig. 2b corresponding to Experiment 8 in Table 3.1), measurements showed that values of PI could double in 25 days. Unlike experiments performed at low temperature, proteolysis kinetics recorded at 13°C allowed simultaneous assessment of the effect of drying and salting on the time course of proteolysis owing to the high number of proteolysis kinetics plotted at this temperature (Experiments 1-3, 5-6, 8 and 10 in Table 3.1). Analysing Fig. 3.2b, which shows the time course of three different proteolysis kinetics in the case of ST muscle, allows these effects to be assessed. Comparing the 1.1% DM salt-68.5% TM water curve with the 1.1% DM salt-56.3% TM water curve of Fig. 3.2b shows that a 12% increase in drying in weakly salted pork meat samples clearly slowed down protein degradation, and the proteolysis rate decreased from 0.14% PI/day to 0.08% PI/day. Costa-Corredor, Muñoz, Arnau and Gou (2010) reported similar results, which could be explained by the inhibitive effect of drying on proteolytic enzymes, leading to a slowed proteolysis time course. Fig. 3.2b also shows that on adding about 14% salt (comparison of the 1.1% DM salt-56.3% TM water curve with the 14.9% DM salt-56.3% TM

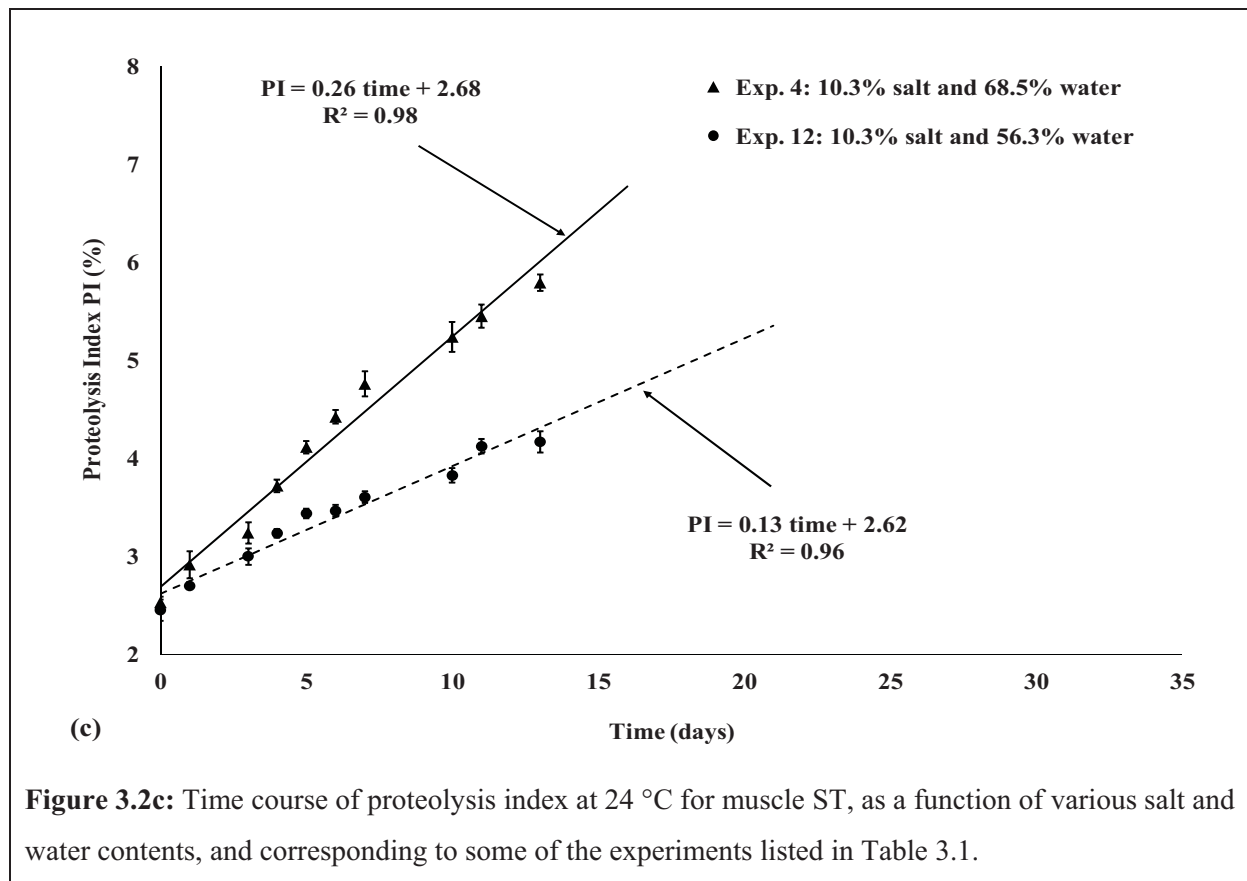
water curve), PIs fell even more for pork meat samples that were already well-dried. This confirms that salting is a key factor during the ham dry-curing process to control proteolysis. These results are consistent with those of Hutton (2002), who indicated that at constant temperature, adding salt and losing water decrease  $a_w$ , which is a key physicochemical variable for biochemical reactions and enzyme activity, and so slows the proteolysis time course.



### Time course of proteolysis at high temperature (24 °C)

Even at high temperature, proteolysis kinetics could be well-represented linearly with time ( $R^2 \geq 0.96$ ). The time course of protein degradation was, as expected, faster than at lower temperatures. Experiment 4 in Table 3.1 plotted in Fig. 3.2c led to PIs that increased from approximately 2.5 to 5.5% in only 13 days, even for pork meat samples salted at 10.3% DM. Comparing the plots in Fig. 3.2c and Fig. 3.2a shows that the proteolysis rates were multiplied by 3 or 4 when temperature increased from 3 to 24 °C, even for a higher salt content (10.3% DM vs. 5.7% DM). These results could be explained by the fact that increasing temperature favours the degradation of muscular proteins by proteolytic enzymes, the activity of which is

increased due to the greater amount of energy available in the medium. Many studies mention that when temperature increases proteolysis also increases (Martin et al., 1998, among others). Fig. 3.2c also shows that drying played an inhibitor role in proteolysis, thus confirming the results obtained at 13 °C for lower salt content. This inhibitor role was more clearly and obviously visible at 24 °C than at the previous temperatures of 13 and 3 °C, as seen from the fourth day (Fig. 3.2c). Also, in spite of a salt content increased by 50% at 24 °C, similar PIs were reached in 10 days at this high temperature against 35 days at 3 °C, for identical water contents. The effect of drying has often been described in several reports, and findings similar to these results have been reported (Toldra (2006), Ruiz-Ramírez, Arnau, Serra, & Gou, 2006; Toldrá, Cerveró, & Part, 1993). For the same reasons as at low temperature, the effect of salting could not be analysed at this temperature.



### Statistical analysis

Table 3.1 shows the slopes of all the proteolysis kinetics plotted corresponding to the Doehlert design for each of the five muscles investigated: SM, BF, ST, RF and GM. Globally, the values of the slopes ranged from 0.02 to 0.37% PI/day. Those of the repeated kinetics, i.e. the centre point of the Doehlert design, were very close: mean values of  $0.09 \pm 0.01\%$  PI/day for



SM;  $0.07 \pm 0.01\%$  PI/day for BF;  $0.09 \pm 0.01\%$  PI/day for ST;  $0.09 \pm 0.003\%$  PI/day for RF;  $0.06 \pm 0.01\%$  PI/day for GM, showing that there was no very marked inter-animal effect (standard deviation values lower than  $0.01\%$  PI/day). Statistical analyses were then carried out on the values of these slopes.

For each muscle, ANOVA showed that the temperature had a highly significant effect ( $p < 0.001$ ), the salt content a very significant effect ( $p < 0.01$ ) and the water content a significant effect ( $p < 0.05$ ) on the proteolysis time course. On the other hand, macroscopically, the muscle type had no significant effect on proteolysis, especially considering SM, BF and ST muscles ( $p > 0.05$ ). A Fisher LSD test confirmed the difference between the three temperatures used in this study. This test also showed that there was no difference between the proteolysis rates of the muscles, which could thus be lumped together, except for the GM muscle, which displayed specific behaviour (data not shown).

By means of multiple linear regressions, proteolysis time course models were built for all the muscles. ‘Component+Residual’ plots indicated that the effect of factors was linear. No outlier point was identified by the examination of hat values, Studentized residuals and Cook’s distances. Table 3.2 contains all the coefficients statistically calculated to build the proteolysis rate models, relating the factors studied and their interactions. Also, as stated above, considering that all the muscles exhibited approximately the same behaviour (except for the GM muscle), a global phenomenological model was also built in which all these muscles were considered together.

**Table 3.2** : Details of multiple linear regression coefficients calculated from experimentally-quantified proteolysis rates for five different pork muscles, plus another one combining muscles SM, BF, ST and RF. *T* represents the temperature (°C), *S* the salt content (% dry matter) and *W* the water content (% total matter).

	Muscle SM	Muscle BF	Muscle ST	Muscle RF	Muscle GM	SM+BF+ST+RF
Intercept	$3.45 \cdot 10^{-2}$	$-7.99 \cdot 10^{-3}$	$4.84 \cdot 10^{-3}$	$-2.80 \cdot 10^{-2}$	$2.53 \cdot 10^{-2}$	$8.29 \cdot 10^{-4}$
T	$-1.41 \cdot 10^{-2}$	$-2.01 \cdot 10^{-3}$	$-9.18 \cdot 10^{-3}$	$-1.57 \cdot 10^{-2}$	$-5.73 \cdot 10^{-3}$	$-1.024 \cdot 10^{-2}$
S	$-5.83 \cdot 10^{-3}$	$3.56 \cdot 10^{-3}$	$-7.28 \cdot 10^{-4}$	$3.46 \cdot 10^{-3}$	$-5.88 \cdot 10^{-3}$	$1.147 \cdot 10^{-4}$
W	$-4.26 \cdot 10^{-4}$	$2.76 \cdot 10^{-4}$	$1.69 \cdot 10^{-4}$	$5.68 \cdot 10^{-4}$	$-9.77 \cdot 10^{-5}$	$1.47 \cdot 10^{-4}$
T S	$-1.57 \cdot 10^{-4}$	$-1.15 \cdot 10^{-4}$	$-3.92 \cdot 10^{-4}$	$-3.84 \cdot 10^{-4}$	$-3.45 \cdot 10^{-4}$	$-2.62 \cdot 10^{-4}$
T W	$3.68 \cdot 10^{-4}$	$1.52 \cdot 10^{-4}$	$3.25 \cdot 10^{-4}$	$4.56 \cdot 10^{-4}$	$2.57 \cdot 10^{-4}$	$3.25 \cdot 10^{-4}$
S W	$9.23 \cdot 10^{-5}$	$-6.00 \cdot 10^{-5}$	$5.21 \cdot 10^{-6}$	$-4.46 \cdot 10^{-5}$	$8.91 \cdot 10^{-5}$	$-1.75 \cdot 10^{-6}$
R <sup>2</sup>	0.95	0.95	0.94	0.94	0.84	0.91
Adj. R <sup>2</sup>	0.93	0.93	0.92	0.91	0.78	0.90
RSE	0.030	0.025	0.034	0.044	0.057	0.037

Adj. R<sup>2</sup>: Adjusted R<sup>2</sup> ; RSE: Residual Standard Error



In the present study, only the proteolysis time course model found for the ST muscle is reported. The  $R$ -squared coefficient determined in this case was high (0.94), which means that the model that gives the time course of proteolysis rate ( $\text{Rate}_{\text{PI,ST}}$ ) fits the experimental data closely:

$$\begin{aligned} \text{Rate}_{\text{PI,ST}} = & 4.84 \cdot 10^{-3} - 9.18 \cdot 10^{-3} T - 7.28 \cdot 10^{-4} S + 1.69 \cdot 10^{-4} W \\ & - 3.92 \cdot 10^{-4} T \cdot S + 3.25 \cdot 10^{-4} T \cdot W + 5.21 \cdot 10^{-5} S \cdot W \end{aligned} \quad \text{Eq. (3.2)}$$

where  $T$  is the temperature ( $^{\circ}\text{C}$ ),  $S$  is the salt content (% DM) and  $W$  is the water content (% TM).

As an example, Fig. 3.3 shows the response surface plot of the proteolysis time course for ST muscle, at 4% DM salt content. At low temperature, the values of the slopes of proteolysis kinetics are low, and the inhibitor effect of drying is not clearly visible in this figure. Gradually, as the temperature increases, protein degradation also increases, until at high temperature ( $24^{\circ}\text{C}$ ) the inhibitor effect of the drying is clearly visible (Fig. 3.3). Results also show that increasing salt content slows down the proteolytic activity, especially at low water content. On the basis of all the phenomenological models built, the coefficients of which are listed in Table 3.2, the rate of protein degradation could be quantified as a function of time, for any of the five muscles studied, and for any of the conditions of temperature, water and salt content.

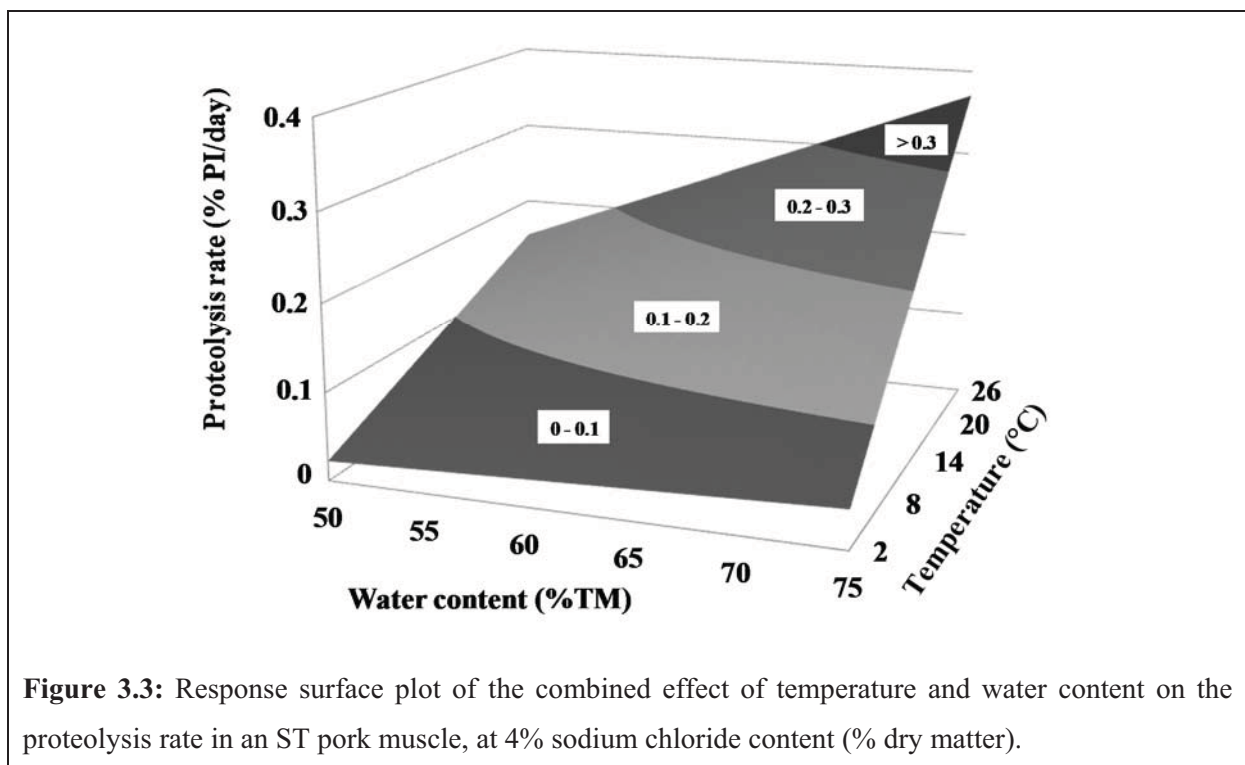


**Figure 3.3:** Response surface plot of the combined effect of temperature and water content on the proteolysis rate in an ST pork muscle, at 4% sodium chloride content (% dry matter).

## Discussion

During their production process, French dry-cured hams are generally subjected to a variable temperature regime that can be summarized as: about 11 weeks at 4 °C (salting and post-salting stages) optionally followed by 1 week at 23 °C (pre-ripening stage), and from the 13<sup>th</sup> week until the end, at 12 °C (drying and ageing stages). Phenomenological models were built and used to predict PIs at the end of particular stages of the production process: salting and post-salting, pre-ripening, drying and ageing, for SM, BF and RF muscles of pork hams cured and dried for 10 months. To achieve this, mean values of water and salt content measured in whole SM, BF and RF muscles extracted from industrial dry-cured hams at various stages during the production process, in the framework of a previous study (internal unpublished data), were introduced into these models.

For each stage and muscle type, Table 3.3 shows the experimental values of water and salt content used for calculating the corresponding proteolysis rates and indices. In Table 3.3, a study of the sensitivity of the PI values to variations in temperature ( $\pm 2^\circ\text{C}$ ), water content ( $\pm 2\%$  TM) and salt content ( $\pm 0.5\%$  TM) commonly found in industrial practice is also reported. Table 3.3 indicates globally that the highest increase in proteolysis occurs during the ageing stage due to its long duration, with a mean PI increase of 2 to 2.5% a month. At this particular stage, thorough analysis shows that the three muscles investigated can be ranked in order of increasing PI: RF > BF > SM. Regarding the pre-ripening stage, although high proteolysis rates (0.2% PI/day) were calculated as a result of a high temperature, a very restricted PI increase (< 2%) occurred since this stage only lasts one week. Whatever the muscle type, similar values of proteolysis rates and indices were calculated using the phenomenological models during the salting and resting time periods compared with the drying stage due to offset between the temperature effect (main variable allowing proteolysis to be controlled during the salting and post-salting stages) and the drying and salting effects (main variables affecting proteolysis during drying) on the proteolysis time course (Table 3.3). In the case of SM muscle, the lower value of PI during drying compared with that during salting and post-salting can even be attributed to drying only, because similar values of salt content over these stages are reported in Table 3.3. Analysis of the sensitivity study reveals that the highest changes in PI are attributable to temperature before the water content and then the salt content, in accordance with the results of statistical analysis. This confirms that an accurate control of temperature and drying, and to a lesser extent, salting, is crucial throughout the dry-cured ham production process (except during the pre-ripening stage, given its short duration) to limit heterogeneity in terms of final PI values.

**Table 3.3:** Calculation of proteolysis indices (PIs) and their variation as a function of temperature, water and salt contents during each main stage of the dry-cured ham production process using the phenomenological models built in this study, for three different pork muscles (SM: semimembranosus, BF: biceps femoris, and RF: rectus femoris).

Stages of dry-cured ham production process	Salting and post-salting	Pre-ripening	Drying	Ageing
Duration (day)	77	7	70	150
Air temperature (°C)	4	23	12	12
Muscle SM				
Mean water content (% TM)	66.0	61.5	58.0	55.0
Mean salt content (% TM)	3.4	3.2	3.0	3.2
Mean proteolysis rate (%/day)	0.04	0.17	0.08	0.07
PI (%)	5.9 <sup>d</sup>	1.2	5.6	10.0
$\Delta_{T,PI}$ (%) <sup>a</sup>	1.3	0.1	0.9	1.5
$\Delta_{X_w,PI}$ (%) <sup>b</sup>	0.3	0.1	0.6	1.3
$\Delta_{X_{NaCl},PI}$ (%) <sup>c</sup>	< 0.1	< 0.1	0.2	0.4
Muscle BF				
Mean water content (% TM)	71.0	68.0	66.0	62.5
Mean salt content (% TM)	1.9	2.5	3.0	4.0
Mean proteolysis rate (%/day)	0.04	0.18	0.09	0.08
PI (%)	5.5 <sup>d</sup>	1.2	6.4	12.4
$\Delta_{T,PI}$ (%) <sup>a</sup>	1.3	0.1	1.0	1.9
$\Delta_{X_w,PI}$ (%) <sup>b</sup>	< 0.1	< 0.1	0.15	0.3
$\Delta_{X_{NaCl},PI}$ (%) <sup>c</sup>	0.15	< 0.1	0.2	0.3
Muscle RF				
Mean water content (% TM)	68.0	65.0	62.0	57.5
Mean salt content (% TM)	3.2	4.2	4.2	4.9
Mean proteolysis rate (%/day)	0.06	0.23	0.11	0.09
PI (%)	7.2 <sup>d</sup>	1.6	8.0	13.7
$\Delta_{T,PI}$ (%) <sup>a</sup>	1.8	0.1	1.2	2.0
$\Delta_{X_w,PI}$ (%) <sup>b</sup>	0.2	0.1	0.6	1.4
$\Delta_{X_{NaCl},PI}$ (%) <sup>c</sup>	0.1	0.1	0.4	0.7

TM: total mass;

<sup>a</sup>: Impact of a 2°C variation in air temperature on the variation of PI over the considered stage;

<sup>b</sup>: Impact of a 2% TM variation in water content on the variation of PI over the considered stage;

<sup>c</sup>: Impact of a 0.5% TM variation in salt content on the variation of PI over the considered stage;

<sup>d</sup>: a 2.5% initial value was considered when calculating PI at this particular stage. This initial value corresponds to the mean value of PI measured for the laboratory-prepared pork meat samples before salting and drying, i.e. for a few days-old “fresh” pork meat.

These results are globally in line with those of Zhao et al. (2008), who indicated that the highest PI increase in BF muscle occurred during ageing, and with those of Toldra, Flores and Sanz (1997) and Ruiz-Ramirez et al. (2006), who reported a more intense proteolysis in BF muscle than in SM muscle, probably due to constantly higher moisture content.

## **Conclusion**

The present results confirm that temperature, water and salt contents are key processing factors, strongly influencing proteolysis during the ageing of laboratory-prepared pork meat samples mimicking dry-cured ham production. Temperature rise favoured proteolysis, whereas salting and drying slowed it down. Statistical analyses supported the highly significant effect of temperature on proteolysis, highlighting a very high significant effect of water content and high significant effect of salting. On the other hand, the muscle type had no significant effect on proteolysis, especially for the most often studied and voluminous muscles in dry-cured ham, i.e. BF, SM and ST.

To the authors' knowledge, several phenomenological models were built here for the first time. These models relate proteolysis to temperature and water and salt content for five types of muscle. Some of them were used to predict PIs and to assess the impact of some variations in the control of temperature, drying and salting on PI values at the end of the main stages of the production process: salting and post-salting, pre-ripening, drying and ageing. It was highlighted that introducing a one-week-long pre-ripening stage during the process had very little influence on the PI time course. However, the great advantage of these phenomenological models is that they can be easily integrated into a 3D multi-physical numerical model to predict simultaneously the time course of proteolysis as a function of salt diffusion, water migration and heat transfer throughout the ham dry-curing process, which can last from 6 to more than 18 months. A total of six phenomenological models have thus been built (one for each type of muscle, plus one corresponding to an "average muscle" combining SM, ST, BF and RF) with the prospect of integrating them into a real geometry of 'numerical' ham built up from morphological images.

## **Acknowledgements**

This work was funded by the Na- integrated programme (ANR-09-ALIA-013-01) financed by the French National Research Agency. This paper forms part of the thesis of Rami Harkouss, who works for this research program. We thank S. Portanguen for his technical assistance and ATT for language editing.

### 3.3. Article n°4 (soumis à Food Chemistry en Novembre 2013)

#### Is there any relationship between proteolysis, structure and texture during the manufacture of dry-cured ham?

Rami Harkouss<sup>a</sup>, Thierry Astruc<sup>a</sup>, André Lebert<sup>b</sup>, Philippe Gatellier<sup>a</sup>, Olivier Loison<sup>a</sup>,  
Stéphane Portanguen<sup>a</sup>, Emilie Parafita<sup>c</sup>, Pierre-Sylvain Mirade<sup>a</sup>

<sup>a</sup> INRA, UR370 Qualité des Produits Animaux, F-63122 Saint-Genès-Champanelle, France.

<sup>b</sup> Institut Pascal, UMR6602 UBP/CNRS/IFMA, 24 avenue des Landais, BP80026,  
63171 Aubière Cedex, France.

<sup>c</sup> ADIV, 10 rue Jacqueline Auriol, ZAC Les Gravanches, 63039 Clermont-Ferrand Cedex 2,  
France.

#### Abstract

Temperature, salt and water content are key processing factors in dry-cured ham production. They affect how proteolysis, structure and texture evolve, and thus determine the sensory properties and final quality of dry-cured ham. The literature offers little quantitative information about the interrelationships between proteolysis, texture and structure. The aim of this study was to quantify the effects of the three processing factors on the time course of (i) proteolysis, (ii) five textural parameters: hardness, fragility, cohesiveness, springiness, and adhesiveness, and (iii) four structural parameters: fiber numbers, extracellular spaces, cross section area, and connective tissue area. Applying multiple polynomial regression enabled us to build phenomenological models relating proteolysis, salt and water content to the textural and structural parameters investigated. These texture-structure-proteolysis models, combined with salt penetration, water migration and heat transfer models, can dynamically simulate all these phenomena throughout dry-cured ham manufacturing.

*Keywords: dry-cured ham; proteolysis; structure; texture; polynomial regression model*

#### Introduction

Dry-cured ham can be an important source of essential amino acids for humans. Proteolysis, one of the main biochemical reactions during dry-cured ham processing, is considered to be the source of many of these free amino acids. Proteolysis generally refers to endogenous enzyme activity (Cordero & Zumalacarregui, 2000), such as that of cathepsins B, L, H and D, calpains, peptidases and cytosolic enzymes (Luccia et al., 2005). Proteolytic activity depends on many factors. Zhao, Zhou, Wang, Xu, Huan, and Wu (2005) found that potential activities

of cathepsin B and L were reduced during processing to only 9.3% and 13.7% of their original potential activity, as a result of the inhibitory role of salting. According to Morales, Serra, Guerrero, and Gou (2007b), temperature also has a strong influence on these enzymes. They showed that ageing biceps femoris (BF) muscle at 30 °C increased proteolysis intensity significantly compared with hams aged at 5 °C. It has also been observed that high temperatures during the drying-ageing stage promote the formation of non-protein nitrogen compounds, and in turn affect the course of proteolysis. Many authors have found that proteolysis rate is affected by several processing parameters such as temperature, relative air humidity, and salt content (Arnau, Gou, & Comaposada, 2003; Ruiz-Ramirez, Arnau, Serra, & Gou, 2006; Toldrá, Flores, & Sanz, 1997). High water content has been found to increase proteolytic activity as a result of high water activity ( $a_w$ ) values (Serra, Ruiz-Ramirez, Arnau, & Gou, 2005). In addition, some studies have shown that proteolysis remains stable during one week of storage at 30 °C and increases after one month of storage in the same conditions (Arnau, Guerrero, & Gou, 1997; Morales et al., 2007b). The anatomic location of muscles inside the ham, whether external like semimembranosus (SM) or internal like BF, also plays a major role in the time course of proteolysis during the dry-cured ham production process, owing to different salt and water transfer kinetics in each muscle. It is well-known that proteolysis impacts the final texture (hardness, cohesiveness, etc.) of the product, and is considered as a crucial parameter to obtain good quality sensory characteristics at the end of the process (García-Garrido, Quiles-Zafra, Tapiador, & Luque de Castro, 2000; Toldra, 1998; Zhao, Tian, Liu, Zhou, Xu, & Li, 2008). Thus a better understanding and control of proteolysis rates can favor an optimized texture in dry-cured ham.

In parallel, lipid oxidation is an important degradative change during processing and storing that strongly affects the quality and safety of muscle foods. It is also an essential factor for the development of the typical aroma of dry-cured ham. Few research studies have characterized this phenomenon or examined the effect of NaCl and temperature on it. Rhee, Smith, and Terrell (1983) showed that NaCl promoted lipid oxidation at low concentrations, but inhibited it at concentrations greater than 2% in minced pork muscle. Aidos, Lourenco, Van der Padt, Luten, and Boom (2002) found that elevating temperature could accelerate the degradation of hydroperoxides. Recently, Jin, He, Zhang, Yu, Wang, and Huang (2012) reported that even at 4% salt content, lipid oxidation gradually increased in minced pork muscles, but differently according to the process temperature; in other words, lipid oxidation is strongly affected by both salt content and temperature, and probably by their interaction. Jin et al. (2012)



confirmed that as the temperature increased, so the threshold value of NaCl content affecting lipid oxidation in pork muscle progressively decreased.

In general, the sensory quality of dry-cured ham is evaluated through flavor, appearance and texture criteria. Although color and flavor are highly important for reaching a high final product quality, texture remains a major sensory characteristic to be tested. Texture problems such as softness, pastiness and crusting frequently impede slicing and give a mouth-coating sensation, whence the important role of texture for both retailer and consumer acceptability. Hams are usually classified into four texture types: very pasty, pasty, soft, and normal, each identified by various properties. It has been shown that textural defects are closely related to anomalous proteolysis (Virgili, Parolari, Schivazappa, Soresi-Bordini, & Borri, 1995). Studies have shown that NPN values are highest in pasty hams and lowest in soft hams. Ruiz-Ramirez, Serra, Gou, and Arnau (2005) observed that high proteolysis rates led to poor cohesiveness and sliceability, as a result of abnormal softness. The role of several process factors (salt content, temperature, etc.) on texture has also been investigated. Gou, Morales, Serra, Guàrdia, and Arnau (2008) studied the effect of salt, and observed that as NaCl content decreased, so texture problems increased; these results were in line with those of Desmond (2006), who showed that limiting salt tended to decrease fiber swelling, leading to poor texture. Also, Sforza et al. (2001) showed that high temperature in the final ageing period played an important role in lowering ham dryness. These results were confirmed by Morales, Arnau, Serra, Guerrero, and Gou (2008a), who observed a decreased pastiness in BF with no increased hardness in SM muscle, after one week of storage at 30 °C. Most texture problems in dry-cured hams could be related to a short processing time and low salt content. Consequently, studies have to be more narrowly focused on processing factors (time, temperature, salt amount, etc.) in association with textural properties (e.g. hardness) and biochemical changes (proteolysis, oxidations, lipolysis, etc.) to ensure a dry-cured ham of high final quality. To achieve this aim, structural properties must also be thoroughly studied and combined with the properties stated above.

Few studies have been carried out to study the main biochemical changes influencing the structural proteins, especially those related to the thick and thin filaments, the Z-disks and the costamere proteins (Fritz, Mitchell, Marsh, & Greaser, 1993). Electronic microscopy highlighted the effect of endogenous proteolytic enzymes on muscle ultrastructure during dry-cured ham processing. Larrea, Perez-Munuera, Hernando, Quiles, and Lluch (2007) related dry-cured ham quality to its microstructure, and observed modifications in the structural proteins that could explain the texture and flavor time course of the final product. They

reported that after the salting stage, the Z-disks inside the myofibrils were no longer in line, and a marked degradation of the cell membranes was detected; in the last stage of ripening, several accumulated proteolysis products were observed. This brief literature review shows that little quantitative information about the interrelationships between proteolysis, texture and/or structure is available. Here we aim to devise a model quantitatively relating proteolysis to several textural and/or structural parameters, through a statistical analysis of experimental results obtained on samples extracted from industrial dry-cured ham at five key times during their manufacture.

## Materials and methods

### Extraction of samples of Bayonne dry-cured hams

The work described here evaluates changes in the time course of proteolysis, texture and structure that occur in PDO Bayonne dry-cured hams during their manufacture. A total of 15 dry-cured hams were selected on the basis of an initial pH value in the range 5.6–5.9.

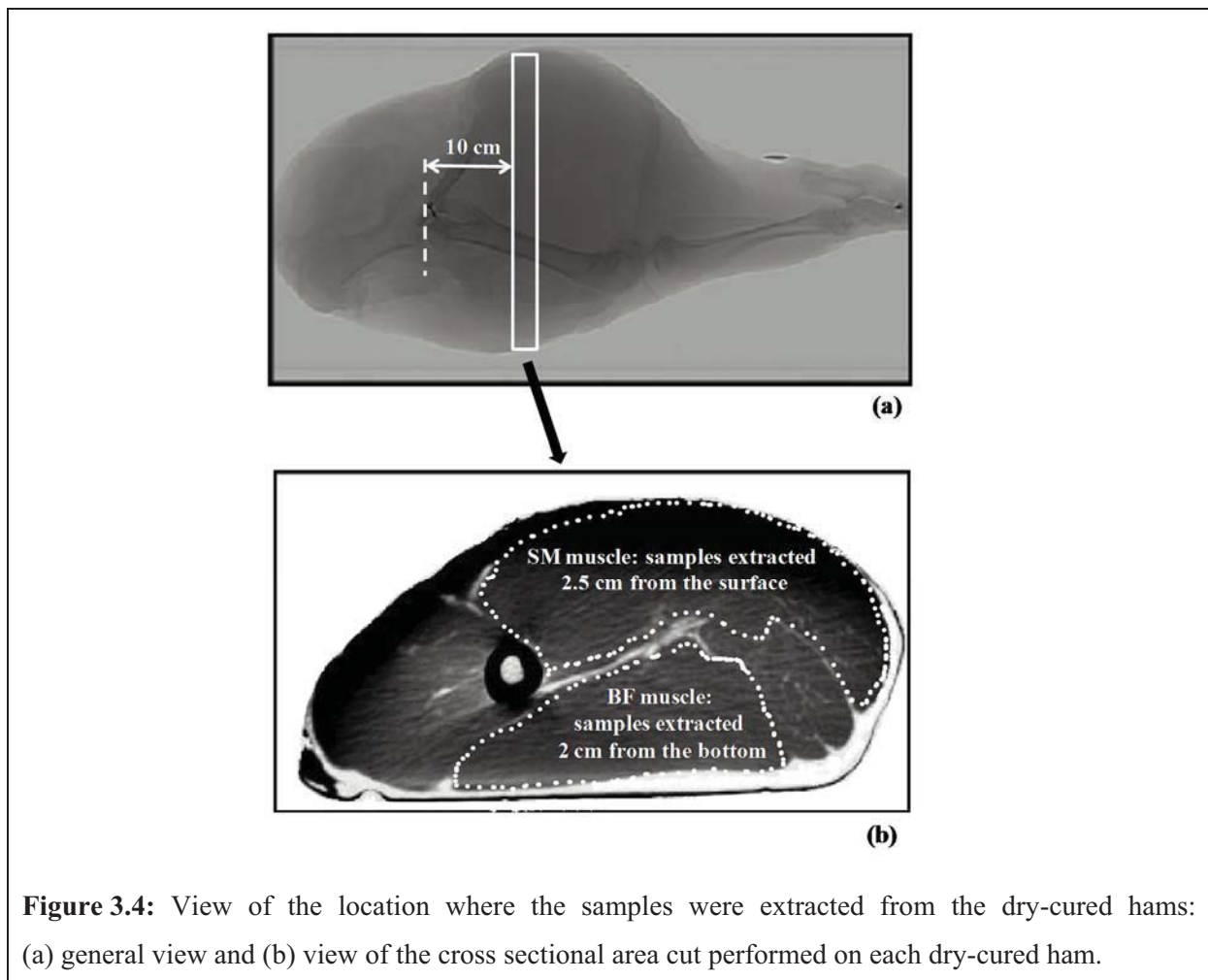


**Figure 3.4:** View of the location where the samples were extracted from the dry-cured hams: (a) general view and (b) view of the cross sectional area cut performed on each dry-cured ham.



Two muscles, BF and SM, were extracted from these 15 hams, corresponding to three hams removed from the process at five different processing times: (i) four days *post mortem* (“fresh hams”), (ii) at the end of the resting period (11 weeks), (iii) at the end of the drying period (21 weeks), (iv) at mid-period (35 weeks), and (v) at the end of the ageing period (12 months). At a distance of 10 cm from the coaxial bone, a 3 cm-thick cross sectional area section was cut on each of the 15 hams (Fig. 3.4a). On each section, slabs (2 × 3 × 5 cm) of muscle were cut 2 cm from the bottom (BF), and 2.5 cm from the top (SM) of the ham (Fig. 3.4b). In this way, we expected to have similar salt and water contents in all the samples obtained from each ham for the various experimental measurements, and to keep constant the geometrical position where the samples were cut for the 15 dry-cured hams.

### **Biochemical measurements**

#### **Quantification of proteolysis**

The proteolysis index (PI) of dry-cured ham samples was determined to evaluate the proteolysis intensity using the fluorometric-based procedure described in Harkouss, Mirade, and Gatellier (2012). Briefly, this procedure comprises the following successive phases: (i) grinding of the samples, (ii) dilution of the extracts with trichloroacetic acid to precipitate proteins, (iii) centrifuging, (iv) measurement of the peptide and amino acid concentrations in a portion of the supernatant, (v) addition of fluorescamine to another portion of the supernatant, and (vi) 1 h later, measurement of fluorescence, and determination of the level of amino groups by reference to a calibration curve of glycine treated in parallel, under exactly the same conditions as the pork meat extracts. This procedure determines the level of N-terminal  $\alpha$ -amino groups of peptides and amino acids, and so reflects the real intensity of proteolytic activity occurring in the hams throughout the drying and curing processes. PI was defined as the percent ratio of N-terminal  $\alpha$ -amino group content to total protein content of the ham sample. A complete description of this powerful and rapid technique for quantifying proteolysis can be found in Harkouss et al. (2012).

#### **Quantification of lipid oxidation**

Lipid oxidation was quantified using 2-thiobarbituric acid-reactive substances (TBARS). TBARS were determined using the method developed by Mercier, Gatellier, Viau, Remignon, and Rennerre (1998) based on the technique of Lynch, and Frei (1993). Muscle samples (1 g) were homogenized with 10 ml of deionized distilled water, using a Polytron blender (1 min at medium speed). Homogenates (0.5 ml) were incubated with 1% (w/v) 2-thiobarbituric acid in

50 mM NaOH (0.25 mL) and 2.8% (w/v) trichloroacetic acid (0.25 mL) in a boiling water bath, for 10 min. After cooling at room temperature for 30 min, the pink chromogen was extracted with n-butanol (2 mL), and its absorbance measured at 535 nm against a blank of n-butanol. TBA-RS concentrations were calculated using 1,1,3,3 tetrathoxypropane (0–0.8  $\mu$ M) as standard. Results are expressed as mg of MDA per kg of meat (TBA units).

## **Structural analyses**

### **Preparation of dry-cured ham samples**

The dry-cured ham samples were frozen in cooled isopentane ( $-160\text{ }^{\circ}\text{C}$ ) chilled with liquid nitrogen ( $-196\text{ }^{\circ}\text{C}$ ), and stored at  $-80\text{ }^{\circ}\text{C}$  until analysis. Serial fiber cross-sections 10  $\mu\text{m}$  thick were sliced at  $-25\text{ }^{\circ}\text{C}$  in a cryostat (Microm HM 560, Thermo Fisher Scientific Inc., United States), mounted on glass slides, and then air-dried at  $20\text{ }^{\circ}\text{C}$ . Sections were stained with hematoxylin-eosin-safran (HES) to reveal general structure, and with picro-Sirius red to reveal perimysial and endomysial collagen. After staining, the slices were mounted using a synthetic resin (Eukitt, Kindler GmbH & Co, Germany) to preserve the section.

### **Acquisition and analysis of images**

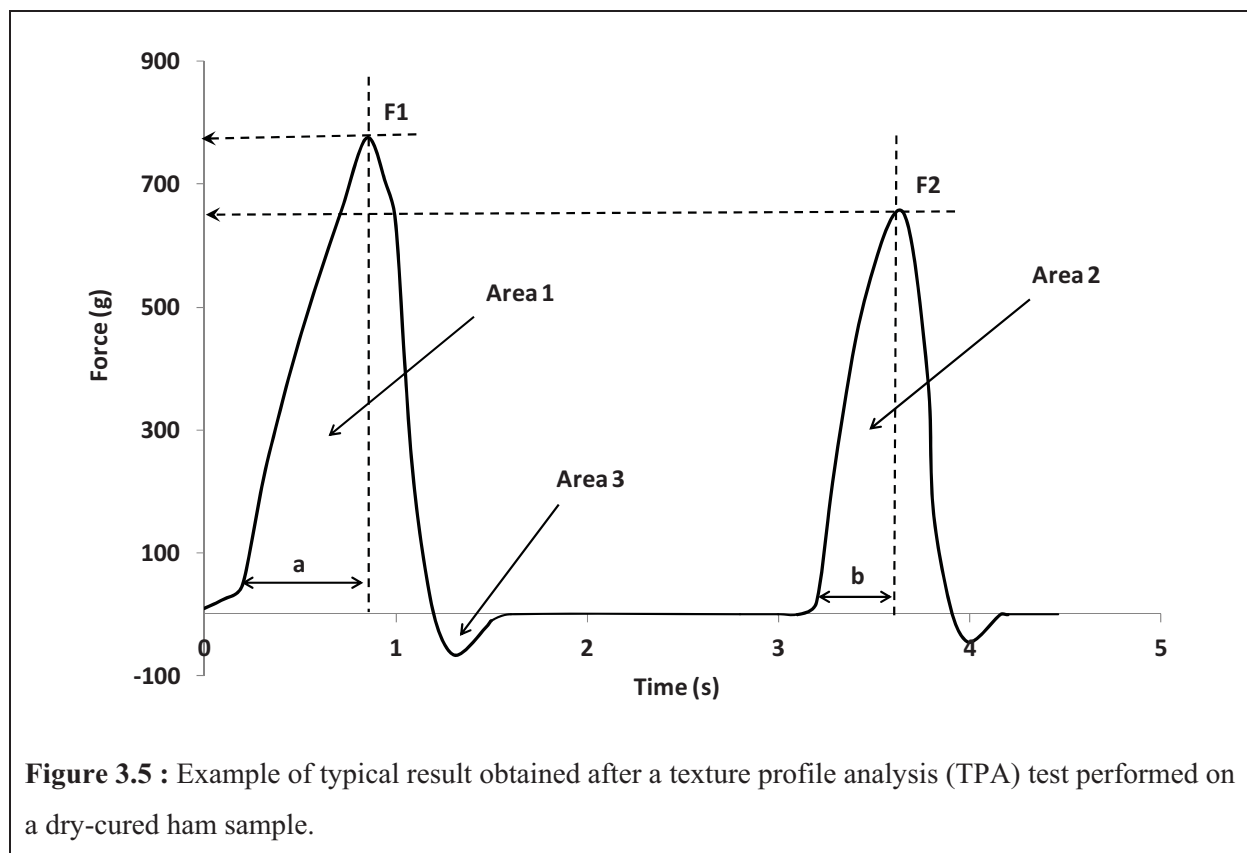
Observations were made on a transmission microscope coupled to a digital acquisition kit (Olympus BX61 microscope, Olympus DP 71 digital camera and Cell F software, Olympus France SAS, Rungis, France). Images were recorded at  $\times 10$  magnification. The  $\times 10$ -magnified cross section images were quantitatively analyzed with the open source ImageJ image processing software, applying the exact same acquisition parameters for all the images. Each RGB-colored image was separated into its three monochromatic components (red, green and blue) to keep only the green component of the image, thereby improving the contrast between extracellular spaces and muscle fibers. To prevent distortion of the fiber size evaluation, the only fields of observation taken into account were those where muscle fibers were perfectly cut transversely to the main axis of fiber orientation.

Fiber morphology parameters and extracellular spaces were determined on six HES stained images corresponding to six different optical fields, forming a total of approximately 500 muscle fibers for each drying condition. Extracellular space was extracted after thresholding segmentation of the gray levels. Its relative area was assessed by its pixel count relative to the whole field-of-view area. The same approach was used to extract and individualize muscle fibers, eliminating any cropped cells touching the edge of each field of view. The surface area of each fiber was assessed by its pixel count. A conversion factor was applied to express the

measured surface areas in  $\mu\text{m}^2$ . Connective tissue area was determined in the same way on six micro-Sirius red stained images corresponding to six different optical fields.

### Texture profile analysis (TPA) test

Before texture measurement, the dry-cured ham samples were removed from the freezer and placed in a cooler maintained at  $4\text{ }^\circ\text{C}$  to thaw for approximately 24 h. A universal Texture Analyser TA.XT plus (Stable MicroSystems Ltd., Surrey, England) was used to perform the texture profile analysis (TPA) test (Bourne, 2002), at room temperature. Duplicate cubes  $10 \times 10 \times 10\text{ mm}$  of SM and BF muscles were analyzed. The 10 mm-high cubic samples were placed so that the fiber bundles were oriented parallel to the compression plate surface (flat plunger 50 mm in diameter), and were then compressed axially twice to 50% of their original height, with a time interval of 2 s between the two successive compressions. Force-time curves were recorded with a 15 kg load cell applied at a crosshead speed of 1 mm/s. The following TPA parameters were obtained using the XT.RA Dimension software package: hardness, fragility, springiness, adhesiveness, and cohesiveness (Fig. 3.5).



Hardness was defined by peak force during the first compression cycle (F1) and expressed in N, and fragility by the ratio  $F2/F1$ . Cohesiveness was calculated as the ratio of the area under

the second curve (Area 2) to the area under the first curve (Area 1). Springiness was defined as the ratio of the time recorded between the start of the second area (b) and the second probe reversal to the time recorded between the start of the first area and the first probe reversal (a). Adhesiveness corresponded to the “negative” area under the curve obtained between the two cycles (Area 3), and expressed in N.s (Fig. 3.5). The mean of the replicates of each sample was used for statistical analyses.

### **Physicochemical analyses**

To determine the salt content, samples (1 g) were homogenized (Ultra-Turrax system, Ika, Germany) with 10 mL of ultrapure water. After a 2 h rest period, the homogenate was centrifuged at  $11,300 \times g$  for 10 min at room temperature (MiniSpin Plus, Eppendorf, France). The supernatant was recovered, diluted in ultrapure water, and run through an ion chromatography system (850 professional IC, Metrohm France SAS, France) to measure chloride ion content. The NaCl content (%) was then calculated from this value.

Water content was determined by drying samples (2–3 g) at  $103 \pm 2 \text{ }^\circ\text{C}$  in a controlled-temperature chamber (Model FT127U, Firlabo, France) to constant weight (AOAC, 1990), i.e. at least 24 h. Water content was expressed on a total matter (TM) basis (kg H<sub>2</sub>O/kg TM).

### **Statistical analyses**

Statistical analyses were performed using R 3.0.1 software (R Development Core Team, 2013), the statistical packages 'car' (Fox & Weisberg, 2011), 'HH' (Heiberger, 2013), 'leaps' (Lumkey, 2009) and the graphical package 'rgl' (Adler & Murdoch, 2013). They were carried out at different stages of this work. Firstly, an analysis of variance (ANOVA) was performed at the five different times of dry-cured ham production to test the effects of the processing stages and muscle types on the PI and TBARS values. When a significant effect was observed by ANOVA, the unpaired Student *t*-test was used to determine the levels of statistical significance between groups. Secondly, morphometry data acquired by image analysis was expressed as mean  $\pm$  standard error of the mean (SEM). Changes in cross section area of fibers, extracellular spaces and fiber numbers were quantitatively analyzed by one-way ANOVA, and an unpaired Student *t*-test was used to determine levels of statistical significance between groups. Thirdly, a three-way ANOVA was performed on all the data obtained for the two muscles, SM and BF. The objective was to assess the effect of each factor (PI, water and salt content) on all the textural and structural parameters. When the *F*-test was significant ( $p < 0.05$ ) a *post hoc* procedure was used: multiple comparisons among means were examined by Fisher's least

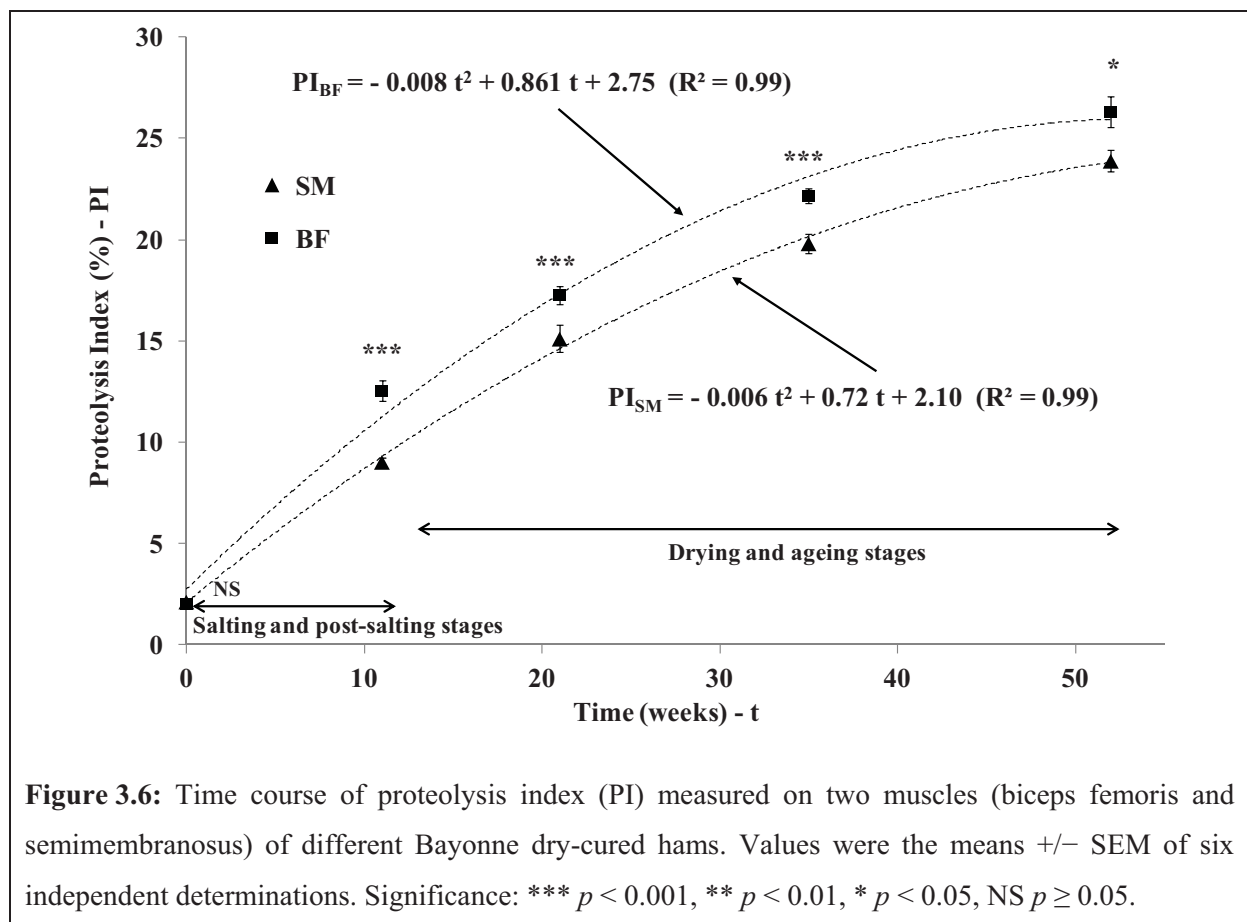
significant difference (LSD) test. Multiple linear or polynomial regressions were performed to find the best model of each of the textural and structural parameters as a function of the factors studied for each muscle, and their interactions. As advocated by Fox and Weisberg (2011), regression diagnostics such as 'Component+Residual' plots were performed to investigate non-linearity problems, hat values, Studentized residuals and Cook's distances to identify outlier points, and finally model factor selection by exhaustive search, forward or backward stepwise, or sequential replacement (Mallows's Cp and Schwartz's information criterion: BIC).

## Results and discussion

### Time course of biochemical parameters

#### Proteolysis index (PI) values

PI was measured on samples of industrial Bayonne hams over a 12-month period (Fig. 3.6).



To characterize the time course of proteolysis, the increase in PI value with time was fitted by a second-order polynomial regression. Despite the biological variability, high correlation coefficients were obtained from the different curves ( $R^2 > 0.99$ ). As shown in Fig. 3.6, the

increase in PI value was higher in BF than in SM muscle. These results are consistent with the results obtained in a previous study (Harkouss et al., 2012), where similar coefficients of the polynomial regression of PI curves were obtained, together with similar proteolysis levels in both muscles.

The ANOVA showed a high significant effect of muscle and time ( $p < 0.001$ ), with also a highly significant interaction between the two ( $p < 0.001$ ). The results were in line with those of Ruiz-Ramírez et al. (2006) and Toldrá et al. (1997), who reported higher proteolysis in BF muscle than in SM muscle, as a result of a higher residual moisture content in BF muscle, which permits a higher activity of endogenous proteases.

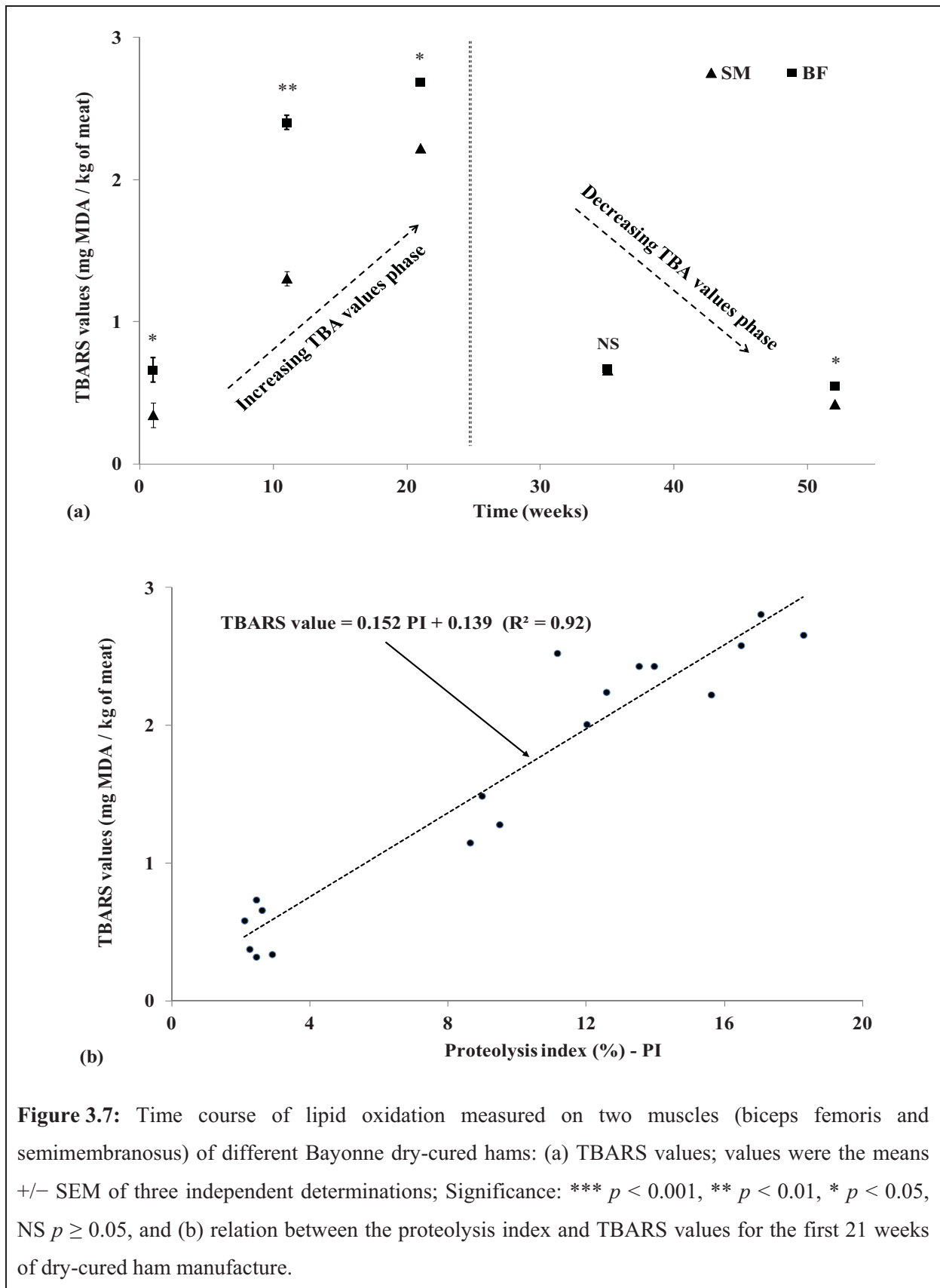
### TBARS values

Fig. 3.7a shows the time course of TBARS values at those stages when proteolysis degradation was assessed. A biphasic curve was observed for lipid oxidation, with an initial increase followed by a decrease beyond 21 weeks. The initial increasing phase, until the first weeks of the drying stage, corresponds to the accumulation of aldehydes such as malondialdehyde. Beyond the lengthy drying-ripening stage of dry-cured hams, the decrease in the TBA values may occur mostly because during long-time processing, either the originally generated thiobarbituric acid (TBA) reactive substances, mainly aldehydes, are unstable and can be further decomposed into other low molecular weight volatile compounds, or else these aldehydes interact with proteins, which prevents their reaction with TBA. Similar decrease in TBA was previously reported by Andrés, Cava, Ventanas, Muriel, and Ruiz (2004) in dry-cured Iberian hams, confirmed by Jin, He, Zhang, Yu, Wang, and Huang (2012) in pork belly muscle, and shown by Gatellier, Santé-Lhoutellier, Portanguen, and Kondjoyan (2009) in cooked beef meat. For lipid oxidation, the ANOVA highlighted a significant effect of muscle and time ( $p < 0.01$ ) and a highly significant interaction between the two ( $p < 0.001$ ).

Actually, lipid oxidation may be continuously increasing during the final stage, but not well detected by TBARS. On that basis, during the increasing TBA value phase (0–21 weeks), a relationship was established linking proteolysis to lipid oxidation, whatever the muscle type (Fig. 3.7b). This relationship was closely fitted with the following linear regression model:

$$\text{TBARS value} = 0.152 \cdot \text{PI} + 0.139 \quad (r = 0.96, p < 0.001) \quad \text{Eq. (3.3)}$$

We note that this correlation is clearly valid only so long as the PI determinations are performed in the conditions described above. Other protocols will require a new formula.



**Figure 3.7:** Time course of lipid oxidation measured on two muscles (biceps femoris and semimembranosus) of different Bayonne dry-cured hams: (a) TBARS values; values were the means +/- SEM of three independent determinations; Significance: \*\*\*  $p < 0.001$ , \*\*  $p < 0.01$ , \*  $p < 0.05$ , NS  $p \geq 0.05$ , and (b) relation between the proteolysis index and TBARS values for the first 21 weeks of dry-cured ham manufacture.



### **Time course of structural parameters**

Accurate quantitative analysis of the microscopy images revealed that the cross sectional area of muscle fibers decreased by about 35% and 39% for BF and SM muscles, respectively, during the first 21 weeks of processing, and then stabilized for both (Fig. 3.8a). Regarding the extracellular spaces (ECS), results showed that these were minimal after 11 weeks of processing (93% and 72% decrease for BF and SM, respectively), and again came close to values for the fresh muscle during the subsequent stages. Overall, similar behavior in terms of time course of ECS was detected in both BF and SM muscles (Fig. 3.8b). This intense decrease in the ECS seems not to be associated to cell swelling, since their cross section area did not increase. It more probably results from the evacuation of the water initially contained in the cells and ECS towards the outside of the muscle. This hypothesis is confirmed by the increase in the fiber numbers, which reflect the surface reduction of the muscle fibers related to the water release (Fig. 3.8c). During the subsequent weeks of processing, the decrease in cross sectional fiber area was associated with an increase in the ECS, which implies a lateral cell contraction. This observation is probably attributable to an intracellular water loss during the drying stage. Contrary to BF, the significant surface reduction of the SM fibers between 35 and 52 weeks of processing is probably related to the external position of this muscle, where the water transfers are correspondingly higher than for the internal BF muscle (Monin et al., 1997).

The surface area of the connective tissue increased significantly following the salting for both muscles (data not shown). It is related to the decrease in the volume of muscle during the drying, which increases the relative proportion of the extracellular matrix. It is also possible that certain essential proteins of the extracellular matrix could be partially distorted because of the increase in the ionic strength. These molecular modifications could lead to an expansion of the connective tissue, thus increasing its calculated surface area.

As a result, the dry-cured ham processing gives rise to dramatic structural modifications of muscle tissue and fibers. Generally speaking, BF and SM showed the same trends in their time course. To complete this work, it would be of interest to study the structural modifications by electron microscopy, in order to gain a better understanding of how salting modifies the muscular ultrastructure, and to obtain more relevant information about mechanisms involved during all the stages in the dry-curing ham process.



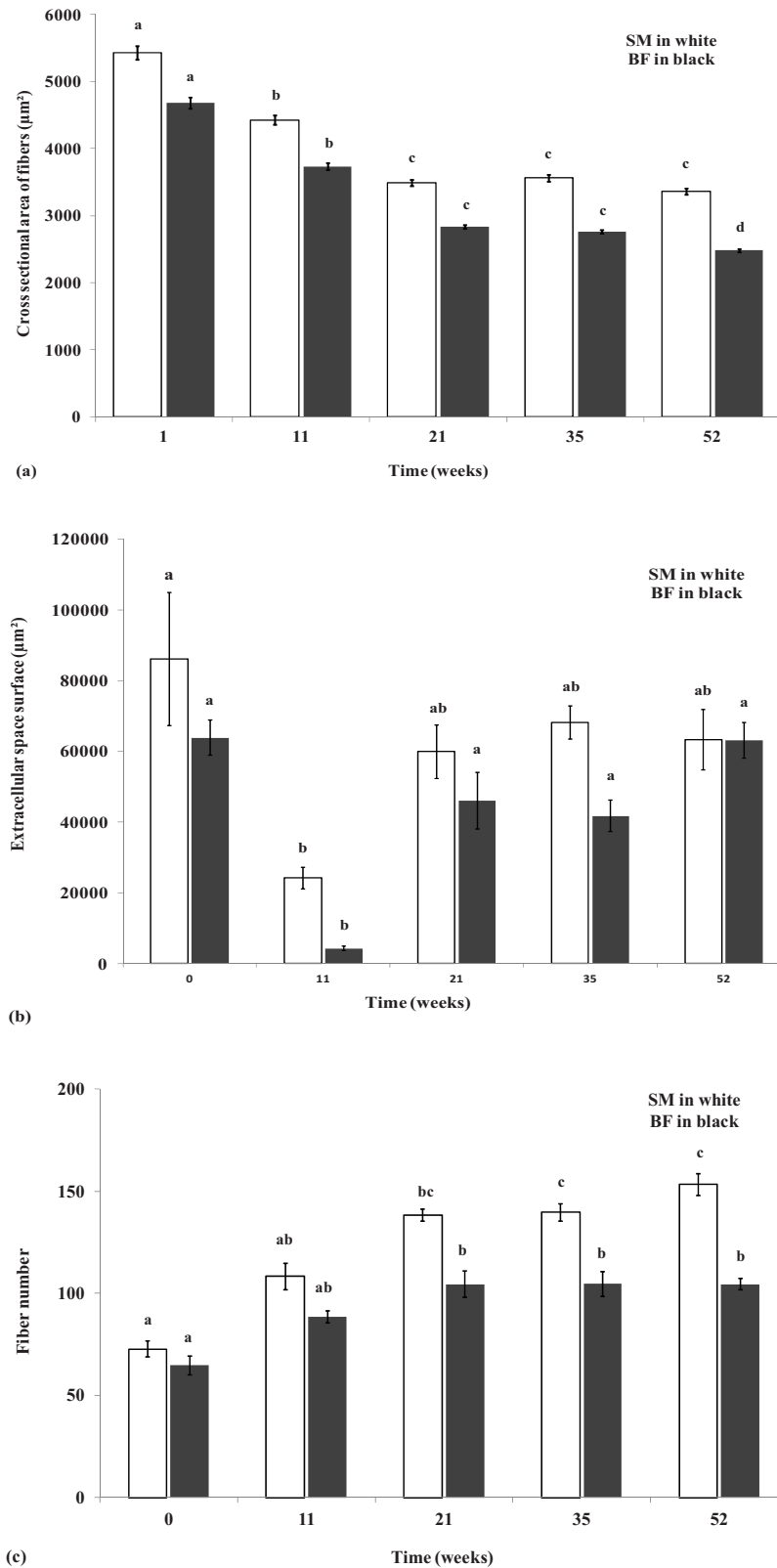


**Figure 3.8:** Time course of three structural parameters investigated in this study on two muscles (biceps femoris and semimembranosus) of different Bayonne dry-cured hams: (a) cross sectional fiber area, (b) extracellular space surface area, and (c) fiber numbers. Values not bearing common superscripts for each muscle differed significantly ( $p < 0.05$ ).

### Time course of textural parameters

Table 3.4 shows how the mean values of the five textural parameters measured, for the SM and BF pork muscles, are modified according to the status of the manufacturing process for dry-cured ham.

**Table 3.4:** Time course of the five textural parameters investigated (hardness, fragility, cohesiveness, springiness and adhesiveness) on two muscles (biceps femoris and semimembranosus) of different Bayonne dry-cured hams. Values were the means  $\pm$  SEM of two independent determinations.

SM pork muscle					
Time (week)	Hardness (N)	Fragility	Cohesiveness	Springiness	Adhesiveness (N.s)
0	122 $\pm$ 23	0.825 $\pm$ 0.028	0.483 $\pm$ 0.062	0.857 $\pm$ 0.008	-3.1 $\pm$ 1.0
11	52 $\pm$ 3	0.860 $\pm$ 0.001	0.504 $\pm$ 0.010	0.727 $\pm$ 0.022	-5.1 $\pm$ 1.8
21	97 $\pm$ 8	0.872 $\pm$ 0.007	0.480 $\pm$ 0.005	0.709 $\pm$ 0.026	-16.1 $\pm$ 5.1
35	108 $\pm$ 17	0.887 $\pm$ 0.005	0.462 $\pm$ 0.034	0.578 $\pm$ 0.024	-27.1 $\pm$ 13.3
52	198 $\pm$ 14	0.875 $\pm$ 0.028	0.488 $\pm$ 0.014	0.663 $\pm$ 0.019	-37.1 $\pm$ 5.2
BF pork muscle					
Time (week)	Hardness (N)	Fragility	Cohesiveness	Springiness	Adhesiveness (N.s)
0	185 $\pm$ 41	0.813 $\pm$ 0.021	0.410 $\pm$ 0.035	0.854 $\pm$ 0.057	-3.3 $\pm$ 1.3
11	74 $\pm$ 7	0.866 $\pm$ 0.014	0.468 $\pm$ 0.035	0.805 $\pm$ 0.028	-6.4 $\pm$ 0.2
21	89 $\pm$ 18	0.848 $\pm$ 0.016	0.471 $\pm$ 0.007	0.821 $\pm$ 0.042	-8.5 $\pm$ 0.9
35	118 $\pm$ 52	0.840 $\pm$ 0.024	0.465 $\pm$ 0.028	0.757 $\pm$ 0.027	-16.1 $\pm$ 3.5
52	183 $\pm$ 3	0.853 $\pm$ 0.013	0.489 $\pm$ 0.024	0.751 $\pm$ 0.001	-13.3 $\pm$ 1.1

Accurate analysis of results reveals that hardness of dry-cured ham samples increased when water content strongly decreased, as soon as the salting and post-salting stages occurring at low temperature were complete. Hardness thus increased significantly between 10 and 52 weeks of processing. Similar behavior was found by Cilla, Martinez, Beltran and Roncales (2005) in Spanish dry-cured ham, with longer ripening (up to 26 months). In addition, the hardness values of Bayonne dry-cured ham samples were approximately the same for both muscles, SM and BF (Table 3.4). These results are in agreement with the observations of Serra et al. (2005), who found an increase in hardness with decreasing water content values in BF muscle of Spanish dry-cured ham. Cohesiveness tended to be higher in SM than in BF muscle at high water content values, but had approximately the same value at the final stage of the process (Table 3.4). Similar results were reported by Ruiz Ramirez et al. (2006) in the

first stages of the dry-cured ham process, while they noted somewhat lower values at the final stages of processing. The same behavior was detected for both muscles throughout the process. Adhesiveness increased with time in both muscles, but the SM values were higher, especially at the final stages of the dry-curing process. Springiness tended to decrease when PI increased, and this particular behavior was observed in both muscles, with lower values for SM (Table 3.4).

### Results of multivariate statistical analysis

For each muscle, ANOVA allowed the effect of several factors on the different textural and structural properties to be assessed (Table 3.5). It showed that PI had a highly significant effect on the extracellular spaces and the cross sectional area for BF muscle ( $p < 0.001$ ), and a significant effect for SM muscle ( $p < 0.05$ ). PI also had a very significant effect on the fragility of BF muscle and the springiness of SM muscle ( $p < 0.01$ ). The water content had a highly significant effect on the hardness for BF muscle ( $p < 0.001$ ), and a significant effect on the cross sectional area and the extracellular spaces for SM muscle ( $p < 0.05$ ). Analyzing the results of the ANOVA showed that salt content had a very highly significant effect on the adhesiveness for SM muscle and on the extracellular spaces for BF muscle ( $p < 0.01$ ) and a significant effect on the hardness for both muscles ( $p < 0.05$ ).

By means of multiple polynomial regressions, different structural and textural models were then built, for SM and BF muscles, for the entire dry-cured ham production process. Table 3.5 contains all the coefficients statistically calculated to build these models, which allow the textural and structural parameters investigated to be quantified from knowledge of the PI values, the water and salt contents, and their interaction.

In the present study, the ‘hardness’ model, as an example for a textural model, and the fiber numbers model, as an example of a structural model, established for the SM muscle are reported. The  $R$ -squared coefficients determined for these two models are relatively high: 0.87 and 0.84, respectively, which means that the phenomenological models that give these two textural and structural parameters fit the experimental data closely:

$$\text{Fiber Number}_{\text{SM}} = 551.55 + 2.12 \text{ PI} - 84.18 \text{ S} - 6.41 \text{ W} + 1.16 \text{ S.W} \quad \text{Eq. (3.4)}$$

$$\text{Hardness}_{\text{SM}} = -7.77.10^2 - 2.96 \text{ PI} + 0.258 \text{ PI}^2 + 2.42.10^2 \text{ S} + 12.05 \text{ W} - 3.57 \text{ S.W} \quad \text{Eq. (3.5)}$$

Where  $PI$  is the proteolysis index (%),  $S$  is the salt content (% DM) and  $W$  is the water content (% TM).

**Table 3.5:** Details of multiple polynomial regression coefficients calculated from experimentally quantified textural and structural parameters, for BF and SM pork muscles. PI represents the proteolysis index (%), T the temperature (°C), S the salt content (% dry matter) and W the water content (% total matter).

BF muscle	Textural parameters					Structural parameters			
	Hardness	Fragility	Cohesiveness	Springiness	Adhesiveness	Fiber number	Extracellular spaces	Cross sectional area	Connective tissue area
Intercept	4.48.10 <sup>3</sup>	0.476	1.678		6.115	47.80	-2.50.10 <sup>6</sup>	6.71.10 <sup>3</sup>	
(PI) <sup>0.5</sup>	9.99.10 <sup>2</sup>	1.058*	0.765		-9.396	41.82	-	-2330.3***	
PI	-7.35.10 <sup>2</sup> *	-0.62**	-0.529		-	-	-2.33.10 <sup>4</sup> ***	-	
PI <sup>2</sup>	-	-	-		-	-	514.2***	-	
W	-60.63***	4.30.10 <sup>-4</sup>	-0.020		-	-	4.77.10 <sup>3</sup>	-	
S	-89.16*	0.233	-		3.80	-	4.91.10 <sup>4</sup> **	-	
W S	-	3.49.10 <sup>-3</sup>	-		-	-	-	-	
R <sup>2</sup>	0.81	0.67	0.54		0.60	0.47	0.77	0.58	
Adjusted R <sup>2</sup>	0.73	0.46	0.40	< 0.25	0.52	0.43	0.68	0.55	< 0.25
RSE	37	0.026	0.041		3.98	17.6	1.57.10 <sup>4</sup>	784.6	
SM muscle	Hardness	Fragility	Cohesiveness	Springiness	Adhesiveness	Fiber number	Extracellular spaces	Cross sectional area	Connective tissue area
Intercept	-7.77.10 <sup>2</sup>	-0.292		0.932	-5.19.10 <sup>2</sup>	551.55	2.74.10 <sup>6</sup>	-3.29.10 <sup>4</sup>	
(PI) <sup>0.5</sup>	-	1.086*		-	-	-	-1.47.10 <sup>6</sup>	1.57.10 <sup>4</sup>	
PI	-2.956	-0.483*		-0.030**	4.682	2.121	6.44.10 <sup>5</sup> *	-7.56.10 <sup>3</sup>	
PI <sup>2</sup>	0.258	-		7.35.10 <sup>-4</sup>	-0.108	-	-	-	
W	12.05	0.010		-	6.778	-6.41	-2.89.10 <sup>4</sup> *	4.33.10 <sup>2</sup> *	
S	2.42.10 <sup>2</sup> *	0.166		-	124.2**	-84.18	-3.60.10 <sup>5</sup> *	5.22.10 <sup>3</sup>	
W S	-3.57	-0.0029		-	-1.759	1.158	5.49.10 <sup>3</sup>	-79.09	
R <sup>2</sup>	0.87	0.68		0.75	0.79	0.84	0.66	0.79	
Adjusted R <sup>2</sup>	0.80	0.51	< 0.25	0.70	0.68	0.77	0.47	0.67	< 0.25
RSE	24.2	0.025		0.055	9.9	15.7	3.20.10 <sup>4</sup>	6.16.10 <sup>2</sup>	

RSE: Residual Standard Error / Significance: \*\*\* p < 0.001, \*\* p < 0.01, \* p < 0.05

For the first time, different quantitative structural models based on PI values, water and salt contents and their interaction are established that should remain valid throughout the dry-cured ham process. The results in Table 3.5 show that structural properties are strongly affected by all these factors, in particular the extracellular space surface area. The PI factor was present in all the structural models, showing its effective and crucial role in structural changes during the entire dry-cured ham process. Salt content had to be included quite often in these phenomenological models, thus showing its very marked effect, in particular on the extracellular spaces. Generally speaking, we also observed a greater role of water content in SM muscle than in BF muscle. This may be because SM muscle dries rapidly as soon as the process begins; consequently, quantifying many structural and textural parameters of this superficial ham muscle absolutely requires taking into account water content. The interaction between water and salt content had to be introduced in the SM structural models, whereas it

was not necessary in any of the BF ones. Again, this observation could be related to the intense salt diffusion and water evaporation that occur in the SM muscle compared with the BF muscle, especially during the first stages of the process, thus leading to these differences between the two muscles, and showing again the importance of the geometrical location of the muscles in the 3D ham.

A small number of studies sought to relate some textural parameters, such as hardness or fragility, to other factors such as PI, water content and/or salt content. We note that Ruiz-Carrascal, Ventanas, Cava, Andres and Garcia (2000) found a negative correlation relating hardness to fat content in Iberian ham. In this study, we have established that hardness is related to PI, as shown in Eq. (3.5), in agreement with Virgili et al. (1995), who found a correlation between proteolysis and hardness in Parma dry-cured ham. The statistical analyses performed here also clearly show that PI was crucial in explaining the time course of cohesiveness for BF muscle, and springiness for SM muscle; these results confirm those of Ruiz-Ramirez et al. (2005), who reported that cohesiveness and springiness were proportional to PI values. Table 3.5 also shows that adhesiveness can be reasonably estimated as a function of PI values, water content and salt content, this last factor having a very significant effect on adhesiveness, in particular for SM muscle.

However, all the results reported in Table 3.5 need to be confirmed by further experiments to highlight both truly significant correlations and complete absence of correlation (i.e. when adjusted R-squared coefficients are lower than 0.25). For instance, for connective tissue area, no statistical model was found for either muscle investigated. This could be because this particular structural parameter does not depend on PI or water and salt content, but it could also be because not enough samples were analyzed to establish a significant correlation. It is clear that the statistical significance of the correlations reported in Table 3.5 would gain from being based on a larger number of dry-cured ham samples. This is planned in future work. We must bear in mind that in the present study, the phenomenological models reported were statistically built on the basis of experiments performed on samples extracted from 15 dry-cured hams, corresponding to three dry-cured hams and five process times. Even so, this study has the merit of giving, often for the first time, statistical models allowing the quantitative estimation of several structural and textural parameters as a function of proteolysis index and some basic physicochemical parameters, such as water and salt content.

## **Conclusion**

Quantitative information about the interrelationships between proteolysis, texture and/or structure is provided in this study by the development of several statistical models allowing the time course of some textural parameters, such as hardness, cohesiveness, springiness, fragility and adhesiveness, and of some structural parameters of dry-cured ham, such as fiber numbers, extracellular spaces and cross sectional area of muscle fibers, to be estimated, with greater or lesser accuracy, as a function of proteolysis index, salt and water contents, and their interaction. Few studies of this type are available in the literature. However, we are aware that the robustness of the correlations established in this study would be improved by increasing sample size.

The phenomenological models built here could be then incorporated into a numerical finite-element model dedicated to predicting salt diffusion, water migration and heat transfer inside a 3D ham geometry, to simulate the time course of proteolysis and of some textural and structural parameters throughout the dry-cured ham process. Once validated, this complete “numerical” ham model could then be used to test different scenarii to allow salt content to be reduced in dry-cured hams, while avoiding excessive proteolysis leading to a too-soft product, and preserving the textural properties that consumers demand.

## **Acknowledgments**

This work was funded by the Na- integrated programme (ANR-09-ALIA-013-01) financed by the French National Research Agency. This paper forms part of the thesis of Rami Harkouss, who works for this research program. We thank Riziki Ali for her participation in image analysis, Annie Venien and Raphaël Favier for their technical assistance, ADIV for measuring the textural parameters in Bayonne dry-cured ham samples, and ATT for language editing.

### 3.4. Article n°5 (projet à soumettre à Food and Bioprocess Technology)

**Building a 3D “numerical ham” that simulates and couples water and salt transfers to proteolysis during the dry-cured ham process. Application to the modelling of the salting and post-salting stages of process.**

Harkouss R., Chevarin C., Daudin J.D., and Mirade P.S.

INRA, UR370 Qualité des Produits Animaux, F-63122 Saint-Genès-Champanelle, France

#### **Abstract**

Since salting is essential during the dry-cured ham elaboration process, reducing salt content could affect the final product quality. The aim of this study was to build a 3D numerical model which estimates the biochemical evolution (proteolysis) as well as the distribution of salt and water contents during the first stages of dry-cured ham process, i.e. the salting and the post-salting stages. The first approach of the simulation showed a very good prediction of profiles of salt and water content in the ham. The robustness of the model was evaluated by comparing the predicted values of proteolysis index (PI) at the end of post-salting stage with the experimental PI values measured in samples extracted from industrial Bayonne dry-cured hams. The crucial role of the thin film of fat existing inside the ham was also numerically highlighted and assessed. The 3D “numerical ham” built can be considered as an original software tool that could be useful to reduce the final salt content in dry-cured hams, without altering their final quality.

*Keywords: simulation, numerical ham, water migration, heat transfer, proteolysis, dry-cured ham.*

#### **Introduction**

Generally speaking, salt is essential to maintain humans in good health. It controls blood pressure, helps in transmitting nerve cell impulses and enhances the proper balance of fluids in the body. In industrialized countries, most surveys showed an averaged daily salt consumption of 6-8 g per person, whereas 2 g per day are physiologically sufficient for a 60 kg person. This extra sodium intake has been linked to hypertension, increasing risk of stroke and cardiovascular disease, as well as raising calcium excretion which can lead to osteoporosis (Karppanen & Mervaalaa 2006; Lawes, Van der Hoorn, Law, Elliott, MacMahon, & Rodgers 2006). Therefore, many research projects, such as the French “Na”

project, are performed to find technological ways allowing salt content to be reduced in manufactured food products, and thus obtaining healthier food products. In the dry-cured ham elaboration process, salt is a multifunctional element that influences the final product in terms of quality and safety. Salt contributes to water holding capacity, texture and flavour development and limits the growth of pathogens and spoilage microorganisms (Benedini, Parolari, Toscani, & Virgili 2012; Taormina 2010). On the other hand, the final dry-cured ham quality is also affected by the time-course of proteolysis which depends on various factors, such as temperature, pH, salt and water contents (Toldrá & Flores 2000; Arnau, Guerrero, & Gou 1997; Serra, Ruiz-Ramirez, Arnau, & Gou 2005). It has been shown that during the drying-ageing stage, moderate air temperatures and drying inhibited the formation of non-protein nitrogen compounds and decreased water activity ( $a_w$ ) and in turn, the proteolysis intensity. Moreover, many authors have studied the effect of salt on the action of proteolytic enzymes. Zhao, Zhou, Wang, Xu, Huan, and Wu (2005) observed that salting decreased the potential activities of cathepsin B and L down to only 9.31% and 13.66% of their original potential activity, thus confirming the inhibitory role of salt. Very recently, similar results were obtained by Harkouss, Safa, Gatellier, Lebert, and Mirade (2014) who highlighted the promoting role of temperature and on the contrary, the inhibitory role of salting and drying on the time-course of proteolysis measured in laboratory-prepared pork meat samples.

Although salt is essential during the dry-cured ham manufacturing, many efforts have been made to reduce the final salt content, without altering the final dry-cured ham quality. To achieve this, NaCl reduction was mainly performed through two different approaches: (a) direct reduction of NaCl content or (b) partial substitution of NaCl by other salts. Results of the first approach showed that longer post-salting time was needed for lower-sodium hams to reach the same  $a_w$  values as hams normally salted with 100% NaCl. No more than 25% salt reductions can be obtained using this first approach. Besides, Grau, Albarracin, Toldra, Antequera, and Barrat (2008) reported that freezing then thawing hams before the salting process, reduced the salting time and provided hams with a lower final salt content. However, particular caution has to be paid when using this approach to avoid any microbiological stability problem and final defective texture as a result of abnormal proteolysis (Desmond 2006; Ruiz-Ramirez, Serra, Gou, & Arnau 2005). Given these concerns, NaCl substitution by potassium chloride, calcium chloride, magnesium chloride or K-lactate constitutes the second approach that can be used. However, manufacturing hams with salt mixtures with low-sodium content may lead professionals to modify the dry-curing ham process, especially by extending



the time of the post-salting stage at low temperature (Aliño, Grau, Fuentes, and Barrat 2010). As a result, many studies have indicated that KCl and K-lactate could be considered as effective NaCl alternatives; hence these salts are commonly employed in meat products to lengthen shelf-life and increase food safety. In fact, to better understand how partial substitution of NaCl by other salts can be performed in meat processes, a perfect knowledge of their diffusion properties is required. Some authors determined the diffusion coefficient of salt ( $D$ ) in meat. These authors confirmed that using salts that rapidly diffuse inside hams, such as potassium, would contribute to accelerate the salt distribution, allowing salting time to be reduced and finally, low-sodium dry-cured ham to be obtained (Barat, Baigts, Aliño, Fernandez, & Perez-Garcia 2011; Blesa, Aliño, Barat, Grau, Toldrá, & Pagán 2008).

In food industry, salting and drying are mass transfer processes leading to time-variable water and salt content profiles. It is of high interest to assess the time-course evolution and to quantify these two parameters, e.g. to better understand their effects on the biochemical evolution and textural properties that occur during the dry-cured ham manufacture. Traditional measurement techniques are time- and product-consuming. Non-destructive methodologies, such as Nuclear Magnetic Resonance (NMR), are now well used to estimate local salt and water values in dry-cured hams (Fantazzini, Gombia, Schembri, Simoncini, & Virgili 2009). Recently, Santos-Garcés, Muñoz, Gou, Sala, and Fulladosa (2012) and Haseth, Sørheim, Høy, and Egelanddal (2012) used Computed Tomography (CT) to build salt and water content models in different stages of dry-curing hams and concluded that CT is a suitable technology for characterizing and optimizing dry-cured ham salting processes. Although these analysis tools are not invasive, they have to be repeatedly used during the elaboration process that lasts several months to pursue water migration and salt diffusion patterns in the ham. On account of this, numerical modelling and simulation could be a good way to replace the experimental tools mentioned above, since it is non-invasive, non-destructive, less expensive, and these techniques do not necessitate much time to obtain the requested information.

There are a lot of researches that studied the salt and water transfers in dried meat products using a numerical modelling approach. Effective moisture diffusivity coefficients in SM and BF muscles were determined by Gou, Comaposada, and Arnau (2004), but they built a simple diffusive model. In addition, Barat et al. (2011) represented salt transfer by mathematical models and estimated the NaCl and KCl diffusion coefficients on pork meat samples. However, very few studies aimed at modelling salt and water transfers during the different stages of dry-curing hams. One of them was performed by Said, Schüller, Young, Aastveit,

and Egelanddal (2007) who numerically simulated in three dimensions the salt diffusion in bacon pork. On the other hand, there has not been a single study that predicted the time-course of proteolysis during the dry-cured ham production process. Very recently, Harkouss et al. (2014) established phenomenological models allowing proteolysis to be quantified, for five various pork muscles, as a function of temperature, water and salt content. However, quantitative modelling of salt diffusion, water migration, heat transfer and proteolysis evolution using finite element method has, to our knowledge, never been attempted in dry-cured ham. On account of this, this study aims at presenting a multi-physical 3D model developed under the Comsol<sup>®</sup> Multiphysics software that combines a determination of proteolysis through the phenomenological models developed by Harkouss et al. (2014) with salt penetration, water migration and heat transfer modelling. For practical reason, this paper is focused on the modelling of what happens in terms of water and salt transfers and proteolysis during the first stages of the dry-curing ham elaboration process, those carried out at low temperature, i.e. the salting and post-salting stages. The final ambition of this research project is to provide to meat industry an adequate and practical simulation tool allowing ambitious technological scenarios leading to the manufacture of low-sodium dry-cured hams to be easily and freely tested.

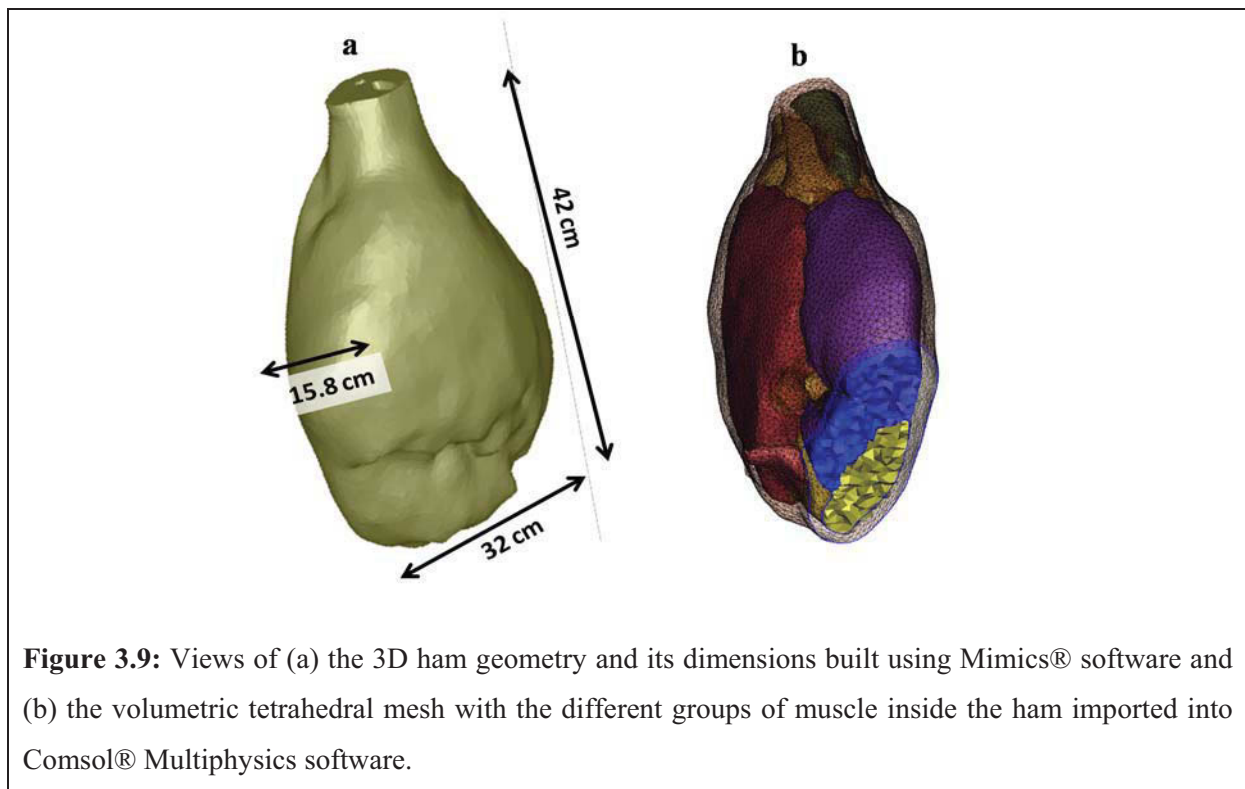
## **Materials and methods**

Before integrating the biochemical models (proteolysis) and the physical models (mass and heat transfer) into the multi-physical model built using Comsol<sup>®</sup> multiphysics software, a complete 3D ham geometry was built.

### **3D ham geometry and meshing**

The process of constructing an accurate 3D ham representation required a series of 2D slices of a fresh ham that can be typically provided by Computed Tomography (CT), which is a rapid and non destructive X-ray imaging technique. Images of high quality have to be used since it has a direct impact on subsequent steps in the overall procedure. Automated tools for noise reduction, smoothing and contrast sharpening were used as well as other data manipulation tools such as re-sampling and rescaling. The process was automated by thresholding, meaning that the different parts of the ham, i.e. rind, muscles, bone and thin film of fat between the SM and BF muscles, were identified by specifying minimum and maximum values for the signal. In total, the segmentation of 181 X-ray CT images of green

ham was made using specific software called Mimics® (Materialise, Leuven, Belgium). The segmented objects were then simultaneously connected and meshed based on an orthotropic grid intersected by interfaces defining the boundaries. The obtained 3D ham geometry was then smoothed and meshed many times in order to obtain a high quality surface mesh (Figure 3.9a). After that, a volumetric tetrahedral mesh with extra smooth boundary was obtained, corresponding to a 42 cm-long, 32 cm-wide and 15.8 cm-depth ham. Finally, the 3D ham model consisting in 202,000 tetrahedral meshes and containing five different groups of muscle was imported into Comsol® Multiphysics software (Figure 3.9b).



### Proteolysis model

Knowing that proteolysis in dry-cured ham depends on muscle type, temperature, salt and water contents, several phenomenological models allowing proteolysis rate to be quantified as a function of the factors previously mentioned have been built and recently published in Harkouss et al. (2014). In the present study, modelling of proteolysis was performed from solving Eq. (3.6) and assuming that the proteolysis rate could be calculated at each time step from a global phenomenological model (Eq. (3.7)) in which four different pork muscles (semi-membranous, semitendinosus, biceps femoris and rectus femoris) were considered together, on account of similar behaviour in terms of time-course of proteolysis (Harkouss et al. 2014):

$$\frac{d PI}{d t} = R_i \quad \text{Eq. (3.6)}$$

with

$$R_i = 8.286.10^{-4} - 1.024.10^{-2}.T + 1.147.10^{-4}.S + 1.466.10^{-4}.W - 2.62.10^{-4}.T.S \\ + 3.254.10^{-4}.T.W - 1.746.10^{-6}.S.W \quad \text{Eq. (3.7)}$$

where PI is the proteolysis index (%) which characterizes the proteolysis intensity, T is the temperature (°C), S is the salt content (kg salt.kg dried matter<sup>-1</sup> or % DM) and W is the water content (kg water.kg total matter<sup>-1</sup> or % TM).

These equations were solved in all domains of the numerical ham, except the bone which was logically excluded from the PI calculation. In addition to these equations, an initial condition was applied to PI. Indeed, a PI<sub>(t=0)</sub> value of 2.5% was considered, which represents the mean average of a huge number of experimental PI measurements carried out on fresh small pork meat samples prepared from different ham muscles.

### Heat transfer modelling

Fourier law was introduced to numerically simulate heat transfer inside the ham and predict how ham temperature changes in response to the modification of air temperature during the pre-drying or drying/ripening stages. The simplified equation that was solved for calculating the distribution of the ham temperature T as a function of space and time is:

$$\rho c_p \frac{\partial T}{\partial t} = \nabla \cdot (k \nabla T) \quad \text{Eq. (3.8)}$$

where t is the time (s), ρ is the ham density (1072 kg.m<sup>-3</sup>), c<sub>p</sub> is the ham specific heat capacity (3200 J.kg<sup>-1</sup>.K<sup>-1</sup>) and k is the ham thermal conductivity (0.45 W.m<sup>-1</sup>.K<sup>-1</sup>).

This equation was applied and solved in all domains of the numerical ham, except the bone which was considered as thermally insulated. At time 0, i.e. at the beginning of the salting stage, we assumed that a green ham having an initial temperature of 3°C was placed in a cold room with air at 4°C.

At the air-ham interface, the following thermal boundary condition was imposed in the model, thus allowing the heat flow rate q to be calculated taking into account the thermal convection and the energy exchanged during water evaporation:

$$q = h (T_{air} - T_{surface}) + \phi_{water} \cdot L_v \quad \text{Eq. (3.9)}$$

In the previous equation,  $h$  represents the convective heat transfer coefficient. A value of  $h$  equal to  $7 \text{ W.m}^{-2}.\text{K}^{-1}$  was considered in the present model as a result of low air velocity (Kondjoyan & Daudin 1997).  $T_{\text{surface}}$  represents either the temperature of the muscle surface where salt is added or the temperature of the ham rind surface where no salt is added since we modelled here a “limited salt input” salting procedure consisting in salting only the muscle part of the ham without salting the rind. At last, in Eq. (3.9),  $L_v$  represents the latent heat due to the water evaporation (equal to  $2450 \text{ kJ.kg}^{-1}$ ) and  $\phi_{\text{water}}$  is the water flow rate that evaporates from the muscle or the rind surface. How  $\phi_{\text{water}}$  is calculated is explained in the next section (‘Mass transfer modelling’).

### Mass transfer modelling

We assumed that the mass transfer phenomena that occur during the dry-cured ham elaboration process, i.e. salt diffusion and water migration, can be modelled by the following Fick equation:

$$\frac{\partial c_i}{\partial t} + \nabla \cdot (-D_i \nabla c_i) = 0 \quad \text{Eq. (3.10)}$$

where  $c_i$  is the salt or water concentration. In Eq. (3.10),  $D_i$  represents the diffusion coefficient of salt or water inside the ham. For these coefficients, in the lean meat of ham, we assumed a constant  $D_{\text{salt}}$  equal to  $5.10^{-10} \text{ m}^2.\text{s}^{-1}$ , but a  $D_{\text{water}}$  varying as a function of the water content expressed on dry basis ( $X_{\text{water}}$ ) according to the following relation (Ruiz-Cabrera et al. 2004):

$$D_{\text{water}} = 4 \cdot 10^{(0.625 \cdot X_{\text{water}} - 12)} \quad \text{Eq. (3.11)}$$

The Fick equation was solved in all domains, except in the bone which was logically excluded from the calculation. An initial salt content of 0% TM and an initial water content of 75% TM, i.e. values corresponding to fresh meat, were imposed in the model.

As previously indicated, the “numerical ham” model was used first to assess what happens in terms of water and salt transfers and proteolysis during the first 11 weeks of process performed at low air temperature. This period of time included a first stage of salting corresponding to a “limited salt input” salting procedure applied for 15 days only on the muscle side of the ham. From a numerical point of view, salting on the muscle side was modelled through the application of a brine solution composed of a variable mass of salt added to a constant volume of water. Indeed, at each time step of the salting stage, the mass of salt that penetrated inside the ham was calculated as well as the mass of salt that stayed at the

ham surface and thus the new salt concentration of the brine solution in contact with the muscle side of the ham. The salting stage was then followed by 62 days of post-salting during which salt diffused inside the ham. Simultaneously to salt diffusion, water migration occurred from inside the ham to the outer zones where evaporation took place. For that purpose, specific boundary conditions had to be imposed at the ham-air interface in terms of mass flow rates.

The water flow rate can be calculated from the following classical equation:

$$\varphi_{water} = k \cdot \left( a_{w,surface} \cdot P_{sat,T_{surface}} - \frac{RH_{air}}{100} \cdot P_{sat,T_{air}} \right) \quad \text{Eq. (3.12)}$$

With an air relative humidity value  $RH_{air}$  of 70% and in the range of temperature 0-40°C:

$$P_{sat,T} = \exp \left( -\frac{6764}{T} - 4.915 \cdot \log T + 58.75 \right) \quad \text{Eq. (3.13)}$$

In Eq. (3.12),  $k$  which is the water transfer coefficient ( $\text{kg} \cdot \text{m}^{-2} \cdot \text{Pa}^{-1} \cdot \text{s}^{-1}$ ) can be calculated from the convective heat transfer coefficient  $h$  using the relation (Kondjoyan & Daudin 1997):

$$k = \frac{h \cdot M_{water}}{Cp_{air} \cdot M_{air} \cdot P_{atm} \cdot Le^{2/3}} \quad \text{Eq. (3.14)}$$

with  $M_{water} = 18 \text{ g} \cdot \text{mol}^{-1}$ ;  $Cp_{air} = 1004 \text{ J} \cdot \text{kg}^{-1} \cdot \text{K}^{-1}$ ;  $M_{air} = 29 \text{ g} \cdot \text{mol}^{-1}$ ;  $P_{atm} = 1 \text{ atm}$ ; and  $Le$  is the Lewis number which is equal to 0.777 for air. On the rind side of the ham, we arbitrary assumed that the water transfer coefficient  $k$  was divided by a factor 20 to indirectly account for the barrier effect against water transfer played by the fat layer located just under the rind.

In Eq. (3.12), the term ‘surface’ is associated either to the muscle side or to the rind side depending on the boundary condition considered (Figure 3.10). On the rind side of the ham, we arbitrary considered that the water activity at the rind surface was equal to 1 due to the presence of a few mm-thick fat layer. On the other hand, on the muscle side of the ham, owing to the presence of salt, the water activity at the muscle surface obeyed to the following relations (Rougier 2006; Rougier et al. 2007):

$$a_{w,salted\ meat} = a_{w,meat\ with\ no\ salt} \cdot a_{w,salted\ water\ in\ meat} \quad \text{Eq. (3.15)}$$

With:

$$a_{w,meat\ with\ no\ salt} = a_{w,gelatin\ with\ no\ salt} = 0.993 \cdot \exp(-0.0204 \cdot X_{water}^{-1.96}) \quad \text{Eq. (3.16)}$$

$$a_{w,salted\ water} = -0.4553 \cdot X_{salt}^{water^2} - 0.5242 \cdot X_{salt}^{water} + 0.999 \quad \text{Eq. (3.17)}$$

Where  $X_{salt}^{water}$  represents the salt content expressed on water basis ( $\text{kg salt} \cdot \text{kg water}^{-1}$ ).



In a real green ham, there is a fat film (approximately 2 to 5 mm of thickness) between the SM and BF muscles, which separates the upper part of the ham from the lower part. In practice, this internal fat film acts as a barrier and affects the salt and water transfers inside the ham. Consequently, we took into account this fat film in the “numerical ham” model by defining a thin diffusion layer at the interface between the two groups of muscles with the following characteristics: a mean thickness of the fat film of 3 mm and lower diffusion coefficients for salt and water equal to  $10^{-10}$  m<sup>2</sup>/s and to  $10^{-12}$  m<sup>2</sup>/s, respectively, in this fat region (Lebert and Daudin 2013).

As previously indicated, salting on the muscle side of the ham was numerically modelled through the application of a brine solution on the muscle surface (Figure 3.10).

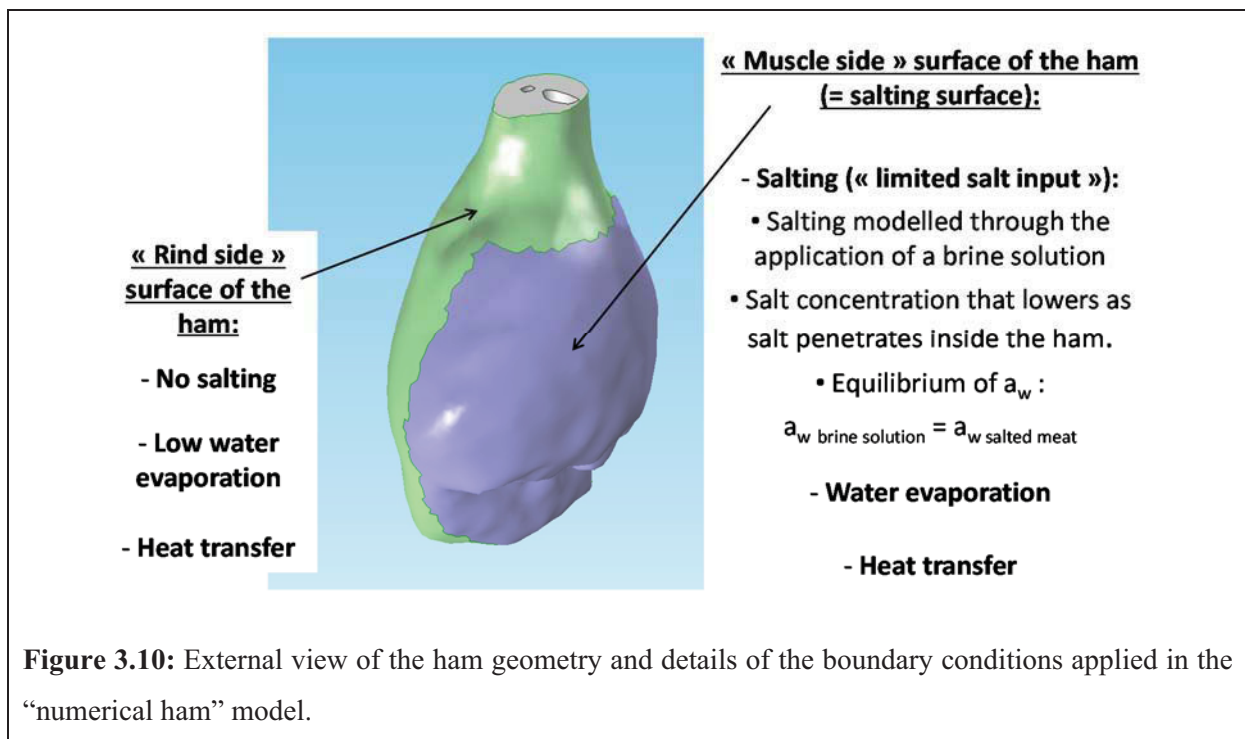


**Figure 3.10:** External view of the ham geometry and details of the boundary conditions applied in the “numerical ham” model.

In terms of salting, the boundary condition applied to the muscle side of the ham consists in writing the equality of water activities between the brine solution and the first layer of meat in contact with this brine solution. This assumption leads to:

$$a_{w\text{brine solution}} = a_{w\text{salted meat}} \quad \text{Eq. (3.18)}$$

The first term of this equation ( $a_{w\text{brine solution}}$ ) was calculated using Eq. (3.17) and from the salt balance performed at each time step of the salting stage on the salting surface allowing the mass of salt to be calculated and thus, for the brine solution, the term  $X_{\text{salt}}^{\text{water}}$ . Note that, in the salting conditions tested in the numerical model presented here, i.e. an initial mass of salt

equal to 655 g added to a constant water volume of 100 ml, the brine solution stayed saturated throughout the salting stage, thus leading to a water activity of the brine solution equal to 0.759.

The right-hand-side term of Eq. (3.18) ( $a_{w_{salted\ meat}}$ ) corresponds to Eq. (3.15). Solving Eq. (3.18) allows, for the salted meat, the term  $X_{salt}^{water}$  to be assessed, and then the salt concentration in the first layer of meat in equilibrium with the brine solution.

Once implemented in the “numerical ham” model, solving all these equations lasted about 3.5 h on a 3 GHz Xeon 8-processors PC with 48 Go of RAM to model what happened during the salting and post-salting stages in terms of time course of proteolysis and water and salt transfers.

## Results and discussion

In this paper, only the results corresponding to the first two stages performed at low temperature, i.e. salting and post-salting, will be shown. After convergence, spatial and time distribution of the following parameters can be visualized in the 3D ham geometry: salt content, water content, PI and  $a_w$  values. In addition to these spatial and time values, mean values of the same parameters can be easily calculated in each group of muscles or in the whole ham geometry, if necessary. The barrier role played by the thin fat film existing between the SM muscle, on one hand, and the ST and BF muscles, on the other hand, will be also discussed in this article.

### Distribution of spatial and time values of salt content, water content and PI

Figure 3.11 shows the distribution of PI, water and salt contents predicted by the numerical model during the salting stage, after one week or two weeks of process. In this figure, each view presents the distribution of water content, in the range 50%-75% TM, on the section located in the lower part of the ham geometry, the distribution of salt content, in the range 0%-10% TM, on the section located in the middle part of the ham geometry, and that of PI, in the range 2.5%-12.5%, on the section located in the upper part of the ham geometry. Analysis of these sections highlights the heterogeneity in the distribution of these parameters inside the ham during the first weeks of the process. After one week of process, the salt penetration is only visible in the few first centimeters from the salting surface, leading to a salt concentration reaching 10% TM in this region, whereas it is lower in the middle part of the ham (2%-3% TM) and negligible near to the rind side of the ham opposite the salting surface.



Concerning the water migration and distribution, Figure 3.11 shows that just the superficial area of the “muscle side” of the ham has lost water during the first week of process.

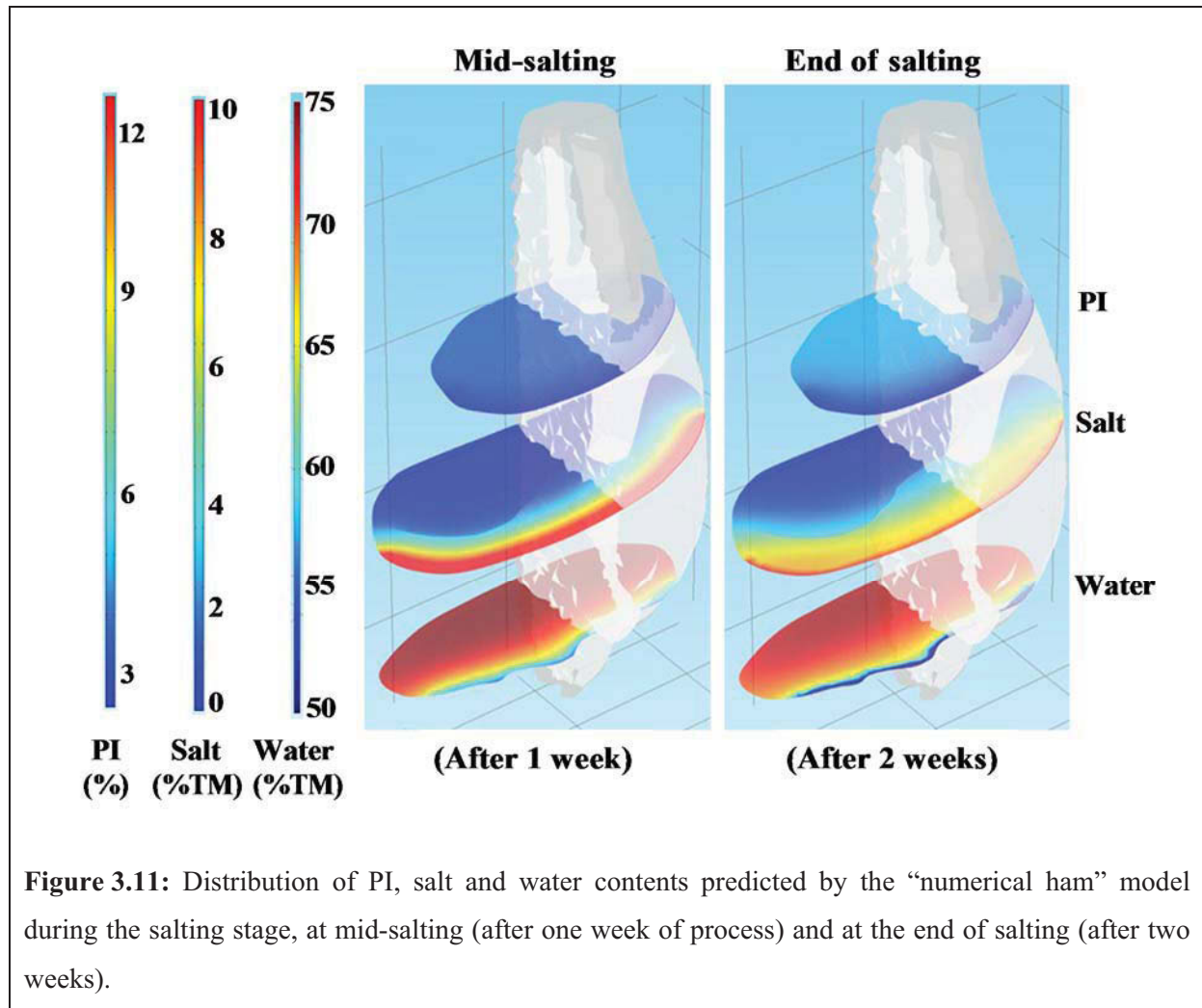


**Figure 3.11:** Distribution of PI, salt and water contents predicted by the “numerical ham” model during the salting stage, at mid-salting (after one week of process) and at the end of salting (after two weeks).

After two weeks of process, i.e. at the end of salting, Figure 3.11 shows that salt has diffused more inside in the ham, increasing obviously the salt concentration, in particular in the middle part of the ham where concentration values reach 5% TM; however, the salt concentration is still relatively low in the deeper zones of the ham. Due to water evaporation, the water content of the ham continued to decrease until the end of salting, but this is still visible close to the salting surface, in particular in the few first millimetres of this surface where the water content decreased to 55% TM. As a result of the short duration of process, PI values did not increase clearly during these two weeks, even if, in the deeper zones of the ham, predicted PI was equal to approximately 4-5% compared to 2.5%-3% close to the salting surface. Actually, owing to the behaviour highlighted by the phenomenological models of proteolysis built, the predicted PI values were logically lower in areas highly dried and highly salted, as close to the salting surface. Inside the ham, the proteolysis logically increased due to high water content

values combined to low salt content values, thus leading to a 2-3% increase in PI values during the two first weeks of process (Figure 3.11).

During the post-salting stage, numerical simulation showed that, some weeks after the end of salting, homogeneity started to take place in the different domains of the ham (Figure 3.12). This homogeneity is more and more visible, especially when visualizing the distribution of salt content at the end of the post-salting stage (Figure 3.12). During this stage, salt showed a great ability to penetrate deeply towards the inner zones of the ham. After six weeks, the salt content gently increased in the middle of the ham (4%-5% TM) and slightly in the deepest zones of the ham where values of 2%-3% TM were predicted. Meanwhile, the water content of the ham gradually decreased in the inner zones (68%-70% TM) and the very dried zone still exists close to the salting surface. Due to the evolution of the salt and water content, PI values logically increased inside the ham where indices ranging from 7% to 9% were predicted, leading to the apparition of a gradient of PI between the inner zone of the ham and the zone located in close proximity to the salting surface where salting and drying highly inhibited the proteolysis evolution (Figure 3.12).

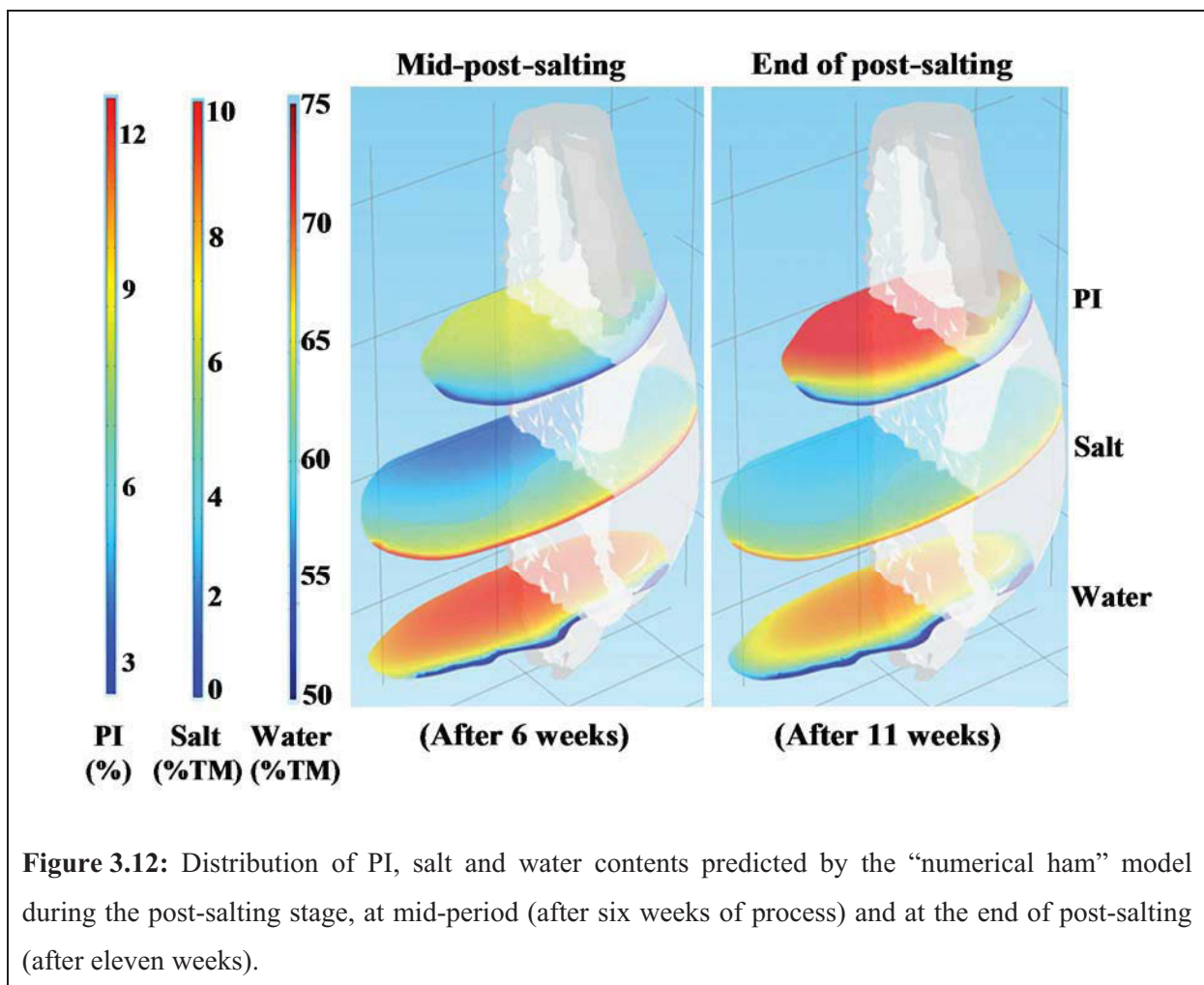


**Figure 3.12:** Distribution of PI, salt and water contents predicted by the “numerical ham” model during the post-salting stage, at mid-period (after six weeks of process) and at the end of post-salting (after eleven weeks).

At the end of the post-salting stage, i.e. after 11 weeks of process, due to diffusion, the distribution of salt appeared as more and more homogeneous inside almost all the ham volume with values of salt content of about 4-5% TM. The salt content even decreased in the zone close to the salting surface where high salt content values were now predicted only on the few first millimetres (Figure 3.12). During this period, the water content obviously decreased inside the ham (65%-67% TM) and the thickness of the very dried zone close to the salting surface slightly increased (Figure 3.12). Eleven weeks were finally necessary to raise the predicted PI values in a noticeable manner, especially in the inner domains of the ham where PI exceeded 10%. Figure 3.12 also shows that a gradient of PI is created between the surface where salt was deposited and the inner zones of the ham. In fact, these calculated PI values globally were in agreement with those measured on samples extracted from two types of muscle (BF and SM) of industrial Bayonne dry-cured hams, at the end of the post-salting stage. The experimental PI values were equal to  $12\% \pm 1\%$  and  $9\% \pm 1\%$  for BF and SM, respectively, i.e. values which are relatively close to the calculated PI, thus demonstrating the accuracy of prediction of the 3D “numerical ham” model built.

### **Predicted profiles of salt and water content**

Thanks to the different outputs of the “numerical ham” model, it is also possible to analyse the predicted results according to profiles, which allows the time course of salt and water contents to be accurately assessed as well as the barrier effect played by the 3 mm-thick fat film against internal salt diffusion and water migration.

Figure 3.13 shows the profiles of salt content predicted by the “numerical ham” model during the salting and post-salting stages of the dry-cured ham elaboration process, from the “muscle side” surface, on the left-hand side, to the “rind side” surface, on the right-hand side. In the upper part of this figure, on the right-hand side, accurate information about the location where the profiles presented were extracted can be found. Analysis of Figure 3.13 reveals that, after 5 days of salting (green dotted lines in the figure), the salt concentration rised upon 15% TM at the salting surface because this first meat layer was in equilibrium (in terms of  $a_w$ ) with the saturated brine solution in direct contact with this surface. The barrier effect played by the internal 3 mm-thick fat film located at 3 cm from the salting surface is clearly visible on this profile, with a difference in salt content reaching 2% TM between the upstream and downstream of the fat film. Downstream of the barrier, the salt content is lower than 1% TM. After 10 days of salting (red dotted lines), the salt content increased obviously in the ham part located upstream of the thin fat film, with a salt content of 6% TM just before the fat film;

downstream of the fat film; salt succeeded to penetrate until a distance of 8 cm from the “muscle side” surface (Figure 3.13). At the end of the salting stage (light blue curve), salt continued to accumulate upstream of the fat film, but also to diffuse through this barrier; salt now reached almost the “rind side” of the ham. What is also important to underline during the salting stage is that the predicted salt content at the salting surface is decreasing progressively with time, from 14%-15% TM after 5 days to 8%-10% TM beyond 15 days. This could probably result from the decrease of the gradient of the salt content between the saturated brine solution in contact with the first meat layer of the ham whose salt content is increasing during the salting stage. The limited amount of salt in the brine solution decreased continuously due to the salt penetration inside the ham, thus reducing the difference of salt concentrations between the brine solution and the ham surface. During the post-salting stage, salt continued to diffuse through the fat film in the inner zones of the ham, leading to a difference in salt content lower than 1% TM between the upstream and downstream of the fat film (Figure 3.13). At the end of the post-salting stage (yellow curve), after 70 days, the salt diffusion continued to occur so that, downstream of the fat film, the salt content reached approximately 3% TM, even in the deeper zones of the ham, i.e. in close proximity to the “rind side” surface.

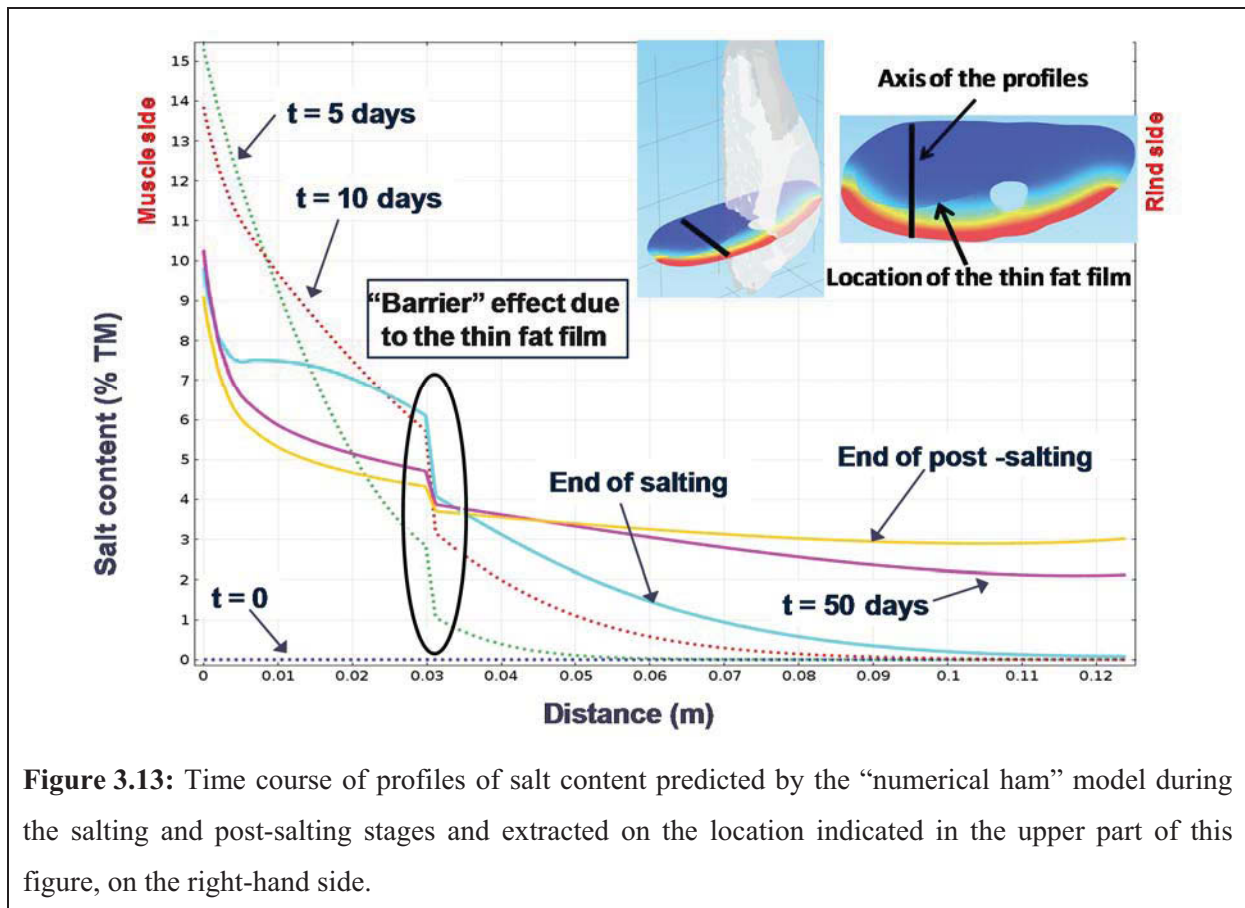
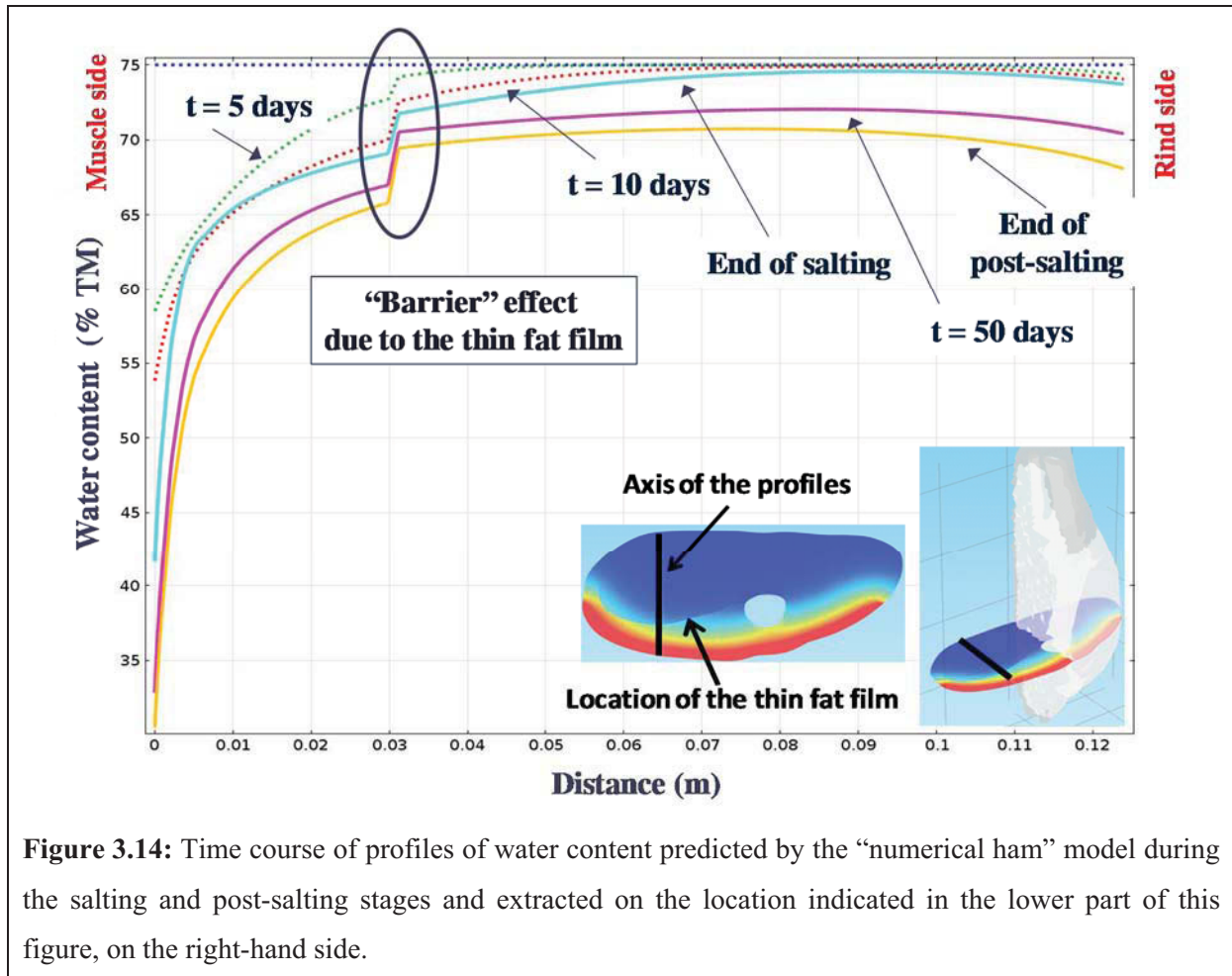


**Figure 3.13:** Time course of profiles of salt content predicted by the “numerical ham” model during the salting and post-salting stages and extracted on the location indicated in the upper part of this figure, on the right-hand side.



The effect of the 3 mm-thick fat layer on water migration was also numerically studied. Figure 3.14 shows the profiles of water content predicted by the “numerical ham” model during the salting and post-salting stages of the dry-cured ham elaboration process, from the “muscle side” surface to the “rind side” surface. It should be remembered that the initial water content was 75% TM in the entire volume of the ham (blue dotted lines in the figure).



During the salting stage, the water content decreased gently in the deeper zones of the ham, with values never lower than 72% TM. Moreover, in spite of 11 weeks of process (yellow curve) that seem to be a long period to make the ham drying, the ham volume located downstream of the fat film did not loose much moisture, thus leading to an average water content of 69%-70% TM at the end of the post-salting stage (Figure 3.14). On the other hand, only 5 days of process were enough to decrease the water content to less than 60% TM in the few first millimetres close to the salting surface, and less than 45% TM after 77 days, thus creating a strong gradient of water content between the “muscle rind” surface and the inner zones of the ham. In addition, similarly as for salt transfer, the thin fat film acted as a barrier

against water transfer, with a barrier effect which increased progressively as ham was dried: e.g. the difference of water content between the upstream and the downstream of the film fat peaked at 4% TM, after 77 days of process. Figure 3.14 also shows that water evaporated from the “rind side” surface, but with a water flux rate lower than the one calculated on the salting surface. This is completely logical since we have assumed that, in the “numerical ham” model, the water transfer coefficient was divided by a factor 20 on the “rind side” surface.

Several published studies highlighted that subcutaneous fat layer and intramuscular fat (IMF) influenced greatly the water migration and salt diffusion inside the ham (Toldra 2002, among others). The results presented here were coherent with information described in Toldra (2002), thus demonstrating the barrier role played by the 3 mm-fat film against water migration from inside the ham to outside and against salt diffusion towards the inner zones of the ham. In practice, the particular role of this internal fat film thus leads to increase the time of salting and post-salting stages to achieve equilibrium in salt content in the entire volume of ham. That is the reason why some scientists suggested trimming away subcutaneous fat would probably reduce the time of salting and post-salting stages and probably the salt content of the hams. Trimming away the subcutaneous fat would also reduce the time of the drying and ripening stages, thus leading to manufacturing dry-cured ham with shortened time of process (Arnau et al. 2007; Marriott et al. 1987).

#### **Predicted mean values of salt content, water content, PI, $a_w$ and weight loss**

The “numerical ham” model also allows calculating mean values of the predicted parameters, such as salt content, water content, PI and  $a_w$  in the different groups of muscles identified in the ham geometry during its construction using Mimics<sup>®</sup> software. Figure 3.15 shows the time course of mean values of salt content predicted by the “numerical ham” model during the salting and post-salting stages in three different groups of muscles: (1) in the SM muscle, called “grosse noix” in a “French butcher” language, (2) in the ‘BF + ST’ muscles, called “sous-noix” in a “French butcher” language, and (3) in all the ham volume. Due to salting, the salt content in these three different groups of muscles increased rapidly, especially since the group of muscles is located close to the salting surface. That is why the salt content in the SM muscle increased more rapidly and exceeded 6% TM, in average, at the end of salting compared to the one of the “sous-noix” whose mean value reached about 1% TM over the same period.

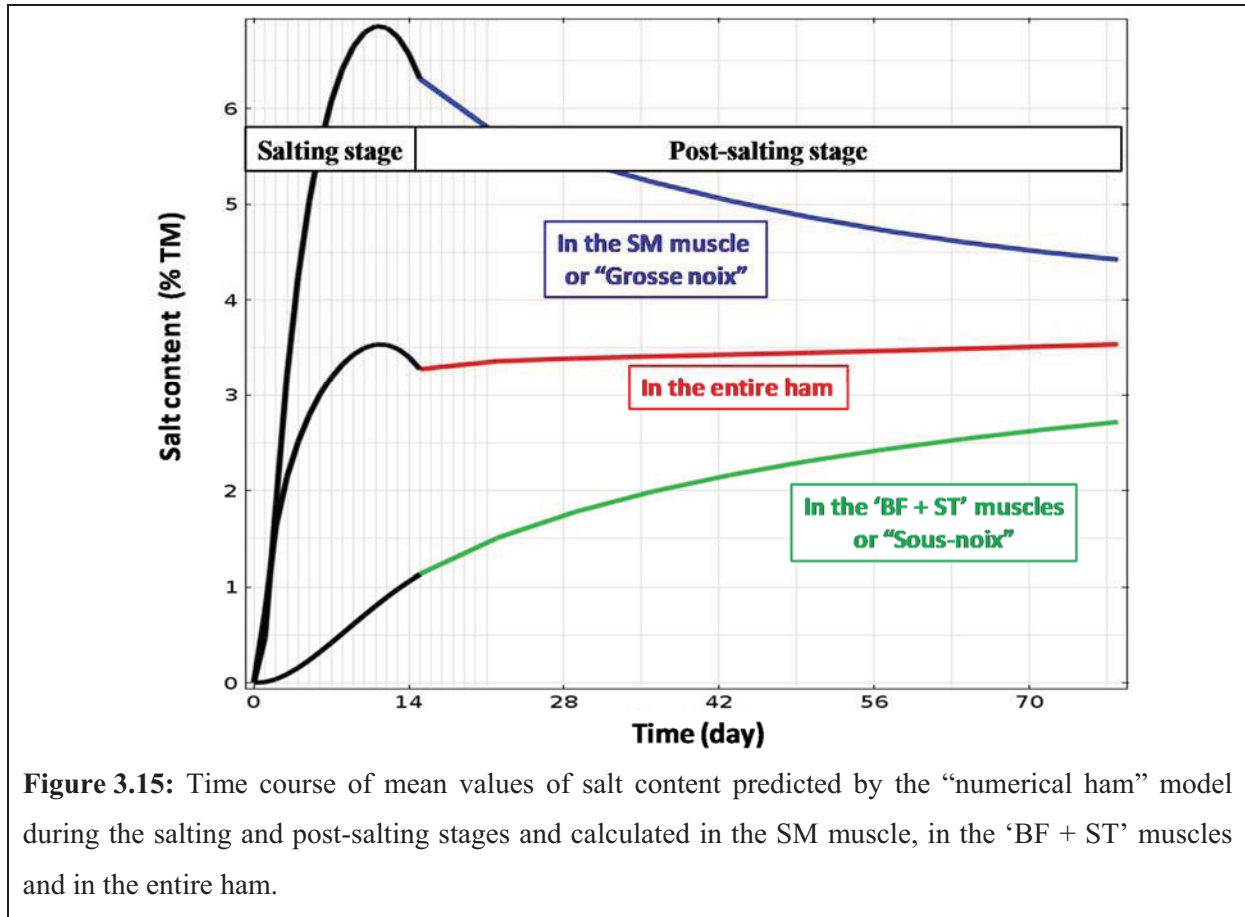


**Figure 3.15:** Time course of mean values of salt content predicted by the “numerical ham” model during the salting and post-salting stages and calculated in the SM muscle, in the ‘BF + ST’ muscles and in the entire ham.

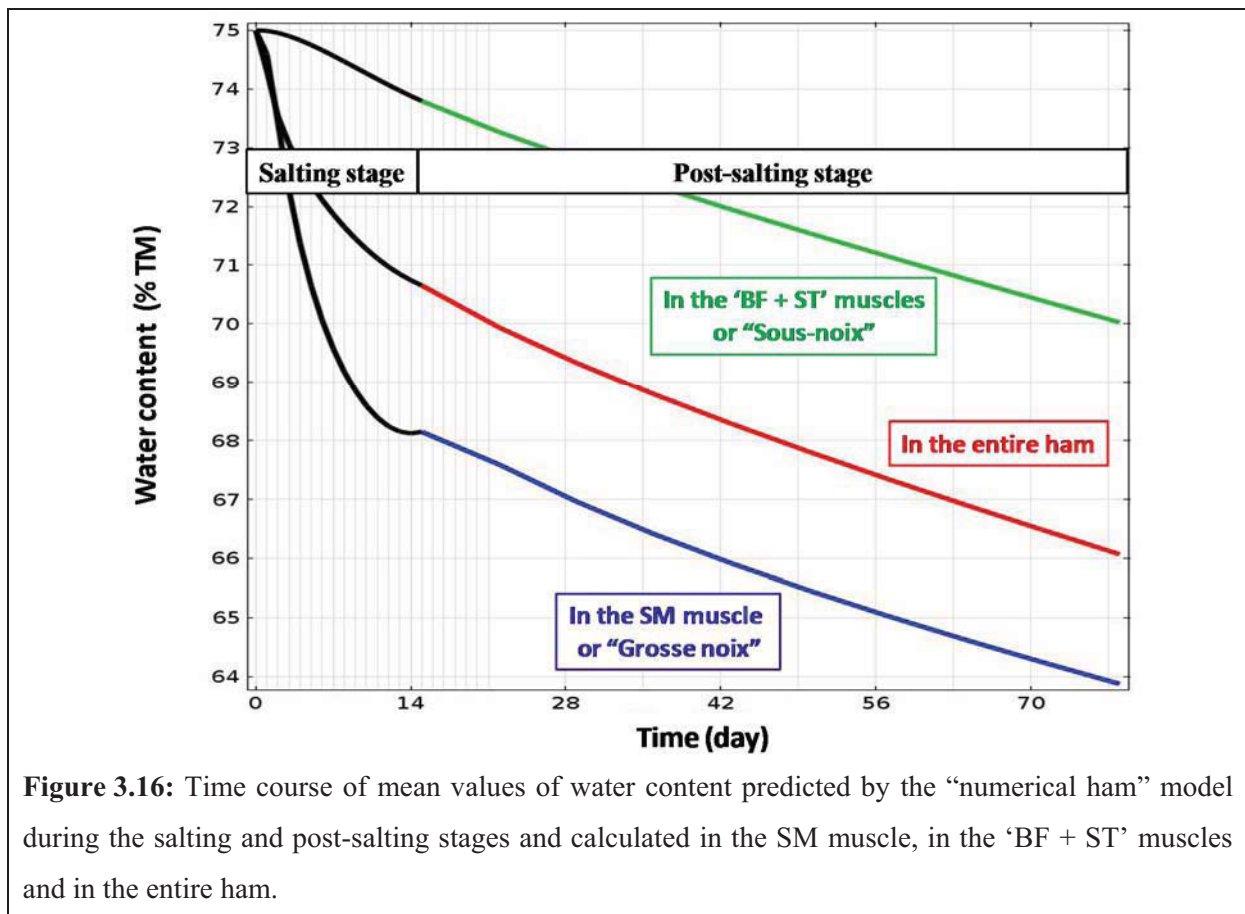


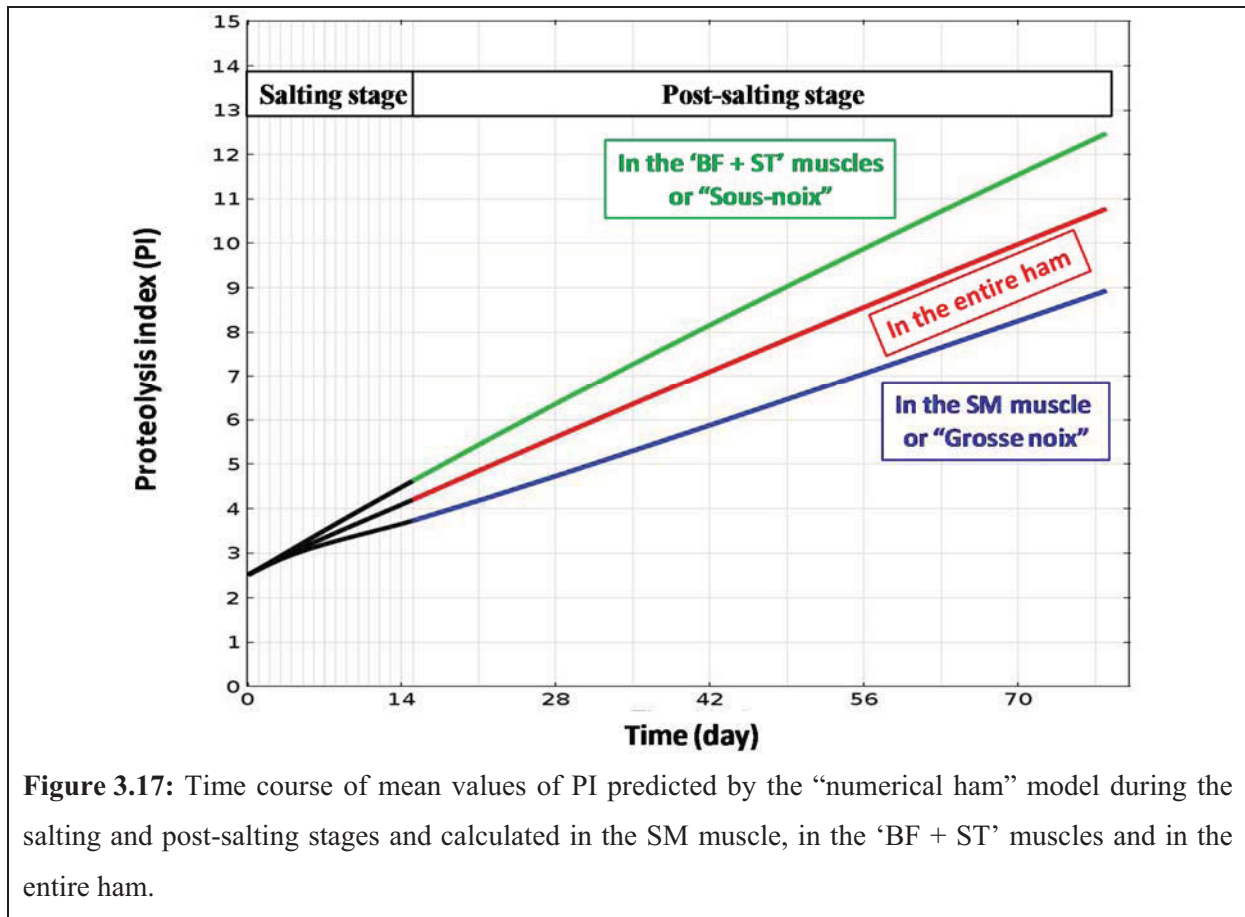
**Figure 3.16:** Time course of mean values of water content predicted by the “numerical ham” model during the salting and post-salting stages and calculated in the SM muscle, in the ‘BF + ST’ muscles and in the entire ham.

During the post-salting stage, the salt content of the group of muscles close to the salting surface decreased in favor of the one located inside the ham, due to diffusion (Figure 3.15). Regarding the entire ham, the behaviour in terms of time course of salt content was logically intermediate compared to the two other groups of muscles, with a mean value equal to 3.3% TM at the end of the salting stage. This value of salt content then increased slightly during the post-salting stage due to the water evaporation which led to a concentration of salt. Salt content in the entire ham thus reached 3.5% TM, after 77 days of process.

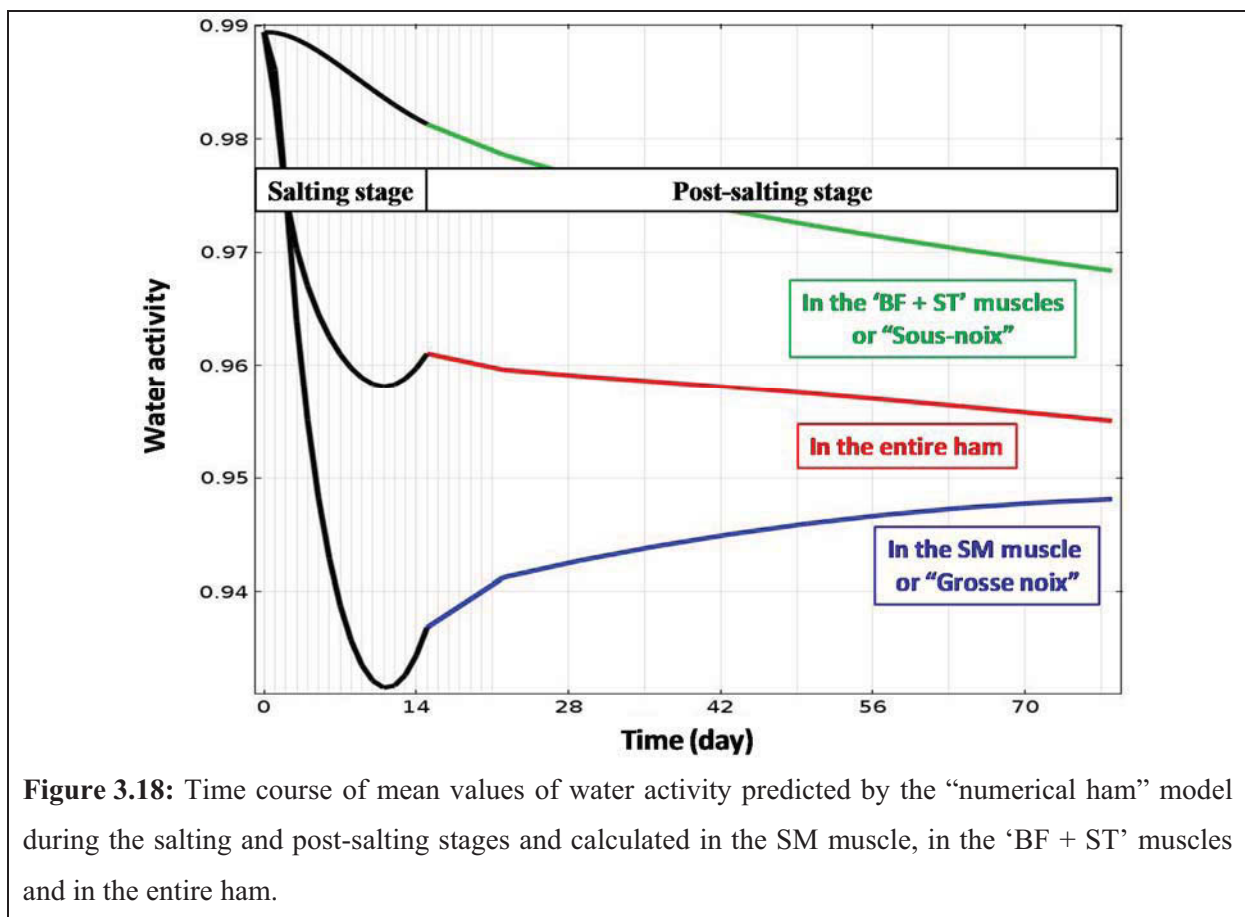
Figure 3.16 shows the time course of mean values of water content predicted by the model during the salting and post-salting stages in the three same groups of muscles than for salt diffusion. Due to water evaporation, the predicted water content in these three groups of muscles logically decreased, but more or less rapidly according to their distance from the ham surface. Since the “muscle side” surface dried more rapidly than the “rind side” surface of the ham, the water content in the “grosse noix” decreased more rapidly than in the “sous-noix”. The difference in water content between these two groups of muscles reached 6% TM, in average, at the end of the post-salting stage (64% TM vs. 70% TM). As previously, the behaviour of the entire ham in terms of decrease in water content was intermediate when comparing to the two other groups of muscles, thus leading to a final mean value of water content in the entire ham equal to 66% TM, after 77 days of process.

Figure 3.17 shows the evolution of mean values of PI predicted over the 77 days period in the “grosse noix”, the “sous-noix” and in the entire ham, from the phenomenological models implemented in the “numerical ham” model. Since the temperature has not changed during the two stages modelled here, the predicted mean values of PI were directly linked to the time course of salt content and water content previously described. So the lower mean values of PI were predicted in the most dried and salted group of muscles, i.e. the “grosse noix”. The difference in PI values exceeded 4% between the “sous-noix” (12.5%) and the “grosse noix” (9%); the mean PI value of the entire ham was intermediate (approximately 10.7%). As previously reported when analysing the distribution of the spatial and time values of PI (Figure 3.12), the predicted PI values, at the end of the post-salting stage, were in agreement with those measured on samples extracted from BF and SM muscles of industrial Bayonne dry-cured hams:  $12\% \pm 1\%$  and  $9\% \pm 1\%$  for the BF and SM muscles, respectively, thus confirming the accuracy of prediction in terms of proteolysis of the 3D “numerical ham” model. Accurate analysis of Figure 3.17 reveals that the difference in terms of time course of mean values of PI between the different groups of muscles appeared early in the second or third day of salting; these differences becoming more pronounced afterwards.





**Figure 3.17:** Time course of mean values of PI predicted by the “numerical ham” model during the salting and post-salting stages and calculated in the SM muscle, in the ‘BF + ST’ muscles and in the entire ham.



**Figure 3.18:** Time course of mean values of water activity predicted by the “numerical ham” model during the salting and post-salting stages and calculated in the SM muscle, in the ‘BF + ST’ muscles and in the entire ham.

The mean values of water activity ( $a_w$ ) and the weight loss kinetics were also calculated by the “numerical ham” model during this study. Figure 3.18 shows the time course of mean values of  $a_w$  predicted during the salting and the post-salting stages in the “grosse noix”, in the “sous-noix” and also in the entire ham. The increase of salt content in the muscles combined to the decrease of the water content due to drying globally led to a decrease in mean  $a_w$  values in all the groups of muscles with the objective of reaching the microbial stability, which is the aim of the salting and drying operations performed during the dry-cured ham elaboration process. It is interesting to note that, in Figure 3.18, the mean  $a_w$  value of the “grosse noix” increased during the post-salting stage as a result of an increase in  $a_w$  due to the salt diffusion from the “grosse noix” to the “sous-noix” as shown in Figure 3.15 not counterbalanced by the decrease in  $a_w$  due to the drying that occurred at the same period. However, the mean value of  $a_w$  in the entire ham decreased progressively during the post-salting stage, from 0.96, after 15 days, to 0.955, after 77 days (Figure 3.18).

Since the “numerical ham” model predicts the time course of water content in the ham, the total weight loss of the ham can be calculated by volume integration. Figure 3.19 depicts the weight loss kinetic predicted over 77 days by the model.

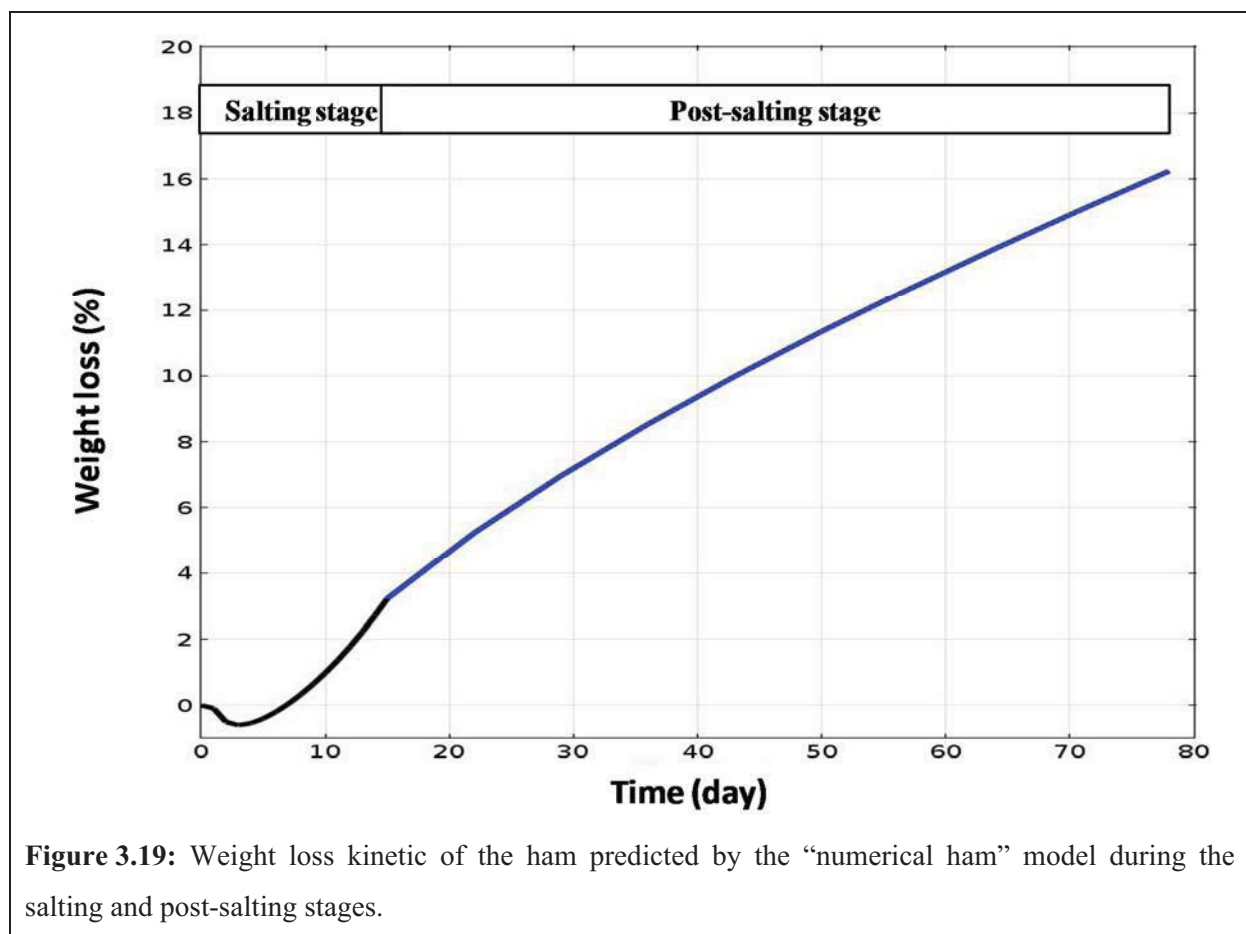


**Figure 3.19:** Weight loss kinetic of the ham predicted by the “numerical ham” model during the salting and post-salting stages.

During the three first days, the weight of the ham increased because the weight of the salt that penetrated inside the ham is higher than the water lost by evaporation over the same period. Beyond three days of process, the salt uptake became lower than the water evaporation, thus the ham globally lost weight. Once the salting stage is ended, i.e. after 15 days of process, the weight loss of the ham corresponded only to the water loss by evaporation. At the end of the post-salting stage, the predicted weight loss of the ham reached 16% of its initial weight, which is in agreement with the weight loss values measured commonly in industry.

### **Conclusion**

This study presented the development of a numerical model that simulates water and salt transfers in a real ham, and couples the time course prediction of the salt and water content to PI evolution through the implementation of a specific phenomenological model established in a previous study. For the time being, PI was calculated at each time step from a global phenomenological model in which four different pork muscles were considered together on account of similar behaviour in terms of time-course of proteolysis. The present “numerical ham” model is able to predict the time course of salt and water content, PI, and  $a_w$ , and profiles can be extracted anywhere in the ham to make the interpretation of the phenomena easier to understand. Mean values of these parameters can also be calculated on five different groups of muscles. Due to the prediction of the water evaporation and salt uptake, the ham weight loss kinetic can also be predicted. In this study, the “numerical ham” model was used to simulate what happens during the first crucial stages of dry-cured ham production, i.e. the salting and the post-salting phases carried out at low temperature. The predicted PI values were in close agreement with the PI measured on samples extracted from industrial dry-cured hams, thus showing the accuracy of prediction of the numerical model built. Numerical results also confirmed the barrier role of the thin fat layer existing inside the ham that highly affects internal water and salt transfers. One possible improvement of the model would be the integration of five phenomenological models allowing PI to be calculated specifically in each group of muscles. This could probably change the values of the predicted PI inside each domain.

To the authors’ knowledge, a complete 3D multiphysical numerical model of dry-cured ham was built for the first time. This “3D numerical ham” model constitutes a new numerical tool that would be greatly useful for helping industrials and professionals to experiment and investigate various process scenarios in order to reduce the final salt content of dry-cured hams, without modifying their final quality in terms of proteolysis, texture and flavour. To

achieve this, the numerical model should be completed by the implementation of new phenomenological models that relate some structural parameters (size of fibers, extracellular spaces...) and textural parameters (hardness, adhesiveness...) to PI values and salt and water contents. However, the actual version of the “numerical ham” model needs to be improved by taking into account the decrease in the volume of the ham due to the drying, knowing that this decrease can represent until 40% of its initial volume at the end of the process.

### **Acknowledgements**

This work was funded by the Na- integrated programme (ANR-09-ALIA-013-01) financed by the French National Research Agency. This paper forms part of the thesis of Rami Harkouss, who works for this research program. We thank IFIP for providing CT images.

### **3.5. Discussion**

Une discussion critique et objective des principaux résultats de ce travail est faite dans la dernière partie de ce chapitre. Trois points sont discutés :

- les avantages de la méthode rapide de mesure de l'indice de protéolyse mise au point au laboratoire par rapport à la méthode de dosage classique ;
- les différences observées sur le plan des évolutions dynamiques de la protéolyse mesurées, respectivement, dans des échantillons de viande de porc préparés au laboratoire ou directement extraits de jambons secs industriels ;
- le développement du simulateur de procédé de fabrication de jambon sec, résultat majeur de ce travail de thèse, avec, d'une part, la non prise en compte dans ce modèle numérique de la diminution du volume du jambon au cours du séchage, et d'autre part, la prédiction de la dynamique d'évolution de l'IP, tout au long du procédé de fabrication, de par l'intégration des modèles phénoménologiques.

#### **3.5.1. Nouvelle méthode de mesure de l'indice de protéolyse**

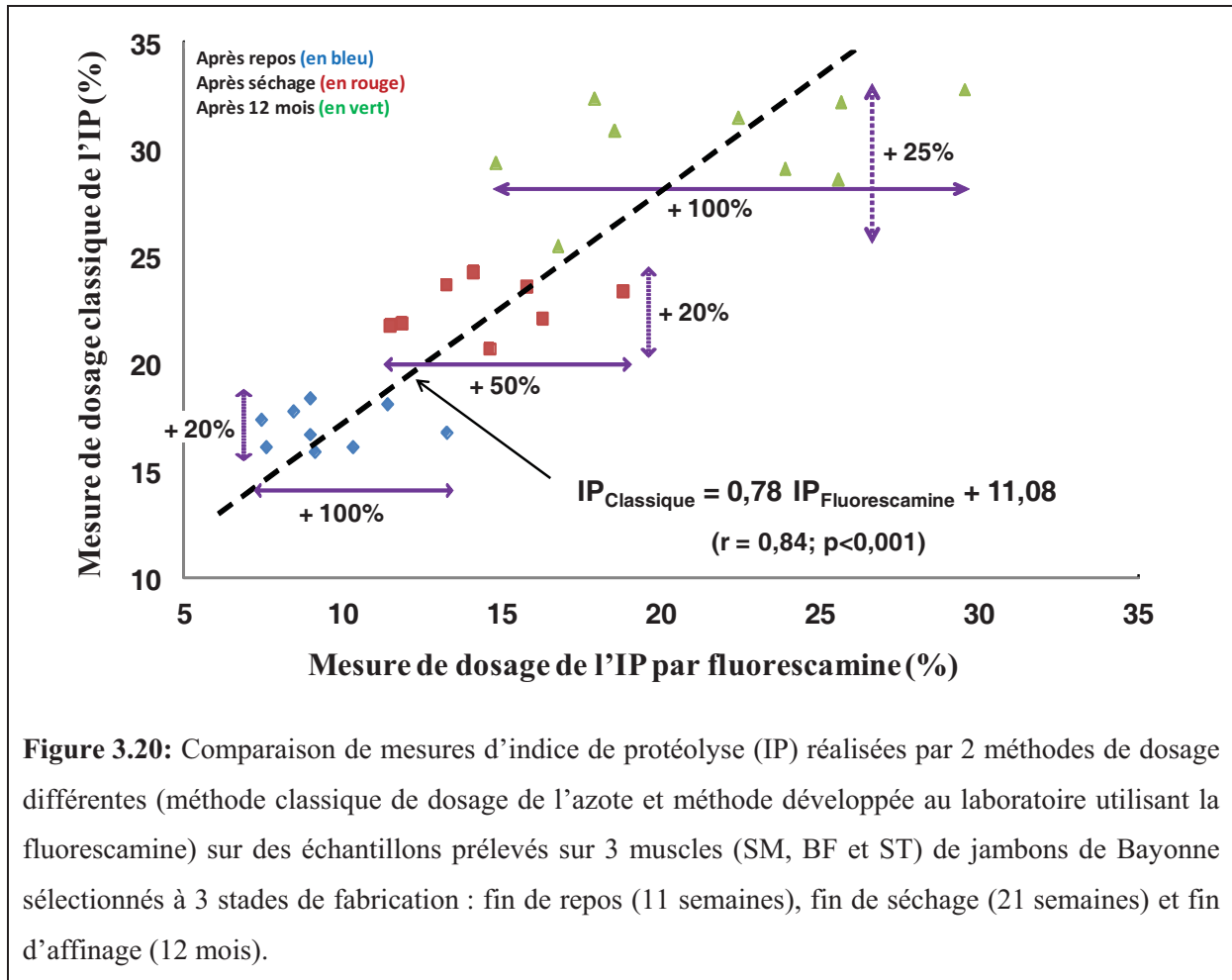
Le développement de modèles phénoménologiques robustes a nécessité de quantifier la protéolyse dans un grand nombre d'échantillons de viande de porc, environ 600 mesures d'IP par muscle étudié. De ce fait, une méthode de mesure rapide de l'IP a été mise au point au laboratoire, autorisant la réalisation d'une cinquantaine de mesures par jour par un utilisateur entraîné. L'étape limitante restant la préparation des extractions à partir de l'échantillon à

analyser : broyage, homogénéisation, dilution, agitation, centrifugation. Contrairement à la méthode classique de dosage de l'azote (rapport de la concentration de l'azote non protéique sur l'azote total), cette nouvelle méthode ne nécessite que très peu de matière, moins de 0,5 g contre plusieurs dizaines de grammes pour la méthode classique ; des essais concluants ont même été réalisés avec moins de 0,1 g d'échantillon. Grâce à cette méthode, il a donc été possible de travailler à partir de petites lamelles de muscle de porc ne faisant que quelques millimètres d'épaisseur, dans lesquelles un salage et un séchage homogène ont été obtenus en moins de 24 h au laboratoire.

De plus, du fait de l'utilisation de fluorescamine, la nouvelle méthode de mesure de l'IP offre *a priori* une plus grande spécificité que la méthode classique. En effet, la fluorescamine ne réagit pas avec la majorité des substances azotées non protéiques communément présentes dans le muscle, à savoir l'urée, l'acide urique, la créatinine et l'ammoniac (Klein and Standaert, 1976). Par contre, la fluorescamine pouvant réagir avec les fonctions amines de la lysine, qui ne sont pas des produits spécifiques de la protéolyse (Dhaunta *et al.*, 2011), les conditions expérimentales (pH égal à 9,2) ont été choisies de façon à ce que la réaction de la fluorescamine se fasse le plus spécifiquement possible avec les fonctions amines en position N-terminale. Enfin, la fluorescamine n'entre pas non plus en réaction avec les groupements amines secondaires présents dans les acides aminés comme l'histidine et l'arginine (Dhaunta *et al.*, 2011 ; Weigele *et al.*, 1972).

Enfin, nous pouvons aussi affirmer que la méthode mise au point est plus discriminante que la méthode classique de dosage de l'azote, du fait qu'elle conduit à une description plus fine de la dynamique d'évolution de l'activité protéolytique. Prenons l'exemple théorique de la dégradation complète d'un décapeptide. En faisant un dosage avec la méthode classique, aucune discrimination ne pourra être faite entre le décapeptide contenant 10 atomes d'azote et l'ensemble des 10 acides aminés obtenus après dégradation qui contiennent chacun un atome d'azote. Dans ce cas théorique, l'IP devrait rester inchangé. A l'inverse, la quantification de l'IP au moyen de la nouvelle méthode utilisant la fluorescamine devrait conduire à une valeur d'IP dix fois supérieures, une fois la dégradation complète opérée, puisque le décapeptide et chaque acide aminé obtenu contiennent chacun une fonction amine en position N-terminale. La figure 3.20 illustre parfaitement le pouvoir discriminant plus fort de la méthode de dosage utilisant la fluorescamine. En effet, quelle que soit la période de fabrication des jambons de Bayonne : fin de repos, fin de séchage ou fin d'affinage, la nouvelle méthode conduit à des variations d'IP comprises entre 50% et 100%, alors que la méthode classique ne permet de

décèler que des variations de l'ordre de 20% pour les mêmes échantillons analysés (Figure 3.20).



### 3.5.2. Comparaison de la dynamique d'évolution de la protéolyse mesurée dans des échantillons préparés au laboratoire et extraits de jambons industriels

La dynamique d'évolution de la protéolyse mesurée dans les échantillons de viande de porc préparés au laboratoire dans les différentes conditions correspondant au plan d'expériences mis en place a été représentée par une droite, et donc caractérisée par une pente. Selon la température de conditionnement des échantillons, pour s'affranchir de tout problème microbiologique qui se serait traduit par une intensification de la protéolyse, les cinétiques ont été mesurées sur une période comprise entre 13 et 35 jours, soit au maximum 5 semaines. Le traitement statistique des valeurs des différentes pentes obtenues a ensuite permis d'établir, pour chacun des 5 muscles du jambon étudiés, un modèle phénoménologique qui permet de calculer la vitesse de protéolyse à partir de la température et des teneurs en eau et en sels.

Quel que soit le muscle étudié (SM, BF ou ST), la dynamique d'évolution de la protéolyse mesurée sur 12 mois sur des échantillons prélevés sur des jambons industriels a pu être approximée par un polynôme du 2<sup>nd</sup> degré et non pas par une droite (Figures 2.12 et 3.6). Les valeurs maximales d'IP obtenues en fin de fabrication étaient de l'ordre de 23 à 25% (Figure 3.6). A ce stade du travail, le fait que les dynamiques d'évolution de la protéolyse obtenues entre les deux types d'échantillons soient différentes peut être expliqué par :

- des temps d'expérimentation totalement différents : la figure 3.6 montre clairement que, sur les 5 premières semaines du procédé de fabrication, la variation de l'IP dans les échantillons industriels peut aussi tout à fait être considérée comme linéaire ;
- les phénomènes de diffusion du sel à l'intérieur du jambon et le séchage qui font que les teneurs en sel augmentent et que les teneurs en eau diminuent dans les différents muscles, au fur et à mesure de l'avancement du procédé de fabrication ; ces variations continues de teneurs en sel et en eau peuvent entraîner une diminution de la vitesse de protéolyse, comme l'ont montré les modèles phénoménologiques, ce qui conduirait progressivement à un infléchissement de la cinétique d'évolution de la protéolyse.

L'exploitation du modèle de « jambon numérique » et la réalisation d'une simulation complète du procédé de fabrication d'un jambon sec devraient permettre d'apporter des réponses à ces interrogations.

### 3.5.3. Modèle de « jambon numérique »

#### 3.5.3.1. Variation de volume

Le gros point faible de la version actuelle du modèle de « jambon numérique » développée à ce jour réside dans la non-prise en compte dans la modélisation de la rétractation du jambon au cours du séchage, variation de volume qui peut correspondre au final à 40% du volume initial. C'est pour cette raison que la série d'images de tomographie X qui a été retenue et qui a servi de base à la construction de la géométrie 3D du « jambon numérique » correspondait à un jambon en fin de phase de repos, où la perte de volume généralement constatée industriellement équivaut pratiquement à la moitié de la perte totale. De plus, lors des calculs de prédiction de concentrations en eau et en sel réalisés en concentrations volumiques, les concentrations prédites dans les volumes apparents (sans déformation) constituant le jambon ont été transformées en concentrations massiques (kg sel ou kg eau.kg jambon<sup>-1</sup>), ce qui a nécessité de calculer en fonction de l'espace, mais aussi, en



fonction du temps, la masse volumique du jambon qui varie du fait de la migration de l'eau et de la diffusion du sel ; la concentration en protéine restant constante. Toutefois, cette transformation n'équivaut pas à une réelle prise en compte de la déformation du milieu dans lequel les phénomènes physiques de transferts d'eau et de sel se déroulent. En tout cas, cela ne permet pas de prédire les dynamiques d'évolution de teneurs en sel mesurées dans des jambons industriels et représentées sur la figure 3.21, qui montrent, qu'à partir d'un moment donné, la teneur en sel moyenne du muscle BF situé en profondeur devient supérieure à celle du muscle SM situé en surface du jambon (Figures 3.21a et 3.21b). En fin de procédé, au bout de 52 semaines, les écarts de teneur en sel mesurés dans ces deux muscles atteignent 0,75% et 5,35%, respectivement, lorsque ces teneurs sont exprimées par rapport à la matière totale (le jambon) ou par rapport à la matière sèche dessalée (les protéines). En réalité, le sel migrant dans l'eau, la diffusion du sel s'opère jusqu'à ce que l'équilibre soit atteint dans tout le volume du jambon, soit environ 34 semaines si l'on se réfère à la figure 3.21c. Ce délai long s'explique par le fait que le séchage plus important du muscle situé à proximité de la surface accentue les différences de concentrations en sel (exprimées en  $\text{kg sel.kg eau}^{-1}$ ) entre la surface et l'intérieur du jambon, ce qui conduit à la création de gradients forts entre ces zones et donc à une intensification du transport du sel vers les zones profondes du jambon.

Pour bien comprendre les phénomènes de migration couplée eau-sel se déroulant dans un jambon sec, il est capital de s'intéresser aux travaux de Broyart *et al.* (2007) portant sur la mesure et la modélisation des profils de teneurs en eau et en sels se développant lors d'un séchage à température constante et à flux d'évaporation d'eau fixés de cylindres de gélatine salée (diamètre : 25 mm et longueur : 55 mm). Dans leurs travaux, pour un flux d'évaporation d'eau égal à  $100.10^{-6} \text{ kg.s}^{-1}.\text{m}^{-2}$ , ces auteurs ont mis en évidence une accumulation de sel à une distance de 2-3 mm de la surface du gel qui s'assèche, avec des teneurs en sel supérieures de 14% après 3 h de séchage et supérieures de 20% après 3 jours de séchage à la teneur en sel initiale du gel. Ces maximums de teneur en sel étant prédits à une distance par rapport à la surface d'évaporation comprise entre 2 et 8 mm, distance augmentant au fil du temps. Il est à noter que, dans le cas d'un flux d'évaporation trois fois supérieurs, des accumulations de sel plus élevées ont été décelées, avec des teneurs en sel supérieures de 16%, après 1 h de séchage, et supérieures de 35%, après seulement 6 h de séchage, à la teneur en sel initiale du gel, et ce, à une distance de 2 à 3 mm sous la surface en contact avec l'air. L'accumulation de sel a été donc observée et prédite à une distance de la surface d'évaporation qui varie selon les conditions limites de séchage et selon la durée du séchage, et non pas au niveau de la surface séchée du gel salée.

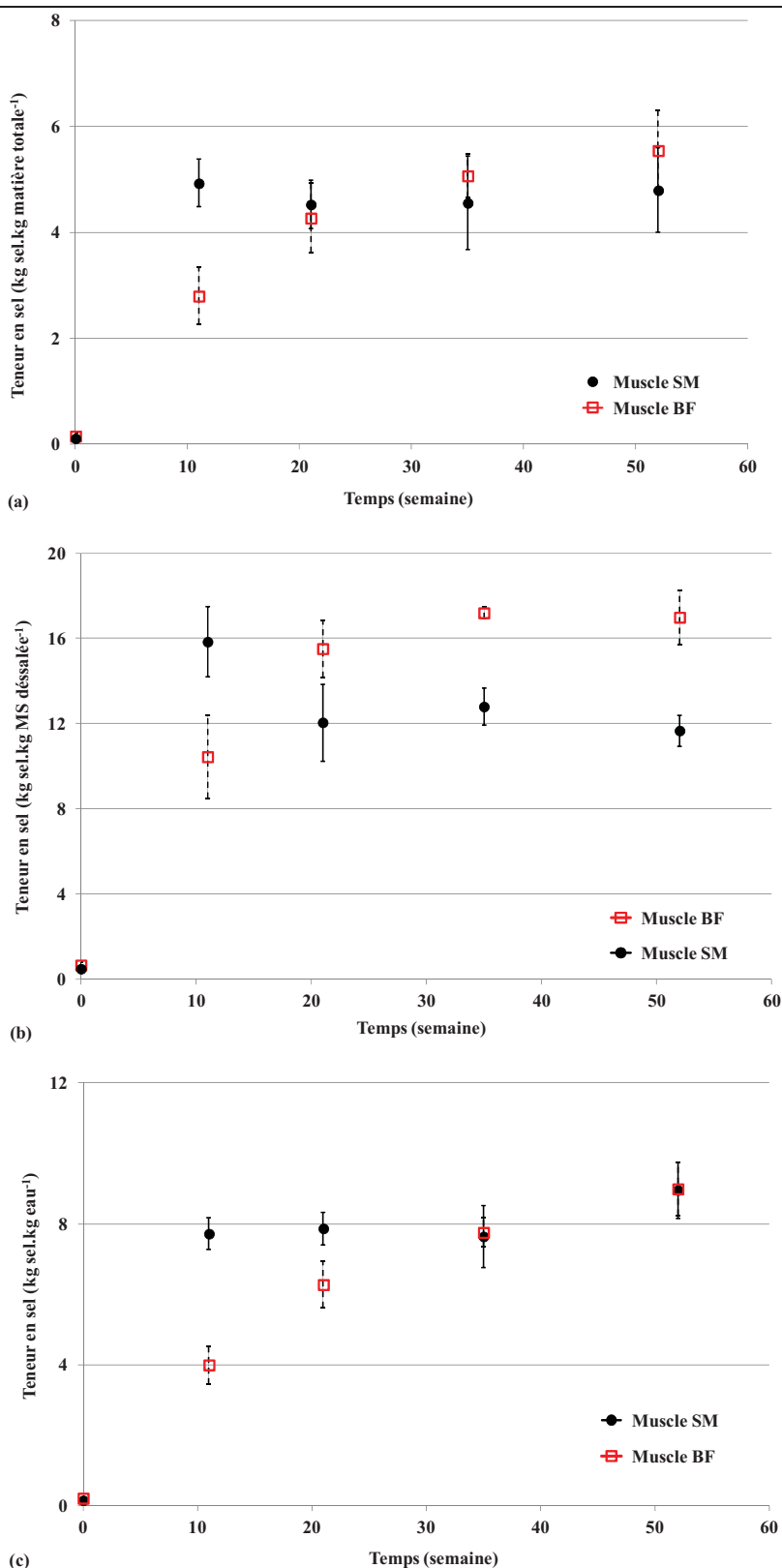


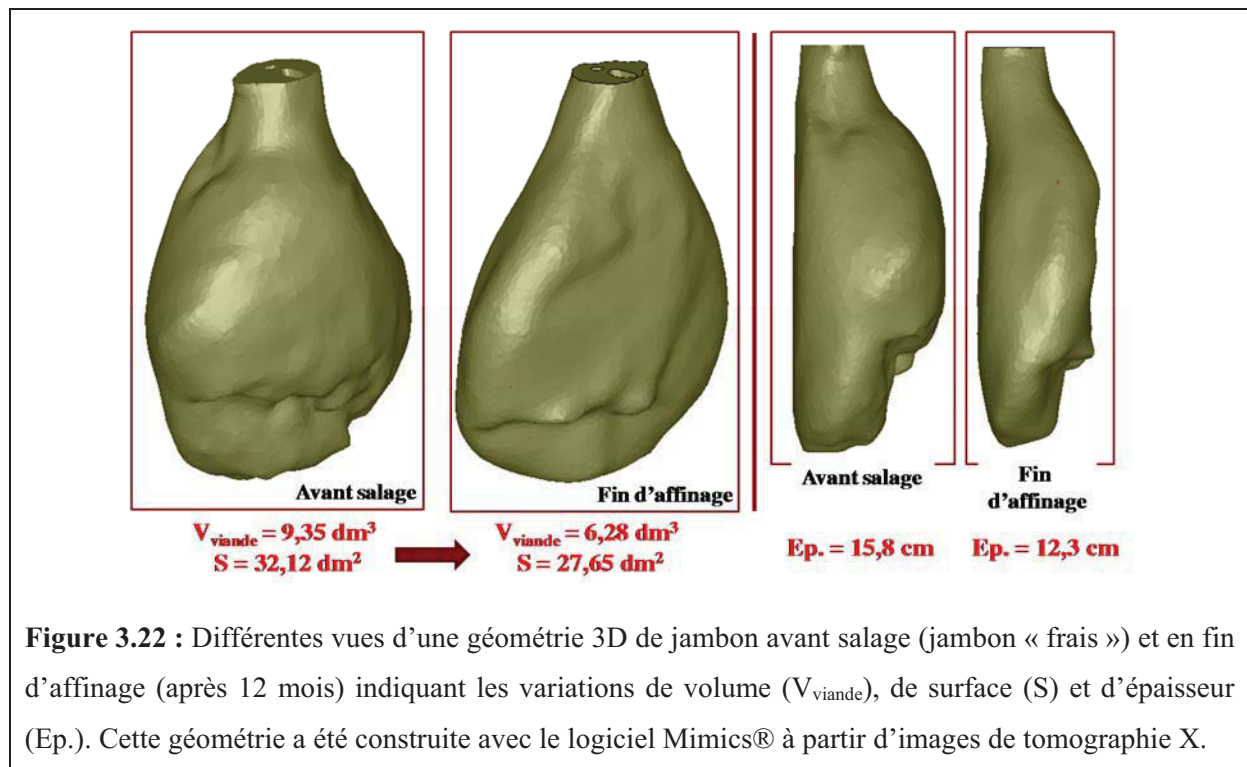
**Figure 3.21 :** Dynamique d'évolution du pourcentage de teneur en sel mesurée par chromatographie ionique dans 2 muscles (*Semimembranosus* et *Rectus femoris*) de jambons de Bayonne et exprimé en : (a) kg sel.kg matière totale<sup>-1</sup>, (b) kg sel.kg matière sèche dessalée<sup>-1</sup> et (c) kg sel.kg eau<sup>-1</sup>. Chaque point de la figure correspond à la moyenne et à l'écart-type calculés à partir d'une mesure sur 3 échantillons.

Cela suggère que, même pour des flux d'évaporation élevés atteignant  $300.10^{-6} \text{ kg.s}^{-1}.\text{m}^{-2}$  et quelle que soit la teneur initiale en sel du gel, le phénomène de transport par convection est négligeable devant le phénomène de diffusion du sel vers l'intérieur du gel provoqué par l'augmentation spectaculaire de la concentration en sel dans l'eau dans les premiers millimètres du gel. Des résultats similaires ont été mis en évidence dans le cas du séchage de saucissons secs où les flux d'évaporation d'eau sont pourtant beaucoup plus faibles que ceux imposés dans l'étude portant sur les gels (Daudin & Kondjoyan, 1992). Broyart *et al.* (2007) ont conclu que, dans la gamme de flux d'évaporation retenue pour leur étude, le phénomène de diffusion du sel qui se produit de la surface qui s'assèche vers le fond du gel était prépondérant devant le phénomène de migration d'eau qui a lieu en direction de la surface d'évaporation. Le même type de phénomènes se produit lors de la fabrication du jambon sec, avec, toutefois, des dynamiques d'évolution beaucoup plus lentes par rapport à celles mises en évidence dans le cas du séchage des gels salés, du fait d'un volume plus gros et d'un flux d'évaporation plus faible.

Dans l'étude de Broyart *et al.* (2007), le bon accord entre les profils de teneurs en eau et en sel mesurés et ceux simulés a nécessité la prise en compte dans la modélisation du rétrécissement du cylindre de gélatine du fait du séchage, de par une formulation des équations de conservation en coordonnées Lagrangiennes dans un référentiel se déplaçant à la vitesse de la phase solide, ici en l'occurrence, la matière sèche anhydre dessalée. En fait, le modèle développé par Broyart *et al.* (2007) correspondait à une adaptation d'un modèle développé par Bohuon (1995) dans ses travaux de thèse visant à étudier les phénomènes de transport de matière (eau, solutés) lors du procédé de déshydratation-imprégnation par immersion en solutions binaires et ternaires de gels et de chairs de poisson. Le même type d'approche mathématique et numérique a été récemment appliqué par Briffaz *et al.* (2014) pour modéliser le transfert d'eau et le gonflement de grains de riz lors de la cuisson qui provoque une gélatinisation de l'amidon. Cette formulation mathématique et numérique spécifique des équations de conservation est connue sous le nom de méthode « ALE (arbitrary Lagrangian-Eulerian) » ; la méthode « ALE » est particulièrement adaptée à la description du transport de quantités dans un milieu se déformant (Donea *et al.*, 2004), comme dans les quelques exemples cités précédemment (Bohuon, 1995, Briffaz *et al.*, 2014 ; Broyart *et al.*, 2007).

L'application de la méthode « ALE » au cas du séchage du jambon sec permettrait de prendre en compte dans la modélisation la variation de volume du jambon résultant de la prise de sel (environ 400 g), mais surtout de la perte d'eau par évaporation (environ 4 kg).

Toutefois, il paraît déraisonnable de vouloir appliquer une telle démarche à une géométrie 3D et un maillage aussi complexes que ceux d'un jambon en cours de séchage. D'ailleurs, les modèles développés dans les travaux de Broyart *et al.* (2007) et de Briffaz *et al.* (2014) mettant en application la méthode « ALE » étaient des modèles monodimensionnels. Par contre, mettre en place une formulation « ALE » sur une coupe 2D de jambon (par exemple, sur la « tranche » la plus épaisse) est une solution envisageable et sûrement réaliste, dans la mesure où les transferts et la déformation de la géométrie se font surtout selon la largeur et l'épaisseur du jambon, et beaucoup moins selon la hauteur, comme le montre la figure 3.22.



Une telle démarche permettrait de juger si la prise en compte de la déformation dans la modélisation permet de prédire des transferts de sel conduisant à une accumulation du sel à l'intérieur du jambon, qui soit en accord avec la réalité expérimentale.

### 3.5.3.2. Dynamique d'évolution de la protéolyse prédite par le modèle

Même si les phénomènes de transferts de sel sont actuellement mal modélisés du fait de la non-prise en compte de la diminution du volume, le modèle de « jambon numérique » a été utilisé afin de prédire la dynamique d'évolution de la protéolyse sur une période de 360 jours. Les résultats numériques obtenus (non présentés ici) ont mis en évidence (1) des valeurs d'IP dépassant les 40%, soit des valeurs beaucoup plus élevées que celles qui ont été mesurées sur

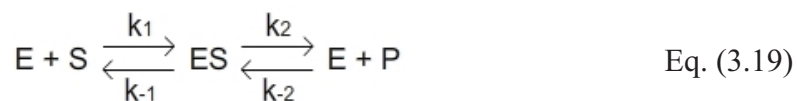
les jambons de Bayonne, qui étaient de l'ordre de 25% au bout de 52 semaines, et (2) une dynamique d'évolution de la protéolyse prédite beaucoup plus « linéaire » que la réalité expérimentale (Figures 2.12 et 3.6). Cette surestimation de la prédiction des indices de protéolyse ne peut raisonnablement pas être expliquée par une sous-estimation des teneurs en sel dans les groupes de muscle situés à l'intérieur du jambon. Il paraît difficile aussi, à ce stade du travail, de remettre totalement en cause la pertinence et l'exactitude des expérimentations de quantification de la protéolyse qui ont été faites au laboratoire sur les petits échantillons de viande de porc pour établir les modèles phénoménologiques. Une autre explication est donc à trouver pour expliquer le fort ralentissement du phénomène de protéolyse lors de l'étape de séchage/affinage des jambons secs... peut-être du côté des mécanismes enzymatiques impliqués dans la protéolyse ?

Les enzymes sont des catalyseurs biologiques, *i.e.* des molécules capables d'accélérer des réactions chimiques spécifiques et qui sont retrouvées dans leur état initial à l'issue de la réaction catalysée. La fonction des enzymes est liée à la présence dans leur structure d'un site particulier appelé site actif. Schématiquement, il a la forme d'une cavité ou d'un sillon dans lequel vont se fixer les substrats grâce à plusieurs liaisons chimiques faibles. Une fois fixés, les substrats vont réagir et se transformer en produit. Le site actif est subdivisé en deux parties : le site de liaison/fixation/reconnaissance qui reconnaît la complémentarité de forme avec un substrat spécifique à l'enzyme et le site catalytique qui permet la réaction transformant le substrat en produit.

Plusieurs mécanismes enzymatiques différents existent selon l'enzyme considérée. Une enzyme dite « michaelienne » (Johnson & Goody, 2011) fonctionne de la manière suivante : un substrat S se lie avec une enzyme E pour donner un intermédiaire ES, puis cet intermédiaire se dissocie pour donner un produit P et conduire à la régénération de l'enzyme E (cf. Eq. (3.19)). Dans ce cas, il convient de préciser que chaque site actif doit se comporter indépendamment des autres, qu'il y ait un site actif ou plusieurs par molécule. Bien entendu, il existe bien d'autres mécanismes enzymatiques, notamment les enzymes dites « allostériques » qui possèdent nécessairement au moins deux sites actifs par molécule et pour lesquelles les caractéristiques cinétiques d'un site actif vont varier selon l'état des autres sites de la même molécule.

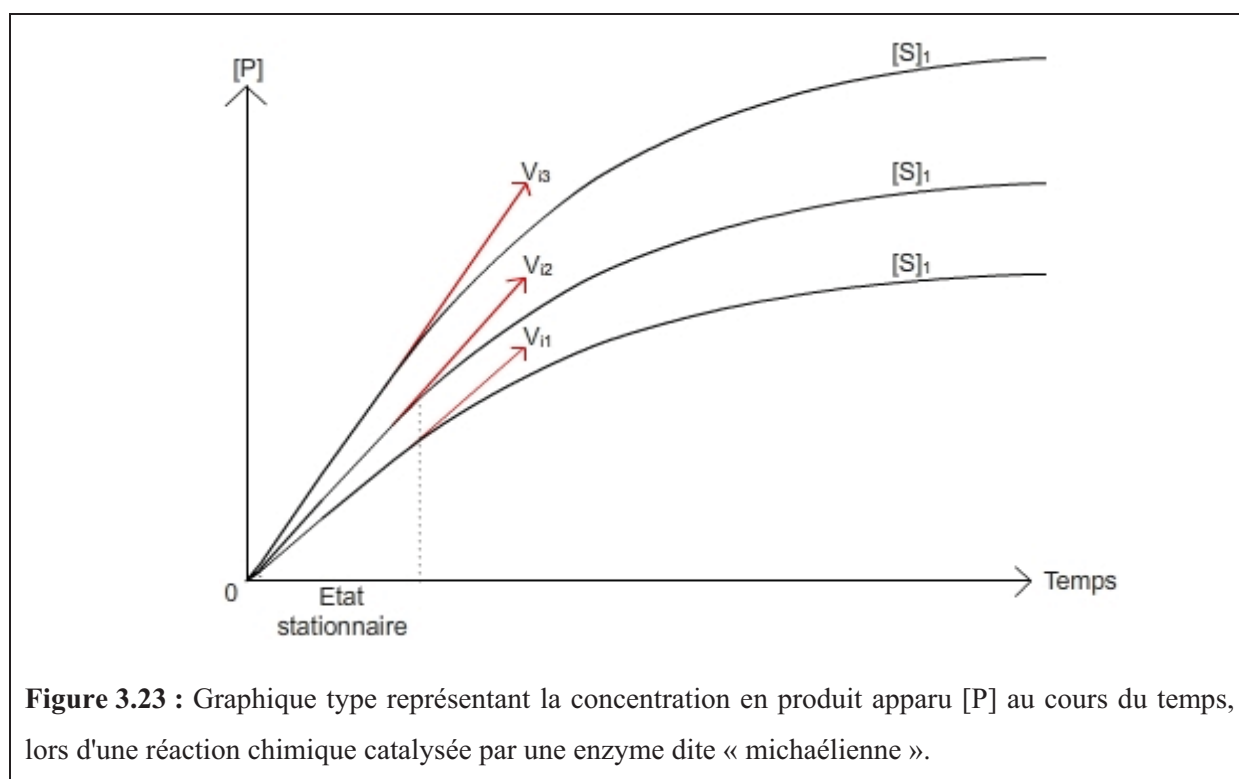
L'équation de Michaelis-Menten est une expression mathématique décrivant les paramètres cinétiques d'une réaction chimique catalysée par une enzyme dite « michaelienne » (Johnson & Goody, 2011 ; Garrido-Del Solo *et al.*, 1994 ; Goldbeter, 2013). Elle se base sur deux termes : les concentrations des différentes molécules et les constantes

d'association et de dissociation des ces molécules entre elles. Ces différents paramètres se retrouvent dans l'équation de la réaction suivante :



où  $k_1$  est la constante d'association de E+S ;  $k_{-1}$ , la constante de dissociation du complexe ES ;  $k_2$ , la constante de réaction de ES en E+P et  $k_{-2}$ , la constante d'association de E+P.

La vitesse de réaction caractérisée par la vitesse d'apparition du produit P va évoluer avec le temps, de la manière indiquée sur la Figure 3.23.



L'évolution de la concentration en produit apparu [P] représentée sur la Figure 3.23 peut être interprétée de la manière suivante. Au début de la réaction, comme aucun produit P n'est formé, la réaction inverse ( $E + P \rightarrow ES$ ) est impossible, la vitesse de la réaction est donc constante. Cette vitesse initiale est une grandeur importante car elle ne dépend que de la concentration initiale en substrat et de la concentration en enzyme. Ensuite, au fil du temps, la quantité de substrat S diminue et la quantité de produit P augmente, les deux entraînant une diminution progressive de la vitesse de réaction jusqu'à atteindre une vitesse nulle. A ce moment-la, soit la réaction est totale et une fois le substrat épuisé, il n'y a plus de réaction

possible, soit un équilibre va s'instaurer entre la formation de produit et sa destruction, ce qui signifie aussi une vitesse de réaction nulle. La quantité maximale de produit pouvant apparaître dépend de la quantité de substrat introduite au début de l'expérience et des constantes cinétiques de la réaction qui conditionnent le point d'équilibre qui sera atteint.

L'équation de Michaelis-Menten (Johnson & Goody, 2011 ; Goldbeter, 2013) relie la vitesse de la réaction à la concentration de substrat et à des paramètres constants, caractéristiques de l'enzyme. Selon le modèle de Michaelis et Menten, l'équation décrivant la vitesse de réaction enzymatique est la suivante :

$$v_i = \frac{V_{max} \cdot [S]_0}{K_M + [S]_0} \quad \text{Eq. (3.20)}$$

Dans l'équation (3.20) :

- $v_i$  représente la vitesse initiale, donc en absence de produit P, de la réaction enzymatique pour une concentration de substrat  $[S]_0$  ; cette vitesse a la dimension d'une concentration par unité de temps ;
- $V_{max}$  représente la vitesse initiale maximale, mesurée pour une concentration saturante de substrat ; cette vitesse a aussi la dimension d'une concentration par unité de temps ;
- $[S]_0$  est la concentration initiale en substrat ;
- $K_M$  est la constante de Michaelis spécifique de l'enzyme ; elle a la dimension d'une concentration ; elle correspond à la concentration en substrat pour laquelle la vitesse initiale de la réaction est égale à la moitié de la vitesse initiale maximale.

Graphiquement, l'équation de Michaelis-Menten correspond à une branche d'hyperbole. Les paramètres de Michaelis-Menten d'une enzyme ( $K_M$  et  $V_{max}$ ) peuvent être obtenus par régression non linéaire (Bezerra *et al.*, 2013). L'équation (3.20) est adaptée à de nombreuses enzymes, cependant elle ne permet pas de rendre compte de comportements complexes, comme la multiplicité des substrats ou l'existence de plusieurs sites actifs sur les molécules.

Il est intéressant de noter que l'allure des courbes représentées sur la figure 3.23 qui donne la dynamique d'évolution de la concentration en produit apparu au cours d'une réaction chimique catalysée par une enzyme « michaélienne » est tout à fait similaire à l'allure des courbes décrivant la dynamique d'évolution de l'IP mesurée dans deux muscles de jambons industriels (Figure 3.6, article n°4). Ceci laisserait à penser que la protéolyse, phénomène biochimique correspondant à une hydrolyse des protéines suite à l'action d'enzymes et au final, à la production de peptides et d'acides aminés, pourrait être globalement assimilée à un



mécanisme enzymatique de type « michaélien ». Si tel était le cas, cela impliquerait que la modélisation de la protéolyse dans le modèle de « jambon numérique » serait plus complexe que celle qui a été réalisée jusqu'à maintenant, qui correspond à une intégration temporelle de vitesses de protéolyse calculées à partir des lois phénoménologiques statistiquement établies et qui varient seulement en fonction de la température et des teneurs en eau et en sel. Si l'on retient l'idée d'un mécanisme enzymatique globalement « michaélien » pour la protéolyse, il faut prendre en compte aussi le fait que la vitesse de protéolyse peut diminuer en fonction du temps, au fur et à mesure de l'évolution du rapport de la concentration en substrat, qui correspond dans le cas de la protéolyse, à la concentration en protéines hydrolysables, sur la concentration en produits issus de la protéolyse (peptides, acides aminés). Il est facile d'imaginer que la concentration en protéines hydrolysables diminue tout au long du procédé de fabrication d'un jambon sec au profit de celle en produits de la protéolyse, et que donc, la vitesse de protéolyse à prendre en compte dans le modèle de « jambon numérique », par exemple, au bout de 30 semaines de procédé, n'est qu'une fraction de la vitesse de protéolyse calculée à partir des modèles phénoménologiques développés dans l'article n°3. Les vitesses de protéolyse déterminées expérimentalement sur les petits échantillons de viande de porc préparés au laboratoire correspondant à des valeurs maximales de vitesse (état stationnaire de la Figure 3.23) où les conditions expérimentales étaient les plus favorables, à savoir une concentration en protéines hydrolysables maximale, très largement supérieure à la concentration en produits de protéolyse. Le modèle de « jambon numérique » devrait donc calculer aussi la variation locale et temporelle de la concentration en protéines hydrolysables afin de pouvoir corriger, d'un facteur compris entre 0 et 1, les vitesses de protéolyse données par les modèles phénoménologiques.

Cette diminution de la vitesse de protéolyse en fonction du temps expliquerait aussi pourquoi, par exemple, les jambons de Parme et de Bayonne ont des valeurs de teneurs en sel, de teneurs en eau, mais aussi d'IP sensiblement identiques à la fin de leur procédé de fabrication respectif, alors que les temps d'affinage sont au moins deux fois plus longs dans le cas des jambons de Parme par rapport à ceux de Bayonne.

### **3.6. Conclusions partielles**

Les principaux résultats de ces travaux de thèse ont été présentés et détaillés, dans ce 3<sup>ème</sup> chapitre, au travers de trois articles scientifiques. Des modèles phénoménologiques permettant de quantifier l'indice de protéolyse dans des échantillons de viande de porc, salés

et séchés, préparés à partir de différents muscles d'un jambon, connaissant la température de traitement et leurs teneurs en eau et en sel, ont été bâtis suite à l'application d'un traitement statistique de type régression linéaire multiple à des données expérimentales issues d'un plan d'expériences. Le même type d'approche statistique a été adopté et appliqué à des données expérimentales obtenues sur des jambons industriels de Bayonne dans le but d'établir des corrélations permettant de calculer certains paramètres de structure et de texture au sein d'un jambon sec, connaissant l'IP et les teneurs en sels et en eau. Enfin, une présentation du modèle de « jambon numérique » couplant les modèles physiques de transferts de chaleur et de matière avec les modèles phénoménologiques de quantification de la protéolyse a été faite. Cet outil numérique permet de prédire quantitativement, en 3D, la dynamique d'évolution de l'IP, des teneurs en eau et en sel, ainsi que de l' $a_w$ , à l'intérieur d'une géométrie réelle de jambon. Toutefois, la version du modèle de « jambon numérique » développée à ce jour ne permet pas de prédire avec précision la dynamique d'évolution de toutes ces grandeurs lors de l'étape de séchage/affinage du jambon, et ce, pour deux raisons : (1) du fait de la non-prise en compte dans la modélisation de la diminution importante du volume du jambon due au séchage, ce qui entraîne une mauvaise prédiction du transport du sel depuis la surface vers l'intérieur du jambon et (2) une surestimation des indices de protéolyse due à une surestimation des vitesses de protéolyse par les modèles phénoménologiques qui n'intègrent pas le fait que cette vitesse de protéolyse doit diminuer avec le temps, compte tenu de la diminution de la quantité de substrat à dégrader dont il faudrait aussi faire un bilan dans la prochaine version du modèle numérique complet.

## **CONCLUSION GENERALE et PERSPECTIVES**

---



Le jambon sec est un produit typique et traditionnel, qui joue un rôle économique majeur dans plusieurs pays producteurs, comme l'Espagne, l'Italie ou la France. Plusieurs facteurs influencent sa fabrication : (1) la qualité de la matière première en lien avec le type génétique (pH initial, teneur en matière grasse, poids initial) et (2) les facteurs technologiques liés au procédé de fabrication tels, par exemple, la quantité du sel qui a pénétré dans le jambon lors de l'étape du salage et les conditions de température et de ventilation auxquelles le jambon a été soumis tout au long du procédé de transformation.

La protéolyse, un des phénomènes biochimiques majeurs se déroulant lors du procédé, dépend des teneurs en eau et en sel, de la température et du pH, et sa maîtrise conditionne en grande partie la qualité finale du jambon sec, notamment ses propriétés sensorielles, comme la texture et la flaveur. Les résultats préliminaires obtenus sur de petits échantillons de viande de porc salés et séchés, et sur des échantillons extraits de jambons de Bayonne, ont permis de valider la technique de quantification de la protéolyse par fluorescence mise au point au laboratoire au début de ce travail de thèse. Cette nouvelle technique de mesure présente l'avantage d'être plus informative et plus précise que la technique classique de dosage de l'azote, surtout dans la phase intermédiaire d'évolution de la protéolyse. De plus, elle est rapide, peu coûteuse en termes de quantité de matière et d'être très sensible, du fait de la détection par fluorescence. Une corrélation linéaire permettant de passer d'un IP mesuré par la « fluorescamine » à son indice équivalent déterminé par la méthode classique a été établie à partir de mesures effectuées sur un lot de 27 échantillons industriels. Toutefois, la validité de cette corrélation mériterait d'être testée sur un nombre d'échantillons beaucoup plus élevé. Enfin, cette technique pourrait être utilisée pour quantifier la protéolyse dans d'autres types de charcuteries, comme les saucissons secs, voire dans d'autres types de produits alimentaires.

L'analyse des résultats obtenus sur de petits échantillons de viande de porc conditionnés en teneurs en eau et en sel et préparés au laboratoire selon un protocole expérimental de préparation et un plan d'expériences de Doehlert spécifiquement mis au point, a montré que les évolutions protéolytiques pour 5 types de muscle de porc (BF, SM, ST, RF et GM) pouvaient être représentées par des droites, donc caractérisées par une valeur de pente. Ces évolutions étaient (1) fortement accélérées par l'augmentation de la température, (2) freinées par la réduction de la teneur en eau, du fait du séchage et (3) efficacement inhibées par l'ajout d'une forte quantité de chlorure de sodium. L'augmentation de la protéolyse dans un jambon est donc positivement corrélée avec la température et la teneur en eau, mais négativement avec la teneur en chlorure de sodium. Ces évolutions sont en très bon accord avec les résultats de la littérature et prouvent l'intérêt du salage, du séchage et du contrôle de la température

tout au long du procédé de fabrication d'un jambon sec, où pour des raisons de stabilité microbiologique, une température basse est maintenue pendant les premiers mois, en attendant que la diffusion du sel et le séchage du produit, et donc un abaissement suffisant de  $a_w$ , s'opèrent avant d'augmenter la température de l'air. Les traitements statistiques effectués sur l'ensemble des valeurs de pente obtenues pour les 5 muscles ont montré que la température avait un effet hautement significatif, que la teneur en sel avait un effet très significatif et que la teneur en eau avait un effet significatif sur l'évolution de la protéolyse. De plus, les résultats correspondant à la double répétition du point central du plan de Doehlert ont montré qu'il n'y avait pas d'effet inter-animal très marqué et que la variabilité biologique n'avait aucun effet significatif sur la protéolyse. Ensuite, à partir d'une régression linéaire multiple, des modèles phénoménologiques permettant de calculer la vitesse de protéolyse en fonction des effets simples des facteurs étudiés (température, teneurs en sel et en eau) et des interactions entre ces facteurs ont été statistiquement établies pour l'ensemble des 5 muscles investigués. Enfin, des surfaces de réponse ont été tracées de façon à visualiser aisément l'effet des différents facteurs sur l'évolution de la vitesse de protéolyse. L'analyse de ces surfaces de réponse a révélé qu'à basse température, les valeurs des vitesses de protéolyse sont faibles et que l'effet du séchage est difficilement visible. Par contre, à température modérée et à température élevée, les effets des différents facteurs sont plus nets : la vitesse de protéolyse augmente rapidement, notamment lorsque la teneur en eau est élevée et lorsque la teneur en chlorure de sodium est faible.

Les mesures d'IP effectuées sur des échantillons extraits de jambons de Bayonne (muscles BF, SM et ST) ont mis en évidence que l'évolution de la protéolyse dans un jambon sec suivait une fonction polynomiale du second degré, et non pas une fonction linéaire, comme dans le cas des mesures faites sur les échantillons préparés au laboratoire. Ces différences de comportement en termes de dynamique d'évolution de la protéolyse ont été interprétées, au moment où ces mesures ont été analysées, comme résultant du fait que, dans la pratique industrielle, les facteurs influençant la protéolyse (température, teneurs en chlorure de sodium et en eau) évoluent continûment au cours des différentes étapes de fabrication. De ce fait, compte tenu du séchage et de la diffusion du sel, la vitesse de protéolyse dans un muscle situé à l'intérieur du jambon doit diminuer avec le temps, ce qui doit conduire à une évolution de la protéolyse dans un jambon sec qui peut être décrite par un polynôme de degré 2 et non pas simplement par une fonction linéaire. De plus, dans un jambon entier, la position géométrique de chaque muscle dans le volume fait que l'IP mesuré à un moment donné peut différer d'un muscle à l'autre, du fait de teneurs en eau et en chlorure de sodium différentes.

En parallèle de ces mesures de protéolyse, des mesures d'oxydation des lipides par un dosage des « TBARS » ont été réalisées sur des échantillons extraits de jambons industriels (muscles BF et SM). Ceci a révélé que la dynamique d'évolution des oxydations lipidiques suivait une forme en cloche. La concentration maximale en « TBARS » était observée pendant la semaine 21 du procédé, avec une valeur 5 fois supérieures à celle mesurée dans les jambons « frais ». Ensuite, une diminution progressive de la quantité de « TBARS » a été mise en évidence durant le séchage et la maturation des jambons, avec au final des valeurs semblables à celles obtenues dans les jambons « frais », ce qui n'est pas logique. En effet, vu que le niveau d'oxydation lipidique est un indicateur du développement aromatique des jambons secs qui ne cesse de s'intensifier au fil du temps, il n'y a aucune raison pour que l'oxydation lipidique baisse aussi fortement en fin de procédé de fabrication, si ce n'est une inaptitude de la méthode expérimentale utilisée à la quantifier dans cette période. Il est donc logique d'envisager d'utiliser une autre méthode de quantification de l'oxydation lipidique que celle du test « TBA », pour pouvoir suivre ce phénomène biochimique même dans les étapes finales du procédé de fabrication des jambons secs. Pour l'instant, une corrélation valable que sur les 21 premières semaines de fabrication a été établie, permettant de calculer la quantité de « TBARS » simplement à partir de la valeur de l'IP. Le même type de corrélation, mais établie de manière fiable sur l'ensemble des étapes de fabrication, y compris lors de l'étape de séchage/affinage, pourrait permettre, dans le futur, de fournir des informations sur la dynamique d'évolution du développement aromatique des jambons secs, à condition d'intégrer cette corrélation dans le modèle de « jambon numérique » développé.

Les mesures texturales réalisées sur les muscles BF et SM extraits de plusieurs jambons de Bayonne pris à des stades de fabrication différents ont confirmé que la dureté d'un échantillon était inversement proportionnelle à la teneur en eau, que l'adhésion évoluait de manière proportionnelle avec le temps et que l'élasticité diminuait quand l'IP augmentait. Parallèlement à ces mesures de texture, les mesures structurales effectuées sur les mêmes échantillons de muscles ont mis en évidence que le salage et le séchage du jambon provoquaient d'importantes modifications de structure aux échelles tissulaire et cellulaire, avec des évolutions similaires entre les muscles BF et SM. La surface de section transversale des fibres musculaires a significativement diminué pendant les 21 premières semaines de fabrication, avant de se stabiliser ensuite. Les espaces extracellulaires (EEC) ont sensiblement diminué pendant les 11 premières semaines de fabrication, avant d'augmenter jusqu'à la 21<sup>ème</sup> semaine et se stabiliser ensuite. Ces évolutions morphologiques sont probablement liées aux mouvements de sel et d'eau dans les muscles lors de la fabrication des jambons. Par ailleurs,



il a été observé une très forte variabilité des paramètres de structure entre les jambons au même stade de fabrication. De ce fait, malgré les fortes contraintes expérimentales que cela génère, il serait judicieux de suivre les évolutions structurales dans les mêmes jambons, tout au long de leur fabrication. Il serait aussi intéressant de faire une étude en microscopie électronique afin de voir comment le sel modifie l'ultrastructure au sein des muscles, ce qui pourrait permettre d'apporter de plus amples informations sur les mécanismes mis en jeu.

Les traitements statistiques appliqués à l'ensemble des données de structure et de texture obtenues sur les muscles SM et BF ont fait apparaître que (1) la valeur de l'IP avait un effet très significatif sur les EEC, la taille des fibres, la fragilité et l'élasticité, que (2) la teneur en eau influençait significativement la dureté, la taille des fibres et des EEC, et que (3) la teneur en sel agissait significativement sur l'adhésion, la dureté et la taille des EEC. Enfin, pour les deux muscles SM et BF, une régression polynômiale multiple a permis d'établir des modèles phénoménologiques permettant de calculer certains paramètres structuraux (EEC, nombre de fibres, taille des fibres), mais aussi texturaux (élasticité, dureté, adhésion) en fonction des valeurs d'IP et des teneurs en eau et en sel. Ces modèles établissent clairement un lien entre les dynamiques d'évolution de la protéolyse, et celles de la structure et de la texture au sein des jambons secs au cours de leur fabrication. De plus, ils présentent l'avantage d'être facilement intégrables dans le modèle de « jambon numérique ».

L'objectif initial et très ambitieux de ce travail de thèse était de développer un simulateur de procédé de fabrication de jambons secs permettant de quantifier les effets biochimiques (protéolyse, oxydation lipidique), texturaux, structuraux et microbiologiques induits par une forte réduction de la teneur en sel lors de la fabrication d'un jambon sec. En couplant des modèles physiques de transferts de chaleur et de matière avec les modèles phénoménologiques de quantification de la protéolyse qui ont été établis, la version du modèle de « jambon numérique » développée à ce jour permet de prédire quantitativement la dynamique d'évolution de l'IP, des teneurs en eau et en sel, ainsi que celle de l' $a_w$ , à l'intérieur d'une géométrie réelle de jambon. A court terme, le modèle de « jambon numérique » peut être facilement complété, en implémentant les dernières corrélations statistiquement établies, de façon à pouvoir aussi prédire la dynamique d'évolution de l'oxydation lipidique et de certains paramètres structuraux ou texturaux en fonction des valeurs locales d'IP et des teneurs en sel et en eau. Néanmoins, cela implique de tester la validité des relations statistiques établies sur un nombre beaucoup plus grand d'échantillons et aussi, dans le cas de l'oxydation lipidique, d'appliquer une autre méthode de dosage que la méthode « TBA » afin d'obtenir des informations quantitatives correctes, en particulier lors

de l'étape de séchage/maturation des jambons secs. Le modèle de « jambon numérique » développé permet déjà de prédire la dynamique d'évolution de l' $a_w$  à l'intérieur du jambon, à partir des teneurs en eau et en sel. Le couplage de cette dynamique d'évolution avec des modèles de microbiologie prévisionnelle permettrait de prédire le devenir microbiologique de germes comme *Staphylococcus aureus*, *Listeria monocytogenes*, ou *Salmonella*, pouvant potentiellement contaminer un jambon sec. La contamination pouvant se faire, soit initialement lorsque le produit est entier, mais le risque est faible si les étapes de salage et de repos à basse température ont été bien conduites et s'il n'y a pas de perforations, soit lors de l'étape de désossage et de tranchage où le risque d'une recontamination est beaucoup plus fort. A ce moment-là, le risque microbiologique dépend surtout des caractéristiques physico-chimiques de la tranche de jambon ( $a_w$ , teneurs en sel et en eau) et du processus de conservation appliqué (température, atmosphère modifiée...). Or, un des avantages du modèle de « jambon numérique » est de pouvoir fournir la distribution spatiale et la dynamique d'évolution des concentrations en sel et en eau, et aussi celles relatives à l' $a_w$ , dans tout le volume du jambon. Moyennant un couplage avec des modèles de microbiologie prévisionnelle, il est donc possible de modéliser le devenir microbiologique en termes de croissance ou non-croissance de micro-organismes qui se seraient déposés à tel ou tel endroit sur une tranche de jambon sec, en tenant compte de l'hétérogénéité de la distribution des grandeurs physico-chimiques ( $a_w$ ,  $X_{sel}$ ,  $X_{eau}$ ) sur la surface de cette tranche.

Toutefois, la version actuelle du modèle de « jambon numérique » doit absolument être améliorée afin : (1) de prendre en compte la variation importante du volume du jambon due au séchage, de façon à prédire avec plus de précision le transport du sel vers l'intérieur du jambon et (2) de tenir compte de la diminution de la vitesse de protéolyse en fonction du temps qui serait liée à une diminution de la quantité de protéines hydrolysables.

La première amélioration peut être réalisée en mettant en place une formulation de type « ALE » des équations de transferts consistant en une déformation du maillage de calcul en fonction de la variation locale des teneurs en eau et en sel. Dans cette approche, le volume de chaque cellule du maillage de calcul doit être considéré comme étant la somme d'un volume de matière sèche anhydre déssalée qui reste constant, d'un volume de sel et d'un volume d'eau qui eux varient temporellement en fonction de la diffusion et du séchage. Cependant, mettre en place une formulation « ALE » sur le volume 3D d'un jambon semble trop difficile à réaliser ; par contre, compte tenu du fait que les transferts de sel et d'eau, ainsi que la déformation de la géométrie du jambon, se font surtout selon sa largeur et son épaisseur, la méthode « ALE » pourrait être développée sur une coupe 2D du jambon.

La seconde amélioration peut être réalisée en calculant la vitesse de protéolyse, non plus simplement à partir des modèles phénoménologiques qui ont été bâtis, mais à partir, par exemple, de l'équation de Michaelis-Menten, qui tient compte du fait que la vitesse d'une réaction enzymatique peut diminuer en fonction de la concentration initiale en substrat dégradé. Toutefois, une approche de ce type implique d'ajuster deux constantes caractéristiques de la réaction enzymatique pour pouvoir calculer la vitesse de protéolyse, à savoir la vitesse maximale de la réaction ( $V_{\max}$ ) et la constante de Michaelis ( $K_M$ ). Normalement, la détermination des constantes  $V_{\max}$  et  $K_M$  se fait suite à l'application d'une régression non linéaire sur des données expérimentales de réaction enzymatique obtenues pour différentes quantités initiales de substrat à dégrader. Cette méthode de détermination des 2 constantes paraît difficilement applicable à la réaction de protéolyse dans la mesure où faire varier la quantité de protéines hydrolysables dans des échantillons de viande semble purement impossible. Néanmoins, il est raisonnable de penser que les vitesses de protéolyse qui ont été mesurées dans ce travail renseignent sur les vitesses maximales ( $V_{\max}$ ) que peut atteindre la réaction de protéolyse dans les conditions de température, de salage et de séchage imposées par le plan d'expériences de Doehlert. Ces valeurs ayant été obtenues dans des conditions très favorables : durées courtes, quantités de substrat à dégrader non limitantes et présence de quantités faibles de produits issus de protéolyse. Il reste, cependant, à déterminer les valeurs des  $K_M$  correspondant à chacune de ces conditions testées, ce qui peut être fait par ajustement, soit en traitant différemment les données expérimentales de protéolyse déjà obtenues sur les petits échantillons préparés au laboratoire, soit en s'appuyant sur les données de protéolyse mesurées dans les échantillons extraits de jambons secs industriels. Ce n'est donc qu'une fois que toutes ces améliorations auront été réalisées que le modèle de « jambon numérique » pourra réellement être considéré comme un simulateur de procédé de fabrication d'un jambon sec. Le simulateur pourra, à ce moment-là, être utilisé pour définir entièrement le chemin technologique, *i.e.* les conditions d'application et la durée de chacune des étapes, permettant d'aboutir à la fabrication de jambons secs à teneur réduite en sodium, mais aux qualités sanitaires, sensorielles et organoleptiques préservées. Comme indiqué dans la littérature, deux voies technologiques sont possibles pour réduire la teneur finale en sodium des jambons secs : une réduction directe de la quantité du sel lors du salage, avec une limite à 25%, ou une substitution partielle du sodium par d'autres ions (potassium, magnésium...) avec une limite à 30 à 40%, moyennant un allongement de la phase de repos à basse température.

## **REFERENCES BIBLIOGRAPHIQUES**

---



---

- A -

---

- Adler, D., & Murdoch, D. (2013). Rgl: 3D visualization device system. R package version 0.93.945. URL <http://cran.r-project.org/web/packages/rgl/>. Accessed 11.07.13.
- AFSSA, Agence Française de Sécurité Sanitaire des Aliments. (2002). Rapport sel : évaluation et recommandations, Paris.
- AFSSA, Agence Française de Sécurité Sanitaire des Aliments. (2008). Présentation de l'étude INCA 2, Paris.
- Aidos, I., Lourenco, S., Van der Padt, A., Luten, J.B., & Boom, R.M. (2002). Stability of crude herring oil produced from fresh byproducts: Influence of temperature during storage. *Journal of Food Science*, 67(9), 3314–3320.
- Aliño, M., Grau, R., Fuentes, A., & Barat, J.M. (2010). Characterisation of pile salting with sodium replaced mixtures of salts in dry-cured loin manufacture. *Journal of Food Engineering*, 97(3), 434-439.
- Andrés, A.I., Cava, R., Ventanas, J., Muriel, E., & Ruiz, J. (2004). Lipid oxidative changes throughout the ripening of dry-cured Iberian hams with different salt contents and processing conditions. *Food Chemistry*, 84(3), 375–381.
- Andrés, A.I., Ventanas, S., Ventanas, J., Cava, R., & Ruiz, J. (2005). Physicochemical changes throughout the ripening of dry-cured hams with different salt content and processing conditions. *European Food Research and Technology*, 221, 30-35.
- Antequera, T., Caro, A., Rodriguez, P.G., & Perez, T. (2007). Monitoring the ripening process of Iberian ham by computer vision on magnetic resonance imaging. *Meat Science*, 76, 561-567.
- Antequera, T., Lopez, B.C.J., Cordoba, J.J., Garcia, C., Asensio, M.A., & Ventanas, J., et al. (1992). Lipid oxidative changes in the processing of Iberian pig hams. *Food Chemistry*, 45(2), 105-110.
- AOAC (1990). Association of official analytical chemist (15th ed., 931–935). Virginia: Arlington.
- Arnau, J., Gou, P., & Comaposada, J. (2003). Effect of the relative humidity of drying air during the resting period on the composition and appearance of dry-cured ham surface. *Meat Science*, 65, 1275-1280.
- Arnau, J., Gou, P., & Guerrero, L. (1994). The effect of freezing, meat pH, and storage temperature on the formation of white film and tyrosine crystals in dry-cured ham. *Journal of the Science of Food and Agriculture*, 66, 279-282.
- Arnau, J., Guerrero, L., & Gou, P. (1997). Effects of temperature during the last month of ageing and of salting time on dry-cured ham aged for six months. *Journal of the Science of Food and Agriculture*, 74, 193-198.
- Arnau, J., Guerrero, L., & Sarraga, C. (1998). The effect of green ham pH and NaCl concentration on cathepsin activities and sensory characteristics of dry-cured ham. *Journal of the Science of Food and Agriculture*, 77, 387-392.
- Arnau, J., Guerrero, L., Casademont, G., & Gou, P. (1995). Physical and chemical changes in different zones of normal and PSE dry-cured ham during processing. *Food Chemistry*, 52, 63-69.

Arnau, J., Guerrero, L., Maneja, E., & Gou, P. (1992). Effect of pH and genetics on texture characteristics of dry cured ham. In 38th ICOMST (pp. 229-232).

Arnau, J., Serra, X., Comaposada, J., Gou, P., & Garriga, M. (2007). Technologies to shorten the drying period of dry-cured meat products. *Meat Science*, 77(1), 81-89.

- B -

---

Bantan-Polak, T., Kassai, M., & Grant, K.B. (2001). A comparison of fluorescamine and naphthalene-2,3-dicarboxaldehyde fluorogenic reagents for microplate-based detection of amino acids. *Analytical Biochemistry*, 297, 128-136.

Barat, J.M., Grau, R., Ibanez, J., & Fito, P. (2005). Post-salting studies in Spanish cured ham manufacturing. Time reduction by using brine thawing-salting. *Meat Science*, 69, 201-208.

Barat, J.M., Baigts, D., Aliño, M., Fernández, F.J., & Pérez-García, V.M. (2011). Kinetics studies during NaCl and KCl pork meat brining. *Journal of Food Engineering*, 106(1), 102-110.

Benedini, R., Parolari, G., Toscani, T., & Virgili, R. (2012). Sensory and texture properties of Italian typical dry-cured hams as related to maturation time and salt content. *Meat Science*, 90(2), 431-437.

Berg, J.M., Tymoczko, J.L., & Stryer, L. (2007). *Biochemistry*; 6th ed. W.H. Freeman and Company: New York, NY.

Bezerra, R.M.F., Fraga, I., & Dias, A.A. (2013). Utilisation of integrated Michaelis-Menten equations for enzyme inhibition diagnosis and determination of kinetic constants using Solver supplement of Microsoft Office Excel. *Computer Methods and Programs in Biomedicine*, 109, 26-31.

Bezerra, M.A., Santelli, R.E., Oliveira, E.P., Villar, L.S., & Escalera, L.A. (2008). Response surface methodology (RSM) as a tool for optimization in analytical chemistry. *Talanta*, 76, 965-977.

Blesa, E., Aliño, M., Barat, J.M., Grau, R., Toldrá, F., & Pagán, M.J. (2008). Microbiology and physico-chemical changes of dry-cured ham during the post-salting stage as affected by partial replacement of NaCl by other salts. *Meat Science*, 78, 135-142.

Bohlen, P., Stein, S., & Udenfriend, S. (1974). Studies on the reaction of fluorescamine with primary amines. *Archives of Biochemistry and Biophysics*, 163, 390-399.

Bohuon, P. (1995). Déshydratation-Imprégnation par immersion en solutions ternaires : Etude des transports d'eau et de solutés sur gel et produits d'origine animale. *Ph-D Thesis*, Université de Montpellier II, Montpellier, France, 216 p.

Bourne, M.C. (2002). Principles of objective texture measurement. In M. C. Bourne (Ed.), *Food texture and viscosity: Concept and measurement* (pp. 107-188). SanDiego, USA

Briffaz, A., Bohuon, P., Méot, J.M., Dornier, M., & Mestres, C. (2014). Modelling of water transport and swelling associated with starch gelatinization during rice cooking. *Journal of Food Engineering*, 121, 143-151.



- Brøndum, J., Munck, L., Henckel, P., Karlsoon, A., Tornberg, E., & Engelsen, S.B. (2000). Prediction of water-holding capacity and composition of porcine meat by comparative spectroscopy. *Meat Science*, 55, 177-185.
- Broyart, B., Boudhrioua, N., Bonazzi, C., & Daudin, J.D. (2007). Modelling of moisture and salt transport in gelatine gels during drying at constant temperature. *Journal of Food Engineering*, 81, 657-671.
- Buscailhon, S., Touraille, C., Girard, J.P., & Monin, G. (1995). Relationships between muscle tissue characteristics and sensory qualities of dry-cured ham. *Journal of Muscle Foods*, 6, 9-22.
- Buscailhon, S., Berdague, J.L., Gandemer, G., Touraille, C., & Monin, G. (1994). Effects of initial pH on compositional changes and sensory traits of French dry-cured hams. *Journal of Muscle Foods*, 5, 257-270.

- C -

- Careri, M., Mangia, A., Barbieri, G., Bolzoni, L., Virgili, R., & Parolari, G. (1993). Sensory property relationships to chemical data of Italian-type dry-cured ham. *Journal of Food Science*, 58(5), 968-972.
- Castell, J.V., Cervera, M., & Marco, R. (1979). A convenient micromethod for assay of primary amines and proteins with fluorescamine: a re-examination of the conditions of reaction. *Analytical Biochemistry*, 99, 379-391.
- Cilla, I., Martinez, L., Beltran, J.A., & Roncales, P. (2005). Factors affecting acceptability of dry-cured ham throughout extended maturation under “bodega” conditions. *Meat Science*, 69, 789-795.
- Cilla, I., Martinez, L., Beltran, J.A., & Roncales, P. (2006). Effect of low temperature preservation on the quality of vacuum-packaged dry-cured ham: Refrigerated boneless ham and frozen ham cuts. *Meat Science*, 73, 12-21.
- Comaposada, J., Arnau, J., & Gou, P. (2007). Sorption isotherms of salted minced pork and of lean surface of dry-cured hams at the end of the resting period using KCl as substitute for NaCl. *Meat Science*, 77(4), 643-648.
- Cordero, M.R., & Zumalacarregui, J.M. (2000). Characterization of micrococccaceae isolated from salt used for Spanish dry-cured ham. *Letters in Applied Microbiology*, 31(4), 303-306.
- Costa-Corredor, A., Serra, X., Arnau, J., & Gou, P. (2009). Reduction of NaCl content in restructured dry-cured hams: Post-resting temperature and drying level effects on physicochemical and sensory parameters. *Meat Science*, 83(3), 390-397.
- Costa-Corredor, A., Muñoz, T., Arnau, J., & Gou, P. (2010). Ion uptakes and diffusivities in pork meat brine-salted with NaCl and K-lactate. *LWT-Food Science and Technology*, 43, 1226-1233.
- Coutron-Gambotti, C., & Gandemer, G. (1999). Lipolysis and oxidation in subcutaneous adipose tissue during dry-cured ham processing. *Food Chemistry*, 64(1), 95-101.
- Cruz, J. (2005). La producción y comercialización de jamón curado en España. *Eurocarne*, 135, 1-10.

- D -

---

- Daudin, J.D, Kondjoyan, A., & Sirami, J. (1992). Water and salt transfers analysis in drying of sausages. In: *Proceedings of the 38<sup>th</sup> International Congress of Meat Science and Technology*, 38<sup>th</sup> ICoMST, Clermont-Ferrand, 23-28 August, (p. 1199-1202).
- Del Olmo, A., Calzada, J., Gaya, P., & Nunez, M. (2013). Proteolysis, texture, and sensory characteristics of Serrano hams from Duroc and Large White pigs during dry-curing. *Journal of Food Science*, 78(3), 416-424.
- Desmond, E. (2006). Reducing salt: A challenge for the meat industry. *Meat Science*, 74, 188-196.
- Dhaunta, N., Fatima, U., & Guptasarma, P. (2011). N-Terminal sequencing by mass spectrometry through specific fluorescamine labelling of  $\alpha$ -amino groups before tryptic digestion. *Analytical Biochemistry*, 408, 263-268.
- Djelveh, G., & Gros, J.B. (1988). Measurement of effective diffusivities of ionic and non-ionic solutes through beef and pork muscles using a diffusion cell. *Meat Science*, 23, 11-20.
- Doehlert, D.H. (1970). Uniform shell designs. *Applied Statistics*, 19, 231-239.
- Donea, J., Huerta, A., Ponthot, J.P., & Rodriguez-Ferran, A. (2004). Arbitrary Lagrangian-Eulerian methods. In: Stein, E., de Borst, R., Hughes, T.J.R. (Eds.), *Encyclopedia of Computational Mechanics*, Volume 1: *Fundamentals*, John Wiley & Sons, (p. 413-437).

- E -

---

- EC. (2006). Regulation (EC) No 1924/2006 of the European Parliament and of the Council of 20 December 2006 on nutrition and health claims made on foods. Official Journal of the European Union, L404, p. 9-25.

- F -

---

- Fantazzini, P., Gombia, M., Schembri, P., Simoncini, N., & Virgili, R. (2009). Use of Magnetic Resonance Imaging for monitoring Parma dry-cured ham processing. *Meat Science*, 82(2), 219-227.
- FDA. (2008). Guidance for industry: A food labeling guide. U.S. Department of Health and Human Services, Food and Drug Administration, Center for Food Safety and Applied Nutrition, (Chapter IX), Available online at <http://www.fda.gov/Food>.
- Fox, J.B. (1980). Diffusion of chloride, nitrite and nitrate in beef and pork. *Journal of Food Science*, 45, 1740-1744.
- Fox, J., & Weisberg, S. (2011). An R companion to applied regression. 2nd Edition. Thousand Oaks CA: Sage. URL <http://socserv.socsci.mcmaster.ca/jfox/Books/Companion>. Accessed 11.09.13.
- Friguet, B., Stadtman, E.R., & Szewda, L.I. (1994). Modification of glucose-6-phosphate dehydrogenase by 4-hydroxy-2-nonenal. Formation of cross-linked protein that inhibits the multicatalytic protease. *Journal of Biological Chemistry*, 269, 21639-21643.

- Fritz, J.D., Mitchell, M.C., Marsh, B.B., & Greaser, M.L. (1993). Titin content of beef in relation to tenderness. *Meat Science*, 33(1), 41–50.
- Fulladosa, E., Serra, X., Gou, P., & Arnau, J. (2009). Effects of potassium lactate and high pressure on transglutaminase restructured dry-cured hams with reduced salt content. *Meat Science*, 82(2), 213-218.
- Fulladosa, E., Santos-Garcés, E., Picouet, P., & Gou, P. (2010). Prediction of salt and water content in dry-cured hams by computed tomography. *Journal of Food Engineering*, 96(1), 80-85.

- G -

- Gandolfi, G., Pomponio, L., Ertbjerg, P., Karlsson, A.H., Nanni Costa, L., Lametsch, R., Russo, V., & Davoli, R. (2011). Investigation on CAST, CAPN1 and CAPN3 porcine gene polymorphisms and expression in relation to post-mortem calpain activity in muscle and meat quality. *Meat Science*, 88(4), 694-700.
- García-Garrido, J.A., Quiles-Zafra, R., Tapiador, J., & Luque de Castro, M.D. (2000). Activity of cathepsin B, D, H and L in Spanish dry-cured ham of normal and defective texture. *Meat Science*, 56(1), 1-6.
- García-Rey, R.M., García-Garrido, J.A., Quiles-Zafra, R., Tapiador, J., & Luque de Castro, M.D. (2004a). Relationship between pH before salting and dry-cured ham quality. *Meat Science*, 67(4), 625-632.
- García-Rey, R.M., García-Garrido, J.A., Quiles-Zafra, R., Tapiador, J., & Luque de Castro, M.D. (2004b). Characterization of defective textures in dry-cured ham by compositional and HPLC analysis of soluble substances of low-molecular weight. *Food Chemistry*, 85(4), 617-622.
- García-Rey, R.M., García-Olmo, J., De Pedro, E., Quiles-Zafra, R., & Luque de Castro, M.D. (2005). Prediction of texture and colour of dry-cured ham by visible and near infrared spectroscopy using a fiber optic probe. *Meat Science*, 70(2), 357-363.
- Garrido, R., Domínguez, R., Lorenzo, J.M., Franco, I., & Carballo, J. (2012). Effect of the length of salting time on the proteolytic changes in dry-cured lacón during ripening and on the sensory characteristics of the final product. *Food Control*, 25, 789-796.
- Garrido-Del Solo, C., Varon, R., Garcia-Canovas, F., & Havsteen, B.H. (1994). Kinetic analysis of the Michaelis-Menten mechanism in which the substrate and the product are unstable. *International Journal of Biochemistry*, 26(5), 645-651.
- Gatellier, P., Santé-Lhoutellier, V., Portanguen, S., & Kondjoyan, A. (2009). Use of meat fluorescence emission as a marker of oxidation promoted by cooking. *Meat Science*, 83, 651–656
- Geleijnse, J.M., Witteman, J.C., Bak, A.A., den Breeijen, J.H., & Grobbee, D.E. (1994). Reduction in blood pressure with a low sodium, high potassium, high magnesium salt in older subjects with mild-moderate hypertension. *British Medical Journal*, 309, 436-440.
- Goldbeter, A. (2013). Oscillatory enzyme reactions and Michaelis-Menten kinetics. *FEBS Letters*, 587, 2778-2784.
- Gornall, A.G., Bardawill, C.J., & David, M.M. (1949). Determination of serum proteins by means of biuret reaction. *Journal of Biological Chemistry*, 177, 751-766.

- Gou, P., Comaposada, J., & Arnau, J. (2004). Moisture diffusivity in the lean tissue of dry-cured ham at different process times. *Meat Science*, 67(2), 203-209.
- Gou, P., Guerrero, L., & Arnau, J. (1995). Sex and crossbreed effects on the characteristics of dry-cured ham. *Meat Science*, 40(1), 21-31.
- Gou, P., Morales, R., Serra, X., Guàrdia, M.D., & Arnau, J. (2008). Effect of a 10-day ageing at 30°C on the texture of dry-cured hams processed at temperatures up to 18°C in relation to raw meat pH and salting time. *Meat Science*, 80(4), 1333-1339.
- Graiver, N., Pinotti, A., Califano, A., & Zaritzky, N. (2006). Diffusion of sodium chloride in pork tissue. *Journal of Food Engineering*, 77(4), 910-918.
- Grau, R., Albarracín, W., Toldrá, F., Antequera, T., & Barat, J.M. (2008). Study of salting and post-salting stages of fresh and thawed Iberian hams. *Meat Science*, 79(4), 677-682.
- Guerrero, L., Gou, P., & Arnau, J. (1999). The influence of meat pH on mechanical and sensory textural properties of dry-cured ham. *Meat Science*, 52(3), 267-273.

- H -

---

- Hansen, C.L., van der Berg, F., Ringgaard, S., Stødkilde-Jørgensen, H., & Karlsson, A.H. (2008). Diffusion of NaCl in meat studied by <sup>1</sup>H and <sup>23</sup>Na magnetic resonance imaging. *Meat Science*, 80, 851-856.
- Harkouss, R., Mirade, P.S., & Gatellier, P. (2012). Development of a rapid, specific and efficient procedure for the determination of proteolytic activity in dry-cured ham: definition of a new proteolysis index. *Meat Science*, 92(2), 84-88.
- Harkouss, R., Safa, H., Gatellier, P., Lebert, A., & Mirade, P.S. (2014). Building phenomenological models that relate proteolysis in pork muscles to temperature, water and salt content. *Food Chemistry*, 151, 7-14.
- Haseth, T.T., Sørheim, O., Høy, M., & Egelanddal, B. (2012). Use of computed tomography to study raw ham properties and predict salt content and distribution during dry-cured ham production. *Meat Science*, 90, 858-864.
- He, F.J., & MacGregor, G.A. (2009). A comprehensive review on salt and health and current experience of worldwide salt reduction programmes. *Journal of Human Hypertension*, 23, 363-384.
- Heaney, R.P. (2006). Role of dietary sodium in osteoporosis. *Journal of American College of Nutrition*, 25, 271S-276S.
- Heiberger, R.M. (2013). HH: statistical analysis and data display. R package version 2.3.37. URL <http://cran.r-project.org/web/packages/HH/>. Accessed 11.07.13.
- Hernandez-Cazares, A.S., Aristoy, M.C., & Toldra, F. (2011). Nucleotides and their degradation products during processing of dry-cured ham, measured by HPLC and an enzyme sensor. *Meat Science*, 87(2), 125-129.
- Hortos, M., Gil, M., & Sarraga, G. (1994). Effect of calpain and cathepsin activities on myofibrils from porcine longissimus muscle during conditioning of normal and exudative meat. *Sciences des Aliments*, 14, 503-515.
- Hutton, T. (2002). Technological functions of salt in the manufacturing of food and drink products. *British Food Journal*, 104, 126-152.

---

**- J -**

---

- Jakobsen, M., & Bertelsen, G. (2000). Colour stability and lipid oxidation of fresh beef. Development of a response surface model for predicting the effects of temperature, storage time, and modified atmosphere composition. *Meat Science*, 54, 49-57.
- Jee, S.H., Miller, E.R., Guallar, E., Singh, V.K., Appel, L.J., & Klag, M.J. (2002). The effect of magnesium supplementation on blood pressure: a meta-analysis of randomized clinical trials. *American Journal of Hypertension*, 15, 691-696.
- Jimenez-Colmenero, F., Ventanas, J., & Toldra, F. (2010). Nutritional composition of dry-cured ham and its role in a healthy diet. *Meat Science*, 84(4), 585-593.
- Jin, G., He, L., Zhang, J., Yu, X., Wang, J., & Huang, F. (2012). Effects of temperature and NaCl percentage on lipid oxidation in pork muscle and exploration of the controlling method using response surface methodology (RSM). *Food Chemistry*, 131, 817-825.
- Johnson, K.A., & Goody, R.S. (2011). The original Michaelis constant: Translation of the 1913 Michaelis-Menten paper. *Biochemistry*, 50, 8264-8269.

---

**- K -**

---

- Karppanen, H., & Mervaala, E. (2006). Sodium intake and hypertension. *Progress in Cardiovascular Diseases*, 49(2), 59-75.
- Klein, B., & Standaert, F. (1976). Fluorimetry of plasma amino nitrogen, with the use of fluorescamine. *Clinical Chemistry*, 22, 413-416.
- Kondjoyan, A., & Daudin, J.D. (1997). Heat and mass transfer coefficients at the surface of a pork hindquarter. *Journal of Food Engineering*, 32, 225-240.

---

**- L -**

---

- Larrea, V., Hernando, I., Quiles, A., Lluch, M.A., & Pérez-Munuera, I. (2006). Changes in proteins during Teruel dry-cured ham processing. *Meat Science*, 74(3), 586-593.
- Larrea, V., Perez-Munuera, I., Hernando, I., Quiles, A., & Lluch, M.A. (2007). Chemical and structural changes in lipids during the ripening of Teruel dry-cured ham. *Food Chemistry*, 101, 1327-1336.
- Lautenschläger, R. (1995). Diffusion of sodium chloride and sodium nitrite in raw meat model systems. Proceedings of the 41st Annual ICoMST, San Antonio, USA, 507-508.
- Lawes, C.M.M., Van der Hoorn, S., Law, M.R., Elliott, P., MacMahon, S., & Rodgers, A. (2006). Blood pressure and the global burden of disease 2000: part I Estimates of blood pressure levels; part II Estimates of attributable burden. *Journal of Hypertension*, 24, 413-430.
- Lebert, A., & Daudin, J.D. (2013). Modelling the distribution of  $a_w$ , pH and ions in marinated beef meat. *Meat Science*, <http://dx.doi.org/10.1016/j.meatsci.2013.10.017>.



- Leistner, L. (1985). Hurdle technology applied to meat products of the shelf stable product and intermediate moisture food types. In Simatos D, Multon JL, editors. Properties of water in foods in relation to quality and stability. Dordrecht: Martinus Nijhoff Publishers. p 309-329.
- Lorenzen, A., & Kennedy, S.W. (1993). A fluorescent-based protein assay for the use with a microplate reader. *Analytical Biochemistry*, 214, 346-348.
- Luccia, A.D., Picariello, G., Cacace, G., Scaloni, A., Faccia, M., Liuzzi, V., Alviti, G., & Musso, S.S. (2005). Proteomic analysis of water soluble and myofibrillar protein changes occurring in dry-cured hams. *Meat Science*, 69(3), 479-491.
- Lumkey, T. (2009). Leaps: regression subset selection. R package version 2.9. URL <http://CRAN.R-project.org/package=leaps>. Accessed 11.07.13.
- Lynch, S.M., & Frey, B. (1993). Mechanisms of copper and iron dependent oxidative modification of human low density lipoprotein. *Journal of Lipid Research*, 34, 1745-1751.

- M -

---

- MAPA. (2005). Estudio sobre el conocimiento, hábitos de compra y consumo en España de jamón de cerdo Ibérico y sus denominaciones de calidad actitud de los consumidores ante las denominaciones de origen. Available on 02/08/07 at URL: [http://www.mapa.es/alimentacion/pags/comercializacion/estudios/jamon\\_iberico.pdf](http://www.mapa.es/alimentacion/pags/comercializacion/estudios/jamon_iberico.pdf).
- Marañón Di Leo, J., & Marañón, J. (2005). Hydration and diffusion of cations in nanopores. *Journal of Molecular Structure: Theochem*, 729, 53-57.
- Marriott, N.G., Graham, P.P., Shaffer, C.K., & Phelps, S.K. (1987). Accelerated production of dry-cured hams. *Meat Science*, 19, 53-64.
- Martín, L., Córdoba, J.J., Antequera, T., Tímon, M.L., & Ventanas, J. (1998). Effects of salt and temperature on proteolysis during ripening of Iberian ham. *Meat Science*, 49, 145-153.
- McMahon, E.J., Campbell, K.L., Mudge, D.W., & Bauer, J.D. (2012). Achieving salt restriction in chronic kidney disease. *International Journal of Nephrology*, doi:10.1155/2012/720429.
- Mendez, E., & Gavilanes, J.G. (1976). Fluorimetric detection of peptides after column chromatography or on paper: o-phthalaldehyde and fluorescamine. *Analytical Biochemistry*, 72, 473-479.
- Mercier, Y., Gatellier, P., Viau, M., Remignon, H., & Renner, M. (1998). Effect of dietary fat and vitamin E on lipid and protein oxidation in turkey meat during storage. *Meat Science*, 48, 301-317.
- Miedel, M.C., Hulmes, J.D., & Pan, Y.C.E. (1989). The use of fluorescamine as a detection reagent in protein microcharacterization. *Journal of Biochemical and Biophysical Methods*, 18, 37-52.
- MØller, J.K.S., Jakobsen, M., Weber, C.J., Martinussen, T., Skibsted, L.H., & Bertelsen, G. (2003). Optimisation of colour stability of cured ham during packaging and retail display by a multifactorial design. *Meat Science*, 63, 169-175.

- 
- Monin G., Marinova P., Talmant A., Martin, J.F., Cornet M., Lanore D., Grassot F. (1997). Chemical and structural changes in dry-cured hams (Bayonne Hams) during processing and effect of the dehairing technique. *Meat Science*, 47, 29-47.
- Mora, L., Sentandreu, M., Koistinen, K., Fraser, P., Toldra, F., & Bramley, P. (2009). Naturally generated small peptides derived from myofibrillar proteins in Serrano dry-cured ham. *Journal of Agriculture and Food Chemistry*, 57, 3228-3234.
- Morales, R., Guerrero, L., Serra, X., & Gou, P. (2007a). Instrumental evaluation of defective texture in dry-cured hams. *Meat Science*, 76(3), 536-542.
- Morales, R., Serra, X., Guerrero, L., & Gou, P. (2007b). Softness in dry-cured porcine biceps femoris muscles in relation to meat quality characteristics and processing conditions. *Meat Science*, 77, 662-669.
- Morales, R., Arnau, J., Serra, X., Guerrero, L., & Gou, P. (2008a). Texture changes in dry-cured ham pieces by mild thermal treatments at the end of the drying process. *Meat Science*, 80, 231-238.
- Morales, R., Guerrero, L., Claret, A., Guardia, M.D., & Gou, P. (2008b). Beliefs and attitudes of butchers and consumers towards dry-cured ham. *Meat Science*, 80(4), 1005-1012.
- Morzel, M., Gatellier, P., Sayd, T., Renner, M., & Laville, E. (2006). Chemical oxidation decreases proteolytic susceptibility of skeletal muscle myofibrillar proteins. *Meat Science*, 73, 536-543.
- Motilva, M.J., Toldra, F., Nieto, P., & Flores, J. (1993). Muscle lipolysis phenomena in the processing of dry-cured ham. *Food Chemistry*, 48(2), 121-125.
- Muñoz, I., Arnau, J., Costa-Corredor, A., & Gou, P. (2009). Desorption isotherms of salted minced pork using K-lactate as a substitute for NaCl. *Meat Science*, 83(4), 642-646.

- N -

- 
- Nazario, C.M., Szklo, M., Diamond, E., Roman-Franco, A., Climent, C., Suarez, E., & Conde, J.G. (1993). Salt and gastric cancer: a case-control study in Puerto Rico. *International Journal of Epidemiology*, 22, 790-797.
- Newton, K.G., & Gill, C.O. (1981). The microbiology of DFD fresh meat: a review. *Meat Science*, 5(3), 223-227.
- Nielsen. (2009). Database for Norwegian meat industry. Report, Nielsen Company.

- P -

- 
- Parolari, G. (1996). Review: Achievements, needs and perspectives in dry-cured ham technology: The example of Parma ham. *Food Science and Technology International*, 2, 69-78.
- Parolari, G., Virgili, R., & Schivazappa, C. (1994). Relationship between Cathepsin B activity and compositional parameters in dry-cured hams of normal and defective texture. *Meat Science*, 38, 117-122.
- Parreño, M., Cussó, R., Gil, M., & Sárraga, C. (1994). Development of cathepsin B, L and H activities and cystatin-like activity during two different manufacturing processes for Spanish dry-cured ham. *Food Chemistry*, 49(1), 15-21.

- Pearson, A.M., Wolzak, A.M., & Gray, J.I. (1983). Possible role of muscle protein in flavor and tenderness of meat. *Journal of Food Biochemistry*, 7, 189-210.
- Phan, V.A., Yven, C., Lawrence, G., Chabanet, C., Reparet, J.M., & Salles, C. (2008). In vivo sodium release related to salty perception during eating model cheeses of different textures. *International Dairy Journal*, 18, 956-963.

- R -

---

- R Development Core Team (2013). R: a language and environment for statistical computing. R Foundation for Statistical Computing, Vienna, Austria. URL <http://www.R-project.org>. Accessed 11.09.13.
- Rastelli, E., Giraffa, G., Carminati, D., Parolari, G., & Barbuti, S. (2005). Identification and characterisation of halotolerant bacteria in spoiled dry-cured hams. *Meat Science*, 70, 241-246.
- Rhee, K., Smith, G.G., & Terrell, R.N. (1983). Effect of reduction and replacement of sodium chloride on rancidity development in raw and cooked pork. *Journal of Food Protection*, 46(7), 578-581.
- Rico, E., Toldrá, F., & Flores, J. (1990). Activity of cathepsin D as affected by chemical and physical dry-curing parameters. *Zeitschrift für Lebensmittel-Untersuchung und Forschung*, 191, 20-23.
- Robert, N., & Lanore, D. (2003). Une mine d'éléments essentiels. Le jambon de Bayonne. *Viandes et Produits Carnés*, 23, 97-101.
- Rodriguez-Nunez, E., Aristoy, M. C., & Toldra, F. (1995). Peptide generation in the processing of dry-cured ham. *Food Chemistry*, 53(2), 187-190.
- Rougier, T. (2006). Caractérisation et modélisation des transferts d'eau et de solutés en vue d'une aide à la formulation des aliments composites. Cas des assemblages base céréalière-fourrage humide protéique. *Ph-D Thesis*, Ecole Nationale Supérieure des Industries Alimentaires, Ecole Doctorale ABIÉS, Massy, France, 271 p.
- Rougier, T., Bonazzi, C., Daudin, J.D. (2007). Modelling incidence of lipid and sodium chloride contents on sorption curves of gelatine in the high humidity range. *Lebensmittel-Wissenschaft-und-Technology*, 40, 1798-1807.
- Ruiz, J., Cava, R., Timón, M.L., & García, C. (1998). Sensory characteristics of Iberian ham: Influence of processing time and slice location. *Food Research International*, 31, 53-58.
- Ruiz-Cabrera, M., Gou, P., Foucat, L., Renou, J.P., & Daudin, J.D. (2004). Water transfer analysis in pork meat supported by NMR imaging. *Meat Science*, 67, 169-178.
- Ruiz-Carrascal, J., Ventanas, J., Cava, R., Andres, A., & Garcia, C. (2000). Texture and appearance of dry-cured ham as affected by fat content and fatty acid composition. *Food Research International*, 33, 91-95.
- Ruiz-Ramirez, J., Arnau, J., Serra, X., & Gou, P. (2006). Effect of pH(24), NaCl content and proteolysis index on the relationship between water content and texture parameters in biceps femoris and semimembranosus muscles in dry-cured ham. *Meat Science*, 72(2), 185-194.



---

Ruiz-Ramirez, J., Serra, X., Gou, P., & Arnau, J. (2005). Profiles of water content, water activity and texture in crusted dry-cured loin and in non-crusted dry-cured loin. *Meat Science*, 69, 519-525.

Ruusunen, M., & Puolanne, E. (2005). Reducing sodium intake from meat products. *Meat Science*, 70 531–541.

- S -

---

Said, R., Schüller, R.B., Young, P., Aastveit, A., & Egelanddal, B. (2007). Simulation of salt diffusion in a pork (bacon) side using 3D imaging. Proceedings of the COMSOL Users Conference 2007, Grenoble, France.

Santé-Lhoutellier, V., Robert, N., Martin, J.F., Gou, P., Hortos, M., Arnau, J., Diestre, A., & Candek-Potokar, M. (2012). PRKAG3 and CAST genetic polymorphisms and quality traits of dry-cured hams--II. Associations in French dry-cured ham Jambon de Bayonne and their dependence on salt reduction. *Meat Science*, 92(4), 354-359.

Santos-Garcés, E., Muñoz, I., Gou, P., Sala, X., & Fulladosa, E. (2012). Tools for studying dry-cured ham processing by using computed tomography. *Journal of Agricultural and Food Chemistry*, 60(1), 241-249.

Sarraga, C., Gil, M., & Garcia-Regueiro, J.A. (1993). Comparison of calpain and cathepsin (B, L and D) activities during dry-cured ham processing from heavy and light large white pigs. *Journal of the Science of Food and Agriculture*, 62(1), 71-75.

Sarraga, C., Gil, M., Arnau, J., Monfort, J.M., & Cussó, R. (1989). Effect of curing salt and phosphate on the activity of porcine muscle proteases. *Meat Science*, 25, 241-249.

Schivazappa, C., Degni, M., Nanni Costa, L., Russo, V., Buttazzoni, L., & Virgili, R. (2002). Analysis of raw meat to predict proteolysis in Parma ham. *Meat Science*, 60(1), 77-83.

Sentandreu, M.A., Stoeva, S., Aristoy, M.C., Laib, K., Voelter, W., & Toldra, F. (2003). Identification of small peptides generated in Spanish dry-cured ham. *Journal of Food Science*, 68(1), 64-69.

Serra, X., Ruiz-Ramirez, J., Arnau, J., & Gou, P. (2005). Texture parameters of dry-cured ham m. biceps femoris samples dried at different levels as a function of water activity and water content. *Meat Science*, 69(2), 249-254.

Sforza, S., Pigazzani, A., Motti, M., Porta, C., Virgili, R., Galaverna, G., Dossena, A., & Marchelli, R. (2001). Oligopeptides and free amino acids in Parma hams of known cathepsin B activity. *Food Chemistry*, 75(3), 267-273.

Skinner, G.E., & Rao, V.N.M. (1986). Linear viscoelastic behaviour of frankfurters. *Journal of Texture Studies*, 17, 421-432.

Soresi-Bordini, C., Virgili, R., Degni, M., Gabba, L., & Schivazappa, C. (2004). Effect of ageing time on the analytical and sensory parameters of Parma ham. *Industria Conserve*, 79, 149-160.

St. John, L. C., Young, C.R., Knabe, D.A., Thompson, L.D., Schelling, G.T., & Grundy, S.M. (1987). Fatty acid profiles and sensory and carcass traits of tissues from steers and swine fed an elevated monounsaturated fat diet. *Journal of Animal Science*, 64, 1441-1447.

- T -

---

- Tabilo, G., Flores, M., Fiszman, S.M., & Toldra, F. (1999). Postmortem meat quality and sex affect textural properties and protein breakdown of dry-cured ham. *Meat Science*, 51, 255-260.
- Taormina, P.J. (2010). Implications of salt and sodium reduction on microbial food safety. *Critical Reviews in Food Science and Nutrition*, 50, 209-227.
- Thorvaldsson, K., & Skjoldebrand, C. (1996). Water transport in meat during reheating. *Journal of Food Engineering*, 29(1), 13-21.
- Toldrá, F. (1998). Proteolysis and lipolysis in flavour development of dry-cured meat products. *Meat Science*, 49, Supplement 1(0), 101-110.
- Toldrá, F. (2002). Dry-cured meat products. Ames, IO: Wiley-Blackwell.
- Toldrá, F. (2006). The role of muscle enzymes in dry-cured meat products with different drying conditions. *Trends in Food Science and Technology*, 17, 164-168.
- Toldrá, F., & Etherington, D.J. (1988). Examination of cathepsins B, D, H and L activities in dry-cured hams. *Meat Science*, 23, 1-7.
- Toldrá, F., & Flores, M. (2000). The use of muscle enzymes as predictor of pork meat quality. *Food Chemistry*, 69, 387-395.
- Toldrá, F., Cerveró, M.C., & Part, C. (1993). Porcine aminopeptidase activity as affected by curing agents. *Journal of Food Science*, 58, 724-726.
- Toldrá, F., Flores, M., & Sanz, Y. (1997). Dry-cured ham flavour: enzymatic generation and process influence. *Food Chemistry*, 59(4), 523-530.

- V -

---

- Ventanas, S., Mustonen, S., Puolanne, E., & Tuorila, H. (2010). Odour and flavour perception in flavoured model systems: Influence of sodium chloride, umami compounds and serving temperature. *Food Quality and Preference*, 21, 453-462.
- Vestergaard, C., Risum, J., & Adler-Nissen, J. (2005). <sup>23</sup>Na-MRI quantification of sodium and water mobility in pork during brine curing. *Meat Science*, 69(4), 663-672.
- Virgili, R., & Parolari, G. (1991). Quality control in the meat industry by multivariate statistics. The case of raw ham. *Meat Science*, 19, 83-96.
- Virgili, R., & Schivazappa, C. (2002). Muscle traits for long matured dried meats. *Meat Science*, 62(3), 331-343.
- Virgili, R., Parolari, G., Schivazappa, C., Bordini, C.S., & Borri, M. (1995). Sensory and texture quality of dry-cured ham as affected by endogenous cathepsin B activity and muscle composition. *Journal of Food Science*, 60, 1183-1186.
- Virgili, R., Saccani, G., Gabba, L., Tanzi, E., & Soresi-Bordini, C. (2007). Changes of free amino acids and biogenic amines during extended ageing of Italian dry-cured ham. *LWT - Food Science and Technology*, 40(5), 871-878.
- Virgili, R., Schivazappa, C., Parolari, G., Bordini, C.S., & Degni, M. (1998). Proteases in fresh pork muscle and their influence on bitter taste formation in dry-cured ham. *Journal of Food Biochemistry*, 22(1), 53-63.

- W -

---

Warnants, N., Van Oeckel, M.J., & Boucque, C.V. (1996). Incorporation of dietary PUFA in pork tissues for the quality of the end products. *Meat Science*, 44, 125-144.

Weigele, M., De Bernardo, S.I., Teng, J.P., Leimgruber, W. (1972). Novel reagent for the fluorimetric assay of primary amines. *Journal of American Chemical Society*, 94, 5927- 5928.

- Z -

---

Zanardi, E., Ghidini, S., Battaglia, A., & Chizzolini, R. (2004). Lipolysis and lipid oxidation in fermented sausages depending on different processing conditions and different antioxidants. *Meat Science*, 66, 415-423.

Zhao, G.M., Tian, W., Liu, Y.X., Zhou, G.H., Xu, X.L., & Li, M.Y. (2008). Proteolysis in biceps femoris during Jinhua ham processing. *Meat Science*, 79(1), 39-45.

Zhao, G.M., Zhou, G.H., Wang, Y.L., Xu, X.L., Huan, Y.J., & Wu, J.Q. (2005). Time-related changes in cathepsin B and L activities during processing of Jinhua ham as a function of pH, salt and temperature. *Meat Science*, 70(2), 381-388.

Zhou, G.H., & Zhao, G.M. (2007). Biochemical changes during processing of traditional Jinhua ham. *Meat Science*, 77(1), 114-120.



**Annexe I :**

**Harkouss, Mirade & Gatellier (2012). *Meat Science*, 92, 84-88**





## Development of a rapid, specific and efficient procedure for the determination of proteolytic activity in dry-cured ham: Definition of a new proteolysis index

Rami Harkouss, Pierre-Sylvain Mirade, Philippe Gatellier\*

INRA, UR370 Qualité des Produits Animaux, F-63122 Saint-Genès-Champanelle, France

### ARTICLE INFO

#### Article history:

Received 7 February 2012

Received in revised form 11 April 2012

Accepted 13 April 2012

#### Keywords:

Dry-cured ham  
Proteolysis index  
Fluorescamine  
Fluorescence

### ABSTRACT

A method was adapted to determine proteolytic activity in dry-cured ham using fluorescamine-specific labelling of N-terminal  $\alpha$ -amino groups of peptides and amino acids. Fluorescence of the complex was measured using a microplate procedure and optimum excitation and emission wavelengths of 375 nm and 475 nm, respectively. A new proteolysis index (PI) was defined as the percentage ratio of the N-terminal  $\alpha$ -amino group content to the total protein content of the ham extract. The robustness of the method was evaluated by measuring PI in pork meat samples subjected to standardized processing conditions and in samples extracted from industrial hams taken at different stages of processing. For the industrial samples, a comparison with the classic nitrogen procedure of PI determination was performed and a formula relating the two PIs was established. The rapidity, sensitivity and specificity of the procedure make it a good candidate for a screening test to evaluate ham quality in industry.

© 2012 Elsevier Ltd. All rights reserved.

### 1. Introduction

In dry-cured ham, one of the main factors affecting final product quality is proteolytic activity. It impacts the flavour, the appearance (e.g. tyrosine crystals, white film, brightness), and the texture (e.g. hardness, cohesiveness, and springiness) of the product (Arnau, Guerrero, & Sárraga, 1998; García-Garrido, Quiles-Zafra, Tapiador, & Luque de Castro, 2000; Toldrá & Flores, 2000; Virgili, Parolari, Schivazappa, Bordini, & Borri, 1995; Zhao et al., 2008). Proteolytic activity depends on many factors, such as pH, water content, NaCl content and drying conditions (Arnau, Gou, & Comaposada, 2003; Arnau, Gou, & Guerrero, 1994; Arnau, Guerrero, & Gou, 1997; Arnau, Guerrero, Maneja, & Gou, 1992; Martín, Córdoba, Antequera, Tímon, & Ventanas, 1998; Toldrá, Flores, & Sanz, 1997). In dry-cured ham, a proteolysis index (PI), defined as the percentage ratio of non-protein nitrogen content to total nitrogen content, is widely used to characterize the intensity of proteolytic activity; nitrogen content is determined by the Kjeldahl method, which measures ammonia after mineralization of the organic matter (Careri et al., 1993; Ruiz-Ramírez, Arnau, Serra, & Gou, 2006; Schivazappa et al., 2002). Although this procedure is commonly used and is standardized (ISO 937–1978 E reference method), it has many drawbacks. It is time- and product-consuming, and it lacks specificity, as there are many nitrogen compounds in meat (ammonium salts, urea, uric acid, creatinine,

etc.) that can interfere in the determination of the proteolysis index. A more rapid and efficient assay of peptides and amino acids would thus greatly facilitate the evaluation of proteolysis in dry-cured ham. To this end, a simple, specific fluorometric procedure was developed to determine the level of N-terminal  $\alpha$ -amino groups of peptides and amino acids, which reflects the intensity of proteolytic activity during the curing process. The procedure is based on the fluorescamine-specific labelling of the N-terminal  $\alpha$ -amino groups present in the fractions of the ham extracts soluble in 10% trichloroacetic acid (TCA). A new proteolysis index was then defined as the percentage ratio of the N-terminal  $\alpha$ -amino group content to the total protein content of the ham extract. Because of the high sensitivity of fluorometric detection, fluorescamine has been extensively used for the quantification of amino acids, peptides and proteins (Bantan-Polak, Kassai, & Grant, 2001; Castell, Cervera, & Marco, 1979; Friguet, Stadtman, & Szewda, 1994; Lorenzen & Kennedy, 1993; Miedel, Hulmes, & Pan, 1989). In this study, this fluorophore was used to evaluate the proteolysis of skeletal muscle myofibrillar proteins (Morzel, Gatellier, Sayd, Renner, & Laville, 2006).

The first objective of this study was to test the applicability of this procedure to the analysis of proteolysis in dry-cured ham at different stages of processing. For this purpose, determinations were performed in small laboratory samples of pork meat processed under well-defined salting and drying conditions, and in industrial dry-cured hams. The second objective was to compare this new procedure with the commonly used nitrogen content procedure and to establish an equation which allows converting the new proteolysis index to the classic one.

\* Corresponding author. Tel.: +33 473 62 41 98.

E-mail address: [pgatel@clermont.inra.fr](mailto:pgatel@clermont.inra.fr) (P. Gatellier).



## 2. Materials and methods

### 2.1. Preparation of the laboratory salted and dried pork meat samples

This preparation mimicked the different steps used in industry processing, but was adapted to small samples. Three different muscles, *biceps femoris* (BF), *semitendinosus* (ST), and *semimembranosus* (SM) from a single animal, were used in the preparation of the samples. pH<sub>24h</sub> were 5.8 for BF, 5.7 for ST, and 5.6 for SM. First, muscle surfaces were decontaminated by using 0.1% peracetic acid for 3 min followed by a 1 min rinse with sterile water. This operation was repeated twice. The muscle superficial layers damaged by the acid treatment were discarded, and samples were cut into small parallelepipeds (5×4×0.3 cm). These operations were performed under sterile air using sterile tools. The small pork meat samples were then salted by covering the surface of the piece with a 300 g.L<sup>-1</sup> NaCl solution using a multichannel pipette (Multipette plus, Eppendorf AG, Hamburg, Germany) adjusted to 4 µl per spot. In these conditions, salt diffused so as to achieve a homogenous distribution in a few hours. The quantity of salt added was calculated on the basis of the salt concentration (4% to 13% of the dry matter) and water content (50% to 75%) required in the final pork meat samples. The percentages of salt obtained in the different samples were always contained between the expected percentage, by -1% to +1%, and the mean values calculated on four samples were close to the expected ones. Drying was then performed at 15 °C for different times (up to 16 h for the driest samples) until each sample reached the weight corresponding to the selected water content. After checking the water content by determining the dry matter and salt content by chlorometry (MKII Chloride Analyser 926, Sherwood, Cambridge, UK), samples were placed under vacuum in plastic bags and kept in temperature-controlled chambers (Model 14 D-78532, Binder GmbH, Tuttlingen, Germany) at different temperatures (4 °C, 14.5 °C and 25 °C) to obtain various proteolysis kinetics. At the end of the processing, samples were stored at -80 °C until analysed. Four samples were prepared for each processing condition.

### 2.2. Preparation of the samples extracted from industrial dry-cured hams

PI determinations were performed on Bayonne dry-cured hams. Bayonne ham obtained a Protected Designation of Origin (PDO) certification in 1998 and its characteristics have been described by Robert and Lanore (2003). Three muscles (*biceps femoris*, *semitendinosus*, and *semimembranosus*) were extracted from three different hams at the end of each main processing stage, i.e. the resting period (11 weeks), drying period (21 weeks), and ageing period (12 months). Samples were taken from each muscle to calculate the new proteolysis index, allowing 24 determinations per muscle type per time (3 hams×8 samples). For the calculation of the classic proteolysis index, only one sample weighing about 50 g was taken from each muscle of the three hams. Some physical and chemical characteristics of these Bayonne hams (pH, water content and salt content) were determined (Table 1).

### 2.3. Determination of the new proteolysis index

Pork meat samples were placed for 1 h in cold water (0.7 g in 7 ml) to facilitate subsequent grinding. Extracts from the pork samples were prepared by homogenization with a Polytron PT-MR 2100 (Kinematica AG, Switzerland) for 30 s at maximum speed (30,000 rpm); 150 µl aliquots of the extract were then removed and diluted with 600 µl of 12.5% trichloroacetic acid to precipitate proteins (TCA final concentration 10%). Samples were shaken for 15 min at 4 °C. After centrifuging at 2000 g for 10 min, the concentration of peptides and amino acids in the

**Table 1**

Characteristics of the Bayonne dry-cured hams at the end of each main processing stage. Water and NaCl contents were calculated on the basis of the total and dry matter, respectively. Values were the means ± SEM of 3 determinations (one determination per muscle). Values not bearing common superscripts differ significantly ( $p < 0.05$ ).

		pH	Water content (%)	NaCl content (%)
11 weeks	SM	5.85 ± 0.05 a	69.8 ± 0.6 ab	2.67 ± 0.42 ab
	ST	5.95 ± 0.09 a	68.0 ± 0.1 a	4.63 ± 0.13 a
	BF	5.90 ± 0.04 a	71.6 ± 0.2 b	2.39 ± 0.28 b
21 weeks	SM	5.88 ± 0.11 a	61.1 ± 1.2 a	3.38 ± 0.47 a
	ST	5.87 ± 0.11 a	65.3 ± 1.0 ab	3.40 ± 0.54 a
	BF	5.95 ± 0.13 a	68.2 ± 0.5 b	3.72 ± 0.59 a
12 months	SM	5.68 ± 0.05 a	56.4 ± 1.0 a	4.94 ± 0.22 a
	ST	5.78 ± 0.03 a	57.2 ± 1.4 a	5.41 ± 0.26 a
	BF	5.83 ± 0.03 a	60.5 ± 0.7 a	5.72 ± 0.33 a

supernatant was measured by the method of Friguet et al. (1994) with slight modifications. First, 300 µl of the supernatant was neutralized with 300 µl of 2 M sodium borate, pH 10. In these conditions, the final pH of the solution was 9.2 ± 0.1, a value suitable for the reaction with fluorescamine. Secondly, 180 µl of fluorescamine (Sigma) at a concentration of 0.6 mg.ml<sup>-1</sup> in acetone was added. Free fluorescamine does not fluoresce, but its reaction with primary amines yields a fluorescent pyrolinone moiety. Fluorescence was measured 1 h after adding fluorescamine by means of a Perkin-Elmer LS 50B spectrofluorometer. A front surface accessory (Perkin Elmer Plate Reader) was installed for measurement in 96-well polystyrene microplates designed for fluorescence. A volume of 200 µl was placed in each well. Analyses were performed at the optimum excitation and emission wavelengths ( $\lambda_{\text{excitation}} = 375$  nm and  $\lambda_{\text{emission}} = 475$  nm) with excitation and emission slit setting to 10 nm. The non-specific fluorescence of corresponding fluorescamine-untreated samples was subtracted. The level of amino groups in the pork meat extracts was determined by reference to a calibration curve of glycine from 5 mM to 50 mM (concentration of the stock solution before TCA treatment) treated under exactly the same conditions and at the same time as the pork meat extracts. Fig. 1 shows that fluorescence increased linearly with glycine throughout the range of concentrations used ( $R^2 = 0.993$ ). The level of N-terminal  $\alpha$  amino groups was then expressed in grams of "glycine equivalent" per gram of ham (A). In parallel, the total protein content was estimated in the pork meat extract, before treatment, by the biuret method (Gornall, Bardawill, & David, 1949). Results were expressed in grams of protein per gram of ham (B). The new proteolysis index was then expressed as the percentage

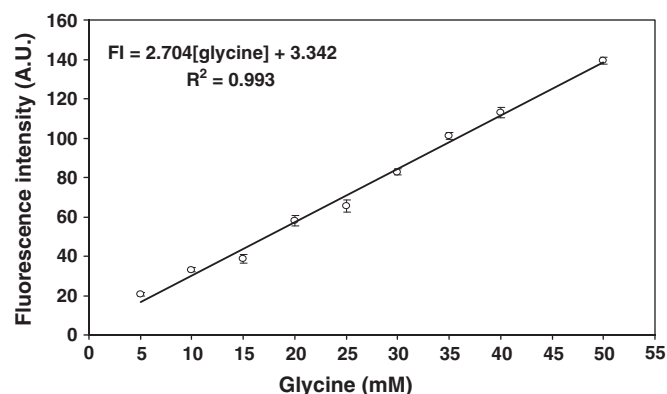


**Fig. 1.** Calibration curve of glycine with fluorescamine. Glycine concentrations were those of the initial stock solutions before the TCA treatment. Values were the means ± SEM of four independent determinations.

ratio of N-terminal  $\alpha$  amino group content to total protein content according to:

$$PI\% = (A/B) \times 100.$$

#### 2.4. Determination of the classic nitrogen proteolysis index

Total nitrogen (TN) was determined by the Kjeldahl method according to the ISO 937-1978(E) reference method, and non-protein nitrogen (NPN) content by precipitation of proteins with TCA followed by determination of nitrogen in the extract by the Kjeldahl method. The proteolysis index was determined as the percentage ratio of NPN to TN (Careri et al., 1993; Ruiz-Ramírez et al., 2006, Schivazappa et al., 2002).

#### 2.5. Statistics

ANOVA was performed at the end of the resting, drying and ageing periods to test the effects of the processing periods and muscle types on the PI values. When a significant effect was observed by ANOVA, the unpaired Student *t*-test was used to determine the statistical significance between groups.

### 3. Results

#### 3.1. Determination of the new proteolysis index in laboratory-dried and salted pork meat samples

The applicability of the new procedure to characterize proteolysis kinetics was tested first in different samples processed under well-defined salting and drying conditions. The use of small pork meat samples enabled the testing of a large number of conditions in muscles of a single animal, thus circumventing lack of reproducibility due to animal effect. In this case, PI variation cannot be produced by differences in raw material (protease activity, inhibitors, pH, etc.). Another advantage of reducing the product size is that rapid salt diffusion and drying, considerably shortens preparation time (16 h at the most). A large number of conditions (salting, drying, temperature, time, and muscle type) were tested, but the complete results will be presented and discussed in a forthcoming paper. The purpose of the present work was only to illustrate the potential of the new procedure for PI determination in a restricted number of conditions and in one muscle only.

The initial value of PI, measured in the *biceps femoris* muscle before processing, was very low (1.04%  $\pm$  0.33%). In Fig. 2 the time course of the PI in pork meat samples prepared from muscle *biceps*

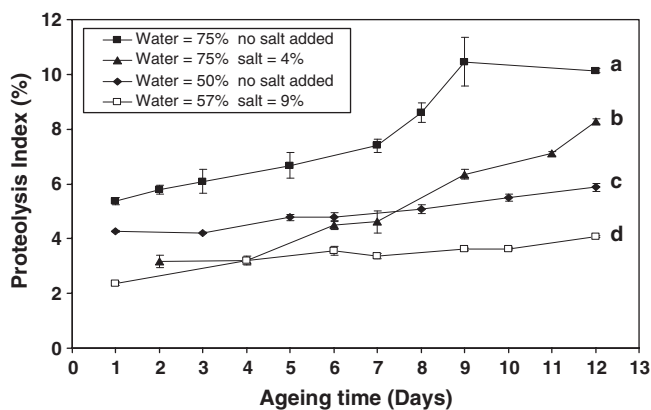


Fig. 2. Proteolysis kinetics in *M. Biceps femoris* at 25 °C under different processing conditions. Values were the means  $\pm$  SEM of four independent determinations. At the end of ageing, values not bearing common superscripts differ significantly ( $p < 0.001$ ).

*femoris* and stored under vacuum for 12 days at 25 °C is seen. The mean coefficient of variation (ratio of standard deviation to mean value) of this parameter calculated from all conditions was 5.3%, demonstrating the good reproducibility of the procedure. Fig. 2 shows that the untreated samples (75% water and no salt added) exhibited the highest proteolysis index. In this case PI reached a maximum of 10.5% after 9 days of ageing and remained stable for the following 3 days of ageing. Salting alone (to 4% of the dry matter) and drying alone (to 50% of water content) reduced the proteolysis intensity. This effect was much more pronounced when both salting and drying processes were applied (9% salt and 57% water). In this case a 60% decrease in PI value was observed after 12 days of ageing, compared with the untreated samples. After 12 days of ageing, the four conditions tested exhibited significant differences in PI values ( $p < 0.001$ ). At lower temperatures (14.5 °C and 4 °C), the PI increase was considerably reduced (data not shown). These results were in line with those generally reported in demonstrating a decrease in proteolysis activity with increasing salt content (Martín et al., 1998; Robert & Lanore, 2003; Ruiz-Ramírez et al., 2006) and with decreasing temperature (Martín et al., 1998; Robert & Lanore, 2003) or water content (Toldrá, Cerveró, & Part, 1993; Toldrá et al., 1997).

#### 3.2. Determination of the new proteolysis index in industrial dry-cured ham samples

The applicability of the new procedure to the characterization of proteolysis kinetics was then tested in more realistic conditions by measuring PI in industrial Bayonne hams over a 12-month period (Fig. 3). Probably owing to the animal effect, the mean coefficient of variation of PI, calculated over the whole conditions, was higher than calculated in laboratory-dried and salted pork meat samples derived from the same animal (19.6% vs. 5.3%). To characterize the kinetics of proteolysis, the increase in PI with time was fitted by a second-order polynomial regression. Despite the biological variability, good correlation coefficients were obtained from the different curves ( $R^2 > 0.99$ ). As seen in Fig. 3, the three muscles tested can be ranked in order of increasing proteolysis speed: BF > SM > ST. BF and SM did not display any significant differences in terms of proteolysis intensity, while proteolysis in ST was always lower than in BF and SM. In the case of the BF muscle, a proteolysis increase of 2200% was observed during the overall period and of 55% during the ageing period only. These results were in line with those of Zhao et al. (2008), who reported a PI increase in BF muscle of 60% during the last 7 months of ageing. Ruiz-Ramírez et al. (2006) and Toldrá et al. (1997) also reported higher proteolysis in BF than in SM muscle. Like these authors, the higher proteolysis in the BF muscle can be

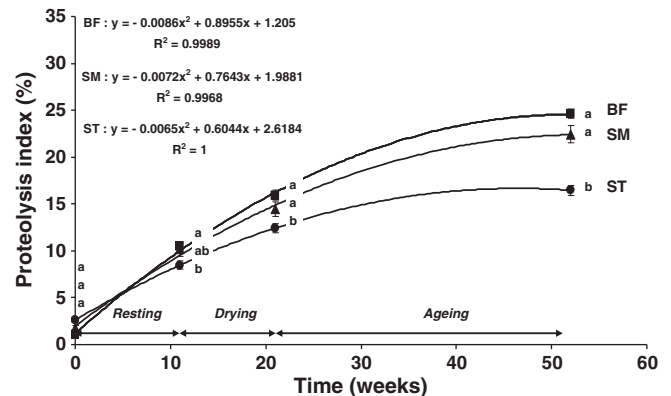


Fig. 3. Proteolysis kinetics in three muscles of different Bayonne dry-cured hams. The zero time values corresponded to PI in the unsalted raw meats. Values were the means  $\pm$  SEM of 24 determinations. Values not bearing common superscripts differ significantly ( $p < 0.05$ ).

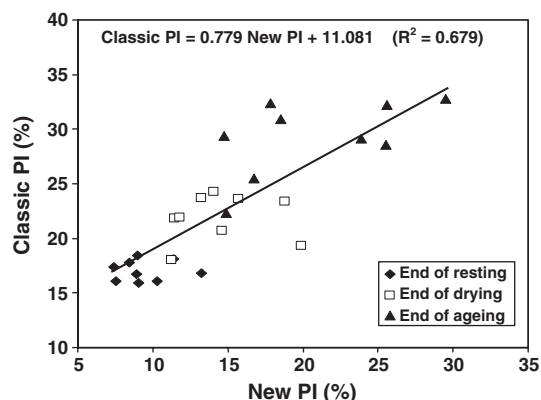


Fig. 4. Relationship between the classic proteolysis index (nitrogen index) and the new proteolysis index (fluorescamine index).

attributed to its higher residual moisture content (Table 1), which allows a higher activity of endogenous proteases. Differences between SM and ST muscles could be explained by the fact that for similar water content, ST muscle had higher salt contents (Table 1).

### 3.3. Relationship between the classic and the new proteolysis indices

Most of the data on dry-cured ham proteolysis have been gained with the classic nitrogen proteolysis index, and so industrial operators use this index routinely. Hence although we have demonstrated the applicability of this new procedure in different conditions has been demonstrated and its many advantages compared with the classic procedure (Section 4. discussion), to be accepted in the dry-cured ham industry, the new proteolysis index must be easily convertible into the classic index. For this purpose, a conversion equation was established by comparison of the two indices in these same Bayonne hams at the end of the resting, drying and ageing periods. Fig. 4 shows the relation between the two PIs. The relationship was well fitted with a linear regression model:

$$PI_{\text{classic}} = 0.779PI_{\text{new}} + 11.081 \quad (r = 0.824, p < 0.001)$$

Clearly, this conversion formula is valid only so long as the determinations are performed in the conditions described above (Sections 2.3 and 2.4). Other protocols will require new formulas.

## 4. Discussion

This new procedure of PI determination offers many advantages over the classic nitrogen procedure. The fluorometric detection lends it a high sensitivity, which allows work on very small product quantities. Samples of 0.7 g were used in the present study, but we have successfully tested this procedure with smaller quantities of meat (less than 0.1 g, data not shown). Using this procedure, dry-cured hams could be tested during industrial fabrication by punching a small hole in the muscle, without depreciation of the products. In addition, the procedure is rapid; the use of a microplate reader allows fluorescence measurement of 96 samples in less than 1 min. The limiting factor in the procedure is the muscle extract preparation, but with trained personnel more than 50 determinations can be performed daily. This procedure also offers high specificity; fluorescamine does not react with the major non-protein nitrogenous substances commonly present in muscle, i.e. urea, uric acid, creatinine and ammonia (Klein & Standaert, 1976). Fluorescamine can react with the  $\epsilon$ -amino groups of lysine (Dhaunta, Fatima, & Guptasarma, 2011), which are not specific products of proteolysis. To avoid this, conditions were chosen such that the reaction of fluorescamine with amino groups was specific for adduction of fluorescamine only to the N-terminal  $\alpha$ -amino groups.

The reaction with fluorescamine requires the amino group to be in its unprotonated form (Bantan-Polak et al., 2001; Bohlen, Stein, & Udenfriend, 1974; Castell et al., 1979; Mendez & Gavilanes, 1976). Since the  $pK_a$  of the N-terminal  $\alpha$ -amino groups of peptides (8.0) is lower than the  $pK_a$  of lysine  $\epsilon$ -amino groups (10.8) (Berg, Tymoczko, & Stryer, 2007), conjugation of the label to the lysine compared with the N-terminal  $\alpha$ -amino groups was minimised by performing the labelling reaction at pH 9.2; using the Henderson equation, at pH 9.2, 94% of the N-terminal  $\alpha$ -amino groups were in the reactive unprotonated form ( $NH_2$ ), while the  $\epsilon$ -amino groups of lysine were almost entirely (98%) in the non-reactive protonated form ( $NH_3^+$ ). It was for that very reason that in peptides containing lysine residues, Dhaunta et al. (2011) failed to detect any evidence of labelling of this residue with fluorescamine in the pH range 8.0 to 10.0. Also, fluorescamine does not react with secondary amines such as the amino groups of histidine and arginine side chains (Dhaunta et al., 2011; Weigele, De Bernardo, Tengi, & Leimgruber, 1972). Finally, it may be safely asserted that the new procedure is more powerful than the classic procedure in that it describes the progress of the proteolytic activity more finely. For example, in the case of the complete degradation of a decapeptide, the classic procedure cannot discriminate between the decapeptide containing 10 nitrogen atoms and the sum of the 10 corresponding amino acids each containing one nitrogen atom. In such a case, the PI remains unchanged. By contrast, the new procedure distinguishes between the decapeptide (one N-terminal  $\alpha$ -amino group) and the corresponding amino acids (10 N-terminal  $\alpha$ -amino groups). In this case the PI is multiplied by ten.

## 5. Conclusion

Based on these results, the fluorescamine-specific labelling of the N-terminal  $\alpha$ -amino groups of peptides and amino acids offers a powerful technique to determine proteolysis intensity in dry-cured ham. This procedure is more rapid and more specific than the classic nitrogen procedure. The easy conversion of PI values obtained with this new procedure into the classic PI values allows the fluorescamine method to be used directly in industry as a reference method for PI determination in dry-cured hams.

## Acknowledgments

This work was funded by the Na-integrated programme (ANR-09-ALIA-013-01) financed by the French National Research Agency. We thank H. Safa for participating in some of the laboratory work, S Portanguen, L. Aubry and J.D. Daudin for discussing the protocol of preparation of the laboratory pork meat samples, ADIV for measuring the classic PI in industrial Bayonne ham samples, and ATT for language editing.

## References

- Arnau, J., Gou, P., & Comaposada, J. (2003). Effect of the relative humidity and drying air during the resting period on the composition and appearance of dry-cured ham surface. *Meat Science*, 65, 1275–1280.
- Arnau, J., Gou, P., & Guerrero, L. (1994). The effect of freezing, meat pH, and storage temperature on the formation of white film and tyrosine crystals in dry-cured ham. *Journal of the Science of Food and Agriculture*, 66, 279–282.
- Arnau, J., Guerrero, L., & Gou, P. (1997). Effects of temperature during the last month of ageing and of salting time on dry-cured ham aged for six months. *Journal of the Science of Food and Agriculture*, 74, 193–198.
- Arnau, J., Guerrero, L., Maneja, E., & Gou, P. (1992). Effect of pH and genetics on texture characteristics of dry cured ham. *38th ICOMST* (pp. 229–232).
- Arnau, J., Guerrero, L., & Sárraga, C. (1998). The effect of green ham pH and NaCl concentration on cathepsin activities and sensory characteristics of dry-cured ham. *Journal of the Science of Food and Agriculture*, 77, 387–392.
- Bantan-Polak, T., Kassai, M., & Grant, K. B. (2001). A comparison of fluorescamine and naphthalene-2,3-dicarboxaldehyde fluorogenic reagents for microplate-based detection of amino acids. *Analytical Biochemistry*, 297, 128–136.
- Berg, J. M., Tymoczko, J. L., & Stryer, L. (2007). *Biochemistry* (6th ed.). New York, NY: W.H. Freeman and Company.

- Bohlen, P., Stein, S., & Udenfriend, S. (1974). Studies on the reaction of fluorescamine with primary amines. *Archives of Biochemistry and Biophysics*, 163, 390–399.
- Careri, M., Mangia, A., Barbieri, G., Bolzoni, L., Virgili, R., & Parolari, G. (1993). Sensory property relationships to chemical data of Italian dry-cured ham. *Journal of Food Science*, 58, 968–972.
- Castell, J. V., Cervera, M., & Marco, R. (1979). A convenient micromethod for assay of primary amines and proteins with fluorescamine: a re-examination of the conditions of reaction. *Analytical Biochemistry*, 99, 379–391.
- Dhaunta, N., Fatima, U., & Guptasarma, P. (2011). N-Terminal sequencing by mass spectrometry through specific fluorescamine labelling of  $\alpha$ -amino groups before tryptic digestion. *Analytical Biochemistry*, 408, 263–268.
- Friguet, B., Stadtman, E. R., & Szewda, L. I. (1994). Modification of glucose-6-phosphate dehydrogenase by 4-hydroxy-2-nonenal. Formation of cross-linked protein that inhibits the multicatalytic protease. *Journal of Biological Chemistry*, 269, 21639–21643.
- García-Garrido, J., Quiles-Zafra, R., Tapiador, J., & Luque de Castro, M. (2000). Activity of cathepsin B, D, H and L in Spanish dry-cured ham of normal and defective texture. *Meat Science*, 56, 1–6.
- Gornall, A. G., Bardawill, C. J., & David, M. M. (1949). Determination of serum proteins by means of biuret reaction. *Journal of Biological Chemistry*, 177, 751–766.
- Klein, B., & Standaert, F. (1976). Fluorimetry of plasma amino nitrogen, with the use of fluorescamine. *Clinical Chemistry*, 22, 413–416.
- Lorenzen, A., & Kennedy, S. W. (1993). A fluorescent-based protein assay for the use with a microplate reader. *Analytical Biochemistry*, 214, 346–348.
- Martin, L., Córdoba, J. J., Antequera, T., Timon, M. L., & Ventanas, J. (1998). Effects of salt and temperature on proteolysis during ripening of iberian ham. *Meat Science*, 49, 145–153.
- Mendez, E., & Gavilanes, J. G. (1976). Fluorimetric detection of peptides after column chromatography or on paper: o-phthalaldehyde and fluorescamine. *Analytical Biochemistry*, 72, 473–479.
- Miedel, M. C., Hulmes, J. D., & Pan, Y. C. E. (1989). The use of fluorescamine as a detection reagent in protein microcharacterization. *Journal of Biochemical and Biophysical Methods*, 18, 37–52.
- Morzell, M., Gatellier, Ph., Sayd, T., Renner, M., & Laville, E. (2006). Chemical oxidation decreases proteolytic susceptibility of skeletal muscle myofibrillar proteins. *Meat Science*, 73, 536–543.
- Robert, N., & Lanore, D. (2003). Une mine d'éléments essentiels. Le jambon de Bayonne. *Viandes et Produits Carnés*, 23, 97–101.
- Ruiz-Ramírez, J., Arnau, J., Serra, X., & Gou, P. (2006). Effect of pH 24, NaCl content and proteolysis index on the relationship between water content and texture parameters in biceps femoris and semimembranosus muscle in dry-cured ham. *Meat Science*, 72, 185–194.
- Schivazappa, C., Degni, M., Nanni-Costa, L., Russo, V., Buttazzoni, L., & Virgili, R. (2002). Analysis of raw meat to predict proteolysis in Parma Ham. *Meat Science*, 60, 77–83.
- Toldrá, F., Cerveró, M. C., & Part, C. (1993). Porcine aminopeptidase activity as affected by curing agents. *Journal of Food Science*, 58, 724–726.
- Toldrá, F., & Flores, M. (2000). The use of muscle enzymes as predictor of pork meat quality. *Food Chemistry*, 69, 387–395.
- Toldrá, F., Flores, M., & Sanz, Y. (1997). Dry-cured ham flavour: enzymatic generation and process influence. *Food Chemistry*, 59, 523–530.
- Virgili, R., Parolari, G., Schivazappa, C., Bordini, C. S., & Borri, M. (1995). Sensory and texture quality of dry-cured ham as affected by endogenous cathepsin B activity and muscle composition. *Journal of Food Science*, 60, 1183–1186.
- Weigele, M., De Bernardo, S. L., Tengi, J. P., & Leimgruber, W. (1972). Novel reagent for the fluorimetric assay of primary amines. *Journal of the American Chemical Society*, 94, 5927–5928.
- Zhao, G. M., Tian, W., Liu, Y. X., Zhou, G. H., Xu, X. L., & Li, M. Y. (2008). Proteolysis in biceps femoris during Jinhua ham processing. *Meat Science*, 79, 39–45.



**Annexe II :**

**Harkouss, Safa, Gatellier, Lebert & Mirade (2014).**

***Food Chemistry, 151, 7-14***







## Building phenomenological models that relate proteolysis in pork muscles to temperature, water and salt content



Rami Harkouss<sup>a</sup>, Hassan Safa<sup>a</sup>, Philippe Gatellier<sup>a</sup>, André Lebert<sup>b</sup>, Pierre-Sylvain Mirade<sup>a,\*</sup>

<sup>a</sup> INRA, UR370 Qualité des Produits Animaux, F-63122 Saint-Genès-Champanelle, France

<sup>b</sup> Institut Pascal, UMR6602 UBP/CNRS/IFMA, 24 avenue des Landais, BP80026, 63171 Aubière Cedex, France

### ARTICLE INFO

#### Article history:

Received 29 July 2013

Received in revised form 23 October 2013

Accepted 30 October 2013

Available online 13 November 2013

#### Keywords:

Proteolysis

Pork muscle

Water and salt content

Temperature

Doehlert design

Response surface methodology

Multiple linear regression

### ABSTRACT

Throughout dry-cured ham production, salt and water content, pH and temperature are key factors affecting proteolysis, one of the main biochemical processes influencing sensory properties and final quality of the product. The aim of this study was to quantify the effect of these variables (except pH) on the time course of proteolysis in laboratory-prepared pork meat samples. Based on a Doehlert design, samples of five different types of pork muscle were prepared, salted, dried and placed at different temperatures, and sampled at different times for quantification of proteolysis. Statistical analysis of the experimental results showed that the proteolysis index (PI) was correlated positively with temperature and water content, but negatively with salt content. Applying response surface methodology and multiple linear regressions enabled us to build phenomenological models relating PI to water and salt content, and to temperature. These models could then be integrated into a 3D numerical ham model, coupling salt and water transfers to proteolysis.

© 2013 Elsevier Ltd. All rights reserved.

### 1. Introduction

During dry-cured ham production, the main biochemical mechanism affecting the tenderization of meat and the quality of the final product (texture, flavour and appearance) is proteolysis, resulting from the action of proteolytic endogenous enzymes, such as cathepsins and calpains, which remain active for a long time (Arnau, Guerrero, & Sárraga, 1998; Garcia-Garrido, Quiles-Zafra, Tapiador, & Luque De Castro, 2000; Tabilo, Flores, Fisman, & Toldra, 1999; Toldrá & Etherington, 1988; Toldrá & Flores, 2000; Virgili, Parolari, Schivazappa, Bordini, & Borri, 1995; Zhao et al., 2008). A literature review showed that many factors influence proteolytic activity, such as temperature, salt content, water content and pH. The effect of temperature has been described in previous studies (Arnau, Guerrero, & Gou, 1997; Parolari, Virgili, & Schivazappa, 1994, among others). Morales, Serra, Guerrero, and Gou (2007) showed that letting biceps femoris (BF) muscle age at 30 °C increased PI significantly compared with hams aged at 5 °C. It is well known that temperature rise promotes cathepsin B and L activity and it has been observed that high temperatures during the drying-ageing stage favour the formation of non-protein nitrogen compounds, which increases PI. However, at the same time, a high enzyme activity results in uncontrolled hydrolysis, leading to

an anomalous texture or even an undesirable colour in the product. The effect of NaCl content has also been widely demonstrated (Garrido, Domínguez, Lorenzo, Franco, & Carballo, 2012; Rico, Toldrá, & Flores, 1991; Sárraga, Gil, Arnau, Monfort, & Cussó, 1989). Studies report that PI increases in hams as salting time is shortened. A high concentration of NaCl may inhibit the enzymes responsible for proteolytic activity. For example, cathepsin D, the most active cathepsin throughout the dry-curing of ham, loses more than 70% of its activity at a salt concentration of 5%. However, the reduction of salt may pose a major problem in terms of colour formation and stability, as reported by Benedini, Parolari, Toscani, and Virgili (2012). High salt concentration significantly affected the yellow colour of fat as a result of a high rate of autoxidation, and the red colour of meat as a result of greater penetration of nitrate and nitrite, generating nitrosomyoglobin, responsible for the characteristic pink colour of cured meats. Martin, Cordoba, Antequera, Timon, and Ventanas (1998) related pasty texture to the amount of salt adsorbed during the salting stage. Garrido et al. (2012) also related increased hardness of meat to an increase in salt content. Studies have often found a relation between salt concentration and water content, another factor affecting proteolysis and texture. High water content increased water activity ( $a_w$ ) and in turn, the proteolytic activity. Serra, Ruiz-Ramirez, Arnau, and Gou (2005) highlighted a negative non-linear relationship between hardness and water content, but a positive relationship with cohesiveness and springiness. Time is also important for proteolysis. Some

\* Corresponding author. Tel.: +33 473624592; fax: +33 473624089.

E-mail address: [pierre-sylvain.mirade@clermont.inra.fr](mailto:pierre-sylvain.mirade@clermont.inra.fr) (P.-S. Mirade).

studies have shown that one month storage at 30 °C augments proteolysis, thereby increasing the pastiness of BF muscle (Arnaud et al., 1997), whereas at the same temperature after one week, pastiness, adhesiveness and softness decrease in BF, without obviously affecting  $a_w$  or proteolysis (Morales et al., 2007). Finally, the activity of proteases, like that of all enzymes, depends on an optimal pH. In dry-cured ham, since the pH rarely exceeds 6.2, only proteases acting in slightly acid pH will be active, such as cathepsins B, D, H and L (Garcia-Garrido, Quiles-Zafra, Tapiador, & Luque De Castro, 2000). By contrast, several studies found greater hardness in hams with  $pH_{24} < 5.8$  than in hams with  $pH_{24} > 6.2$ , whereas others highlighted harder dry-cured hams with  $pH_{24}$  between 5.6 and 6 than with  $pH_{24} < 5.6$  (Arnaud et al., 1998). In addition to these physico-chemical factors (pH, temperature, water and salt content), the type of muscle may also affect the time course of proteolysis during the ham dry-curing process, since the percentage of myofibrillar and sarcoplasmic proteins differs from one muscle to another. Studies have reported that the above factors act on proteolysis in meat. However, the interaction between these factors has not yet been elucidated. Also, no study describes the time course of proteolysis as a function of temperature, salt content, water content and muscle type.

Response surface methodology (RSM) is commonly defined as a collection of mathematical and statistical techniques that explore the relationships between several independent variables, termed input or explanatory variables, and one or more response (or output) variables. RSM is generally based on fitting a polynomial equation to the experimental data obtained through a designed sequence of experiments. Many applications of RSM can be found in the literature, e.g., in analytical chemistry (Bezerra, Santelli, Oliveira, Villar, & Escalera, 2008), and in meat science. For example, Zhao et al. (2005) evaluated the effects of temperature, salt content, pH and nitrite content on the activities of cathepsin B and L, using RSM based on a Box-Behnken design, and calculated the actual activities of these cathepsins during Jinhua ham processing. Jakobsen, and Bertelsen (2000) developed a response surface model to predict the effects of temperature, storage time and oxygen partial pressure on the colour stability and lipid oxidation of fresh beef muscle. They concluded that RSM was a very promising tool for modelling chemical quality changes in meat stored under various conditions, providing that the broad biological variability among animals could be controlled. From the combined use of a RSM approach and a full factorial design with six factors, Møller et al. (2003) found that the interactions between packaging and storage conditions were crucial to limiting light-induced oxidative discoloration of cured ham packaged in a modified atmosphere during the 14 days of chill storage. More recently, Jin et al. (2012) used RSM coupled with central composite design to investigate the effects of temperature (from 15 to 35 °C) and sodium chloride content (from 0.5% to 4.0%) on lipid oxidation in minced pork muscle, demonstrating that both temperature and NaCl content had significant pro-oxidant effects, and also extremely significant interaction for lipid oxidation.

In the present study, RSM was investigated in a way similar to that detailed in Zhao et al. (2005) and Jin et al. (2012) to spotlight the interactive effect of the different factors affecting proteolysis time course in dry-cured ham, and so build phenomenological models that map proteolysis throughout the process. The objective of this study was to quantify the effects of salt content, temperature, water content and muscle type, together with their interactions, on proteolytic activity in laboratory-prepared, dried, salted small pork meat samples, and thereby to determine models to quantify PI as a function of these factors. In future work, these models could be incorporated into a global finite-element model coupling salt and water transfers with proteolysis in a 3D “numerical” ham that is cured and dried for several months.

## 2. Materials and methods

### 2.1. Preparation of the laboratory pork meat samples

This study required a very large number of pork meat samples to be prepared rapidly under pre-defined, accurate temperature, salt content and moisture values. To do this, we decided to work from fresh pork muscles rather than from samples taken directly from dry-cured hams, from which it is very difficult to obtain samples with the desired salt and water content.

Fig. 1 details the experimental protocol followed to prepare and condition the small salted and/or dried pork meat samples, before quantifying proteolysis. Every stage in this figure, i.e., decontamination, cutting, salting, drying and proteolysis quantification, required much preliminary experimental work to determine the best way to proceed. Eight fresh hams of average weight  $10.6 \pm 0.75$  kg were selected at a local slaughterhouse. Five different muscles, biceps femoris (BF), semitendinosus (ST), semimembranosus (SM), rectus femoris (RF) and gluteus medius (GM) were extracted from each ham four days *post mortem*. Their moisture content and pH were respectively,  $74.7 \pm 1.7\%$  and  $5.74 \pm 0.13$ . Entire muscles were vacuum-packed in plastic bags, frozen in an ultra-low temperature freezer (Bio Memory, Froilabo) at  $-80$  °C and stored for later use. Muscle surfaces were decontaminated twice under an extractor fan by treatment with 0.1% peracetic acid for 3 min followed by 1 min rinsing-out with sterile water. Samples were then cut into small slabs ( $5 \times 4 \times 0.3$  cm) after discarding the superficial muscle layers damaged by the acid treatment. These operations were performed under sterile air conditions using sterile tools. Samples were prepared so as to obtain a final mass greater than 5 g per sample in order to perform all the biochemical tests; samples were then vacuum-packed in bags and frozen at  $-80$  °C until needed. The small pork meat samples were then thawed and salted by covering the surface of the piece with a  $300 \text{ g L}^{-1}$  NaCl solution using a pipette (Eppendorf AG, multipette plus, Hamburg, Germany) adjusted to  $4 \mu\text{l}$  per spot. The thinness of the samples allowed the salt to diffuse rapidly, in a few hours, and homogeneously. The quantity of salt added was calculated on the basis of the salt concentration (1–15% of the dry matter – DM) and the water content (50–75% of the total matter – TM) required in the final pork meat sample. The uncertainty of salting of these small pork meat samples was evaluated from preliminary experiments; it was found to range from 0.1% DM for the least salted (1.1% DM) samples to 0.8% DM for the most salted (14.9% DM) samples. The next step was drying; this was carried out under sterile air conditions at 15–16 °C for different periods of time (up to 22 h for the most thoroughly dried samples) until each sample reached the weight corresponding to the selected water content. Applying this simple procedure allowed the uncertainty of drying to be maintained below 1% TM, whatever the final desired water content (from 56.3% to 68.5% TM). Samples were then vacuum-packed in plastic bags and kept in controlled-temperature chambers (Model 14 D-78532, Binder GmbH, Tuttlingen, Germany) at various temperatures (3, 13 and 24 °C) in order to study the proteolysis kinetics.

Preliminary tests gave an estimation of 35, 25 and 13 days, respectively, for the shelf-life of these small samples at these three temperatures, without observing any microbiological growth, so that only proteolysis resulting from endogenous enzyme activity occurred, i.e. that taking place inside hams during the drying and curing processes, and not the degrading action of some microorganisms, which leads to an exponential increase in PI and an increasingly unbearable odour. Once prepared, the samples were finally stored at  $-80$  °C before final analysis (PI, salt and water contents). Four samples were prepared for each processing condition.

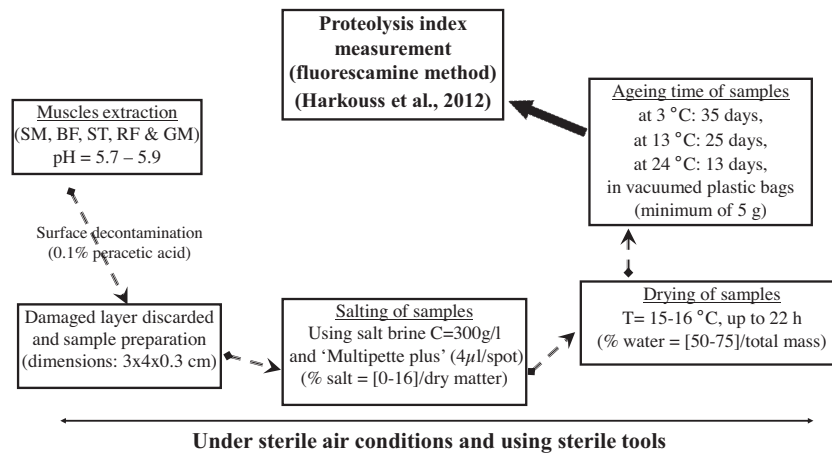


Fig. 1. Experimental protocol for laboratory preparation of the pork meat samples used in this study to determine proteolysis rates.

## 2.2. Quantification of the proteolysis

In parallel to the preparation of the laboratory pork meat samples, to cope with the large number of samples to be analysed, a rapid, accurate, fluorometry-based procedure was developed to determine sample PI. In this procedure, the new PI is defined as the percentage of the ratio of the N-terminal  $\alpha$ -amino group content (A) to the total protein content (B). The content (A), which reflects the real intensity of proteolytic activity occurring during the process, was measured by the fluorescamine method (Harkouss, Mirade, & Gatellier, 2012), and content (B) by the biuret method (Gornall, Bardawill, & David, 1949). This procedure is more rapid, more specific and more economical in raw materials than classical methods, e.g., the classic nitrogen method, and could also be easily used in industry. Full information on this powerful technique can be found in Harkouss et al. (2012).

Preliminary tests of quantification of proteolysis performed on some small laboratory-prepared pork meat samples revealed that over the periods of time investigated (i.e., 13, 25 and 35 days, depending on temperature) proteolysis kinetics could be approximated by straight lines, and thus characterised by a slope representing a rate of protein degradation.

## 2.3. Response surface methodology and Doehlert design

In the present study, a response surface methodology based on a Doehlert design was used to investigate the interaction between temperature, water and salt content on the proteolysis time course in small laboratory pork meat samples, with the final objective of building phenomenological models allowing proteolysis to be quantified in pork muscles as a function of these factors.

A Doehlert design (Doehlert, 1970) was implemented on the basis of three factors for each muscle: temperature, water content and salt content. This particular design offers a uniform distribution of points over the whole experimental region, arranged in a rhomboidal figure. In the case of three-variable designs, a cuboctahedron is produced geometrically. It is important to note that in a Doehlert design, the number of levels is not the same for all variables: in a three-factor problem, the first factor is studied at three levels, the second at five levels and the third at seven levels. Although pH is also a key factor for the proteolysis time course, pH was not included in the present Doehlert design. The pH of green muscles had been previously measured and found to range between 5.6 and 5.9. The selection of the independent variables and their levels was made in accordance with values commonly found in industrial production of dry-cured ham. The different

levels of each factor were chosen as: five levels for water content, centred at 62.5% (50–75% TM), seven levels for salt content, centred at 8% (0–16% DM) and three levels for temperature, centred at 13 °C (approximately 2 to 26 °C). This design allowed the number of manipulations to be decreased from 105 to 13 experiments per muscle (Table 1). Also, the centre of this experimental design was repeated twice to take into account animal variability; at this particular design point, kinetics of proteolysis were recorded on ten small samples prepared from muscles belonging to a different animal each time. Finally, 15 proteolysis kinetics were determined for each muscle, with 10 points (samples) per plot and four measurements per sample, i.e., a total of 3000 experimental proteolysis quantification items for all five muscles.

For each muscle investigated, the quadratic polynomial regression equation was taken as given by RSM:

$$Y = \alpha_0 + \sum \alpha_i X_i + \sum \alpha_{ii} X_{ii}^2 + \sum \sum \alpha_{ij} X_i X_j + \lambda_i, \quad (1)$$

where  $Y$  is the response variable (proteolysis),  $\alpha_0$  is the constant coefficient (intercept),  $\alpha_i$  is the linear coefficient,  $\alpha_{ii}$  is the quadratic coefficient,  $\alpha_{ij}$  is the two-factor interaction coefficient, and  $\lambda_i$  is the random error. Eq. (1) describes the linear, quadratic and interaction effects of the three variables  $T$  (temperature),  $W$  (water content) and  $S$  (salt content) on the response value (proteolysis rate).

## 2.4. Statistical analysis

All statistical analyses were performed using R 3.0.1 software (R Development Core Team, 2013), the statistical packages 'car' (Fox & Weisberg, 2011), 'HH' (Heiberger, 2013), 'leaps' (Lumkey, 2009) and the graphical package 'rgl' (Adler & Murdoch, 2013). A three-way analysis of variance (ANOVA) was performed on all the proteolysis kinetics obtained for the five muscles ST, SM, BF, RF and GM. The objective was to assess the effect of each factor (temperature, water and salt content) on PI. The effect of muscle type was also studied. *Post hoc* procedures were used when the  $F$ -test was significant ( $p < 0.05$ ). Multiple comparisons among means were examined by the Fisher's least significant difference (LSD) test, for temperature, water and salt content. Multiple linear regressions were performed in order to find the best model of proteolysis time course as a function of the factors studied for each muscle, and their interactions. As advocated by Fox, and Weisberg (2011), regression diagnostics such as 'Component+Residual' plots were performed to investigate non-linearity problems, hat values, Studentized residuals and Cook's distances to identify outlier points, and finally model factors selection by exhaustive search, forward or backward stepwise, or sequential replacement (Mallows's  $C_p$

**Table 1**  
Details of the Doehlert design built and results of proteolysis rate obtained as a function of pork muscle type (SM: semimembranosus, BF: biceps femoris, ST: semitendinosus, RF: rectus femoris and GM: gluteus medius).

List of experiments of Doehlert design	Temperature (°C)	Salt content (% dry matter)	Water content (% total mass)	Muscle SM (% PI/day)	Muscle BF (% PI/day)	Muscle ST (% PI/day)	Muscle RF (% PI/day)	Muscle GM (% PI/day)
Exp. 1a (centre)	13	8.0	62.5	0.09	0.06	0.10	0.09	0.06
Exp. 1b (centre)	13	8.0	62.5	0.10	0.07	0.09	0.09	0.05
Exp. 1c (centre)	13	8.0	62.5	0.09	0.08	0.08	0.10	0.07
Exp. 1 (mean)	13	8.0	62.5	0.09	0.07	0.09	0.09	0.06
Exp. 2	13	8.0	75.0	0.08	0.10	0.13	0.22	0.08
Exp. 3	13	14.9	68.5	0.11	0.11	0.10	0.10	0.08
Exp. 4	24	10.3	68.5	0.31	0.17	0.26	0.37	0.35
Exp. 5	13	8.0	50.0	0.05	0.06	0.05	0.06	0.05
Exp. 6	13	1.1	56.3	0.06	0.08	0.08	0.13	0.08
Exp. 7	3	5.7	56.3	0.04	0.04	0.05	0.06	0.04
Exp. 8	13	1.1	68.5	0.13	0.12	0.16	0.19	0.13
Exp. 9	3	5.7	68.5	0.03	0.06	0.08	0.12	0.06
Exp.10	13	14.9	56.3	0.02	0.05	0.04	0.02	0.03
Exp. 11	3	12.6	62.5	0.04	0.05	0.09	0.04	0.04
Exp. 12	24	10.3	56.3	0.12	0.18	0.13	0.24	0.17
Exp. 13	24	3.4	62.5	0.25	0.21	0.33	0.27	0.35

and Schwartz's information criterion: BIC). Using the previous models, the response surface of proteolysis rate was plotted in 3D as a function of temperature, salt and water content.

### 3. Results and discussion

#### 3.1. Time course of proteolysis at low temperature (3 °C)

Results confirmed that the proteolysis time course could be described linearly with time ( $R^2 \geq 0.93$ ) in the laboratory-prepared pork meat samples, at 3 °C. In general, at this temperature protein degradation of the different muscles was very slow ( $0.06 \pm 0.02\%$  PI/day). Similar results were obtained by Costa-Corredor, Serra, Arnau, and Gou (2009), who indicated that increasing post-resting temperature to above 5 °C reduced processing time. Hence at low temperature, proteolysis needs more time to progress. In the present study, at 3 °C, the proteolysis indices were generally low; more than 35 days being required to increase PI from  $2.97 \pm 0.59\%$  to  $4.95 \pm 0.99\%$ . The same results have been reported in several previous studies, thus confirming that PI at low temperature ( $\leq 5$  °C) is lower than at higher temperatures (Martin et al., 1998). Fig. 2a shows that there was also a slight effect of drying on proteolytic activity of the enzymes, clearly visible from day 20 (Fig. 2a). Similar results were reported by Toldra (2006) in his review, denoting that drying decreased water activity values, which affected the muscle proteolytic enzymes activity. The averages of proteolysis kinetics slopes for all muscle types at 5.7% DM salt content, and 68.5% TM and 56.3% TM water content were  $0.07 \pm 0.03\%$  PI/day and  $0.05 \pm 0.01\%$  PI/day, respectively (Experiments 7 and 9, Table 1). This could be because at low temperature there is not enough energy to sufficiently activate the enzymes (cathepsins, calpains, etc.) responsible for protein degradation. Unfortunately, the effect of salt at 3 °C could not be investigated directly from graph analysis because the Doehlert design did not provide for experiments at this temperature (Table 1). The interpretation of salt effect will therefore be discussed later when analysing the 3D response surface plots. The overall conclusion is that all muscles behaved in approximately the same way at 3 °C in terms of the proteolysis time course.

#### 3.2. Time course of proteolysis at moderate temperature (13 °C)

As at low temperature, proteolysis index increased markedly and linearly with time ( $R^2 \geq 0.95$ ), at 13 °C (Fig. 2b). Generally,

the progress of proteolysis at moderate temperature was faster and stronger than at low temperature; the average of slopes of all the muscle proteolysis kinetics at 13 °C were globally higher than at 3 °C ( $0.11 \pm 0.04\%$  PI/day), except for kinetics with high salt content combined with low water content, where low values of slope were obtained, e.g., for the 14.9% DM salt-56.3% TM water curve in Fig. 2b (Experiment 10, Table 1). When pork meat samples were weakly dried and salted (i.e., the 1.1% DM salt-68.5% TM water curve of Fig. 2b corresponding to Experiment 8 in Table 1), measurements showed that values of PI could double in 25 days. Unlike experiments performed at low temperature, proteolysis kinetics recorded at 13 °C allowed simultaneous assessment of the effect of drying and salting on the time course of proteolysis owing to the high number of proteolysis kinetics plotted at this temperature (Experiments 1–3, 5–6, 8 and 10 in Table 1). Analysing Fig. 2b, which shows the time course of three different proteolysis kinetics in the case of ST muscle, allows these effects to be assessed. Comparing the 1.1% DM salt-68.5% TM water curve with the 1.1% DM salt-56.3% TM water curve of Fig. 2b shows that a 12% increase in drying in weakly salted pork meat samples clearly slowed down protein degradation, and the proteolysis rate decreased from 0.14% to 0.08% PI/day. Costa-Corredor, Muñoz, Arnau, and Gou (2010) reported similar results, which could be explained by the inhibitive effect of drying on proteolytic enzymes, leading to a slowed proteolysis time course. Fig. 2b also shows that on adding about 14% salt (comparison of the 1.1% DM salt-56.3% TM water curve with the 14.9% DM salt-56.3% TM water curve), PIs fell even more for pork meat samples that were already well-dried. This confirms that salting is a key factor during the ham dry-curing process to control proteolysis. These results are consistent with those of Hutton (2002), who indicated that at constant temperature, adding salt and losing water decrease  $a_w$ , which is a key physicochemical variable for biochemical reactions and enzyme activity, and so slows the proteolysis time course.

#### 3.3. Time course of proteolysis at high temperature (24 °C)

Even at high temperature, proteolysis kinetics could be well-represented linearly with time ( $R^2 \geq 0.96$ ). The time course of protein degradation was, as expected, faster than at lower temperatures. Experiment 4 in Table 1 plotted in Fig. 2c led to PIs that increased from approximately 2.5% to 5.5% in only 13 days, even for pork meat samples salted at 10.3% DM. Comparing the plots in Fig. 2c and a shows that the proteolysis rates were multiplied by 3 or 4 when temperature increased from 3 to 24 °C, even for a



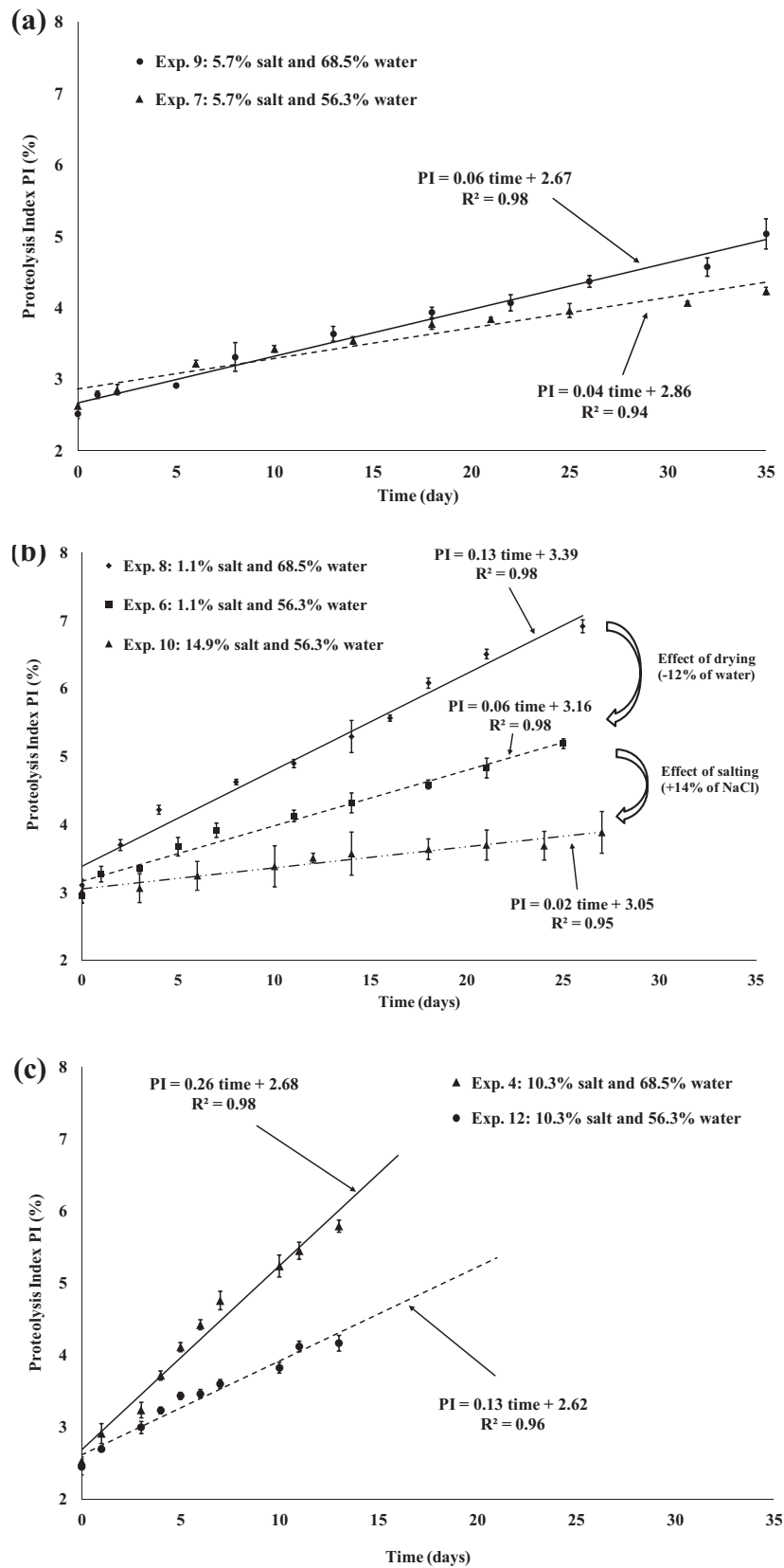


**Fig. 2.** Time course of proteolysis index (a) at 3 °C for muscle BF, (b) at 13 °C for muscle SM and (c) at 24 °C for muscle ST, as a function of various salt and water contents, and corresponding to some of the experiments listed in Table 1.

higher salt content (10.3% DM vs. 5.7% DM). These results could be explained by the fact that increasing temperature favours the degradation of muscular proteins by proteolytic enzymes, the activity

of which is increased due to the greater amount of energy available in the medium. Many studies mention that when temperature increases proteolysis also increases (Martin et al. (1998), among

others). Fig. 2c also shows that drying played an inhibitor role in proteolysis, thus confirming the results obtained at 13 °C for lower salt content. This inhibitor role was more clearly and obviously visible at 24 °C than at the previous temperatures of 13 and 3 °C, as seen from the fourth day (Fig. 2c). Also, in spite of a salt content increased by 50% at 24 °C, similar PIs were reached in 10 days at this high temperature against 35 days at 3 °C, for identical water contents. The effect of drying has often been described in several reports, and findings similar to these results have been reported (Ruiz-Ramírez, Arnau, Serra, & Gou, 2006; Toldra (2006); Toldrá, Cerveró, & Part, 1993). For the same reasons as at low temperature, the effect of salting could not be analysed at this temperature.

### 3.4. Statistical analysis

Table 1 shows the slopes of all the proteolysis kinetics plotted corresponding to the Doehlert design for each of the five muscles investigated: SM, BF, ST, RF and GM. Globally, the values of the slopes ranged from 0.02% to 0.37% PI/day. Those of the repeated kinetics, i.e., the centre point of the Doehlert design, were very close: mean values of  $0.09 \pm 0.01\%$  PI/day for SM;  $0.07 \pm 0.01\%$  PI/day for BF;  $0.09 \pm 0.01\%$  PI/day for ST;  $0.09 \pm 0.003\%$  PI/day for RF;  $0.06 \pm 0.01\%$  PI/day for GM, showing that there was no very marked inter-animal effect (standard deviation values lower than 0.01% PI/day). Statistical analyses were then carried out on the values of these slopes.

For each muscle, ANOVA showed that the temperature had a highly significant effect ( $p < 0.001$ ), the salt content a very significant effect ( $p < 0.01$ ) and the water content a significant effect ( $p < 0.05$ ) on the proteolysis time course. On the other hand, macroscopically, the muscle type had no significant effect on proteolysis, especially considering SM, BF and ST muscles ( $p > 0.05$ ). A Fisher LSD test confirmed the difference between the three temperatures used in this study. This test also showed that there was no difference between the proteolysis rates of the muscles, which could thus be lumped together, except for the GM muscle, which displayed specific behaviour (data not shown).

By means of multiple linear regressions, proteolysis time course models were built for all the muscles. 'Component+Residual' plots indicated that the effect of factors was linear. No outlier point was identified by the examination of hat values, Studentized residuals and Cook's distances. Table 2 contains all the coefficients statistically calculated to build the proteolysis rate models, relating the factors studied and their interactions. Also, as stated above, considering that all the muscles exhibited approximately the same behaviour (except for the GM muscle), a global phenomenological model was also built in which all these muscles were considered together.

In the present study, only the proteolysis time course model found for the ST muscle is reported. The *R*-squared coefficient

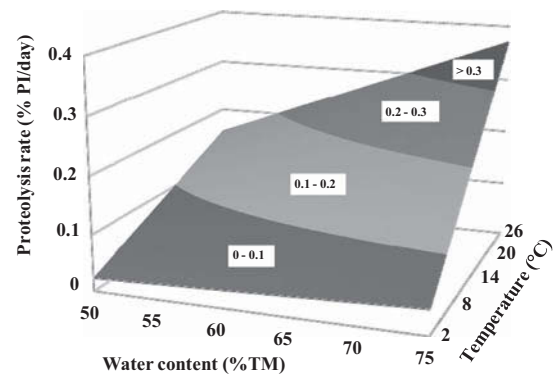


Fig. 3. Response surface plot of the combined effect of temperature and water content on the proteolysis rate in an ST pork muscle, at 4% sodium chloride content (% dry matter).

determined in this case was high (0.94), which means that the model that gives the time course of proteolysis rate ( $\text{Rate}_{\text{PI,ST}}$ ) fits the experimental data closely:

$$\begin{aligned} \text{Rate}_{\text{PI,ST}} = & 4.84 \cdot 10^{-3} - 9.18 \cdot 10^{-3}T - 7.28 \cdot 10^{-4}S \\ & + 1.69 \cdot 10^{-4}W - 3.92 \cdot 10^{-4}T \cdot S + 3.25 \cdot 10^{-4}T \cdot W \\ & + 5.21 \cdot 10^{-5}S \cdot W, \end{aligned} \quad (2)$$

where *T* is the temperature (°C), *S* is the salt content (% DM) and *W* is the water content (% TM).

As an example, Fig. 3 shows the response surface plot of the proteolysis time course for ST muscle, at 4% DM salt content. At low temperature, the values of the slopes of proteolysis kinetics are low, and the inhibitor effect of drying is not clearly visible in this figure. Gradually, as the temperature increases, protein degradation also increases, until at high temperature (24 °C) the inhibitor effect of the drying is clearly visible (Fig. 3). Results also show that increasing salt content slows down the proteolytic activity, especially at low water content. On the basis of all the phenomenological models built, the coefficients of which are listed in Table 2, the rate of protein degradation could be quantified as a function of time, for any of the five muscles studied, and for any of the conditions of temperature, water and salt content.

## 4. Discussion

During their production process, French dry-cured hams are generally subjected to a variable temperature regime that can be summarised as: about 11 weeks at 4 °C (salting and post-salting stages) optionally followed by 1 week at 23 °C (pre-ripening stage) and from the 13th week until the end, at 12 °C (drying and ageing

Table 2  
Details of multiple linear regression coefficients calculated from experimentally-quantified proteolysis rates for five different pork muscles, plus another one combining muscles SM, BF, ST and RF. *T* represents the temperature (°C), *S* the salt content (% dry matter) and *W* the water content (% total matter).

	Muscle SM	Muscle BF	Muscle ST	Muscle RF	Muscle GM	SM+BF+ST+RF
Intercept	$3.45 \cdot 10^{-2}$	$-7.99 \cdot 10^{-3}$	$4.84 \cdot 10^{-3}$	$-2.80 \cdot 10^{-2}$	$2.53 \cdot 10^{-2}$	$8.29 \cdot 10^{-4}$
<i>T</i>	$-1.41 \cdot 10^{-2}$	$-2.01 \cdot 10^{-3}$	$-9.18 \cdot 10^{-3}$	$-1.57 \cdot 10^{-2}$	$-5.73 \cdot 10^{-3}$	$-1.024 \cdot 10^{-2}$
<i>S</i>	$-5.83 \cdot 10^{-3}$	$3.56 \cdot 10^{-3}$	$-7.28 \cdot 10^{-4}$	$3.46 \cdot 10^{-3}$	$-5.88 \cdot 10^{-3}$	$1.147 \cdot 10^{-4}$
<i>W</i>	$-4.26 \cdot 10^{-4}$	$2.76 \cdot 10^{-4}$	$1.69 \cdot 10^{-4}$	$5.68 \cdot 10^{-4}$	$-9.77 \cdot 10^{-5}$	$1.47 \cdot 10^{-4}$
<i>T S</i>	$-1.57 \cdot 10^{-4}$	$-1.15 \cdot 10^{-4}$	$-3.92 \cdot 10^{-4}$	$-3.84 \cdot 10^{-4}$	$-3.45 \cdot 10^{-4}$	$-2.62 \cdot 10^{-4}$
<i>T W</i>	$3.68 \cdot 10^{-4}$	$1.52 \cdot 10^{-4}$	$3.25 \cdot 10^{-4}$	$4.56 \cdot 10^{-4}$	$2.57 \cdot 10^{-4}$	$3.25 \cdot 10^{-4}$
<i>S W</i>	$9.23 \cdot 10^{-5}$	$-6.00 \cdot 10^{-5}$	$5.21 \cdot 10^{-6}$	$-4.46 \cdot 10^{-5}$	$8.91 \cdot 10^{-5}$	$-1.75 \cdot 10^{-6}$
<i>R</i> <sup>2</sup>	0.95	0.95	0.94	0.94	0.84	0.91
Adj. <i>R</i> <sup>2</sup>	0.93	0.93	0.92	0.91	0.78	0.90
RSE	0.030	0.025	0.034	0.044	0.057	0.037

Adj. *R*<sup>2</sup>: adjusted *R*<sup>2</sup>; RSE: residual standard error.

**Table 3**

Calculation of proteolysis indices (PIs) and their variation as a function of temperature, water and salt contents during each main stage of the dry-cured ham production process using the phenomenological models built in this study, for three different pork muscles (SM: semimembranosus, BF: biceps femoris and RF: rectus femoris).

Stages of dry-cured ham production process	Salting and post-salting	Pre-ripening	Drying	Ageing
Duration (day)	77	7	70	150
Air temperature (°C)	4	23	12	12
<i>Muscle SM</i>				
Mean water content (% TM)	66.0	61.5	58.0	55.0
Mean salt content (% TM)	3.4	3.2	3.0	3.2
Mean proteolysis rate (%/day)	0.04	0.17	0.08	0.07
PI (%)	5.9 <sup>d</sup>	1.2	5.6	10.0
$\Delta T$ , PI (%) <sup>a</sup>	1.3	0.1	0.9	1.5
$\Delta X_w$ , PI (%) <sup>b</sup>	0.3	0.1	0.6	1.3
$\Delta X_{NaCl}$ , PI (%) <sup>c</sup>	<0.1	<0.1	0.2	0.4
<i>Muscle BF</i>				
Mean water content (% TM)	71.0	68.0	66.0	62.5
Mean salt content (% TM)	1.9	2.5	3.0	4.0
Mean proteolysis rate (%/day)	0.04	0.18	0.09	0.08
PI (%)	5.5 <sup>d</sup>	1.2	6.4	12.4
$\Delta T$ , PI (%) <sup>a</sup>	1.3	0.1	1.0	1.9
$\Delta X_w$ , PI (%) <sup>b</sup>	<0.1	<0.1	0.15	0.3
$\Delta X_{NaCl}$ , PI (%) <sup>c</sup>	0.15	<0.1	0.2	0.3
<i>Muscle RF</i>				
Mean water content (% TM)	68.0	65.0	62.0	57.5
Mean salt content (% TM)	3.2	4.2	4.2	4.9
Mean proteolysis rate (%/day)	0.06	0.23	0.11	0.09
PI (%)	7.2 <sup>d</sup>	1.6	8.0	13.7
$\Delta T$ , PI (%) <sup>a</sup>	1.8	0.1	1.2	2.0
$\Delta X_w$ , PI (%) <sup>b</sup>	0.2	0.1	0.6	1.4
$\Delta X_{NaCl}$ , PI (%) <sup>c</sup>	0.1	0.1	0.4	0.7

TM: total mass.

<sup>a</sup> Impact of a 2 °C variation in air temperature on the variation of PI over the considered stage.

<sup>b</sup> Impact of a 2% TM variation in water content on the variation of PI over the considered stage.

<sup>c</sup> Impact of a 0.5% TM variation in salt content on the variation of PI over the considered stage.

<sup>d</sup> A 2.5% initial value was considered when calculating PI at this particular stage. This initial value corresponds to the mean value of PI measured for the laboratory-prepared pork meat samples before salting and drying, i.e., for a few days-old "fresh" pork meat.

stages). Phenomenological models were built and used to predict PIs at the end of particular stages of the production process: salting and post-salting, pre-ripening, drying and ageing, for SM, BF and RF muscles of pork hams cured and dried for 10 months. To achieve this, mean values of water and salt content measured in whole SM, BF and RF muscles extracted from industrial dry-cured hams at various stages during the production process, in the framework of a previous study (internal unpublished data), were introduced into these models.

For each stage and muscle type, Table 3 shows the experimental values of water and salt content used for calculating the corresponding proteolysis rates and indices. In Table 3, a study of the sensitivity of the PI values to variations in temperature ( $\pm 2$  °C), water content ( $\pm 2\%$  TM) and salt content ( $\pm 0.5\%$  TM) commonly found in industrial practise is also reported. Table 3 indicates globally that the highest increase in proteolysis occurs during the ageing stage due to its long duration, with a mean PI increase of 2–2.5% a month. At this particular stage, thorough analysis shows that the three muscles investigated can be ranked in order of increasing PI: RF > BF > SM. Regarding the pre-ripening stage, although high proteolysis rates (0.2% PI/day) were calculated as a result of a high temperature, a very restricted PI increase (<2%) occurred since this stage only lasts one week. Whatever the muscle type, similar values of proteolysis rates and indices were calculated using the phenomenological models during the salting and resting time periods compared with the drying stage due to offset between the temperature effect (main variable allowing proteolysis to be controlled during the salting and post-salting stages) and the drying and salting effects (main variables affecting proteolysis during drying) on the proteolysis time course (Table 3). In the case of SM muscle, the lower value of PI during drying compared with that during salting and post-salting can even be attributed to drying

only, because similar values of salt content over these stages are reported in Table 3. Analysis of the sensitivity study reveals that the highest changes in PI are attributable to temperature before the water content and then the salt content, in accordance with the results of statistical analysis. This confirms that an accurate control of temperature and drying, and to a lesser extent, salting, is crucial throughout the dry-cured ham production process (except during the pre-ripening stage, given its short duration) to limit heterogeneity in terms of final PI values.

These results are globally in line with those of Zhao et al. (2008), who indicated that the highest PI increase in BF muscle occurred during ageing, and with those of Toldra, Flores, and Sanz (1997) and Ruiz-Ramírez, Arnau, Serra, and Gou (2006), who reported a more intense proteolysis in BF muscle than in SM muscle, probably due to constantly higher moisture content.

## 5. Conclusion

The present results confirm that temperature, water and salt contents are key processing factors, strongly influencing proteolysis during the ageing of laboratory-prepared pork meat samples mimicking dry-cured ham production. Temperature rise favoured proteolysis, whereas salting and drying slowed it down. Statistical analyses supported the highly significant effect of temperature on proteolysis, highlighting a very high significant effect of water content and high significant effect of salting. On the other hand, the muscle type had no significant effect on proteolysis, especially for the most often studied and voluminous muscles in dry-cured ham, i.e., BF, SM and ST.

To the authors' knowledge, several phenomenological models were built here for the first time. These models relate proteolysis



to temperature and water and salt content for five types of muscle. Some of them were used to predict PIs and to assess the impact of some variations in the control of temperature, drying and salting on PI values at the end of the main stages of the production process: salting and post-salting, pre-ripening, drying and ageing. It was highlighted that introducing a one-week-long pre-ripening stage during the process had very little influence on the PI time course. However, the great advantage of these phenomenological models is that they can be easily integrated into a 3D multi-physical numerical model to predict simultaneously the time course of proteolysis as a function of salt diffusion, water migration and heat transfer throughout the ham dry-curing process, which can last from 6 to more than 18 months. A total of six phenomenological models have thus been built (one for each type of muscle, plus one corresponding to an “average muscle” combining SM, ST, BF and RF) with the prospect of integrating them into a real geometry of ‘numerical’ ham built up from morphological images.

### Acknowledgements

This work was funded by the Na- integrated programme (ANR-09-ALIA-013-01) financed by the French National Research Agency. This paper forms part of the thesis of Rami Harkouss, who works for this research program. We thank S. Portanguen for his technical assistance and ATT for language editing.

### References

- Adler, D., & Murdoch, D. (2013). Rgl: 3D visualization device system. R package version 0.93.945. URL: <http://cran.r-project.org/web/packages/rgl/> Accessed 11.07.13.
- Arnau, J., Guerrero, L., & Gou, P. (1997). Effects of temperature during the last month of ageing and of salting time on dry-cured ham aged for six months. *Journal of the Science of Food and Agriculture*, 74, 193–198.
- Arnau, J., Guerrero, L., & Sárraga, C. (1998). The effect of green ham pH and NaCl concentration on cathepsin activities and sensory characteristics of dry-cured ham. *Journal of the Science of Food and Agriculture*, 77, 387–392.
- Benedini, R., Parolari, G., Toscani, T., & Virgili, R. (2012). Sensory and texture properties of Italian typical dry-cured hams as related to maturation time and salt content. *Meat Science*, 90, 431–437.
- Bezerra, M. A., Santelli, R. E., Oliveira, E. P., Villar, L. S., & Escalera, L. A. (2008). Response surface methodology (RSM) as a tool for optimization in analytical chemistry. *Talanta*, 76, 965–977.
- Costa-Corredor, A., Muñoz, T., Arnau, J., & Gou, P. (2010). Ion uptakes and diffusivities in pork meat brine-salted with NaCl and K-lactate. *LWT Food Science and Technology*, 43, 1226–1233.
- Costa-Corredor, A., Serra, X., Arnau, J., & Gou, P. (2009). Reduction of NaCl content in restructured dry-cured hams: Post-resting temperature and drying level effects on physicochemical and sensory parameters. *Meat Science*, 83, 390–397.
- Doehlert, D. H. (1970). Uniform shell designs. *Applied Statistics*, 19, 231–239.
- Fox, J., & Weisberg, S. (2011). *An R companion to applied regression* (2nd ed., ). Thousand Oaks, CA: Sage. <http://socserv.socsci.mcmaster.ca/jfox/Books/Companion> Accessed 11.07.13.
- García-Garrido, J. A., Quiles-Zafra, R., Tapiador, J., & Luque De Castro, M. D. (2000). Activity of cathepsin B, D, H and L in Spanish dry-cured ham of normal and defective texture. *Meat Science*, 56, 1–6.
- Garrido, R., Domínguez, R., Lorenzo, J. M., Franco, I., & Carballo, J. (2012). Effect of the length of salting time on the proteolytic changes in dry-cured *lacón* during ripening and on the sensory characteristics of the final product. *Food Control*, 25, 789–796.
- Gornall, A. G., Bardawill, C. J., & David, M. M. (1949). Determination of serum proteins by means of biuret reaction. *Journal of Biological Chemistry*, 177, 751–766.
- Harkouss, R., Mirade, P. S., & Gatellier, P. (2012). Development of a rapid, specific and efficient procedure for the determination of proteolytic activity in dry-cured ham: Definition of a new proteolysis index. *Meat Science*, 92, 84–88.
- Heiberger, R.M. (2013). HH: Statistical analysis and data display. R package version 2.3.37. URL: <http://cran.r-project.org/web/packages/HH/> Accessed 11.07.13.
- Hutton, T. (2002). Technological functions of salt in the manufacturing of food and drink products. *British Food Journal*, 104, 126–152.
- Jakobsen, M., & Bertelsen, G. (2000). Colour stability and lipid oxidation of fresh beef. Development of a response surface model for predicting the effects of temperature, storage time, and modified atmosphere composition. *Meat Science*, 54, 49–57.
- Jin, G., He, L., Zhang, J., Yu, X., Wang, J., & Huang, F. (2012). Effects of temperature and NaCl percentage on lipid oxidation in pork muscle and exploration of the controlling method using response surface methodology (RSM). *Food Chemistry*, 131, 817–825.
- Lumkey, T. (2009). Leaps: Regression subset selection. R package version 2.9. URL: <http://CRAN.R-project.org/package=leaps> Accessed 11.07.13.
- Martín, L., Córdoba, J. J., Antequera, T., Timon, M. L., & Ventanas, J. (1998). Effects of salt and temperature on proteolysis during ripening of Iberian ham. *Meat Science*, 49, 145–153.
- Møller, J. K. S., Jakobsen, M., Weber, C. J., Martinussen, T., Skibsted, L. H., & Bertelsen, G. (2003). Optimisation of colour stability of cured ham during packaging and retail display by a multifactorial design. *Meat Science*, 63, 169–175.
- Morales, R., Serra, X., Guerrero, L., & Gou, P. (2007). Softness in dry-cured porcine *biceps femoris* muscles in relation to meat quality characteristics and processing conditions. *Meat Science*, 77, 662–669.
- Parolari, G., Virgili, R., & Schivazappa, C. (1994). Relationship between cathepsin B activity and compositional parameters in dry-cured hams of normal and defective texture. *Meat Science*, 38, 117–122.
- R Development Core Team (2013). R: A language and environment for statistical computing. R Foundation for Statistical Computing, Vienna: Austria. URL: <http://www.R-project.org> Accessed 11.07.13.
- Rico, E., Toldrá, F., & Flores, J. (1991). Effect of dry-curing process parameters on pork muscle cathepsins B, H and L activities. *Zeitschrift für Lebensmittel-Untersuchung und Forschung A*, 193, 541–544.
- Ruiz-Ramírez, J., Arnau, J., Serra, X., & Gou, P. (2006). Effect of pH 24, NaCl content and proteolysis index on the relationship between water content and texture parameters in *biceps femoris* and semimembranosus muscle in dry-cured ham. *Meat Science*, 72, 185–194.
- Sárraga, C., Gil, M., Arnau, J., Monfort, J. M., & Cussó, R. (1989). Effect of curing salt and phosphate on the activity of porcine muscle proteases. *Meat Science*, 25, 241–249.
- Serra, X., Ruiz-Ramírez, J., Arnau, J., & Gou, P. (2005). Texture parameters of dry-cured ham m. *biceps femoris* samples dried at different levels as a function of water activity and water content. *Meat Science*, 69, 249–254.
- Tabilo, G., Flores, M., Fiszman, S. M., & Toldra, F. (1999). Postmortem meat quality and sex affect textural properties and protein breakdown of dry-cured ham. *Meat Science*, 51, 255–260.
- Toldrá, F. (2006). The role of muscle enzymes in dry-cured meat products with different drying conditions. *Trends in Food Science & Technology*, 17, 164–168.
- Toldrá, F., Cerveró, M. C., & Part, C. (1993). Porcine aminopeptidase activity as affected by curing agents. *Journal of Food Science*, 58, 724–726.
- Toldrá, F., & Etherington, D. J. (1988). Examination of cathepsins B, D, H and L activities in dry-cured hams. *Meat Science*, 23, 1–7.
- Toldrá, F., & Flores, M. (2000). The use of muscle enzymes as predictor of pork meat quality. *Food Chemistry*, 69, 387–395.
- Toldrá, F., Flores, M., & Sanz, Y. (1997). Dry-cured ham flavour: Enzymatic generation and process influence. *Food Chemistry*, 59, 523–530.
- Virgili, R., Parolari, G., Schivazappa, C., Bordini, C. S., & Borri, M. (1995). Sensory and texture quality of dry-cured ham as affected by endogenous cathepsin B activity and muscle composition. *Journal of Food Science*, 60, 1183–1186.
- Zhao, G. M., Tian, W., Liu, Y. X., Zhou, G. H., Xu, X. L., & Li, M. Y. (2008). Proteolysis in *biceps femoris* during Jinhua ham processing. *Meat Science*, 79, 39–45.
- Zhao, G. M., Zhou, G. H., Wang, Y. L., Xu, X. L., Huan, Y. J., & Wu, J. Q. (2005). Time-related changes in cathepsin B and L activities during processing of Jinhua ham as a function of pH, salt and temperature. *Meat Science*, 70, 381–388.



## **Title**

**Effect of salting and drying on the time course of proteolysis, structure and texture during the dry-cured ham elaboration process. Building of a “numerical ham” model that couples water and salt transfers to proteolysis.**

## **Abstract**

Because of public health problems, the food industry must lower sodium content in all food products, therefore in cured meat products. During the dry-cured ham elaboration process, decreasing salt content may induce microbial safety problems and texture defects due to an excessive proteolysis that could affect later the industrial stage of slicing. On account of that, this work of thesis aims at (1) studying the relationship between proteolysis, structure and texture during the various stages of dry-cured ham manufacture, and (2) building a “numerical ham” model to predict spatially the time course of water and salt content, and thus water activity ( $a_w$ ), and to couple these variations with proteolysis.

This work combines experimental studies and numerical modelling and simulation. Firstly, a new and powerful technique for quantifying proteolysis that uses “Fluorescamine” was developed and validated on pork meat samples and samples extracted from industrial dry-cured hams; a new proteolysis index (PI) was defined. Based on an experimental design, the time course of proteolysis was quantified in laboratory-salted and dried pork meat samples prepared from five different types of pork muscle. Applying multiple linear regression enabled us to build phenomenological models relating, for each pork muscle, PI velocity to temperature, and to water and salt content. Using Comsol<sup>®</sup> Multiphysics software, these phenomenological models were then combined with heat and mass transfer models and associated with calculation of  $a_w$ , thus constituting the “numerical ham” model. In addition, the time course of PI, five textural parameters (hardness, fragility, cohesiveness, springiness and adhesiveness), and four structural parameters (fiber number, extracellular spaces, cross section area, and connective tissue area) was quantified on samples extracted from two different muscles of industrial dry-cured hams removed from the process at five different processing times. Multiple polynomial regression was applied to build phenomenological models relating PI, salt and water content to some textural and structural parameters investigated. These last models could be rapidly incorporated in the “numerical ham” model to constitute a real process simulator. In the future, the “numerical ham” model should be improved in order to take into account (1) the strong decrease in ham volume due to drying and also (2) the decrease in proteolysis velocity with time as a result of the reduction in the amount of protein that can be hydrolysed in the ham. Once completed and improved, the process simulator will be available to professionals to test scenarios allowing sodium content to be reduced in dry-cured hams without altering their final quality.

**Keywords:** dry-cured ham; drying; salting; proteolysis; structure; texture; fluorescamine; experimental design; phenomenological model; modelling; numerical ham; process simulator.